Universidade do Minho
Escola de Engenharia

Raquel de Jesus Marques da Silva

Sonoproduction of particles for delivery purposes

Abril, 2011

Raquel de Jesus Marques da Silva **Sonoproduction of particles for delivery purposes**

UMinho | 2011

Universidade do Minho
Escola de Engenharia

Raquel de Jesus Marques da Silva

Sonoproduction of particles for delivery purposes

Tese de Doutoramento em Engenharia Têxtil

Trabalho efectuado sob a orientação do
Professor Doutor Artur Manuel Cavaco-Paulo
e da
Doutora Helena Susana da Costa Machado Ferreira

Abril, 2011

“A scientist in his laboratory is not a mere technician: he is also a child confronting natural phenomena that impress him as though they were fairy tales...”

Marie Curie

To my Family

ACKNOWLEDGMENTS

Last words to be written… the most difficult for me!

I cannot conclude this relevant stage of my life without expressing my most sincere gratitude to all those who gave me constant support and encouragement throughout all these years.

First, I would like to acknowledge my supervisor, Professor Artur Cavaco-Paulo, for all the opportunities given. Looking back, after all these years, I can say that I grew as a researcher and as a person. I admire your strength of character and perseverance, your capability to overcome any challenge.

Thank you for the opportunity to make part of an European project “Lidwine” and to meet such interesting people. You also gave me the opportunity to present my work and participate in the best conferences of the field, being able to present my research; always full of confidence in me, which was decisive in my life as a young scientist. I’m deeply indebted for always believe in me. Thank you also for the opportunity to meet such wonderful places and different cultures that otherwise it would be difficult to meet. Thank you for everything!!!

To my co-supervisor and friend Dra. Helena Ferreira who taught me so much. Your contribution in my life is beyond words. I learned how to plan everything in detail and to be organized. Our fruitful discussions and scientific plans have been memorable. I am tremendously grateful for your belief in me. You are an example of strength and courage. I deeply acknowledge your optimism and confidence. You will never know how important you were in certain moments of my life. My most sincere thanks to you, Helena, an excellent co-supervisor that has made possible the born of a great friendship.

Thank you to Professor Aharon Gedanken, that welcomed me on his work group in Bar-Ilan University, for the personal and professional growth that my staying there represented.

In the Department of Biology I must acknowledge to Dra. Andreia Gomes, for “introducing” me in the amazing world that is a cell culture laboratory.

I would like to thank also to Edith for all her help and support provided in the SEM and STEM analysis. For the many hours that we spent understanding the science behind the morphologic analysis of nano and microparticles.

To my friends that I met in the Bioprocess Research Group but already left: Carla Joana, Zille, Carlos, Collin and Rita. You were so important during the first years in the group that I can never describe how grateful I am because of what you have made for me.

To the Go Team, thank you for all the support and happy hours!!!

I would like to dedicate special words to Carla Manuela and Andreia that share with me this trajectory through all these years to build up this final result. They have been very special friends and they share with me the same values. Thank you for the support, scientific advising and endless friendship that were constant through all these years and that are relevant for many of the achievements described in this thesis. We have been together in both wonderful and bad times. Thank you for your patience (in this last months I almost did not have social life), true opinion, and loyalty.

I need to thank all my closest friends, you know who you are! I must say that I have many special people around me.

Thanks to my wonderful family, because they always understood my choices, they gave me constant support. To my sisters Sofia and Joana and to my brother Pedro and my brother-in-law Hélder, they are very important in my life!!! To my dearest nieces, Inês and Joaninha, for their wonderful smile that make me always forget all my problems….They are my Princesses.

To my dear Nuno, for encouraging me specially throughout the late nights. Thank you for your patience, dedication, sense of humour and for your unconditional love all over these years!

At last but not least, to my parents for encouraging my dreams and supporting my decisions. I would be lost without your advices, support, friendship and love. This thesis would not exist without you.

ABSTRACT

Ultrasound was used to develop particle systems based on phospholipids and protein materials. This technique has proven to be a very effective method of nano and microstructured materials production.

Owing to the variety of the application fields of such particles (nanomedicine, drug delivery, cosmetics, etc.), and as existing nano and microparticles are now available, a thorough knowledge of the formulating processes (and their potentialities) is essential in order to achieve the given purposes and needs for research. Based on this approach, it is necessary to develop or optimize methodologies that can fulfill all the requirements to create devices with delivery ability.

In this work, to obtain large unilamellar vesicles (LUVs) from dipalmitoylphosphatidylcholine (DPPC), it was necessary an extensive characterization of ultrasound, namely power input, distance from ultrasound tip to base of reactor and treatment time, in order to control the maximum cavitation events. Results indicated a dependence on cavitation events that are a function of power input, and consequently on the position of the probe within the reaction vessel and the wave behaviour. Short treatment times were required to achieve nanosized vesicles in anti-nodal ($\lambda/4$; 19 mm) reactor geometries. In this wave point the cavitation phenomenon is more pronounced when compared to the nodal point ($\lambda/2$; 38 mm). The acknowledgment of this was also helpful for the incorporation of peptides in phospholipids aggregates. The developed systems were characterized in terms of morphology, zeta-potential, particle size and size distribution.

Studies were also performed in order to investigate the mechanism of protein microspheres formation by ultrasound sources using different proteins bovine serum albumin (BSA), human serum albumin (HSA) and silk fibroin (SF) as well as diverse peptide constructions. The microspheres were produced by means of ultrasonication of two-phase starting mixture, consisting of protein solution and organic solvent or natural oils. Several parameters, namely protein concentration,

ratio of aqueous/organic phase were tested to study their influence in the physico-chemical properties of the developed particles. It was conclude that the particles size decrease with the use of higher protein concentration (5.0 $g.L^{-1}$ and 10.0 $g.L^{-1}$ for BSA and SF, respectively) and with lower percentage of organic phase (5%). The use of different proteins along with different peptides constructions allowed us to prove that the main mechanism of protein microspheres formation is the mass transport effects, promoted by ultrasound, which led to a change in protein entropy system and, consequently, to an enhancement of hydrophilic and hydrophobic interactions forming a closed ring, a microsphere.

The performance of several stabilizers in microspheres formulation was determined. The results demonstrate that the polyvinyl alcohol (PVA) is the most efficient for these protein devices and that 8% was the amount required to obtain smaller sizes and a monodispersed population [≈ 260 nm of size diameter and ≈ 0.060 of polydispersity index (PDI)]. The developed protein-based systems were also characterized regarding their ability to be used as release systems. Two categories of bioactive agents - natural oils and anti-inflammatory drug - were incorporated within protein microspheres. The results demonstrated that they are non-cytotoxic in a certain range of microspheres concentration. Additionally, the developed materials were able to incorporate and to release, with a defined profile, molecules pertaining to two different groups of bioactive agents (natural oils and anti-inflammatory drugs).

The sonochemical method has been further extended to the application of these microspheres containing piroxicam, onto cotton and nonwoven gauzes. A sustained release of piroxicam was observed over time, greatly supporting their application for textile-based wound dressings.

In summary, the results of this work show that it was possible to develop liposomes and protein microspheres with ultrasound sources, whose characterization showed their ability to incorporate and deliver different bioactive agents.

RESUMO

A técnica de ultra-sons foi usada no desenvolvimento de sistemas de partículas a partir de fosfolipídios e proteínas. Esta técnica provou ser um método muito eficaz na produção de nano e micro-materiais estruturados.

Devido à variedade de áreas de aplicação de tais partículas (nano-medicina, libertação controlada de medicamentos, cosméticos, etc.), e ao grande número de nano e micropartículas existentes, um conhecimento profundo dos processos de formulação (e suas potencialidades) é essencial para alcançar os objectivos pretendidos e as necessidades de investigação. Com base nesta abordagem, mostra-se necessário desenvolver e optimizar metodologias capazes de satisfazer todos os requisitos indispensáveis à criação de dispositivos com capacidade de libertação controlada.

Neste trabalho, para obter vesículas unilamelares grandes (LUVs), a partir do dipalmitoilfosfatidilcolina (DPPC), foi necessária uma extensa caracterização dos ultra-sons, nomeadamente a potência, a distância da sonda de ultra-sons à base do reactor e o tempo de tratamento, de forma a controlar os fenómenos de cavitação máxima. Os resultados obtidos indicaram que os fenómenos de cavitação, para além de dependerem da energia aplicada dependem ainda da posição da sonda dentro do recipiente de reacção e do comportamento da onda. Para atingir vesículas nanométricas no ponto antinodal ($\lambda/4$; 19 mm) do reactor foram suficientes tempos de tratamento de curta duração. Naquele ponto da onda, o fenómeno de cavitação é mais acentuado quando comparado com o ponto nodal ($\lambda/2$; 38 mm). A confirmação desta ocorrência foi também útil para a incorporação de péptidos em agregados de fosfolipídos. Os sistemas desenvolvidos foram caracterizados em termos de morfologia, potencial zeta, tamanho de partícula e distribuição de tamanho.

Foram também realizados estudos para investigar o mecanismo de formação de microesferas de proteína por fontes de ultra-sons utilizando diferentes proteínas como a albumina serum bovina (BSA), albumina serum humana (HSA) e a fibroína da seda (SF), bem como diversas construções peptídicas. As microesferas foram produzidas através da sonicação de uma mistura com duas fases, que consiste em uma solução de proteína e solventes orgânicos ou óleos

naturais. Vários parâmetros, nomeadamente a concentração de proteína, as relações de fase aquosa/orgânica foram testadas para estudar a sua influência nas propriedades físico-químicas das partículas desenvolvidas. Verificou-se uma diminuição no tamanho das partículas com o uso de maior concentração de proteína (5.0 $g.L^{-1}$ e 10.0 $g.L^{-1}$ para BSA e SF, respectivamente) e com menor percentagem de fase orgânica (5%). A utilização de diferentes proteínas, juntamente com diferentes construções peptídicas permitiu concluir que o principal mecanismo de formação de microesferas de proteína são os efeitos de transporte de massa, promovido pelos ultra-sons, que leva a uma mudança na entropia da proteína e, consequentemente, a um aumento de interacções hidrofílicas e hidrofóbicas, formando um anel fechado, a microesfera.

O efeito de estabilizadores nas várias formulações de microesferas foi também determinado. Os resultados demonstram que o polivinil álcool (PVA) é o mais eficiente para estes dispositivos de proteína e 8% é a quantidade necessária para obter tamanhos menores e populações monodispersas [≈ 260 nm de diâmetro e ≈ 0.060 de índice de polidispersão (PDI)]. Os sistemas desenvolvidos baseados em proteína também foram caracterizados quanto à sua capacidade para serem aplicados como sistemas de libertação. Duas categorias de agentes bioactivos - óleos naturais e anti-inflamatórios - foram incorporados no interior das microesferas de proteína. Os resultados revelaram que estas não são cito-tóxicas em determinadas concentrações. Além disso, os materiais desenvolvidos demonstraram ser capazes de incorporar e libertar, com um perfil definido, moléculas pertencentes a dois diferentes grupos de agentes bioactivos (óleos naturais e fármacos anti-inflamatórios).

O método sonoquímico foi ainda utilizado na aplicação das microesferas contendo piroxicam, em gazes de algodão e não-tecido, para obter uma libertação controlada de piroxicam ao longo do tempo, apoiando extraordinariamente a sua aplicação no desenvolvimento de novos depósitos de ferida baseados em materiais têxteis.

Em resumo, foi criada evidência sobre a possibilidade de desenvolver lipossomas e microesferas à base de proteínas através de sistemas de ultra-sons, cuja caracterização traduz a sua capacidade de incorporar e de libertar diferentes agentes bioactivos.

TABLE OF CONTENTS

LIST OF ABBREVIATIONS

A

a.a.	Amino acids
ATCC	American type culture collection
Å	Ångström

B

BSA	Bovine serum albumin
BSA-piroxicam	Bovine serum albumin-piroxicam

C

CMC	Critical micelle concentration
cm	Centimetre
COX	Cyclo-oxygenase
CO	Cotton
Cat	Cationized

D

DS	Delivery system(s)
DDS	Drug delivery system
DPPC	Dipalmitoylphosphatidylcholine
DMPC	Dimyristoylphosphotidylcholine
3-D	Three-dimensional
Da	Dalton
DMEM	Dulbecco's modified Eagle's medium
DLS	Dynamic light scattering
DID	1,1'-dioctadecyl-3,3,3',3'-tetramethylindodicarbocyanine perchlorate
DMSO	Dimethyl sulfoxide

E

e.g.	For example
EPC	Egg yolk phosphatidylcholine
EDTA	Ethylenediaminetetraacetic acid

F

FT-IR	Fourier transform infrared
FITC	Fluorescein isothiocyanate
FBS	Fetal bovine serum
fs	Femtosecond

G

GUVs	Giant unilamellar vesicles
g	gram

H

$H^{\bullet}$	Hydrogen radical
H_2O_2	Hydrogen peroxide
$HO_2^{\bullet}$	Hydroperoxyl radical
H_2	Hydrogen
H_2O	Deionized water
HTA	2-hydroxyl-terephthalic acid
HSA	Human serum albumin
HSA-piroxicam	Human serum albumin-piroxicam
Hb	Hemoglobin
HPLC	High performance liquid chromatography
h	Hours

I

IUVs	Intermediate sized unilamellar vesicles
IR	Infrared
IWLs	Internal wool lipids

J

J	Joule

K

K	Kelvin
kHz	Kilohertz
kDa	KiloDalton
Kg	Kilogram
K/S	Kubelka - Munk relationship (K-absorption coefficient; S-scattering coefficient)

L

LUVs	Large unilamellar vesicles
LBL	Layer-by-layer
LiBr	Lithium bromide

M

µm	Micrometre
µmol	Micromole
µL	Microliters
mL	Millilitres
M	Molar
mM	Milimolar
MHz	Megahertz

mm	Millimetre
MLVs	Multilamellar vesicles
min	Minutes
mV	Millivolts
MTT	3-(4,5-dimethylthiazol-2-yl)-2,5-diphenyltetrazolium bromide
MS	Mass spectrometry
MMP	Matrix metalloproteinases

N

nm	Nanometre
nmol	Nanomole
NaOH	Sodium hydroxide
NSAIDs	Non-steroidal anti-inflammatory drugs
NW	Nonwoven

O

$^{\bullet}OH$	Hydroxyl radical
O_2	Oxygen
$O_2^{\bullet-}$	Superoxide radical

P

PBS	Phosphate buffered saline solution
PDI	Polydispersity index
PCS	Photon correlation spectroscopy
PEG	Polyethylene glycol
PAMAM	Poly(amidoamine)
PVA	Polyvinyl alcohol
PPE	Porcine pancreatic elastase
*p*NA	*p*-nitroanilide

pluronic F68	Pluronic acid F68
P	Statistical level of significance
PDDA	Poly(diallyldimethylammonium chloride)
ps	Picosecond

R

RES	Reticuloendothelial system
RNase A	Ribonuclease A
rpm	Rotations per minute

S

SUVs	Small unilamellar vesicles
s	Second
SF	Silk fibroin
SPG	Sodium polyglutamate
SEM	Scanning electron microscopy
STEM	Scanning transmission electron microscopy
SLIPI	Secretory leukocyte protease inhibitor
Suc$(Ala)_3$-*p*NA	Succinyl-alanine-alanine-*p*-nitroanilide

T

T_c	Temperature of phase transition
Tris-HCl	Tris(hydroxymethyl)aminomethane hydrochloride
TCs	Thermocouples
TA	Terephthalic acid
TAMRA	5(6)-carboxytetramethyl-rhodamine, succinimidyl ester

U

UV	Ultra-violet
U	Unit

V

v/v	Volume/volume
Vs	Versus

W

w/v	Weight/volume

Z

ζ-potential	Zeta-potential

LIST OF FIGURES

LIST OF TABLES

LIST OF EQUATIONS

INTRODUCTION TO THE THESIS FORMAT

Over the past few decades, there have been demands to develop several devices for delivery purposes. In parallel, there was a need to optimize or develop new techniques to produce them.

The main aim of this thesis is to develop nano and microparticles, based on phospholipids and protein materials, using high energy of ultrasound. The specific objectives intend to verify the influence of sonochemical method to produce these systems and at the same time, evaluate the physico-chemical parameters of the developed devices and their ability for delivery purposes.

In agreement with the aims of the present thesis, this dissertation research is divided in four parts containing ten chapters, with one of them experimental. The contents of each one are summarized below.

1st part - Theoretical considerations related to the topics of thesis outline.

- *Chapter I*: give an overview of the state of the art of the sonochemical methodology to prepare two different delivery devices, namely liposomes and polymeric particles. Special focus is devoted on the novel applications and recent work involving sonochemical methodology in the fields of nano and microparticles. Some remarks on the main concepts of those systems to form the nano and microparticles and their applications as delivery systems (DS) is performed. Finally, relates to their uses and potential for textile-based wound dressings.

2nd part- Materials and methods.

- *Chapter II*: contains in detail the materials and the experimental procedures used for the development and characterization of nano and microparticles.

3rd part - Major results in the scope of this thesis (Chapter III to IX).

- *Chapter III*: **Effect of ultrasound parameters for unilamellar liposome preparation**, describes the characterization of ultrasound system providing a guideline for further preparation of unilamellar vesicles.

- *Chapter IV*, **Incorporation of peptides in phospholipid aggregates using ultrasound**, reports the use of ultrasound to prepare liposomes incorporating one of the two different synthesized peptides and their physico-chemical properties.

- *Chapter V*, **Insights on the mechanism of protein microspheres formation**, was designed to investigate the mechanism of proteinaceous microspheres formation by sonochemical method, using bovine serum albumin (BSA) and silk fibroin (SF). Different experimental conditions were investigated to study their influence in microspheres formation, and in their physico-chemical properties.

- *Chapter VI*, **Mechanisms of the formation of proteinaceous microspheres - Highlights from peptide size and sequences**, reports deeper studies on the mechanism of protein microspheres formation, by sonochemical method. For that, new engineered peptides with a different range of sizes and sequences were used and further characterized.

- *Chapter VII*, **Sonochemical proteinaceous microspheres for wound healing**, exploits the benefits of BSA, human serum albumin (HSA) and SF microspheres, incorporating three different organic solvents (*n*-dodecane, mineral and vegetable oil), for wound healing.

- *Chapter VIII*, **Protein microspheres as suitable devices for piroxicam release**, describes the use of a sonochemical method to produce microspheres of BSA and HSA incorporating piroxicam. Besides

microspheres characterization, it was also analysed the release profile of piroxicam from these devices.

- *Chapter IX*, **Cotton and nonwoven gauzes bandages: A support for proteinaceous microspheres**, reports the application of BSA-piroxicam microspheres attached onto cotton and nonwoven gauzes using two different methodologies: incubation and sonochemical methodology.

4th part: General discussion, final remarks and future perspectives.

- *Chapter IX*: contains the general conclusions regarding the overall work carried out under the scope of this thesis, as well as some final remarks. The future perspectives part describes the future work that can follow this thesis outline.

CHAPTER I

SONOPRODUCTION OF PARTICLES FOR DELIVERY PURPOSES

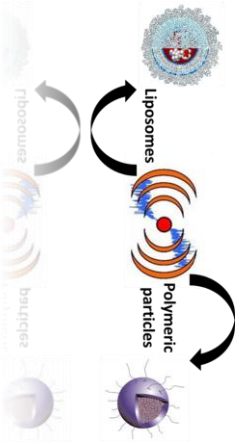

Chapter I

Sonoproduction of particles for delivery purposes*

ABSTRACT

The development of nano and micro delivery systems (DS), so small in size, is growing in importance. In an era where nano is the new trend, micro and nano materials are in the forefront of progress. These systems can be produced by a diversity of methods. However, the use of high intensity ultrasound offers an easy and versatile tool for nano and microstructured materials that are often unavailable by conventional methods. Similarly to the synthesis methods that can be used, several starting materials can be applied to produce particulate systems. In this review, the recent strategic development of DS is discussed with emphasis on liposomes and polymer-based, specially protein-based, nanomedicine platforms for drug delivery. Among the variety of applications that materials in the particulate form can have, the control release of drugs is probably the most prominent one, as these have been in the forefront line of interest for biomedical applications. The basic concepts of sonochemical process pertaining to DS are summarized as well as the role of sonochemical procedure to their preparation. The different applications of these systems wrap up this review.

* This chapter is based on the following publication:
Silva R; Ferreira H, Cavaco-Paulo A, *Sonoproduction of particles for delivery purposes*, submitted.

I-1. GENERAL INTRODUCTION

Nano and microparticles are particulate delivery systems (DS) of nanometre or micron size ranges, respectively, and can incorporate therapeutic agents, such as small drugs or even macromolecules [1]. The term microparticle refers to spherical particles with diameters range between 0.1 and 100 µm. Particles with diameter below 0.1 µm are called nanoparticles [2].

The promising significance of nano and microparticles in the biomedical field and the needs of materials with biocompatibility, biodegradability and non-toxicity have propelled the efforts for developing and optimizing new materials. Various types of particles like solid lipid nanoparticles [3], micelles [4], liposomes [5], dendrimers [6] and polymers [7] have been reported as DS to encapsulate drugs and other bioactive agents (Figure I-1).

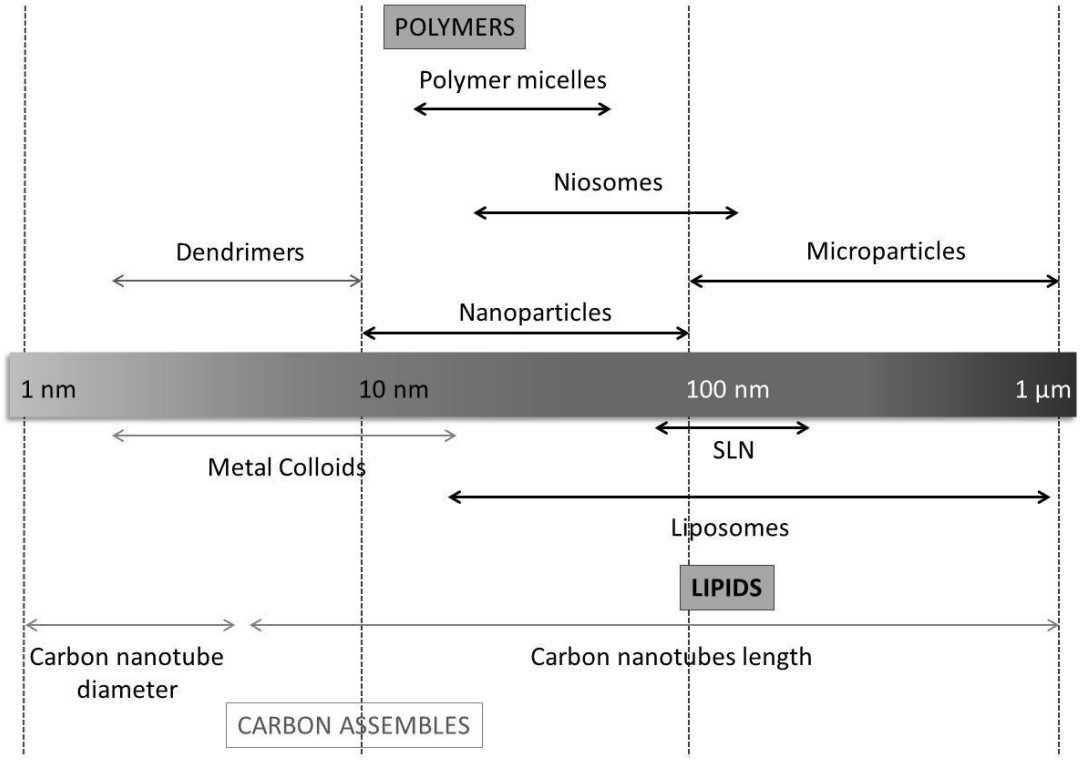

Figure I-1: **Types of nano and microtechnology used for delivery purposes. The major components are either lipids or polymers. The black and grey axis represents the diameter of technology (Adapted from Couvreur, P. and Vauthier C. [8]).**

Over the past few decades, significant advances have been made in delivery technology. Drug delivery, which takes into consideration the carrier, the route of administration and the target, has evolved into a strategy of processes or devices designed to enhance the efficacy of therapeutic agents through controlled release. This may involve enhanced bioavailability, improved therapeutic index (ratio between the efficacy of the drug and its undesirable side effects), or improved patient acceptance or compliance. In fact, the administration of a drug in a DS influences their parameters, in particular concerning the pharmacokinetics, pharmacodynamics and biodistribution, which, in turn, affect their therapeutic index [8, 9]. Thus, the DS can increase the bioavailability of drugs and decrease their toxic effects, leading to an increase in therapeutic index (Figure I-2). Additionally, they can vehicular and release the drugs in a target cell, thereby decreasing the dose required to observe certain action minimizing the side effects [10].

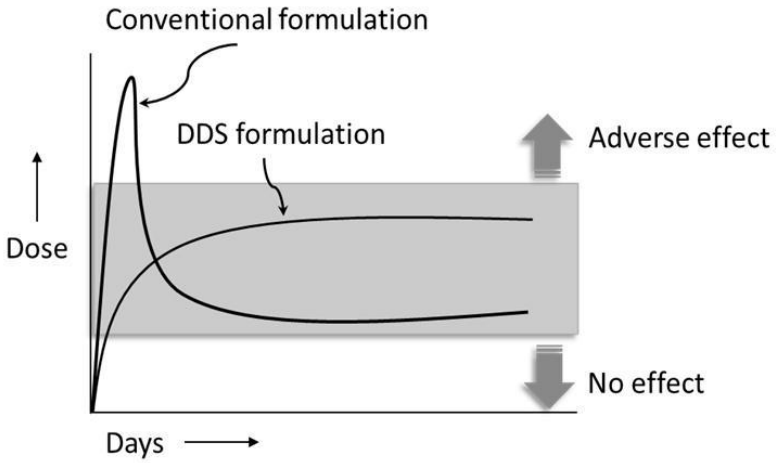

Figure I-2: Release profile of conventional formulation and drug delivery systems (DDS) over time (Adapted from Liechty *et al.* [11]).

The need of developing new DS at nano and microscaled materials is paralleled by attempts to optimize or develop new techniques to produce them. Therefore, numerous protocols exist for synthesizing nano and microparticles based on the type of drug used and the desired delivery route. Among a variety of approaches, the utilization of ultrasound for materials synthesis has been extensively studied, and now is positioned as one of the most powerful tools in nano and micro structured materials synthesis [12]. Once a protocol is chosen,

the parameters must be tailored to create the best possible characteristics for the developed particles.

In this review, the most successful ultrasound-assisted synthetic methods (sonochemistry) will be discussed to provide a fundamental understanding of their basic principles and to demonstrate the powerful and unique aspects of ultrasound in nano and micro structured materials synthesis. This review also focuses on the materials-based drug delivery platform, highlighting the use of phospholipids and proteins. Finally, it will be pointing out to areas requiring focused effort to arrive at an understanding of applications of these devices for textile-based wound dressings.

I-2. SONOCHEMISTRY

Chemistry deals with the interaction between energy and matter, and chemical reactions, require some form of energy (e.g. heat, light, radiation, electric potential, etc.) to proceed [12, 13]. In large part, the properties of a specific energy source determine the course of a chemical reaction.

Sonochemistry is the research area in which molecules can undergo a chemical reaction due to the application of powerful ultrasound radiation (20 kHz-10 MHz) [14]. Considering typical sound velocities in liquids of ≈ 1500 $m.s^{-1}$, acoustic wavelengths range from 10 to 10^{-4} cm, which is far above molecular and atomic dimensions [15]. Thus, no direct molecular level interaction between ultrasound and chemical species take place. Instead, acoustic cavitation, driven by high intensity ultrasound, accounts for the chemical effects of ultrasound [16].

Ultrasonic irradiation differs from traditional energy sources in duration, pressure and energy per molecule [17]. Cavitation occurs over a very wide range of frequencies, from tens of Hz to tens of MHz; above that frequency regime, the intrinsic viscosity of liquids prevents cavitation from occurring. Most high intensity ultrasonic horns operate at 20 or 40 kHz, most cleaning baths near 40 kHz, and there is specialized equipment available in the few hundred kHz to few MHz regime [14, 18].

In general, physical effects of ultrasound (e.g. emulsification and surface damage) are more dominant at lower frequencies, whereas cavitational heating of collapsing bubbles occurs over the full frequency range. Acoustic cavitation appears in the liquids at high and moderate intensities of ultrasonic irradiation. The minimum power intensity required for ultrasonic cavitation increases with the increase of the frequency of ultrasound [19]. When sonicating liquids at high intensities, the sound waves that propagate into the liquid media result in alternating high-pressure (compression) and low-pressure (rarefaction) cycles, with rates depending on the frequency. The liquid expands during the expansion by the sound field (‘‘negative pressure’’, low-pressure). This results in rapid growth of the weak sites of the liquid predominantly containing dissolved gases (‘‘cavitation nuclei’’) thus producing vapour - and gas-filled cavities or microbubbles [20]. Then, the liquid compresses during the compression phase of the sound field (‘‘positive pressure’’, high-pressure). The bubbles continue to grow during the negative/positive cycles of the ultrasound until reaching a critical diameter (Figure I-3), which depends on ultrasound frequency and nature of the liquid. This ‘‘critical’’ bubble is mostly filled with gases and vapour and thus unable to provide stiffness. The compression of bubbles occurring during cavitation is more rapid than thermal transport and generates localized hot-spots. The compression of bubbles during cavitation leads to the enormous concentration of energy within the small volume of the collapsed bubble. The oscillating bubbles can accumulate ultrasonic energy effectively while growing to a certain size (typically tens of mm) [21].

Under the right conditions, a bubble can overgrow and subsequently collapse, releasing the concentrated energy stored in the bubble within a very short time (with a heating and cooling rate of $>10^{10}$ $K.s^{-1}$). This cavitational implosion is very localized and transient with a temperature of ≈ 5000 K and a pressure of ≈ 1000 bar [22].

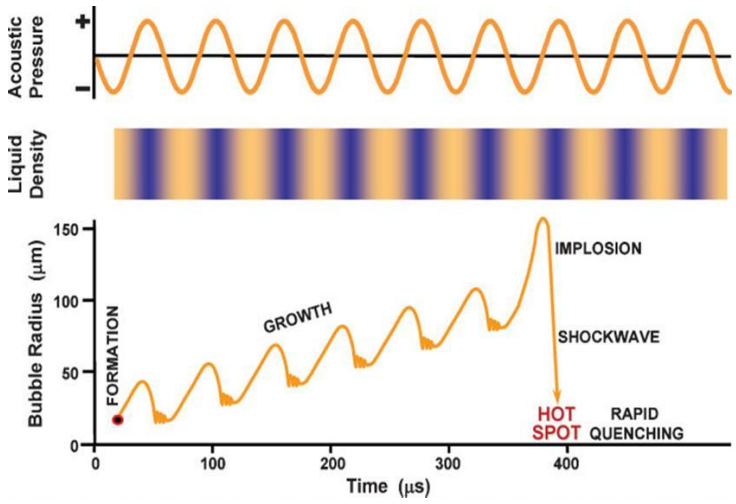

Figure I-3: **Schematic representation of transient acoustic cavitation (Adapted from Bang J. H. and Suslick K. S [23]).**

The chemical effects of ultrasound were explored for many years, specially in water [24-28]. Ultrasonic irradiation of aqueous liquids generates free radicals, and the formation of free radicals by sonolysis of water has been particularly well-studied. Primary sonolysis products in water are hydrogen radicals ($H^{\bullet}$) and hydroxyl radicals ($^{\bullet}OH$) [Equation I-1 (1)] [23]. These radicals can recombine to return to their original form or combine to produce hydrogen (H_2) and hydrogen peroxide (H_2O_2) [Equation I-1 (2) and (3)]. They can also produce hydroperoxyl radicals ($HO_2^{\bullet}$) by combination with oxygen (O_2). These strong oxidants as well as the reductants are used for various sonochemical reactions in aqueous solutions.

$$H_2O \rightarrow H^{\bullet} + {}^{\bullet}OH \quad (1)$$

$$H^{\bullet} + H^{\bullet} \rightarrow H_2 \quad (2)$$

$${}^{\bullet}OH + {}^{\bullet}OH \rightarrow H_2O_2 \quad (3)$$

Equation I-1: **Chemical reactions of sonolysis of water (Adapted from Bang J. H. and Suslick K.S. [23]).**

I-2.1. Sonoproduction of nano and microstructured materials

The ultrasonic irradiation, compared to traditional energy sources, provides rather unusual reaction conditions (a short duration of extremely high temperatures and pressures in liquids) that cannot be realized by other methods

[20]. Major developments in nanotechnology have been achieved, by sonochemistry methodology, synthesising different nano and microstructured materials. A diverse set of applications of ultrasound have been explored to obtain such different materials.

Table I-1 summarizes the most frequently used materials for the synthesis of nano and microstructures by sonochemical method.

Table I-1: Overview of the materials used to achieve different nano and microstructure by sonoproduction. (Information compiled, in the scope of this review, from references [17, 29-89])

Material	Type	Reference
Phospholipids	Liposomes (small unilamellar vesicles and large unilamellar vesicles) and solid lipid nanoparticles	[29-43]
Polymers (proteins, chitosan, polyglutamate/polyethyleimine/polyacrylic acid, polyvinyl alcohol, polyallylamine hydrochloride/polystyrene sulfonate, gum acacia and starch)	Nano and microparticles	[44-76]
Inorganic compounds (metals, metals oxides, carbons and metals chalcogenides and carbides	Nanoparticles nanotubes, nanobelts, nanorods, nanowires, nanocubes, mesoporous and amorphous nanostructured	[17, 77-89]

Among all the materials used, this review details the latest development of liposomes and protein nano and microparticles DS and their potential applications.

I-3. LIPOSOMES

Liposomes are highly versatile structures for research therapeutic and analytical applications [90].

Since Bangham *et al.* [91] described for the first time the preparation of liposomes. They have been often used as membrane model systems to reveal the basic nature of cell membranes. In 1971, Gregory Gregoriadis [92] proposed for the first time, the use of liposomes as drug carrier system, describing the conditions for the entrapment of *Aspergillus niger* amyloglucosidase (EC 3.2.1.3) and ^{131}I-labelled albumin into liposomes composed of phosphatidylcholine, cholesterol and dicetyl phosphate.

The unique physico-chemical properties of liposomes coupled with a structural versatility, explain the great potential of these resources organized as membrane models and vectors of drugs, which translate into huge numbers of studies achieved with these systems [93].

According to the parameters previously described it is important to state the essential physico-chemical characteristics along with their classification. Furthermore, an overview of liposomes preparation using the sonochemical methodology will be highlighted as well as their applications as DS.

I-3.1. Physico-chemical considerations

Phospholipids are the major structural components of biological membranes. They are amphiphatic molecules in which a glycerol bridge links a pair of hydrophobic chains and an hydrophilic polar head group, phosphocholine [32]. The hydrophobic part consists of two hydrocarbon chains of saturated or unsaturated fatty acids, which esterify the same number of hydroxyl groups of glycerol, and each chain can present ten to twenty-eight carbon atoms [94].

Amphipathic lipids have the ability to spontaneously form bilayer aggregates when dispersed in an aqueous solution, involving within a certain volume of solvent. These structures may consist of one or several concentric membranes,

varying in size from 20 nm to a few micrometres in diameter, with a membrane thickness approximately equal to 4 nm [32].

Phospholipids are abundant in nature and certainly the most used in the preparation of liposomes are those containing choline [34]. These are called lecithin or phosphatidylcholine (of the "lekithos, " a Greek word meaning egg yolk) and are dipolar molecules at physiological pH, with the quaternary ammonium group presenting a positive charge and a negative charge in the phosphate group (Figure I-4). Each class of a type of phospholipid, for example phosphatidylcholine, comprises a wide variety of molecules, as regarding the type of fatty acids linked to the glycerol skeleton. Fatty acid part of phospholipids molecule is important, and differences in fatty acid part can change the characteristics of the phospholipids. Fatty acids can differ in the number of carbon atoms chain and degree of unsaturation [95].

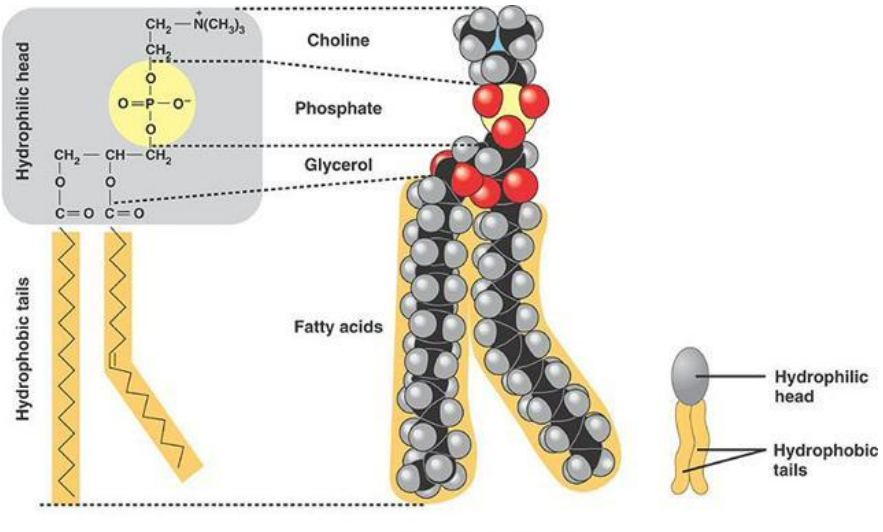

Figure I-4: General chemical structure of phosphatidylcholine (Adapted from Keller A. [96]).

Lecithin from natural sources, as extracted from egg yolk or soybean, is a mixture of several molecules with carbonaceous chains of different lengths and different degrees of saturation. The most abundant fatty acid in lecithin from egg yolk is palmitic acid (35.3%), followed by oleic acid [32]. However, lecithin can also be obtained by synthesis, presenting a well-defined composition, particularly with respect to acyl chains, which can be obtained from saturated or unsaturated hydrocarbon chains, with greater or lesser number of carbon atoms, equal or

different. This type of phospholipids, such as dipalmitoylphosphatidylcholine (DPPC) (Figure I-5) or dimyristoylphosphatidylcholine (DMPC), can be easily characterized for various thermodynamic parameters, compared to the heterogeneous populations that are in the natural phospholipids [34].

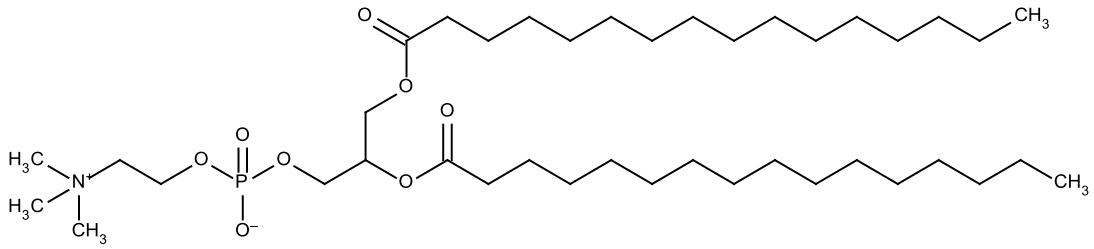

Figure I-5: Chemical structure of DPPC.

Lecithin, as just referred, is the major component of natural membranes, being widely used in the preparation of liposomes for variety applications. Besides phospholipids, the liposomes can also include other molecules, also present in natural membranes, such as cholesterol [97]. Cholesterol improves the fluidity of the membrane bilayer, reduces the permeability of water soluble molecules through the membrane, and improves the stability of bilayer membrane in the presence of biological fluids, such as blood/plasma [98].

One of the main physical characteristics of lipid bilayers is the existence of a certain temperature where the organization of phospholipids suffers a change. Thus, for different values of temperature, lipid bilayers can present itself in two distinct thermodynamically phases, occurring transition from one phase to another by varying the temperature [32]. Therefore, the lipid bilayers can be presented in a phase of great order, designated by solid-gel state, and for higher temperatures, a more fluid phase called liquid-crystal [32, 34], as shown schematically in Figure I-6.

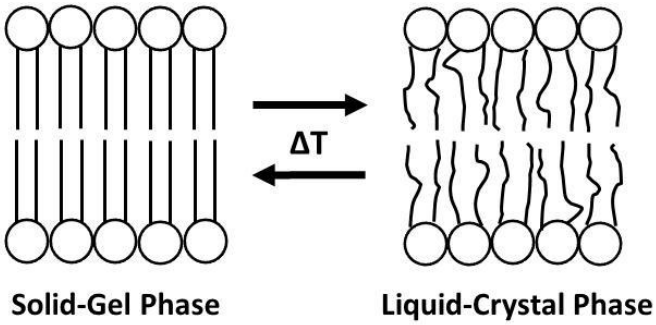

Figure I-6: **Schematic representation of the organizational structure presented by the hydrocarbon chains of phospholipids in the gel-solid state and liquid-crystal. ΔT corresponds to the variation of temperature.**

The temperature of transition from one stage to another is called temperature of phase transition (T_c) and is specific to a particular lipid. Thus, when the temperature of the system is lower than T_c of the phospholipid components of a given bilayer, this presents an ordered structure where the hydrocarbon chains are in an extended conformation and tight packaged, and the freedom of movement is severely restricted. Above T_c, increases the mobility of the acyclic chains in the membrane, the area occupied by each phospholipid molecule is higher and the bilayer thickness decreases [32, 34].

The influence of hydrocarbon chain length and unsaturation (as well as head group) on the value of T_c for a membrane composed of different phospholipids is considerable. In general, increasing the chain length or the saturation of the chains, increases the transition temperature. For a homogeneous composition of membranes is possible to state a value of the phase transition temperature. However, for mixtures of phospholipids, T_c comprises a range of temperatures. The width of this interval depends strongly on the lipid composition and can cover more than 10 ºC or even be absent in certain mixtures of lipids, for example, in the presence of high concentrations of cholesterol (50%). The T_c described for DMPC is 23.5 ºC and for DPPC is 41.4 ºC, while the egg yolk phosphatidylcholine (EPC), an heterogeneous mixture, has a transition temperature of -15 to -7 ºC [32, 34].

An understanding of phase transitions and fluidity of phospholipids membranes is important both in the manufacture and exploitation of liposomes, since the phase behaviour of a liposome membrane determines such properties

as permeability, fusion, aggregation, protein biding, all of which can markedly affect the stability of liposomes and their behaviour in biological systems [32, 99].

Another important feature inherent to the membrane structure is its permeability, which is highly dependent on the dynamics and thermodynamics of membrane phase [34]. The degree of diffusion of molecules and ions through the bilayer varies considerably. The bilayers are sufficiently permeable to hydrophobic molecules but may constitute a barrier to hydrophilic molecules. Thus, compounds that are more hydrophilic can pass through the membrane, but more slowly, or else through typical channels in the membrane. The water and ions such as calcium ions, potassium, sodium and chlorine, for example, pass through the membrane channels (proteins), which control the entry and exit of these compounds in the cell [32].

I-3.2. Classification of liposomes

Apart from their chemical constituents, liposomes can be characterized based on their number of lipid bilayers (lamellae) and size. Thus, without any further processing, the dispersion of phospholipids in water leads to a polydisperse population known as multilamellar vesicles (MLVs), whose sizes are usually ranging from 0.4 and 3.5 µm of diameter [32]. Each vesicle consists of multiple lipid bilayers (around five or more) concentrically arranged, between which there is a fraction of internal aqueous medium. The MLVs were used in early studies being the vesicles with the most immediate preparation. The liposomes formed by a single bilayer are called large unilamellar vesicles (LUVs) if its size exceeds 50 nm, according to some authors [94], or 100 nm according to others [98]. The small unilamellar vesicles (SUVs) are characterized by approximate diameters from 25 to 50 nm and unilamellar vesicles of intermediate size [intermediate sized unilamellar vesicles (IUVs)] for intermediate sizes [32]. In addition to these unilamellar vesicles, it should be also considered the giant unilamellar vesicles (GUVs), larger than 1 µm and can reach the tens of µm size, comparable to size of a eukaryotic cell (10 to 100 µm in diameter [32]). Figure I-7 represents the types of liposomes described.

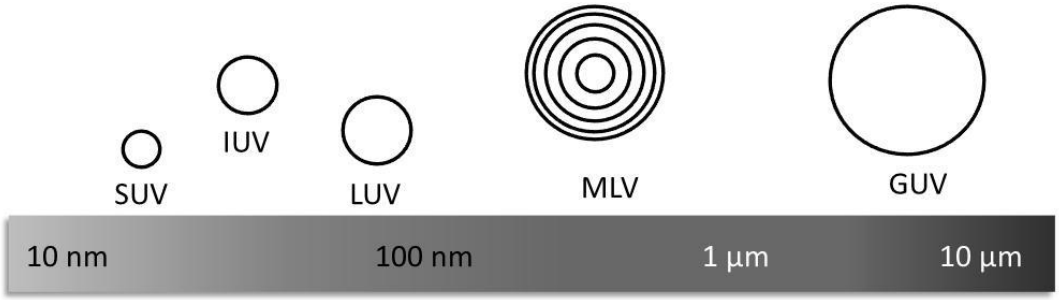

Figure I-7: **Schematic representation of the different types of liposomes classified according to the size and number of lipid bilayers. Each line represents a lipid bilayer.**

According to the aim of study it should be selected the more suitable type of liposomes, usually MLVs, LUVs or SUVs. For example, in the study of structural, dynamic and thermodynamic properties of membranes in which the sensitivity can often be a problem, normally it is preferred the MLVs, due to its higher lipid concentration. On the other hand, unilamellar structures are chosen, particularly the LUVs, in studies of membrane permeability and the roles of proteins. SUVs, due to the high curvature, present anomalies in the packaging of lipids that make them susceptible to degradation in the presence of biological molecules [100]. Additionally, LUVs have a volume fraction for encapsulation much larger than SUVs for the same lipid concentration [5].

When they are applied as vehicles, multilamellar structures are usually preferred in the case of hydrophobic molecules to be encapsulated, while LUVs are more appropriate for the hydrophilic molecules, since they have a large volume/surface. Conversely, the MLVs provide a more sustained drug release than LUVs, as their membranes are being gradually degraded at the site of action. However, if it is desirable rapid delivery of the drugs, the LUVs are the most suitable ones [101]. For the surface studies there is a need of large surface/volume ratio and the obviously preferred choice are SUVs, while GUVs are too fragile for most applications. Although, these vesicles are very useful for studies of basic features, such as elasticity, permeability and tensile strength of bilayers, in which the optical microscope is the main method used [5].

I-3.3. Preparation of liposomes

The widespread use of liposomes for various purposes has created the need to develop preparation methods, which should be efficient, reproducible, and with the greatest simplicity. The methods of preparation of liposomes, currently available, are diverse and may have numerous variants. The classic preparation of liposomes, initiated by Alec Bangham in 1965, and used nowadays, is entitled by thin film hydration method [102]. This preparation process may undergo some changes, particularly regarding the organic solvent used, the possible addition of glass beads, from the drying of lipid and parameters agitation, such as time, intensity, mode of agitation and temperature [34]. However, this method always leads to the formation of MLVs very heterogeneous with regard to size, shape and number of lipid bilayers, and a small percentage of LUVs and SUVs [103]. Therefore, it is necessary to submit MLVs to further processes, when vesicles with specific sizes are needed. These processes include mechanical, chemical or electrostatic methods that allow obtaining unilamellar liposomes. There are also methods that use already preformed vesicles, SUVs to form mainly LUVs, small MLVs and GUVs. These methods are based primarily on melting, freezing and thawing or dehydration/rehydration of liposomes. However, the most frequently used methods are mechanical, and the most widespread of these are the sonication and extrusion, although, the homogenization and French press can also be applied [29, 32, 34].

Sonication is one of the most popular methods to prepare liposomes from the aqueous dispersion of phospholipids, which has been used from the beginning of the study of liposomes [29]. Since that several studies have been performed with ultrasound in order to obtain unilamellar vesicles with defined sizes.

Finer and co-workers [30] found that the collisions produced by ultrasound led to complete disruption of the multilamellar particles, with the formation of short-lived bilayer fragments or other forms of small lecithin aggregates. These fragments then re-aggregate to form single-shelled vesicles of roughly uniform size.

Woodbury and co-workers performed a study where the main goal was to obtain a detailed characterization of the various lipid suspensions produced by using different sonication times [36]. They had shown that mildly sonicated

liposomes generally have a bimodal distribution and are not well described by single mean.

The studies of treatment time of ultrasound have been also performed by Maulucci *et al.* [35]. The results indicate that the lipid film, upon sonication, forms LUVs, which then progressively reduce their size when increasing the sonication time. At shorter sonication time, the total energy transferred by sonication was not sufficient to reduce MLVs and if the treatment is too long, the vesicles are damaged by the generated free radicals. Therefore, an optimal sonication time must be determined for the specific use of the vesicles.

The size changes of liposomes as well as the polydispersity and lamellarity of the systems as a function of the ultrasound power applied, were also studied [37]. They concluded that the increase of ultrasound power decreases the number of lamellae, the vesicle size and the polydispersity, obtaining a homogeneous distribution of lipid vesicles.

Later, the effect of sonication and freezing-thawing on the aggregate size and dynamic surface tension of aqueous DPPC dispersions was studied [38]. When DPPC dispersions were prepared using extensive sonication, they form vesicles that were quite clear, transparent, and stable for at least 30 days. The average dispersed vesicles diameter was 80 nm in water and 90 nm in standard phosphate saline buffer. After a freeze-thaw cycle, this dispersion became turbid, and precipitates of coagulated vesicles were observed with large particles of average size of 1.5×10^3 nm. The vesicle coagulation is due to the local salt concentration increase during the freezing of water. This dispersion had shown much higher equilibrium and dynamic surface tension than those before freezing. When this freeze-thawed dispersion was subjected to a resonication at 55 ºC, smaller vesicles with sizes of 70 nm were produced, and a lower surface tension behaviour was restored as before freezing [38].

Recently, Richardson and co-workers [39] explore also the role of cavitation in manipulating liposome size. They hypothesize that ultrasonic cavitation phenomena play a key role in altering the size distribution of liposomes processed in an ultrasonic bath. They manipulate the size of liposomes by correlating changes in liposome size with cavitation emissions at various acoustic

intensities and static pressures. Richardson and co-workers proved that the microstreaming around oscillating bubbles, and not necessarily collapse cavitation events, create shear sufficient to reduce the size of the liposomes during ultrasonic processing.

Besides various powers, it was also study the influence of different ranges of frequencies (43-480 kHz) to obtain liposomes prepared with L-α-dilauroylphosphatidylcholine. It was observed a faster reduction of the mean size of liposome when a lower frequency was used [40]. The effect of frequency on the size reduction of liposome can be related to the strength of cavitation caused by the difference in the bubble dynamics. The amplitude of the oscillation of a cavitation bubble is larger at lower frequency because the bubble experiences longer time of negative pressure to glow larger [104]. The impulsive shock wave and the microjet stream created by a bubble are thus stronger at the lower frequency and consequently a size reduction of liposome was faster.

More recent studies performed by Silva *et al.* [41, 42] reported the importance of the different parameters of sonication, such as power delivery, time, distance from ultrasound tip to base of reactor, when a transducer of 20 kHz is used to obtain LUVs. The data obtained reveals the importance of LUVs preparation in the nodal (lower production of $^{\bullet}OH$) and anti-nodal (higher production of $^{\bullet}OH$) horn position of ultrasound sources.

Another approach based on the parameters previously mentioned [41, 42] was used to obtain the reduction of liposome sizes prepared with internal wool lipids (IWLs) [43].

I-3.4. Stability of liposomes

Over time, the liposomes can undergo several types of changes, including physical and chemical modifications [91]. However, if prepared and stored under very specific conditions, the occurrence of these changes can be minimized. A stability study program must include the product characterization.

Average size distribution of liposomes determined at the time of their preparation can change upon their storage. Liposomes tend to fuse and grow into

bigger vesicles, which is a thermodynamically more favourable state. Since this phenomenon may occur mainly at the T_c, it is advisable to store the suspensions of liposomes at a temperature different from that. Additionally, it can be advantageous to include a sufficient proportion of cholesterol into the membrane to reduce or eliminate the phase transition, particularly if it occurs in a temperature range near which the liposomes are stored or handled. The macroscopic aspect, average size and size distribution are important parameter to evaluate and can be obtained by examination of the suspension or by using the photon correlation spectroscopy (PCS) and/or electron microscopy [32, 34, 42, 98].

Chemically, phospholipids are susceptible to oxidation and hydrolysis reactions. Although, the most susceptible to degradation are lipids containing double bonds, since the unsaturation permits delocalization of the remaining unpaired electron along the lipid chain, and lower the energy of this state (and hence increase the probability of its being formed). The polyunsaturated fats are thus particularly susceptible to oxidative degradation [32, 34]. The oxidative degradation of the lipids in general can be minimized by protecting the lipid preparations from light, by adding antioxidants or by producing the product under nitrogen or argon environment [34, 98, 105, 106]. The hydrolysis of phospholipids leads to the formation of lysophospholipids and free fatty acids [107-109]. The presence of lysophospholipids enhances the permeability of liposomes and thus it is essential to keep its level to a minimum in a given preparation [109]. Hydrolysis is strongly affected by temperature and pH. In fact, this degenerative chemical process can occur to a lesser extent at low temperatures and pH values close to neutrality [32]. On the other hand, the use of lipids that contain ether linkages instead of ester, such as those found in the membranes of halophilic bacteria, completely avoids the hydrolysis reactions [32, 110, 111].

Oxidation and hydrolysis of phospholipid can be also promoted by free-radicals formed in the cavitation bubbles during the preparation of the sonicated phospholipid suspension [33]. Although, according to Kruus *et al.* [112], the formation of free radicals is not a major problem when low frequencies (≈ 20 kHz) and short sonication times (≈ 20 min) are used. Rabinovich-Guilatt *et al.* [113] proved that the use of a temperature of 50 ºC over 24 h induces only 1.6% of phosphocholine hydrolysis.

Other factors to be taken into consideration prior to starting a stability study are the formulation factors and environmental conditions, which may influence the stability of liposomes. Influence of formulation factors such as pH, buffer species, ionic strength, and solvent system play a major role in stabilizing a liposome formulation [98].

I-3.5. Liposomes as delivery systems

The ability of liposomes to dissolve, protect and drive water-soluble or fat soluble drugs, as well as its biocompatibility with cell membranes and the possibility of adding certain ligands to their surface achieving a particular cell type, were the main reasons for their implementation systems as carriers of drugs in cosmetic, pharmacology and medicine [34, 93, 114, 115]. One of the main advantages of using liposomes as carriers is the easy drug incorporation, independently of their charge or molecular weight, and the accommodation of substances with very different polarity characteristics on the same system [115, 116] (Figure I-8).

Figure I-8: **Possible locations of water-soluble drugs or other compounds without (1) or with electrostatic or ionic bonds (2), hydrophilic (3) or amphipathic (4) drugs in the phospholipid membrane (Adapted from Lasic D. D. [34]).**

As a pharmaceutical formulation, the main advantages conferred by liposome encapsulation of drugs are increased solubility of lipid soluble drugs and the protection granted by these systems to hydrolysis of the drugs, caused for example by the action of degenerative enzymes, adverse pH and action of light [34].

The application of liposomes *in vivo* is limited by its retention at the level of the reticuloendothelial system (RES). In fact, liposomes in the bloodstream are quickly captured by the macrophages, as well as the liver, spleen, lymph nodes, lungs and bone marrow, which have the function of processing the foreign agents that enter in the body [117]. Thus, the half-life in plasma of liposomes can be reduced to few minutes. The problems led to the development of liposomes, with the inclusion of certain molecules in their outer layer, with new transport options in order to prevent their elimination by the RES. Indeed, the physical characteristics and composition of liposomes affects their capture by the RES, such as the size and fluidity. Therefore, larger liposomes are captured more quickly, as well as the more rigid liposomes due, to its constitution [118]. One way to going through this problem is coating liposomal vesicles with a hydrophilic polymer, such as polyethylene glycol (PEG), which reduces uptake by the RES [119-121]. As a result, coated liposomes remain in circulation longer than conventional liposomes. Additionally, incorporating targeting ligands on the surface of the liposomes, it is possible to direct them to certain organs. For example, an association with folic acid or antibodies, which are specific to particular cell [117, 122-126]. The modified liposomes are generically called stealth liposomes and may increase 100 times the half-life [121, 127].

I-4. POLYMERIC PARTICLES

It has recently become a trend to develop new and suitable biomaterials, due to their bioavailability, biocompatibility and biodegradability coupled with low toxicity being the usefulness of polymers in drug delivery systems (DDS) well established. Continued improvement and accelerating research and development in polymeric materials has played a vital role in the progress of most controlled-release technologies. In the past 25 years, there has been a considerable increase in interest in this technology, as is shown by the increasing number of publications and patents in the area of controlled drug-release systems using synthetic, as well as naturally occurring polymeric materials [128].

The furthermost nano and microparticle formulations are effectively based on nano and micrometric-scaled emulsions. Therefore, the study of particle

formulation has to include the knowledge of emulsion formation phenomena. Nano and microemulsion generation is very commonly performed with such high-energy emulsification methods, particularly exploited in polymeric materials [129, 130]. The formation of such nano and micrometric scaled particles is governed by directly controllable formulation parameters, such as the quantity of energy and nature of the components. Two main groups of devices are used in the literature: the rotor/stator devices, which appear in the first articles of nano and microparticles, and high-efficiency devices, including high-pressure homogenizers and ultrasound generators [131].

Polymer-based nano and microparticles templates have been widely developed. Especially in the area of engineered nano and microparticles of polymer origin there is a vast area of possibilities for the chemical composition. They can be divided into two broad classes: protein-based and non-protein-based nano and microparticles platforms. Non-protein-based templates include PEG, poly(amidoamine) (PAMAM), dextran, chitosan, etc. [132].

I-4.1. Protein-based nano and microparticles

Among of polymers systems, those based on proteins are very promising ones. Proteins are a class of natural molecules that have unique functionalities and potential applications in both biological as well as material fields [133]. Nano and microstructures derived from proteins, especially protein particles, are biodegradable, non-antigenic, metabolizable and can also be easily amenable for surface modification and covalent attachment of drugs and ligands [134, 135].

To develop protein-based templates, there are several criteria to be followed: first, the novel matrix should be easy to obtain with relatively low cost; second, the new template has to maintain the cells' viability and not cause any immunogenic reactions; third, the protein-based platform should be stable and keep its chemical and mechanical properties once it has been delivered *in vitro* or *in vivo*; fourth, the drug molecules should also be stable in this new material; and fifth, the biodegradable rate of this new novel platform should be slower than that of the drug molecule release rate [136].

A variety of proteins have been used and characterized for drug delivery, such as albumin [137-139], silk fibroin (SF) [140, 141], casein [142, 143], collagen [144, 145], and gelatin [146-148].

The serum albumin protein has been one of the most extensively studied and applied in the preparation of nano and microparticles, because of its availability, relative low cost, stability and unusual ligand-binding properties. For this reason, its main characteristics will be pointed in this review.

Albumin is a globular protein, which is emerging as a versatile protein carrier for drug targeting and for improving the pharmacokinetic profile of bioactive compounds. This is the most abundant plasma protein (35-50 $g.L^{-1}$ human serum) with a molecular weight of 66.5 kDa [149].

Like most of the plasma proteins, albumin is synthesized in the liver and is responsible for the transport of fatty acids and others lipids that would otherwise be insoluble in the circulating plasma [150].

The three-dimensional (3-D) structure of human serum albumin (HSA) has been elucidated by X-ray structure analysis [151, 152]. The approximate 3-D shape of HSA can be described as an ellipsoid consisting of three flexible spheres in a row (domains I, II, III) and is illustrated schematically in Figure I-9.

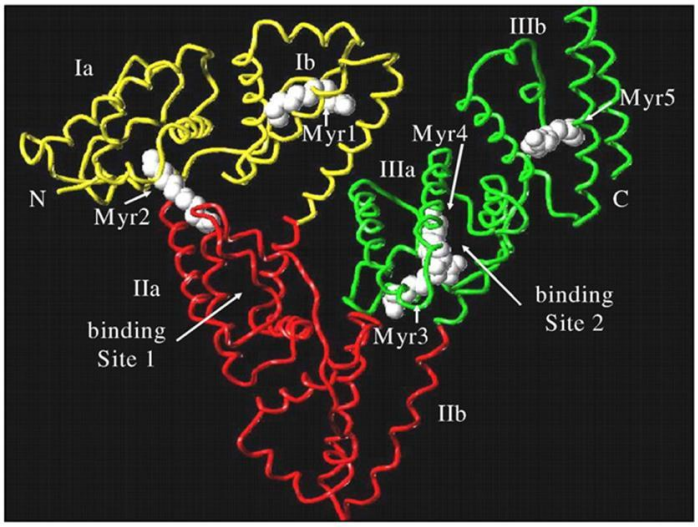

Figure I-9 : X-ray structure of HSA (Adapted from Carter D. C. [152]).

HSA is one of the smallest proteins present in blood plasma. Both size and abundance explain the fact that so many metabolic compounds and therapeutic

drugs are transported by this protein. The binding sites for metabolic substrates and diagnostic, as well as, therapeutic drugs have been extensively studied and reviewed [153, 154]. These properties, as well as its preferential uptake in tumor and inflamed tissue, its ready availability, its biodegradability and its lack of toxicity and immunogenicity make it an excellent candidate for drug delivery [103].

The bovine serum albumin (BSA) is also a very used protein in the preparation of microparticles, due to the lower cost when compared with the HSA. The primary structures of HSA and BSA are homologous by 80% [155].

Albumins are characterized by a low content of Tryptophan, Glycine and Methionine and a high content of Cysteine (seventeen disulphide bonds and one sulfhydryl group) and the charged amino acids (a.a.), Aspartic and Glutamic acids, Lysine and Arginine. The difference between the two proteins is that, in HSA, some hydrophobic a.a. are replaced by other hydrophobic residues, e.g. BSA holds two Tryptophan's a.a. in its structure and HSA has only one [150, 155].

I-4.2. Preparation of protein-based nano and microparticles

In the later of 1960s, Rhodes and co-workers were the first investigators to produce microspheres from natural macromolecules for medical applications [156]. By slightly modifying the method proposed by Zolle [157], they succeed in producing HSA particles with a size bellow one micrometre [157]. The particles were formed by heat denaturation of a water-in-oil emulsion of albumin. However, the heat denaturation can be harmful for the entrapped drugs or bioactive molecules. To solve this problem, the heat denaturation was replaced by the chemical cross-linking agents, such as glutaraldehyde. Nevertheless, this method yields microspheres with a short storage life, low stability and high toxicity. These issues motivate new methods of microparticle manufacture in order to: improve protein stability, allow the further sterilization and eliminate the addition of cross-linking agents.

Suslick and co-workers pioneered sonochemical synthesis of protein microspheres, where simple sonication of a protein solution produces microcapsules filled with air or a non-aqueous liquid [44]. They were made of

BSA and were filled with *n*-dodecane, *n*-decane, *n*-hexane, cyclohexane or toluene. The synthesis was conducted under high intensity ultrasonic probe upon sonicating the precursor solution under air or O_2. The average diameter of the protein microspheres was 2.5 µm with a narrow size distribution. Ultrasonic irradiation of HSA generates similar microspheres to those of the BSA and the same was obtained for the protein microspheres of hemoglobin (Hb) [48].

In-depth mechanistic studies revealed that mechanism of proteinaceous microspheres preparation is a direct result of the chemical effects of ultrasound irradiation on an aqueous medium. Indeed, the microspheres formation is a combination of two acoustic phenomena: emulsification and cavitation. Ultrasonic emulsification is a well-known process and does occur in this biphasic system. Emulsification is necessary for microspheres formation. Nevertheless, in vortex mixing, emulsification occurs but microspheres are not formed. Consequently, emulsification by itself is not sufficient for microspheres formation.

Ultrasonic emulsification creates the microscopic dispersion of the protein solution necessary to form the shape of the proteinaceous microsphere shell. However, ultrasonic irradiation of liquids produces acoustic cavitation: the formation, growth and implosive collapse of bubbles. The collapse of such bubbles creates transient hot-spots with enormous peak temperatures and production of free radicals. Aqueous sonochemistry caused by the implosive collapse of bubbles produces $^{\bullet}OH$ and $H^{\bullet}$ radicals, and in the presence of O_2, superoxide ($O_2^{\bullet-}$) and $HO_2^{\bullet}$ radicals. $^{\bullet}OH$, $O_2^{\bullet-}$, and $HO_2^{\bullet}$ radicals are all potential protein cross-linking agents. Using various trapping agents, they concluded that the important oxidant involved in microsphere formation is superoxide [46, 47]. They proposed that the Cysteine, which is present in BSA, HSA, and Hb, is oxidized by the $O_2^{\bullet-}$. The microspheres are then held together by protein cross-linking through disulphide bounds from Cysteine oxidation (Figure I-10).

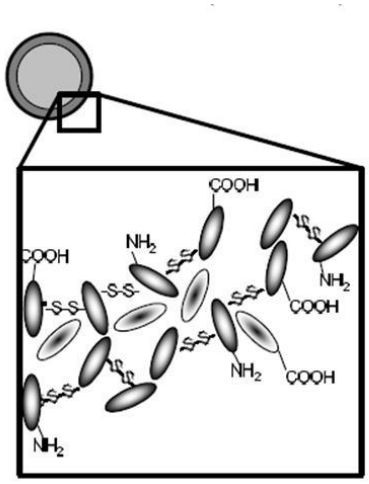

Figure I-10: Disulphide cross-linking holds the protein microspheres together (Adapted by Suslick K.S. [17]).

In a later publication, Suslick and Grinstaff reported on the preparation of aqueous suspensions of air-filled proteinaceous microbubbles [45]. The synthesis involves the ultrasonic irradiation of aqueous protein solutions in the presence of O_2. Yields and size distribution of HSA and BSA microbubbles were determined as a function of various experimental parameters. The ultrasound irradiation was conducted during three minutes [45]. This irradiation time is typical for the optimal formation of the protein microspheres. It is worth mentioning that the difference in the formation of the liquid- and air-filled bubbles is in the position of the sonicator. In a typical synthesis of liquid-filled protein microspheres, the organic liquid is layered over a 5% w/v protein solution and the horn is positioned at the water/organic interface. For air-filled microbubbles, the horn is placed at the water/air interface.

Another approach has been developed about the mechanism of microspheres formation with ultrasound systems [51]. To probe whether the sonochemical microsphere formation process is more general and can be applied to proteins that do not contain Cysteine residues, an attempt was made employing this method to streptavidin. Streptavidin is a protein, which has no sulphur residues [51]. They had extended the sonochemical method to this non-sulphur containing protein and demonstrated the formation of protein microspheres. Nevertheless, no microspheres were obtained when the pH was kept at 7. However, when the pH was lowered to 6.0, by adding a concentrated acidic solution, microspheres were formed. According to the proposed

explanation, hydrophobic or thermal denaturation of the protein after the initial ultrasonic emulsification assists in microsphere formation. A contribution is provided by the lowering of the pH, which helps to neutralize the basic COO^- edges, thus creating a more favourable hydrophobic environment. To verify whether this hypothesis is correct, a poly(Glutamic acid) protein was sonicated [51]. This protein carries only carboxyl groups on the side chain. Microspheres of the poly(Glutamic acid) were formed only at a pH lower than 4.5. Thus, the authors concluded that hydrophobic interactions, which become more dominant in an acidic medium, are responsible for the production of the microspheres in a poly(Glutamic acid), as well as in streptavidin.

In addition, sodium polyglutamate (SPG) microspheres have also been reported that are stabilized by hydrogen bonding networks instead of covalent cross-linking [58]. More specifically, the dominant interaction between the polymer chains are a network of hydrogen bonds or ion pairs: $[RCO_2^-\cdots M^+\cdots O_2CR]$ in which $M^+ = H^+$ or Na^+ [58].

Gedanken and co-workers [67] have synthesized microspheres made of a few different proteins. The three proteins used were BSA, green fluorescent protein (GFP) and cyan fluorescent protein - glucose binding protein - yellow fluorescent fused protein (CFP-GBP-YFP). The two synthesized microspheres made of mixed proteins are BSA-GFP and BSA-(CFP-GBP-YFP). The authors characterized the three possible arrangements from the assembly of two different kinds of proteins in microsphere structures. First, the two combined proteins form the microspheres walls. Second, the first protein forms the microspheres walls and the second one is encapsulated inside the liquid-filled proteinaceous microsphere bubble. Third, each kind of protein forms one-protein microspheres [67].

Recently, Silva *et al.* [72] highlighted the insights on the mechanism of protein microspheres formation using two different proteins, namely BSA and SF from *Bombyx mori*. As it was previously referred, BSA is a globular protein. In contrast, SF is a fibrous protein and is mainly composed of hydrophobic a.a. without Cysteine residues in its structure. The SF from *Bombyx mori* is an insoluble protein and its primary structure has been determined to be composed dominantly of a six a.a. residue motif, i.e., -Gly-Ala-Gly-Ala-Gly-Ser- (Figure I-11) [158-160].

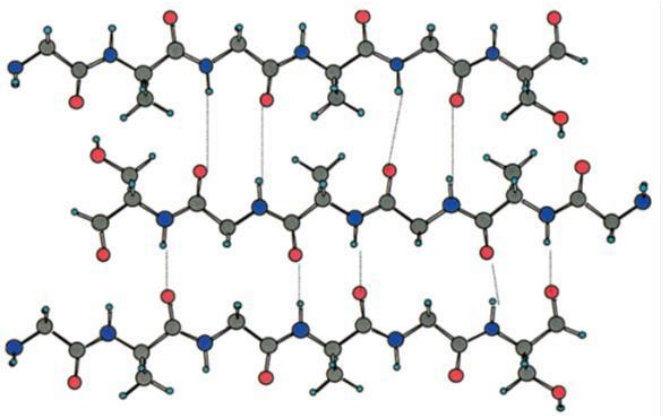

Figure I-11: Three-chain layer of a polypeptide GAGAGS model (Adapted from Zhou *et al.* [161]).

The authors report the influence of different ratios of aqueous/organic phase and protein concentration on microspheres production using BSA and SF. An increase on protein concentration promotes ≈ 100% of yield on particles formation, independently of aqueous/organic ratio used. It was proved that the use of lower organic fraction leads to smaller sizes particles. It was also found that these parameters demonstrate to be an important tool to control the sizes of particles, ranging from 300 to 1500 nm. The conformation assessment obtained with Fourier transform infrared (FT-IR) analysis demonstrated a change on the secondary structure of SF upon sonication treatment, presenting an increase on the amount of β-sheet. Conversely, the sonochemical treatment did not affect the secondary structure of the globular protein, BSA.

Based on these different sonochemical approaches to synthesize protein microspheres, a multitude of parameters should be controlled as well as the physico-chemical protein characteristics, to precise the main mechanism of protein microspheres formation for each protein in particular.

Cavaco-Paulo and co-workers [73] further extended the sonochemical method to new engineering peptides, with a range of sizes and sequences, to highlight the mechanism of proteinaceous microspheres formation. It was reported the importance of some a.a. residues and their arrangement in peptide construction in respect to obtain microspheres with adjustable properties to cover a wide range of applications. The authors proved that the larger peptides with separated and clear hydrophobic and hydrophilic areas lead to small and more stable spheres.

I-4.3. Biological activity of protein-based nano and microparticles

A related effort by Suslick and Wong was the biological activity of microspheres formed with Hb [48]. The microspheres of Hb were filled with air and are described as having many of the ideal characteristics needed for use as blood substitute. The results of the oxygen binding have shown that Hb microspheres can bind and release oxygen at the same oxygen pressures as native Hb. The authors have calculated the oxygen-carrying capacity of the Hb microbubbles and found that for O_2 filled microbubbles it is greater by 50% than whole blood (0.32 mL O_2 per mL microbubble *versus* 0.2 mL O_2 per mL blood) [48].

Later, Avivi and Gedanken performed two other investigations probing the biological activity of proteinaceous microspheres [55, 60]. In the first, it was found that unlike a denaturation process, where the biological activity of the protein is destroyed, the sonochemical process leading to the microspherization of a protein reduces its biological activity but does not destroy it. Avidin microspheres are still active after the sonochemical process. Thus, it was verified that avidin microspheres have ability to bind biotin, but to a lesser degree than the native protein [55]. In a second study related also to the biological activity of proteinaceous microspheres, Avivi [60] formed microspheres of α-amylase (1,4-α-D-glucanohydrolase, endoamylase), a protein known to hydrolyse starch, glycogen, and related polysaccharides by randomly cleaving the internal α-1,4-glucosidic linkages. Microspheres of α-amylase were compared for their catalytic activity with those of the native protein. They concluded one more time that the sonochemical method does not destroy the enzymatic activity of the microspheres. In this research, it was demonstrated that the sonication leading to the modification into microspheres of two enzymes, α-amylase and α-chymotrypsin, is not a denaturation process. The protein microspheres are catalytically active, but their reactivity is reduced as compared to the native protein.

More recently, it was developed a new methodology to recover the biological function of protein [74]. The refolding of ribonuclease A (RNase A) microspheres, assisted by protein disulphide isomerase, is highlighted in this study. The ultrasound application was shown to induce a loss of 35% of RNase A enzymatic

activity when compared to the native RNase A, and protein disulphide isomerase was able to restore it [74]. Moreover, the application of protein disulphide isomerase on RNase A microspheres emulsion, in the presence of appropriate oxidative environment, suggested the refolding of microspheres into the aqueous medium by a protein disulphide isomerase induced-structural change.

I-4.4. Protein nano and microparticles stability

When protein nano and microparticles are used as the DS, their stability becomes a major concern, mainly against aging and aggregation. This issue has been studied for quite long time and a variety of factors are known to influence it. These factors include, but are not limited to, particle size distribution, surfactant type and concentration, aqueous solubility of the dispersed phase, temperature, surface tension and ionic strength [162]. To investigate the stability of prepared particles, a program of study should be performed to measure in appropriate interval time their physical stability.

The most important parameter affecting the stability of microspheres is their size and its distribution, which can be determined by PCS. If the microspheres are even slightly soluble in the aqueous phase, mass transfer will occur from the smaller microspheres to the larger ones. This phenomenon, Ostwald ripening, was first theorized by Ostwald in 1901 [163]. Ripening usually occurs in solution due to the lack of monodispersity of microspheres. If all microspheres have the same size, ripening does not occur. The protein microspheres prepared by sonication usually have a broad size distribution, due to the disruption of acoustic sound.

The addition of a surfactant to the emulsion can help to solve this problem. The surfactant, also called tensioactive agent, is frequently employed for the dispersion of one phase in another immiscible phase and for the stabilization of obtained emulsion. It reduces the surface tension of continuous phase, avoids the coalescence and agglomeration of drops and stabilizes the emulsion.

A suitable surfactant should be able to give microspheres of a regular size with small size distribution, guaranteeing a more predictable and stable drug release.

There are four different types of surfactant classified by the nature of the hydrophilic part of molecule: anionic, cationic, amphoteric and non-ionic. The anionic surfactants have a negative charge in the aqueous solution. They have a relatively high hydrophilic/lipophilic balance level, because they are disposed to be hydrophilic. Contrariwise, the cationic surfactants present a positive charge in aqueous solution. The amphoteric surfactants behave as anionic in alkali pH and as cationic in acid pH. Non-ionic surfactants have no charge [164].

It is unrealistic to find a single surfactant that properly works for all different processes. Different formulations impose different requirements on stabilizers [165-168]. Furthermore, differences in the surfaces characteristics of drug would require different properties of stabilizers [169].

The amount of stabilizer used will also have an effect on the properties of the micro and nanoparticles. Most importantly, if the concentration of the stabilizer is too low, aggregation of the polymer droplets will occur and little if any particles will be recovered. Alternatively, if too much of the stabilizer is used, the drug incorporation could be reduced due to interaction between the drug and stabilizer. However, when the stabilizer concentration is between the “limits”, adjusting the concentration can be a means of controlling particle size [170].

Recently, it was demonstrated the importance of adding stabilizers to obtain a monodisperse population of proteinaceous microspheres by sonochemical synthesis [76]. Several stabilizers were studied and the polyvinyl alcohol (PVA) shown to be the best choice to obtain BSA and HSA microspheres with small size, homogeneous dispersion and high stability. The authors also proved that the presence of PVA increased the entrapment efficiency of an anti-inflammatory drug, piroxicam.

I-4.5. Protein-based nano and microparticles as delivery systems

Another important issue is the possibility of using such devices as DDS for different diseases. Since the first reports on the preparation of uniformly sized albumin microspheres in the early 1970s, these biodegradable, biocompatible particles have found various applications. Initially conceived as a diagnostic tool [171], albumin particles have been utilized as drug-carrier systems [172].

In general, the polymeric DS release bioactive agents by the following mechanisms [173, 174]: diffusion, chemical reaction or solvent activation. The release of a bioactive agent from a particle is primarily controlled by diffusion of the bioactive agent through the polymer [175]. For biodegradable polymers, degradation is a chemical process, whereas erosion is a physical phenomenon dependent on dissolution and diffusion process. As soon as the bioactive agent-containing polymer (A) comes into contact with the external liquid environment, it enters the polymer matrix (B), resulting in a swelling process, which allows the diffusion of the bioactive agent into the external environment [175] (C), as illustrated in Figure I-12.

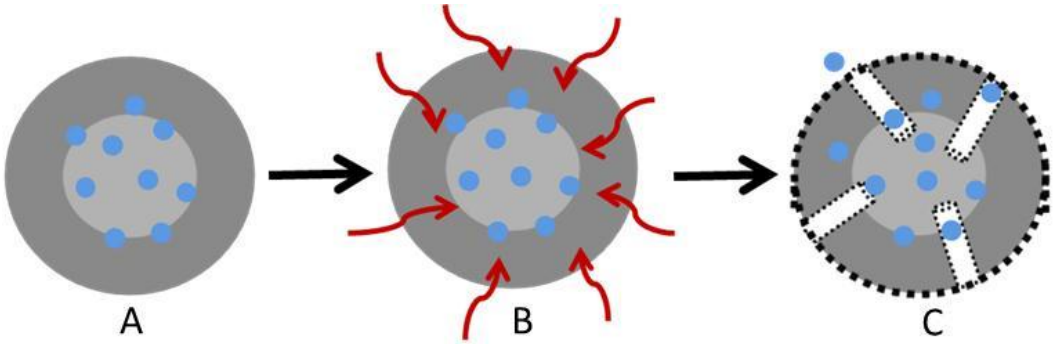

Figure I-12: **Schemes of the release of entrapped drug or bioactive agents from biodegradable polymeric particles. When the polymer device incorporating the bioactive agent (A) is inserted into the environment, the fluid from the surrounding medium enters the particle (B), causing swelling of the device. The fluid creates diffusion channels (C) and the incorporated active agent is released to the external environment. The degradation of material device occurs over time or by chemical reactions (e.g. enzymatic attack and chemical reactions on particular polymeric sites).**

Factors influencing the release rate include the molecular size of the bioactive agent and the entrapped percentage into the nano and microparticle, as well as polymer composition, and the dimensions and shape of the particles [173].

Regarding the release profile, strategies to control or render it more adequate for a particular application, by means of modifying parameters such as the surface (by coating, chemical modification and use of surfactants) or creating dual-release systems (layers of materials that can incorporate different molecules) can greatly improve the properties of several materials. With this, the

obtained microspheres can be changed to increase their stability as well as to target an organ or a tissue.

The availability of numerous exploitable side groups in proteins such as amine, hydroxyl, thiol and carboxyl groups makes it possible to use conjugation routes on prefabricated particles.

The encapsulation of the antibiotic tetracycline (TTCL) in BSA microspheres by sonochemical method, was successfully obtained by Avivi and Gedanken [53]. In the same research group the proteinaceous microspheres of BSA containing an anti-cancer drug (Taxol) were produced and characterized [62]. Later, the gemcitabine, which is also an anti-cancer drug, was encapsulated on BSA microspheres (BSA-Gemzar) [66]. The BSA-Gemzar composite was examined for its anti-cancer activity (*in vitro*) in renal cancer cells (RCC, 786-O cells) using [^{3}H] thymidine incorporation assays. They found that the influence of the Gemzar-loaded microspheres on the cancer cells was significantly greater than that of an equimolar concentration of Gemzar.

Recently, the benefits of encapsulated oil were verified by Silva *et al.* [75]. The authors reported a novel approach using proteinaceous microspheres of BSA, HSA and SF containing different organic solvents, namely *n*-dodecane, mineral oil and vegetable oil, to reduce the activity of human neutrophil elastase (HNE) found in high levels on chronic wounds. The ability of these devices to inhibit HNE was evaluated using porcine pancreatic elastase (PPE) solution as a model of wound exudates. These devices demonstrate an innovative way to control the imbalance of elastase/antielastase found in chronic wounds.

The entrapment of an anti-inflammatory drug, piroxicam, was also achieved, using BSA and HSA [76]. The work performed included the determination of the release kinetics of piroxicam from proteinaceous microspheres in the presence of protease, indicating an Anomalous drug transport mechanism (diffusion and polymer degradation). In the presence of higher protease concentration, BSA microspheres exhibit Case II transport, leading to zero order release (polymer degradation).

Suslick and co-workers [58] reported on a noncovalent, electrostatic layer-by-layer (LBL) modification that successfully targets protein microspheres to the integrin

receptors that are over expressed in several tumor types. Suslick has found that these negatively charged vesicles are excellent templates for LBL electrostatic adhesion.

Multilayer deposition of polyelectrolytes onto air-filled microbubbles is an attractive strategy to design targeted particles. Cavalieri *et al.* [64] report the synthesis of stable and functional microbubbles, coated with chemically reduced lysozyme, using high intensity ultrasound in aqueous solution. In order to demonstrate the possibility of surface functionalization of lysozyme microbubbles, which is of importance in targeted drug delivery, they adsorbed a polyelectrolyte on the surface of the microbubbles. Lysozyme air-filled microbubbles are positively charged colloidal particles and provide a good template for assembly of polyelectrolyte multilayer using the LBL approach. Two layers of poly(styrene sulfonate)/poly(allylamine hydrochloride) were assembled on the lysozyme shell.

I-5. APPLICATION OF DELIVERY DEVICES FOR WOUND DRESSING

Fundamental principles of nanoscience are now increasingly being employed for the manufacturing of innovative textile products with biomedical properties. Medical textiles and biomaterials for healthcare is a culmination of the worldwide research into medical textiles and biomaterials.

The future development of biomedical and protective textiles with selective properties that benefit the patient is based on applying scientific and clinical advances in wound healing, anti-microbial and enzyme-based fabrics [176].

From the ancient times, for effective healing of a wound, a suitable material had to be used to cover the wound in order to prevent any infection [177]. The use of biomedical textiles has being expanding as a result of innovations in medical procedures and textile technology. In each application area of biomedical textiles, advances continue, but they all depend on the properties of the fibre (or fibre blend) and the constructions fabricated from them. Although, medical device engineers have been utilizing textile structures for decades, their complexity is increasing as biomaterial and fabric-forming options become more abundant.

Biomedical textile fibres comprise synthetic fibres and those derived from natural sources designed a textile-based wound dressings [178].

Over the last few decades the wound dressings have undergone an evolutionary process from natural materials that simply covered and concealed the wound, to materials that focused on moisture management and, more recently, to materials that either deliver active ingredients or interact directly with cells or specific chemicals in the local wound environment [179].

The prolonged contact time of a drug with a body tissue, through the use of wound dressings, can significantly improve the performance of many drugs. These improvements range from better treatment of local pathologies to improved drug bioavailability and controlled release to enhanced patient compliance [180]. Furthermore, dressings that will deliver an active substance to a specific target site in a controlled fashion for a sustained period could help solve or minimize the non-compliance patients. In this highlight, the use of DS attached onto textiles-based wound dressings is being exploited for the treatment of several diseases.

There are a variety of methods for the attachment of the DS onto several dressings. The sonochemical method appears as one of the most effective method, once that it is possible to produce and attach the microspheres to fibres by one-step reaction.

BSA and casein microspheres have been attached to cotton and polyester fabrics using sonochemical radiation [181]. Proteinaceous microspheres bound to polyester remain linked to the fabric even after repeated washings in a washing machine, suggesting that these coated fibres can be used either for one-time application or for repeated use.

Gouveia [182] also demonstrate the potentialities of sonochemical methodology to develop a coating process based on BSA/L-Cysteine (L-Cys) microspheres on different textile materials, namely 100% of cotton, wool, polyester, polyamide, cellulose acetate and viscose. The microspheres developed by this process evidence anti-microbial property by themselves, due to the addition of L-Cys.

Recently, it was reported the use of an anti-inflammatory drug, piroxicam, sonochemical entrapped on BSA microspheres and attached onto cotton and nonwoven gauzes [183]. This work demonstrates the ability of the functionalized biomaterial to deliver the pharmaceutical agent.

I-6. MAJOR REMARKS AND FUTURE OUTLOOK

The rapidly developing field of nano and micro structured synthesis constantly attracts new methods and solutions for further improving the process performance.

The usefulness of sonochemical synthesis as a synthetic tool resides in its versatility. In this review it was highlighted the use of ultrasound sources to produce different nano and microparticles starting from phospholipids and polymeric based-proteins. The progress achieved on the synthesis of lipidic and polymeric nano and microstructures has been accompanied by the parallel exploitation of these materials in various fields, among them the controlled release. The sonochemical method has been further extended to the applications of these delivery devices designed to be textile-based wound dressings.

There are still some challenges left to be overcome for further development delivery-based platforms. The variety of natural proteins encourages us to explore more naturally existing proteins for versatile drug delivery, which can be prepared by sonochemical method.

Future developments for delivery devices can focus on the enhanced site-specific drug delivery by using receptor-targeting ligands, improve sustained drug release rates with enhanced permeability, retention time and minimize the undesirable side effects.

Furthermore, there is a demand to obtain preparation methods of the nano and microparticles that are able to be reproducible in an industrial scale.

CHAPTER II

MATERIALS AND METHODS

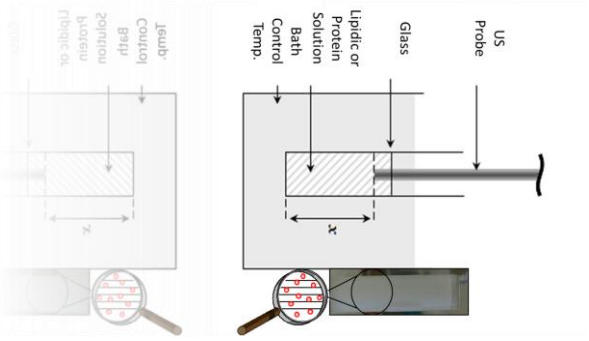

Chapter II

Materials and methods

The main aim of this Chapter is to describe in more detail the experimental work that was employed throughout the thesis. Each of the following seven chapters has a section of “Materials and methods”, but due to constraints of article length it is not possible to show all the details necessary for the correct understanding of the experiments performed. In this Chapter it will be highlighted each technique used and the experiment details are described in the followed Chapters (III to IX).

II-1. MATERIALS

The majority of the chemical reagents, unless otherwise noted, was purchased from Sigma-Aldrich and used as provided.

The lipophilic probe 1,1'-dioctadecyl-3,3,3',3'-tetramethylindodicarbocyanine perchlorate (DID) and the Nile red were purchased from Invitrogen.

All the chemicals were stored and manipulated following the manufacturer’s instructions and safety practices.

Silk cocoons from *Bombyx mori* were donated from “Sezione Specializzata per la Bachicoltura” (Padova).

The gauzes fibres were commercial available in a local pharmacy (100% cotton gauze and nonwoven gauze composed by 67% of viscose and 33% polyester).

The centricon tubes (molecular-weight cut-off of 3 kDa and 100 kDa) were purchased from Amicon.

II-2. ULTRASOUND EQUIPMENT

The experimental set-up used was composed of a probe type ultrasound source (20 kHz Sonics and Materials Vibracell CV 33) fitted with a 3 mm diameter titanium micro-tip. Power delivery was controlled as percentage amplitude (20%, 30% and 40%). The reaction vessel was an open glass cell (diameter 19 mm and height 75 mm), which contained 16 mL of sample solution (Figure II-1).

The sonochemical reactor temperature was controlled via a thermo-stated water bath with a freezer exchanger placed within a thermo jacket cell. Temperature was monitored throughout using K type thermocouples (TCs).

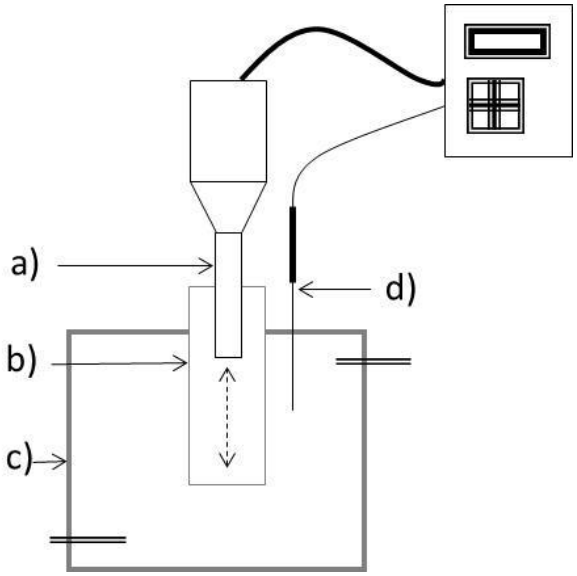

Figure II-1: Experimental set-up: a) ultrasound probe (3 mm diameter); b) glass vessel (diameter 19 mm and height 75 mm); c) jacketed vessel (diameter 130 mm and height 180 mm); d) temperature control bath.

II-3. PREPARATION OF PROTEIN SOLUTIONS

The bovine serum albumin (BSA) was weighted and solubilised, while human serum albumin (HSA) was diluted in phosphate buffered saline solution (PBS, 0.01 M, pH=7.4) or deionized water.

Silk fibroin (SF) was purified from its sericin content, as previously described [184]. The cocoons were cut, cleaned from debris and larvae and autoclaved for

30 min at 120 ºC. SF was then thoroughly washed with deionized water and dried overnight at room temperature.

The solutions of SF were prepared by dissolving 1 g of degummed silk fibres into 10 mL of saturated aqueous lithium bromide (LiBr) at 60 °C for 3 h. The solution was then diluted by adding 90 mL of deionised water, filtered and dialyzed against deionized water until complete removal of salt, using cellulose tubing (molecular - weight cut-off of 12000 - 14000 Da) [184, 185].

II-4. PRODUCTION OF NANO AND MICROPARTICLES

II-4.1. Preparation of unilamellar vesicles

Liposomes were prepared by the thin film hydration method [91]. According to this method, a known amount of dipalmitoylphosphatidylcholine (DPPC) was dissolved in chloroform.

The organic solvent was evaporated under a nitrogen stream and the residual traces of solvent were removed by a further evaporation for, at least, three hours under the same stream. The resulting dried lipid film was dispersed by the addition of phosphate buffer (0.1 M, pH 7.4) in a sufficient volume to obtain a final phospholipid concentration of 1500 µM. These mixtures were then vortexed above their phase transition temperature (41.4 ºC) to produce multilamellar vesicles (MLVs). MLVs suspension were sonicated at 50 ± 1 ºC to produce large unilamellar vesicles (LUVs) and was carried out with a total treatment of 21 min monitored in 3 min increments (Figure II-2). A pulsed duty cycle of 8 s on, 2 s off was used for all the experiments with indicated power delivery of 20%, 30% and 40%.

Preparation of liposomes with peptides (5 µM) followed a similar procedure with the lipid solution in chloroform and the peptides dissolved in pure ethanol and dried together under nitrogen.

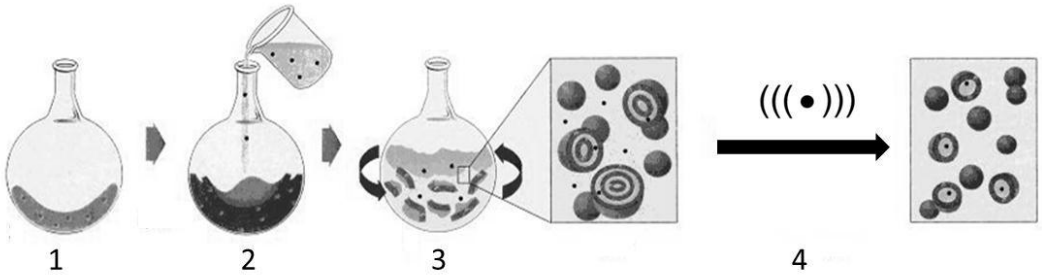

Figure II-2: **Schematic representation of MLVs and LUVs preparation: 1) formation of lipid film on the walls of the flask by evaporation to dryness of the organic solvent, 2) addition of an aqueous solution to the lipid film, 3) agitation to obtain MLVs; 4) Sonication of MLVs leading to the formation of LUVs.**

II-4.2. Preparation of proteinaceous microspheres

The microspheres were prepared by an adaptation of Suslick method. Briefly, the bottom of the high intensity ultrasonic horn was positioned at the aqueous-organic interface employing an amplitude of 40% with a temperature of 10 ± 1 ºC and with a total treatment of 3 min. The organic phase was chosen from different food-grade and/or medical approved oils. The separation of phases was accomplished in a few minutes. However, to obtain a complete separation of the microspheres from the mother solution, the flasks were placed in a refrigerator (4 ºC) for 24 h. After, microspheres were collected by centrifugation (2000 g, 30 min) using the centricon tubes (molecular-weight cut-off of 100 kDa or 3 kDa, for proteins and peptides, respectively) in order to separate the microspheres from the protein/peptide mother solution (supernatant) (Figure II-3).

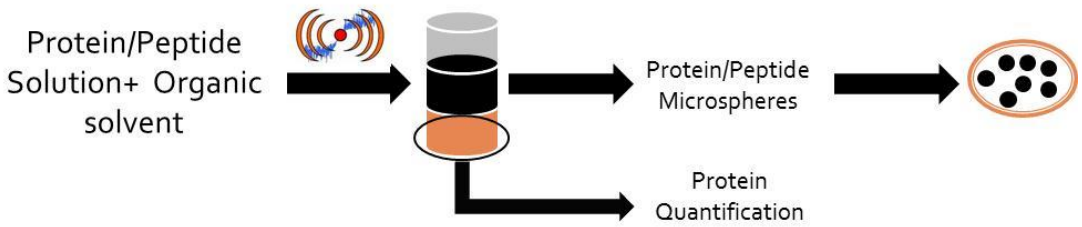

Figure II-3: **Schematic representation of protein/peptide microsphere preparation by sonochemical method.**

II-4.2.1. Preparation of proteinaceous microspheres containing piroxicam

Microspheres with the anti-inflammatory drug selected in this work were employed to determine the percentage of entrapment efficiency of drug, together with the studies of the entrapped molecule *in vitro* release profiles. The microspheres used for these studies are the following: BSA and HSA. The anti-inflammatory drug was the piroxicam (Figure II-4).

Microspheres with anti-inflammatory drug were synthesized using the sonochemical method. The piroxicam (3000 µM) was added to protein solution (5.0 $g.L^{-1}$) and layered with vegetable oil and submitted to ultrasound treatment in the same conditions described above (II-4.2.). The very low solubility of piroxicam required the use of dimethyl sulfoxide (DMSO): water solutions (1:99 v/v).

When stabilizers were used, they were dissolved in the aqueous phase. In this thesis, three different stabilizers were added to the formulation, namely polyvinyl alcohol (PVA), pluronic acid F68 (pluronic F68) and tween 80.

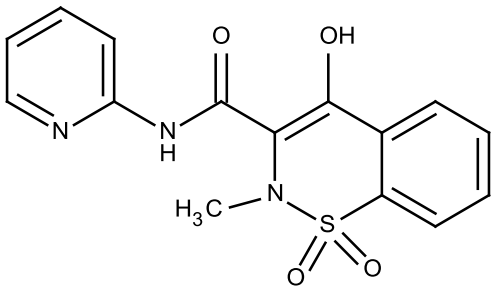

Figure II-4: Chemical structure of piroxicam.

II-5. CHARACTERIZATION OF DEVELOPED MICRO AND NANOPARTICLES

II-5.1. Photon correlation spectroscopy (PCS)

The diameter of the particles, as well as its homogeneity, was determined by photonic correlation spectroscopy (PCS), also known as dynamic light scattering (DLS). This method measures the Brownian motion and relates this to the sizes of the particles.

The Brownian motion is defined as the random movement of particles in a liquid due to the bombardment by the molecules surround them [186]. The particles in a liquid move randomly and their speed of movement is used to determine the size of particle. The randomly moving particles are irradiated with a laser beam and the intensity of the light scattered from a small volume of the sample in a (usually) fixed or variable angle is recorded in dependence on time. Small particles lead to fast intensity fluctuations as a result of their high diffusion coefficient, whereas for larger particles, which move more slowly, the fluctuations are slower [186, 187]. Because PCS relies on the determination of the particle diffusion coefficient (D), it is not a direct method for the determination of particle sizes. Information on the particle size can be obtained by the Stokes - Einstein equation analysing the experimental signals emitted at different sampling times [187]. From the value of D and together with the values of temperature (T) and the medium viscosity (η) it is possible to determine the diameter (d) of particles through the equation of Stokes-Einstein (Equation II-1) [187]. K is the Boltzmann constant and T the temperature in Kelvin (K).

$$D = \frac{KT}{3\pi d}$$

Equation II-1: Determination of particle diameter using Stokes-Einstein equation.

In addition to the determination of particle size it is possible to calculate the value of polydispersity index (PDI), which is indicative of the degree of heterogeneity regarding to the sample size. Thus, the greater the range of diameters which lies between the average diameter, i.e. the higher the standard deviation, the greater is the PDI, whose value ranges between 0.0 and 1.0 [186].

The size and PDI of microparticles was measured using a Malvern zetasizer NS (Malvern Instruments).

The size of liposomes vesicles was determined at 50 ± 0.1 ºC. However, the size of proteinaceous microspheres, as well as the peptide microspheres, was determined at 25 ± 0.1 ºC.

In order to verify the reproducibility of the preparation microparticles assembled under the typical process described above, the procedure was carried

out at least three times for each of the individual nano and microparticles and the results were expressed as mean value ± standard deviation.

II-5.2. Determination of zeta-potential

Almost all particles in contact with a liquid acquire an electric charge on their surface. The electric potential at the shear plane is called the zeta-potential [187].

The determination of zeta-potential was carried out using the same equipment described in the study of the diameter (Malvern zetasizer NS) and provides information on the membrane potential of particles.

Because the surface potential of the particles cannot be measured directly, the zeta-potential (electrical potential at the surface of hydrodynamic shear around the colloidal particles) is usually determined as a characteristic parameter for the nano and microparticle charge (Figure II-5) [187].

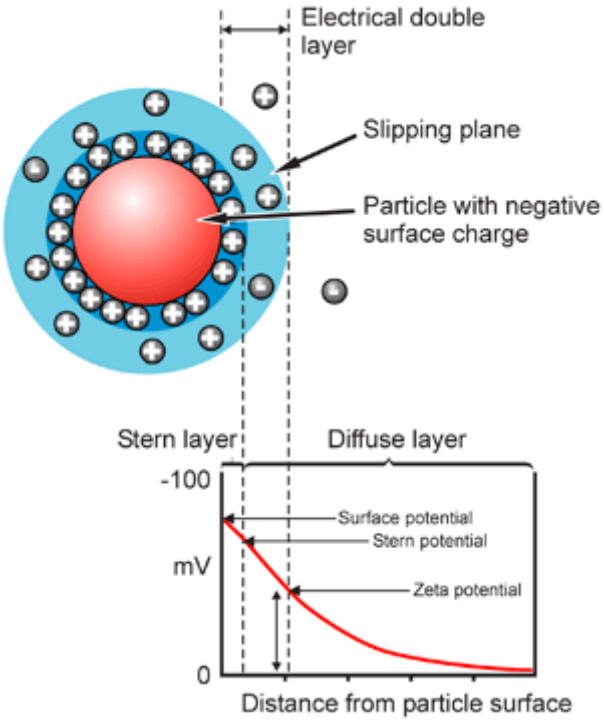

Figure II-5: **Schematic representation of the double layer of charges at the surface of an anionic particle (biological membrane or membrane models) (Adapted from Malvern I. [188]).**

For measurement, a dilute suspension of the particles is subjected to a weak electric field, and the mobility of the particles is commonly determined by laser

Doppler anemometry [188]. This technique is based on the evaluation of a frequency (Doppler) shift that is observed for the light scattered from the particles motion in the electric field [187].

The zeta-potential is based on measuring the electrophoretic mobility of particles, and determined, by the Henry equation, (Equation II-2) where, μ_e is the electrophoretic mobility, the zeta (ζ) -potential, ε is the dielectric constant, f (κa) is the role of Henry and η is the viscosity of the medium [188].

$$\mu_e = \frac{2\varepsilon\zeta - \text{potentialf}(\kappa a)}{3\eta}$$

Equation II-2: Determination of zeta-potential using the Henry equation.

For measuring the electrophoretic mobility, it was used a cell that has two electrodes that create, a potential difference, in which the particles move in suspension (Figure II-6). The displacement speed of particles in this field depends on their electrical charge [188].

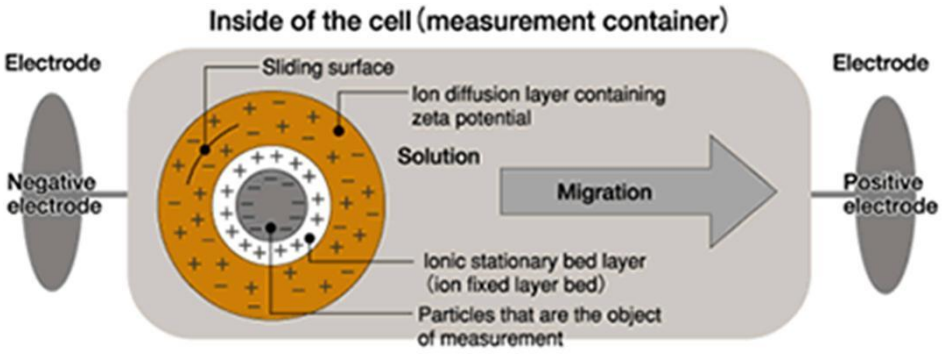

Figure II-6: Schematic representation of a cell used for determining zeta-potential of a sample with a negative charged particle (Adapted from Malvern I. [188]).

To determine the surface charge of nano and microparticles prepared, it was used the technique of electrophoretic laser Doppler anemometry [188].

Liposomes were suspended in PBS and measured at 50 ± 0.1 ºC. However, for the protein microspheres the measurements were performed at 25 ± 0.1 ºC and diluted with deionized water or PBS, according to the solvent used in their preparation. The instrument was routinely calibrated with a ± 66 mV latex standard.

The measurements were performed in triplicate and the results were expressed as mean value ± standard deviation.

II-5.3. Stability studies

A general and crucial aspect of colloid chemistry should be considered, and that is the means by which the particles are stabilized in the dispersing medium, since small particles can be unstable with respect to agglomeration to the bulk solution [189]. The stability of the microspheres was measured in terms of size distribution, zeta-potential and macroscopic aspect. The measurements of size and zeta-potential were done every week by the procedure previously described.

Measurements were recorded in triplicate and the results were expressed as mean value ± standard deviation.

II-5.4. Scanning electron microscopy (SEM)

Scanning electron microscopy (SEM) has been routinely applied for the morphological analysis of nano and microparticles. For investigation, the particles are usually dried and their surface has to be coated with a conductive layer, commonly by sputtering with gold.

In SEM the specimen is scanned point by point with the electron beam, and secondary electrons that are emitted by the sample surface on irradiation with the electron beam are detected. In this way, a three-dimensional (3-D) impression of the structures in the sample, or of their surface, respectively, is obtained [187].

To verify the liposomes morphology, the sample preparation included the drying and covering with a gold layer. The visualization was made using the LEICA S360 microscope.

The microspheres and the attachment of microspheres onto the gauzes were evaluated also by SEM. The samples were previously gold coated in vacuum. However, different equipment was used for their observation. The SEM photographs were obtained with a scanning electronic microscope model NOVA Nano SEM 200 FEI with a backscattered and secondary electrons detected.

II-5.5. Scanning transmission electron microscopy (STEM)

In conventional SEM study, the drastic drying conditions imposed by high vacuum in the microscope chamber have always prevented the directed studies of wet samples and dynamic imaging in a changing sample environment. Thus, scanning transmission electron microscopy (STEM) allows observing directly a liquid layer containing nano/micro objects [190].

For STEM analysis, the diluted microparticles suspension was dropped in Copper grids with carbon film 400 meshes, 3 mm diameter. The shape and morphology of particles were observed using a NOVA Nano SEM 200 FEI.

II-5.6. Lowry method

The Lowry method [191] has been, for decades, the procedure of choice for quantification of soluble proteins, due to its sensitivity, simplicity, and precision. This method was performed to quantify the protein in supernatant, using BSA as standard protein. The total protein concentration is exhibited by a colour change of the sample solution in proportion to protein concentration, which can then be measured using colorimetric techniques. The absorbance was measured at 750 nm, using a Heλios γ spectrophotometer (Unicam).

The efficiency of the microspheres formation was calculated using the Equation II-3, where $[P]_{total}$ and $[P]_{supernatant}$ is the initial and the final protein or peptide concentration in the aqueous solution, respectively.

$$\text{Microspheres formation}\,(\%) = \frac{[P]_{total} - [P]_{supernatant}}{[P]_{total}} \times 100$$

Equation II-3: Determination of efficiency of the microspheres formation.

This process indicates the percentage of protein/peptide that formed microspheres respecting to the total amount used in that preparation.

Measurements were recorded in triplicate and the results were expressed as mean value ± standard deviation.

II-5.7. Quantification of piroxicam entrapped into proteinaceous microspheres

Entrapment efficiency of piroxicam in proteinaceous microspheres was measured by ultraviolet (UV) spectrophotometry, at 353 nm using a Helios γ ThermoSpectronic spectrophotometer (Unicam). The separation of free piroxicam was achieved by centrifugation of samples at 2000 g for 30 min, using the centricon tubes (molecular-weight cut-off of 3 kDa). The entrapment efficiency of piroxicam was determined using the Equation II-4, where $[Piroxicam]_{initial}$ is the initial concentration used and $[Piroxicam]_{final}$ is the final concentration in supernatant.

$$\text{Entrapment}\,(\%) = \frac{[\text{Piroxicam}]_{initial} - [\text{Piroxicam}]_{final}}{[\text{Piroxicam}]_{final}} \times 100$$

Equation II-4: Determination of the entrapment efficiency of piroxicam.

Measurements were recorded in triplicate and the results were expressed as mean value ± standard deviation.

II-5.8. Confocal microscopy

A confocal microscope provides a significant imaging improvement over conventional fluorescence microscopes overcoming some limitations. It creates sharper, more detailed images, and allows collection of data in 3-D [192].

For confocal analysis proteins were labelled with fluorescein isothiocyanate (FITC; 495 nm/521 nm) and 1,1'-dioctadecyl-3,3,3',3'-tetramethylindodicarbocyanine perchlorate (DID), which is an hydrophobic probe with markedly red-shifted fluorescence excitation and emission spectra. However, another dye, Nile red, was used as a probe. The main differences is that Nile red is a dye that exhibits solvatochromism and its absorption band varies in spectral position, shape and intensity with the nature of the solvent [193, 194].

The samples were analysed with a confocal laser scanning microscope Leica TCS SPE. For the 3-D reconstructions it was use the Imaris software (version 7.0, Bitplane, Zurich).

II-5.9. Fourier transform infrared (FT-IR) spectroscopy

The Fourier was used to quantitatively assess protein secondary structure by Fourier transform infrared (FT-IR) spectroscopy. This approach can provide detail information regarding protein conformation without alteration or degradation of the controlled release system [155].

Infrared spectra were recorded at room temperature using a Perkin Elmer Spectrum 100 Infrared spectrophotometer from 4000 cm^{-1} to 500 cm^{-1}. To eliminate spectral contributions, due to atmospheric water vapor, the instrument was continuously purged with dry air. The protein microspheres emulsion was quickly transferred to a potassium bromide (KBr) Liquid Omni Windows support cell in an Omni Cell Assembly accessory, specially designed for liquid solutions.

All samples were measured at least three times.

Gaussian deconvolution of Amide I band region was performed using OriginPro 8.5 software. The number of components and their peak position were determined from the second derivative spectrum of the same region. The secondary structure content was calculated from the areas of the assigned peak as percentage fraction of the total area of the Amide I range. For all data, a linear baseline was fitted and a self-deconvolution was performed using Gaussian function.

II-5.10. Molecular dynamic studies

Molecular dynamics simulations were performed with the GROMACS package, using the GROMOS96 force field with an integration time step of 2 fs. Bond lengths of the solute were constrained with LINCS and the ones of water with SETTLE. Non-bonded interactions were calculated using a twin-range method with short and long range cut-offs of 8 and 14 Å, respectively. The SPC water model was used. The solute and solvent were coupled to two separate heat baths with temperature coupling constants of 0.1 ps and reference temperatures of 300 K. The pressure control was implemented with a reference pressure of 1 atm and a relaxation time of 0.5 ps.

CHAPTER III

EFFECT OF ULTRASOUND PARAMETERS FOR UNILAMELLAR LIPOSOME PREPARATION

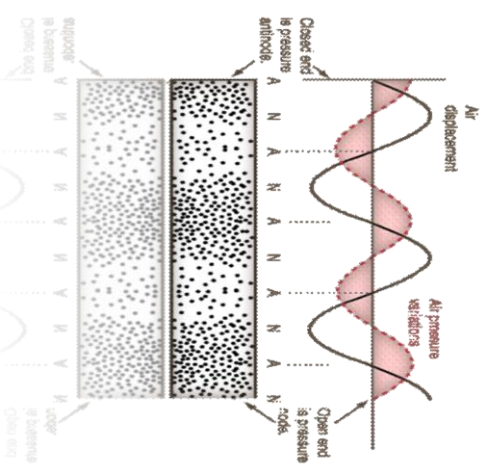

Chapter III

Effect of ultrasound parameters for unilamellar liposome preparation[†]

ABSTRACT

In this study, it was investigated the effects of ultrasound, namely power input, distance from ultrasound tip to base of reactor and treatment time, in the formation of liposomes. Results indicate a dependence on cavitation events that are a function of power input, and consequently dependent on the position of the probe within the reaction vessel and the wave behaviour. Short treatment times are required to achieve nanosized vesicles in anti-nodal ($\lambda/4$; 19 mm) reactor geometries. In this wave point the cavitation phenomenon is more pronounced when compared with the nodal point ($\lambda/2$; 38 mm). Therefore, the consideration of the above parameters is vital if dependable and repeatable results are to be achieved.

[†] This chapter is based on the following publication:
Silva R; Ferreira H, Little C, Cavaco-Paulo A, *Effect of ultrasound parameters for unilamellar liposome preparation*, Ultrasonics Sonochemsitry, 2010 (17), pp 628-632.

III-1. INTRODUCTION

Liposome applications can been found in many different areas as biochemistry, molecular biology, food technology, pharmaceutical and medical. Each application requires vesicles with different characteristics, which will be dependent for example, on the material to be encapsulated, as well as on the different release properties [5, 98, 195]. Different methodologies are described in the literature to produce multilamellar vesicles (MLVs), large unilamellar vesicles (LUVs) and small unilamellar vesicles (SUVs) [5, 32, 98, 103].

The use of ultrasound methods to produce LUVs and SUVs are widely reported in the literature [32, 37, 196]. However, the productions of these phospholipid vesicles are poorly reproducible, since that ultrasound experimental set-up is not well described.

Ultrasound phenomena in liquid media enhance mass transports of their constituents in a non-homogeneous fashion allowing the fast formation of vesicles [197, 198]. Several authors had pointed the fact that the most claimed ultrasound characteristics are in direct dependence of power input and duration of sonication effects [14, 25, 28]. However, the control of these two parameters leaves the possibility of variation sound field intensity arising from the relationship between the frequency of ultrasound, position of probe tip from the base of the vessel and the phase of the sound wave upon reflection at the base.

It is well known that ultrasound mechanical waves generate cavitation in liquids with the formation of local hot spots and free radicals [20, 22]. Previous work, done by Little *et al.*, has shown that variations of the ultrasound path-length had a marked effect on rates of temperature rise and radical production within the bulk solution [199]. Therefore, the power input, the duration of treatment and the position of the ultrasound source within the solution, will have an outcome on the ultrasound conditions imposed on the solution. This will affect the levels of hydroxyl radicals ($^{\bullet}OH$) generated in solution. In fact, the chemical effects of the cavitation bubble collapse, namely $^{\bullet}OH$ radical formation, are rarely considered in detriment of the extent of the tensile stresses imposed by ultrasound, which are usually reported [199].

The present work intends to show the need of control experimental set of operating parameters to engineer the characteristics of phospholipids vesicles. For that it was performed an extensive reactor characterization process. The methodology that was used explored the effects of the three parameters referred, namely power input, sonication time and depth (measure from the base of the vessel), in the production of $^{\bullet}OH$ radicals and consequently in the formation of vesicles. These conditions were related with lipid vesicle size, the polydispersity index (PDI) and surface charge (before and after sonication), usually determined in terms of zeta-potential.

III-2. MATERIALS AND METHODS

III-2.1. Calorimetry and dosimetry procedures

The reactor was characterized via calorimetry and dosimetry by an adaptation of the previously published method [199]. Calorimetry measurements were performed within a custom made enclosure with temperature recorded via four wire ended k-type thermocouples (TCs), three positioned at the outer sides and one at the base of a glass vessel of the same type as that used for dosimetry and liposome formation. The TCs were interfaced with a Pico Technology TC-08 Thermocouple data logger connected to a computer with Pico Log software version R.33. The sonochemical reactor temperature was controlled via a thermo-stated water bath with a heat exchanger placed within a thermo jacket cell. The vessel was filled with 16 mL of deionized water and the probe activated for ninety seconds (90 s) constant ultrasound at the indicated power input settings. The initial temperature (T_i) was taken from the average within the solution for 10 s prior to activation, and the final temperature (T_f) the average in the final 40 s of sampling. Calorimetry was performed using deionized water and the calorific power of the reactor was determined from Equation III-1, where E is the calculated energy (J) to raise the water temperature, ΔT_{Ave} is equal to difference of the final and initial temperature (T_f -T_i; K), m is the mass of H_2O (Kg) and C_p is the heat capacity of H_2O (4186 $J.Kg^{-1}.K^{-1}$). The change in temperature

(ΔT) from the initial to final levels was calculated for each TC position where ΔT, values were averaged from the four TCs positions to give ΔT_{Ave}.

$$E = \Delta T_{Aver} \times m \times C_p$$

Equation III-1: Determination of calorific power (J).

Calorific power was subsequently converted to intensity (I) units of $W.cm^{-2}$ using Equation III-2, where Δt is the time of ultrasound activation and $\pi.r^2$ the surface area of the micro-tip.

$$I = \frac{E}{\Delta t \times \pi \times r^2}$$

Equation III-2: Conversion of calorific power into intensity ($W.cm^{-2}$).

A total sonication time of 90 s using the previously specified duty cycle was used at an indicated power input percentages of 20%, 30% and 40%. The dosimetry procedure was performed by the ultrasonic irradiation of buffered aqueous terephthalic acid (TA) solution [199]. This leads to the breakdown or sonolysis of the water, which results in the formation of $^{\bullet}OH$ and hydrogen ($H^{\bullet}$) radicals. The reaction is specific to $^{\bullet}OH$ radical and results in conversion of TA to 2-hydroxyl-terephthalic acid (HTA), which exhibits fluorescence under UV excitation and accounts for 35% of $^{\bullet}OH$ radical formation [14]. The detection of HTA was performed on a Shimadzu RF-1501 spectrofluorophotometer, using an excitation wavelength of 314 nm and an emission wavelength of 425 nm.

Samples were taken (2 mL) in triplicate and returned after analysis. The HTA decay rate during the 15 min of incubation time was negligible. Fluorescence data was averaged and converted to $nmol.mL^{-1}.s^{-1}$ using the calibration curve of fluorescence *vs* HTA concentration ($nmol.mL^{-1}$). The calorimetry and dosimetry procedures were based on the variations of the distance between the ultrasound tip and the base of the reaction chamber, shown as x in Figure III-1.

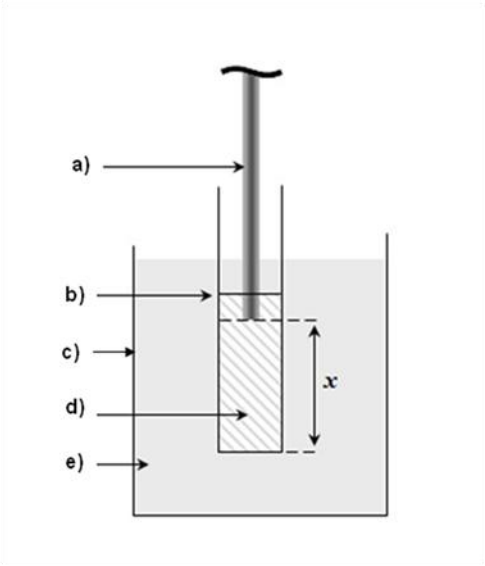

Figure III-1: Experimental set-up: a) ultrasound probe (3 mm diameter); b) glass vessel (diameter 19 mm and height 75 mm); c) jacketed vessel (diameter 130 mm and height 180 mm); d) lipid solution (16 mL, 1500 µM); e) temperature control bath (50 ºC) and x) distance between ultrasound tip and base of the glass vessel.

These distances variations were chosen based on a guideline wavelength. The Marczak equation (Equation III-3) [200] gave us the value of the velocity of sound in pure water (c), and therefore, it is possible to determine the wavelength according to the Equation III-4, where T is the temperature in degrees Celsius and f is the frequency in kHz.

$$c = 1.40238\times10^{-3} + 5.03881T - 5.79913\times10^{-2} + 3.29715\times10^{4}T^{3} - 1.39884\times10^{6}T^{4} + 2.78786\times10^{-9}T^{5}$$

Equation III-3: Determination of velocity of sound in pure water using the Marczak equation.

$$\lambda = \frac{c}{f}$$

Equation III-4: Determination of wavelength.

According to Equation III-3 and Equation III-4 for 50 ºC the wavelength was 77.1 mm.

III-2.2. Preparation and characterization of liposomes

Liposomes were prepared according with the method described in Chapter dedicated to materials and methods. The procedure for the further characterization of liposomes (size distribution and the zeta-potential) is also mentioned in the same Chapter.

III-3. RESULTS AND DISCUSSION

The reactor was characterized via calorimetry and dosimetry procedures, as previously described, prior to testing the liposome behaviour to the sonication. These two procedures were performed at 19 mm (anti-nodal point; $\lambda/4$) and 38 mm (nodal point; $\lambda/2$) of depth, which were calculated based on an estimated wavelength of 77.1 mm. The nodal point is known as a point where the wave has the minimal amplitude. The opposite of a nodal point is an anti-nodal point, where the amplitude of the wave is maximum.

The calorimetry results are presented in Figure III-2. In this figure, it is possible to observe that the energy deposition for these two depths (19 and 38 mm) increase with the power input. The highest value of input energy (about of 50 $W.cm^{-2}$) was obtained at 19 mm of depth and 40% of power input. Although, when it was used the 20% of power input at two different depths (19 and 38 mm), it was obtained the same input energy inside of the reactor (about 15 $W.cm^{-2}$).

After the calorimetry method it was performed the TA dosimeter, which is extensively used as an $^{\bullet}OH$ radical indicator [25, 28]. The extent of the conversion of TA to HTA obtained in the dosimetry procedure is shown in Figure III-3.

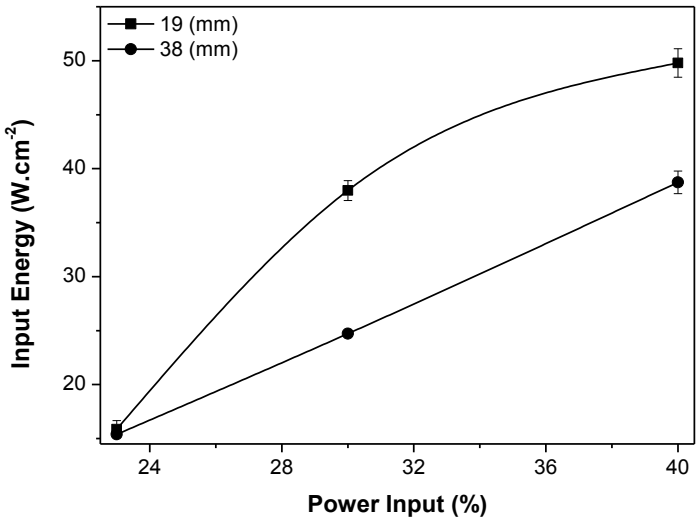

Figure III-2: Variation of measured input energy (W.cm^{-2}) with power input (%), at different depths (19 and 38 mm).

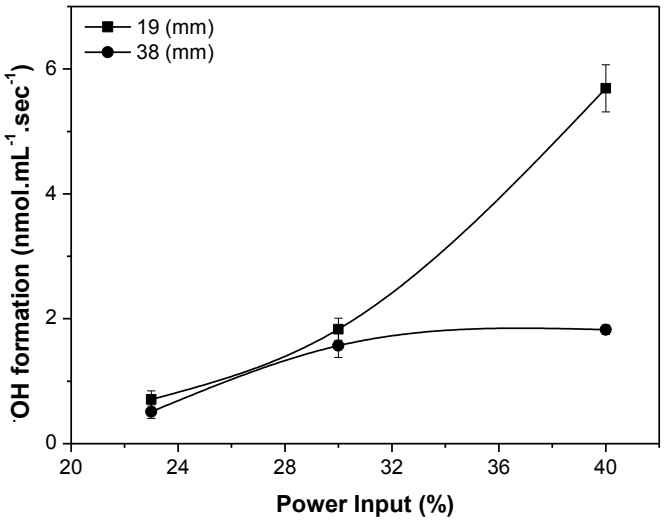

Figure III-3: Variation of rate of $^{\bullet}$OH radical formation (nmol.mL^{-1}.sec^{-1}) with power input (%), at different depths (19 and 38 mm).

The behaviour at the 38 mm (λ/2) position showed an almost linear production of $^{\bullet}$OH radicals. Conversely, the 19 mm (λ/4) position displayed a significant increase in $^{\bullet}$OH radical production at 40% of power input. The possible reason for this is that whilst cavitation bubble implosion is regarded as necessary for $^{\bullet}$OH radical formation, and is also a contributor of heat, other factors are present, which contribute heat to energy to the solution when conditions do not

favour $^{\bullet}$OH radical production. These include cavitation bubble implosion of insufficient energy to form radicals, fluid friction within the bulk solution from the mixing effect, and friction between the bulk solution with the stationary boundary layer adjacent to the side of the vessel. These friction forces could continue to provide heat energy even when the differential in acoustic pressure is not enough to sustain effective cavitation [199]. After this characterization, it was possible to identify the minima and maxima $^{\bullet}$OH radical activity points as occurring at 38 mm (nodal point) and 19 mm (anti-nodal point) positions, respectively.

The characterization described above is essential, once that the ultrasound can promote the hydrolysis and the oxidation of phospholipids, via the free radicals produced in the cavitation bubbles collapse. Additionally, high temperatures accelerate phosphocholine hydrolysis. Thus, during the sonication procedure, temperature should be controlled otherwise oxidation and hydrolysis reactions are favoured [33, 201]. However, according to Rabinovich Guilatt *et al.* [113] a temperature of 50 ºC over 24 h induces only 1.6% of phosphocholine hydrolysis. In this context, in order to minimize the hydrolysis, the temperature was controlled during all the experiment using a thermo-stated bath and the sonication was carried out in time intervals of 3 min. Therefore, in these working conditions the hydrolysis should be negligible.

Afterwards, the ultrasonic treatment of the liposomes was carried out at amplitudes of 20%, 30% and 40%, using the depths of 38 and 19 mm, measured from the base of the vessel. The variation of the vesicles size with sonication time, at different fixed sonication powers and different depths, was analysed by photon correlation spectroscopy (PCS). Size distribution is a crucial parameter for the characterization of liposomes and can be weighted by number, surface area, volume or any other property of the particle being measured. These different measurements are dependable of the liposomes applications. Liposomal delivery of an encapsulated hydrophilic drug, for example, is best described by a volume-weighted histogram to determine the liposome size at which most of the drug is carried. Delivery of a membrane-bound molecule may be better described by a surface-area weighted histogram [37]. In this work, the size of liposomes was measured in terms of volume, so these liposomes can be used as vehicle for controlled release [42].

Figure III-4 shows the vesicle size, after increasing sonication times and using constant sonication amplitudes: 20%, 30% and 40%, for the system containing 1500 µM of dipalmitoylphosphatidylcholine (DPPC). This figure shows a decrease of the particle size with the increase of the sonication time, until a plateau size was obtained after 21 min of sonication. These results also demonstrate that the vesicle sizes decreased when sonication amplitude increased. In addition, using different sonication times and different depths, a difference in the sizes were observed. Considering a constant sonication time and amplitude, a higher value of liposome sizes were observed when the treatment was made at 38 mm. On the other hand, at the anti-nodal point (19 mm) the cavitation phenomenon is more pronounced promoting a higher $^{\bullet}OH$ radical formation. These phenomena could affect the composition of samples and the formation of vesicles with lower sizes. However, in the nodal point (38 mm) the size obtained was not so different, after 21 min of treatment, with the advantage to decrease the possibility of phospholipid oxidation since at this depth the $^{\bullet}OH$ radical production is much lower.

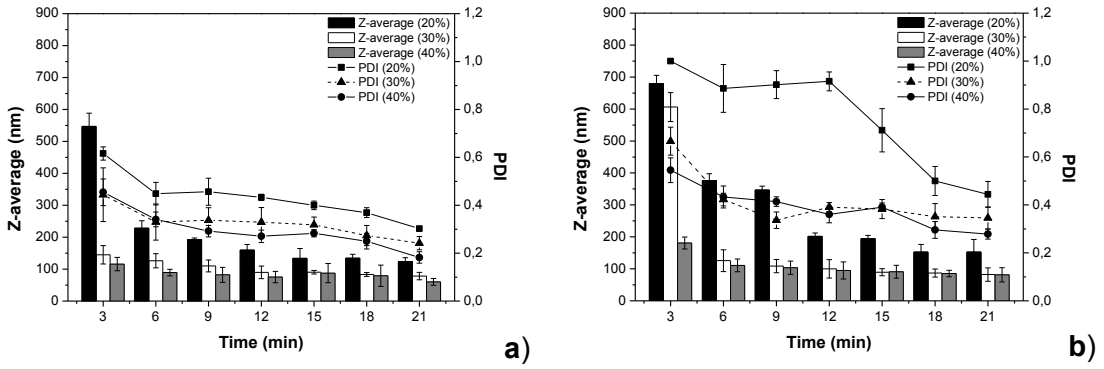

Figure III-4: Effect of sonication on DPPC liposomes (1500 µM) sizes (Z-average; nm) using 19 mm (a) and 38 mm (b) of depth, applying different amplitudes (20, 30, 40%) after 3, 6, 9, 12, 15, 18 and 21 min, at 50 ºC and pH 7.4.

Figure III-4 also shows that using higher amplitude it was possible to obtain a decrease in PDI. In fact, the size and PDI decreased as the higher power exerts greater shear forces within the solution. The greater extent of streaming from the ultrasound source promotes higher mixing of the solution and consequently more homogeneity. Therefore, at 19 mm and after 21 min of treatment a drop in the physical size and PDI was observed. However, at 38 mm the difference of size was not so significant and the possibility of occurring oxidative reactions is lower.

This is very important when it is used polyunsaturated phospholipids, because they are easily oxidised.

In Figure III-5 and Figure III-6 it can be observed two different sizes of population. Current theories postulate that sonication, as other methods of liposome formation, randomly fragment MLVs into what are termed LUVs [5, 202]. These disc-like fragments are thought to fold up into thermodynamically stable liposomes [203]. Alternatively, tiny unstable liposomes, formed during sonication, may fuse together to form slightly larger, stable liposomes [204, 205].

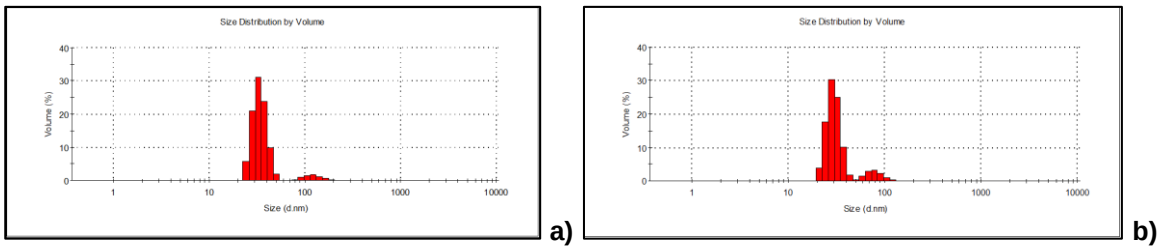

Figure III-5: Size distribution of liposomes (1500 µM) using 19 mm (a) and 38 mm (b) of depth, after 21 min of sonication, with 40% of amplitude, at 50 ºC and pH 7.4.

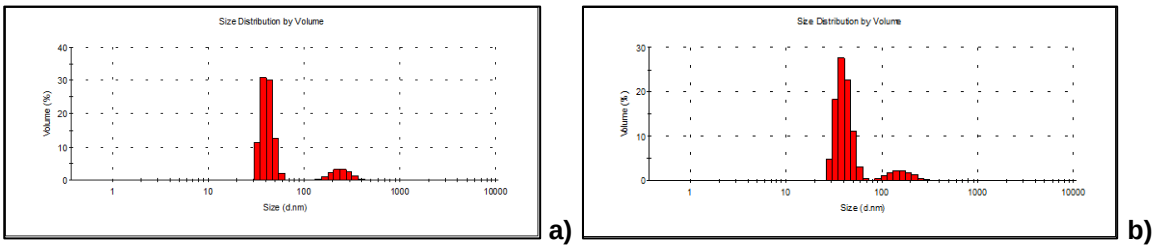

Figure III-6: Size distribution of liposomes (1500 µM) using 19 mm (a) and 38 mm (b) of depth, after 21 min of sonication, with 20% of amplitude, at 50 ºC and pH 7.4.

The determinations of zeta-potential were made before and after sonication. After the measurements it was verified that the potential surface of liposomes did not change significantly by the use of ultrasound (≈ 4 and ≈ 3 mV, before and after ultrasound, respectively).

III-4. CONCLUSION

The results of this work show the importance of reactor characterization to attain the control of liposome sizes using an ultrasonic probe system. It was

considered that the three principal factors of ultrasound which could influence the ranges of size of liposomes are: depth, power input and extent of treatment. Indeed, these factors that could influence the cavitation phenomenon have an impact on the rate and structure of the vesicles formed. At 19 mm of depth, 40% of amplitude and 21 min of treatment, carried out in time intervals of 3 min, it is possible to obtain a more homogeneous population of nanosized vesicles than 38 mm. These two positions are of importance when using ultrasound for the breakup of multilamellar liposome layer stuff, in particular the position at which constructive interference (anti-nodal point; 19 mm) occurs as this maximises cavitation events and associated phenomena.

These findings seem to indicate the usefulness of the ultrasound method to obtain unilamellar liposomes, particularly when the parameters are controlled. The knowledge of this can be further extended to the synthesis of other nanomaterials.

CHAPTER IV

INCORPORATION OF PEPTIDES IN PHOSPHOLIPID AGGREGATES USING ULTRASOUND

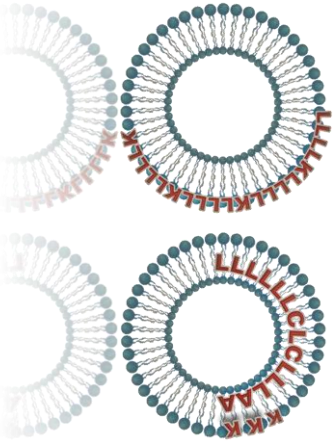

Chapter IV

Incorporation of peptides in phospholipid aggregates using ultrasound‡

ABSTRACT

In the previous Chapter (III) the optimum conditions for ultrasound preparation of liposomes were achieved. Considering these parameters, in this Chapter it was investigated their influence when peptides where incorporated in phospholipid aggregates (liposomes). These liposomes or vesicles are known as transport agents in skin drug delivery and also for cosmetic use. They might be a good model to deliver larger peptides into hair to restore fibre strength after hair coloration, modelling, permanent wave and/or straightening. The preparation of liposomes dipalmitoylphosphatidylcholine (DPPC) with peptides (LLLLKLLLLKLLLLKLLLLK; LLLLLLCLCLLLKAKAK) was made by the thin film hydration method. The large unilamellar vesicles (LUVs) were obtained by sonication, applying different experimental conditions, such as depth (mm) and power input (%). Photon correlation spectroscopy (PCS), zeta-potential and scanning electronic microscopy (SEM) results confirmed that the incorporation of these peptides, with different sequence of amino acids (a.a.), presented differences on the diameter, zeta-potential of membrane surface and shape of liposomes. The liposomes that included peptide LLLLKLLLLKLLLLKLLLLK present an increased in zeta-potential values after using ultrasound and an ‘‘amorphous” morphology. Conversely, the liposomes that incorporated the peptide LLLLLLCLCLLLKAKAK presented a define shape (rod shape) and the potential surface of liposome did not change significantly by the use of ultrasound.

‡ This chapter is based on the following publication:
Silva R, Little C, Ferreira H, Cavaco-Paulo A, *Incorporation of peptides in phospholipids aggregates using ultrasound*, Ultrasonics Sonochemistry, 2008 (15), pp 1026-1032.

IV-1. INTRODUCTION

The potential use of liposomes as microencapsulators for drug delivery and for cosmetics applications has been well-studied [32, 93, 117, 206-209]. Several types of liposomes can be distinguished, depending on the preparation method, such as multi-, oligo- and unilamellar vesicles, containing several, few or only one bilayer shell, respectively [32, 97, 98, 103]. Nevertheless, all liposomes are basically lipid bilayer containers in which several substances could be entrapped or at least anchored into their structure [98]. Due to their unique physical and chemical properties, such as their stability in solution for long periods of time with no significant changes in size or structure [93], and their ability to incorporate lipophilic, amphiphilic and/or hydrophilic compounds [117], liposomes can be used in a wide range of applications.

Multilamellar vesicles (MLVs) have high encapsulation efficiency, but also great variations on the vesicle size, size distribution and lamellarity. The use of mechanical treatments such as: repetitive freezing/thawing cycles, extrusion through polycarbonate membranes, dehydration/rehydration cycles, microfluidation or sonication can transform the MLVs suspension into large unilamellar vesicles (LUVs) and small unilamellar vesicles (SUVs). In addition to a stand-alone treatment, ultrasound can be applied to the other methods to increase efficiency in the formation of hydrated lipid vesicles of the smallest size. Ultrasound has recently been applied to obtain stable nanosuspensions which have emerged as a promising strategy for an efficiency delivery of hydrophobic drugs, because of their versatile features such as very small particle size. The ability to produce the nanoparticles of desired size with great precision (narrow size distribution and small variation) is the key factor of producing the nanosuspensions [37, 210].

The extreme conditions generated within the collapsing cavitational bubbles have been used for the size reduction of the material to the nanoscale. Nanoparticle synthesis techniques include sonochemical processing, cavitation processing and high-energy ball milling. In sonochemistry, an acoustic cavitation process can generate a localized hot zone with an extremely high temperature

gradient and pressure. Such sudden changes in the temperature and pressure assist the destruction of the sonochemical precursor and the formation of nanoparticles [17, 89].

Symmetric collapse of a cavitation bubble results in hot spots of nearly 5000 K within the bulk solution [22] and high velocity shock waves travelling through the solution. Collapse in proximity to surfaces can result in deformation of the bubble, manifesting as asymmetric collapse. This behaviour causes micro-streaming and high velocity shock waves within the bulk solution in the direction of the surface [197].

Myriad applications of ultrasound in medicine and industry have been developed; however, the details of ultrasound-induced damage to biomolecules, especially proteins, remain poorly characterized [211]. Such characterization is difficult, owing to the potentially complex mechanisms of sonication. These may include the formation of liquid-gas interfaces, local heating effects, sheer and tensile stresses and reactions occurring with generated free radicals [14, 212].

Loomis and Wood first reported the damaging effects of ultrasound radiation on biological systems in 1927 [213]. Many applications of ultrasound in common use today may alter protein structures [14]. However, sonication is used to prepare proteinaceous microspheres and these proteins can retain their functionality [45]. These vehicles are widely used as ultrasound contrast agents, and are being investigated as possible gene transfer vehicles [214]. Sonication is also employed in procedures to encapsulate therapeutic proteins, such as asparaginase, insulin for controlled release *in vivo* [215-217].

This work describes the sonication conditions to obtain systems of lipid vesicles with low polydispersity and lamellarity and also study how they can interfere with the physico-chemical properties of liposomes when different peptides were incorporated in the lipid bilayer. For that, it was investigated the size changes as well as the polydispersity index (PDI) using the photon correlation spectroscopy (PCS), and the zeta-potential, usually determined as a characteristic parameter for the particle charge. The morphology, as a function of the ultrasound power and the different depths (from the base of the vessel), were examined using scanning electron microscopy (SEM).

IV-2. MATERIALS AND METHODS

IV-2.1. Peptide development

The two synthesized peptides with approximately 20 amino acids (a.a.) were: C-term: LLLLLLCLCLLLKAKAK and C-term: LLLLKLLLLKLLLLKLLLLK, where L, C, K and A is the one-letter code for the a.a. Leucine, Cysteine, Lysine and Alanine. The peptides were covalently linked by the N-terminal to a fluorescent dye, (5(6)-carboxytetramethyl-rhodamine, succinimidyl ester), i.e., 5(6)-TAMRA, with spectral properties of Abs_{max} = 544 nm and Em_{max} = 572 nm, to facilitate the analysis of peptide penetration. The peptides structures were synthesized by JPT Peptide Technologies GmbH (Berlin, Germany). The peptides were supplied as a lyophilized material. They were analysed by high performance liquid chromatography (HPLC) and mass spectrometry (MS), and their purity was over 70% (HPLC, 220 nm, C18, linear gradient).

IV-2.2. Preparation and characterization of liposomes containing synthetic peptide

Liposomes were prepared according to the method previously described in the Chapter II. The procedure for the further characterization of liposomes containing the bioactive agent (two peptides previously described) including the determination of size and its distribution and the zeta-potential, are also mentioned in Chapter II.

The peptide surface charge analysis was obtained by using the PyMOL v0.99 [218].

IV-3. RESULTS AND DISCUSSION

Prior to testing of the liposome behaviour to the sonication, the reactor was categorized as previously mentioned on the Chapter III. This identified the minima and maxima hydroxyl radical ($^{\bullet}OH$) activity points as occurring at 38 mm (nodal-point $\lambda/2$) and 19 mm (anti-nodal point $\lambda/4$) positions, respectively.

Subsequently, ultrasonic treatment of the liposomes with and without peptides was carried out at amplitudes of 20%, 30%, and 40% and using the depths, measured from the base of the vessel, of 38 mm and 19 mm. First, liposome dispersions without peptides were sonicated at the specified powers and depths. An analysis of size distributions of liposomes before applying ultrasound (MLVs) was performed and it was observed that these MLVs presented a large size (≈ 2400 nm) with a higher PDI (≈ 0.910). This result was attributed to the heterogeneity of MLVs population presented in the sample.

Figure IV-1 shows the size (nm) and the PDI that were obtained after 12 min of sonication. According with the previous results (Chapter III) this time frame was sufficient to promote the size decrease of liposomes vesicles.

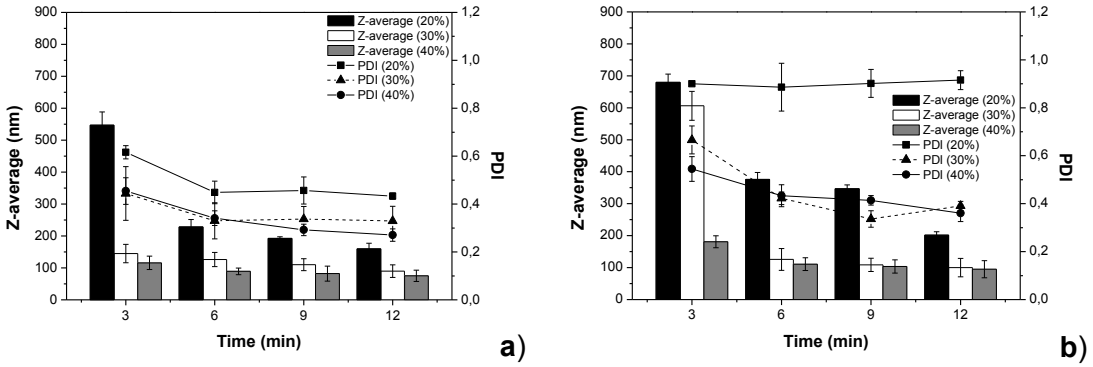

Figure IV-1: Effect of sonication on liposomes (1500 µM, pH=7.4) size (Z-average; nm) using different depths (a) 19 mm, (b) 38 mm, applying different amplitudes (20, 30, 40%) after 3, 6, 9 and 12 min of sonication, at 50 ºC.

Initial data, from the zetasizer, gave a high Z-average with a high PDI during the first minutes. After the treatment with ultrasound, there was a decrease in the PDI with a rapid drop in the Z-average. Physical size and PDI decreased with higher power intensity (40%), since with this power it is possible to achieve more rapid mixing of solution.

The highest value of PDI obtained for the lowest sonication amplitude (20%), is associated with a wide distribution of liposomes size. This fact seems to indicate that this amplitude is not enough to decrease homogeneously the size of particles. A drop in the physical size and PDI at 19 mm was observed.

The production of $^{\bullet}OH$ radicals is notably higher since at this depth the cavitation phenomenon is more pronounced (anti-nodal point) and the greater

extent of streaming from the ultrasound source promotes a decrease in the size of liposomes.

The determinations of liposomes zeta-potential (mV) were made before and after sonication. After the measurements, it was verified that the potential surface of liposomes did not change significantly by the use of ultrasound (≈ 4 and 3 mV, before and after ultrasound, respectively).

Hydrolysis of phospholipids is promoted presumably by free radicals in the cavitation bubbles during the preparation of the sonicated phospholipids suspension in water. However, it is difficult to guarantee a minimum lipid oxidation level by control of temperature [33, 201], due to ultrasonic irradiation of water develops $^{\bullet}OH$ and hydrogen peroxide, which also contributes for lipid oxidation [29]. According to Kruus *et al.* [112], the formation of free radicals is not a major problem when low frequencies (≈ 20 kHz) and short sonication times (≈ 20 min) are used. High temperatures accelerate phosphocholine hydrolysis; however according to Rabinovich-Guilatt *et al.* [113] a temperature of 50 ºC over 24 h induces only 1.6% of phosphocholine hydrolysis. Therefore, this hydrolysis should be negligible with these working conditions. This is extreme important, as the principle goal is the entrapment of peptides in liposomes and the protection of these peptides against the free radicals produced by sonication.

In order to minimise the oxidation, sonication was carried out in time intervals of 3 min and the temperature was controlled during all the experiment using a thermo-stated bath.

After pointing all these parameters for the characterization of liposomes, the incorporation of two different peptides on the LUVs was studied. The peptides were formulated together with a lipid, dipalmitoylphosphatidylcholine (DPPC), which was added to attain a peptide formulation compatible with a water environment.

Due to the large size of the Leucine side chain, the synthesized peptides tend to acquire an alpha helix structure in water. The interaction with phospholipids could further stabilize the alpha helix structure [219, 220]. However, the exact structure of these peptides in water is yet to be confirmed.

The peptide sequences were visualized by a molecular modelling program to identify the major differences in their structure (Figure IV-2). The molecular modelling program allows the creating of the structure based on the a.a. sequence, which differs in the position of the charged group (Lysine represented as K) in the sequence of peptides.

Figure IV-2 shows the structures of C-term and N-term peptides in vacuum. Besides illustrating the amphiphatic nature of the alpha-helix, it also indicates a much narrower spatial distribution of the positively charged side chains in the peptides. These peptides tend to be, therefore, both amphipathic and cationic. Amphipathicity increases their affinity for biological membranes, while the positive charge increases their specificity toward negatively charged membranes [219, 220].

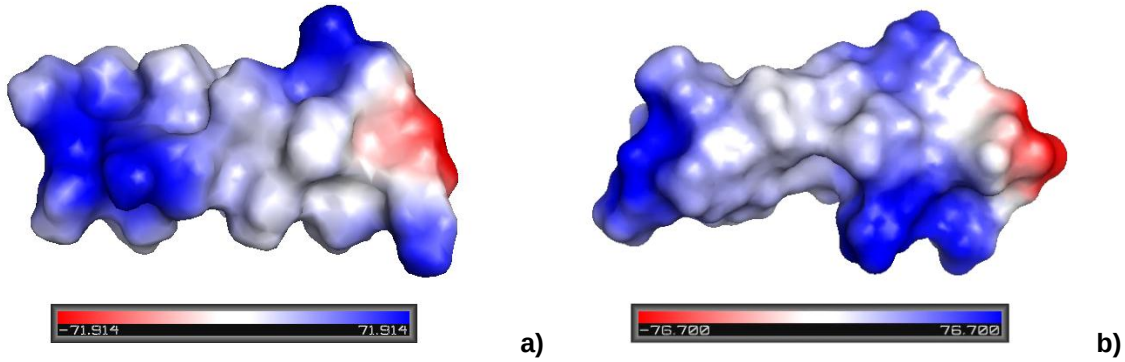

Figure IV-2: Surface charge analysis for the C-term and N-term peptides (a: LLLLKLLLLKLLLLKLLLLK, b: LLLLLLCLCLLLKAKAK), attained by PyMOL v0.99. Red denotes the negatively charged C-terminus while blue denotes the positively charged side chains. The scale represents the charge potential.

It was previously described that different depths and amplitudes have different effects on liposomes. For this reason the extent of this influence was investigated when the peptides were incorporated on liposomes. The peptides inserted on liposomes were sonicated at the minimum amplitude (20%) and the maximum amplitude (40%).

Figure IV-3 shows the influence of power at 19 mm and 38 mm positions, on the LUVs size and PDI. Lower sizes were obtained with 19 mm of depth, most likely due to the higher production of $^{\bullet}OH$ that are related with higher effects of the cavitation phenomenon. The use of the higher amplitude (40%) promoted

size decreases in both peptide formulations. The higher power is associated with greater mixing, promoting a more homogeneous solution and it is possible to obtain particles with lower size and with lower polydispersity.

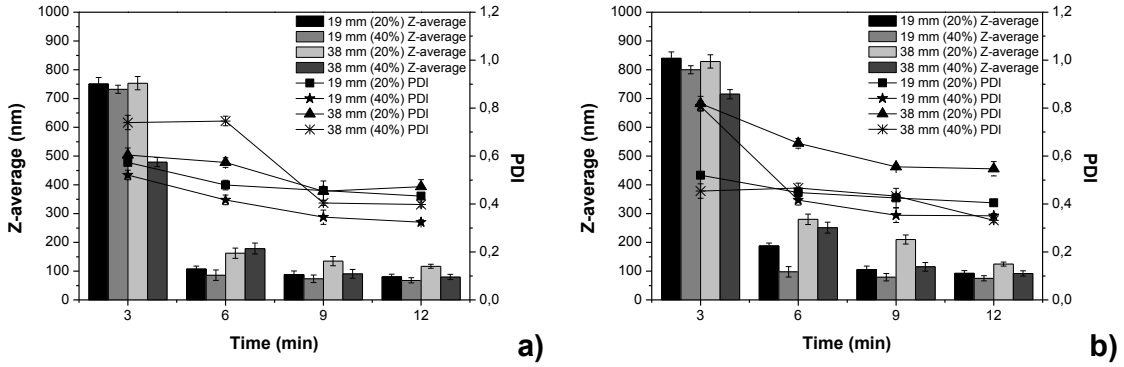

Figure IV-3: Z-average (nm) and PDI values for peptides (5 µM; a: LLLLKLLLLKLLLLKLLLLK, b: LLLLLLCLCLLLKAKAK) entrapped on liposome (1500 µM, pH=7.4) using different depths (19 and 38 mm) and amplitudes (20 and 40%) after 3, 6, 9 and 12 min of sonication, at 50 ºC.

Figure IV-4 shows the influence of sonication on membrane surface of liposomes with the peptides. The Lysine a.a. (indicated in bold) of the peptide LLLL**K**LLLL**K**LLLL**K**LLLL**K** are positively charged, and therefore they can be located on the polar surface of liposomes resulting in an increased positive charge and consequently an increase in the zeta-potential values. Although, compared with the other peptide motif the presence of one more Lysine residue can also lead to an increase on the zeta-potential value.

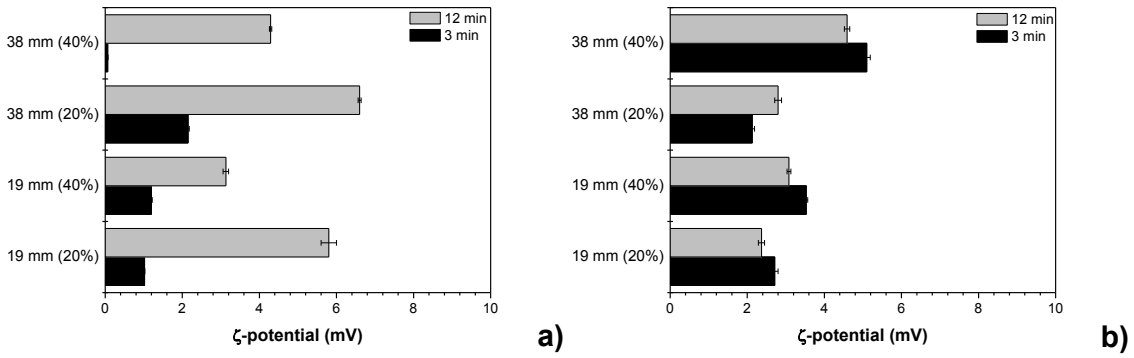

Figure IV-4: Zeta (ζ) -potential (mV) values for peptides (5 µM; a: LLLLKLLLLKLLLLKLLLLK; b: LLLLLLCLCLLLKAKAK) entrapped on liposome (1500 µM, pH=7.4) using different depths (19 and 38 mm) and amplitudes (20 and 40%) after 3 and 12 min of sonication, at 50 ºC.

Conversely, for the other peptide (LLLLLLCLCLLL**K**A**K**A**K**), the values of zeta-potential do not change significantly, here the Lysine a.a. residues are at the extremity of the fragment, allowing the positioning of the other a.a. residues (Cysteine, Alanine and Leucine) to the inside of the liposome as they are more hydrophobic. The zeta-potential values for the maximum of amplitude (40%) were very similar to the results with minimum of amplitude (20%).

Samples of each peptide were analysed by SEM, after treatment with ultrasound at 19 and 38 mm of depth and 40% amplitude. The photographs were taken at different magnifications of x50, x800, and x5000. Figure IV-5 shows that peptide LLLLKLLLLKLLLLKLLLLK has an ‘‘amorphous” aspect, possibly due to the positively charged Lysine amino acid (K) distributed in the sequence of peptide.

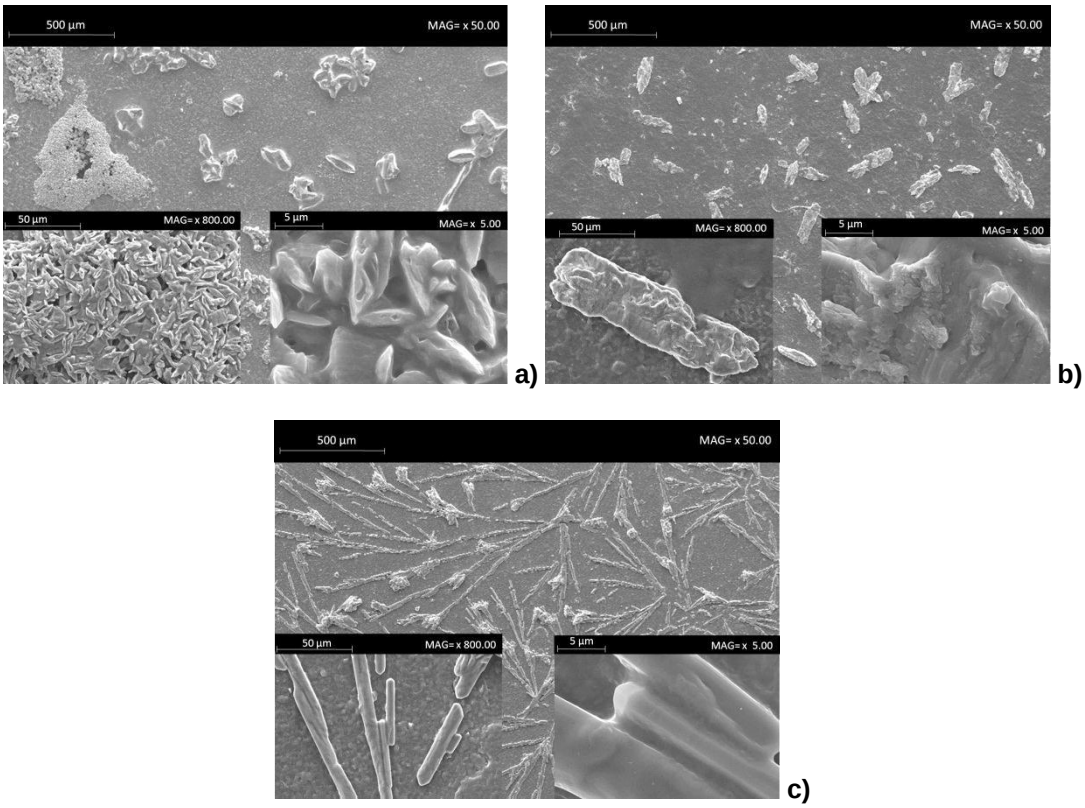

Figure IV-5: SEM microphotographs: a) DPPC; b) LLLLKLLLLKLLLLKLLLLK; c) LLLLLLCLCLLLKAKAK, after 12 min of sonication at 19 mm of depth and 40% of amplitude (the samples were dried after ultrasound treatment), using different magnifications (x50; x800; x5000).

The peptide with the amino acid Cysteine (LLLLLLCLCLLLKAKAK) and with the positive charge on the C-terminal presented a defined rod shape. This

suggests that the peptide can have their hydrophilic part (positive charge) oriented towards the polar part of the lipid bilayers while their hydrophobic segment (not charged) is in the upper part and between lipophilic tails.

Figure IV-6 shows differences between these two peptides that were analysed, nevertheless these differences are not so pronounced when the 38 mm of depth was used. This fact can be related with the effect of cavitation that is more prominent at 19 mm due to an increased production of $^{\bullet}OH$ (anti-nodal point).

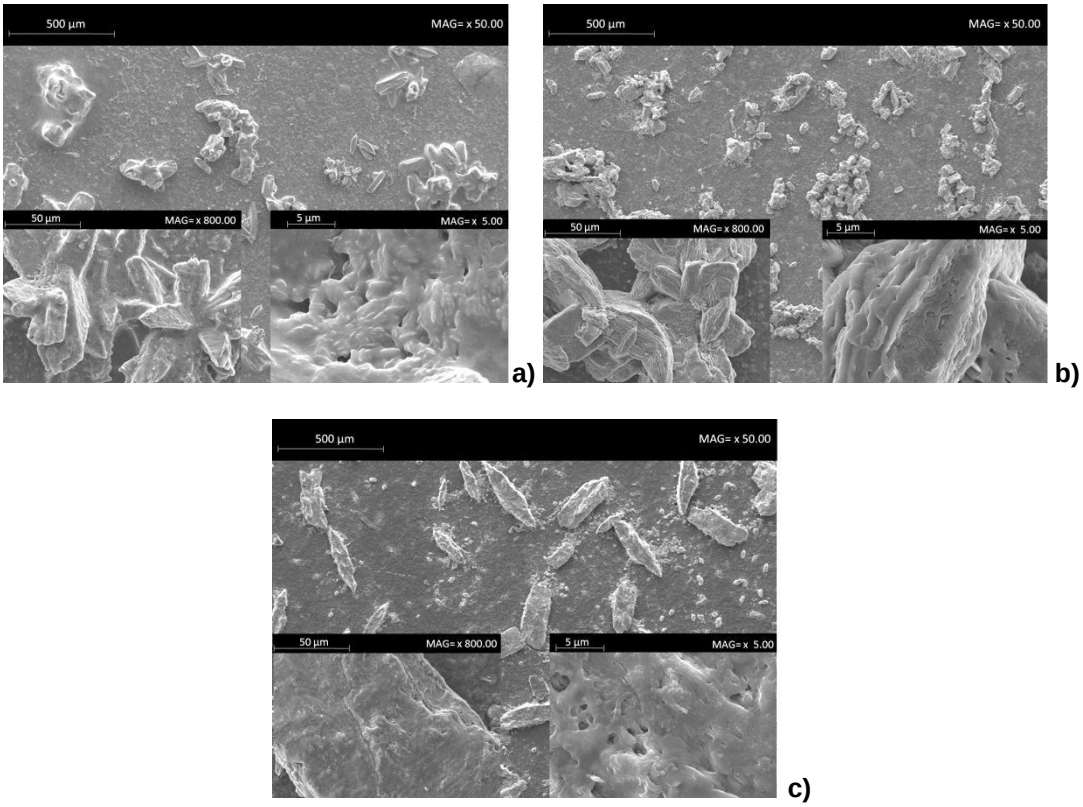

Figure IV-6: SEM microphotographs: a) DPPC; b) LLLLKLLLLKLLLLKLLLLK; c) LLLLLLCLCLLLKAKAK, after 12 min of sonication at 38 mm of depth and 40% of amplitude (the samples were dried after ultrasound treatment), using different magnifications (x50; x800; x5000).

IV-4. CONCLUSIONS

This study shows the three principal factors of ultrasound that could influence the ranges of sizes and zeta-potential: depth, amplitude and time of treatment.

The results from zeta-potential measurements and SEM analysis demonstrated that the insertion of peptides led to a change on the properties of lipidic membrane.

The size and PDI decreased with an increase of amplitude (40%) as the higher power exerts greater shear forces within the solution. The greater extent of streaming from the ultrasound source promotes greater mixing of the solution and consequently more homogeneity. At 19 mm a drop in the physical size and PDI was observed. At this depth the rate of radical production is higher, further promoting the decrease in liposomes size even when peptides are entrapped in phospholipids aggregates. This size reduction increases their surface area and consequently their ability for controlled release of peptides.

CHAPTER V

INSIGHTS ON THE MECHANISM OF PROTEIN MICROSPHERES FORMATION

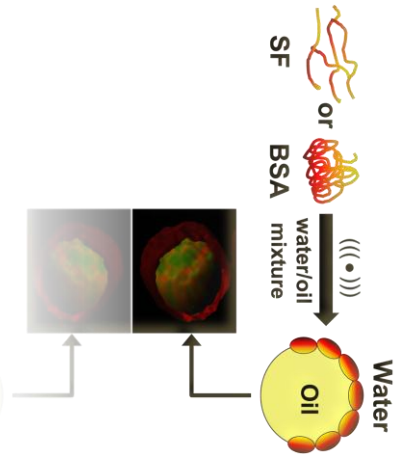

Chapter V

Insights on the mechanism of protein microspheres formation[§]

ABSTRACT

Protein microspheres of bovine serum albumin (BSA) and silk fibroin (SF) were obtained by applying high intensity ultrasound in a biphasic aqueous/organic system. In the study performed in Chapters III and IV, we demonstrated the influence of different parameters of ultrasound system, such as input energy on the reduction of liposome sizes.

In this Chapter, additionally with Suslick's protein microspheres production procedure, this parameter was taken into account for the production of protein structured materials.

The ratios of aqueous/organic phase and protein concentration were investigated on particles production. An increase on protein concentration promotes ≈100% of yield on particles formation, independently of aqueous/organic ratio that was used. It was found that these parameters prove to be an important tool to predict and control the sizes of particles ranging from 300 to 1500 nm. Furthermore, these proteinaceous spheres present a negative surface charge and have a high stability over four months.

The conformation assessment obtained with Fourier transform infrared (FT-IR) analysis show a change on the secondary structure of SF upon sonication treatment, presenting an increase on the amount of β-sheet. Conversely, the sonochemical treatment did not affect the secondary structure of the globular protein, BSA.

[§] This chapter is based on the following publication:
Silva R, Ferreira H, Araujo R, Azoia N, Rollet A, Angel U, Gomes AC, Freddi G, Güebitz G, Gedanken A, Cavaco-Paulo A, *Insights on the mechanism of protein microspheres formation*, submitted.

Molecular dynamic studies indicate that the protein have a change of conformation at water/oil interface and shows the importance of hydrophobic areas on the spheres stability. Those results were confirmed by confocal microscopy.

No significant cytotoxicity was found in a concentration range below 300 $mg.L^{-1}$. All those properties shown here, seems to indicate a great potential for several biomedical applications, such as a vehicle for controlled release of drugs.

V-1. INTRODUCTION

The ability to fabricate, characterize and manipulate artificial and natural structures, whose features are controlled at the micro/nano level, has gained considerable attention in recent years [41, 42, 221-224].

Among these micro/nano devices, the ones based on proteins may be rather promising, since they are biodegradable and non-antigenic [23, 66, 136, 225]. In the late 1960s, a modified polymerization method for the preparation of proteinaceous microspheres was developed by Rhodes and co-workers [156]. The microspheres formation was accomplished by a modified emulsion polymerization method, using either heat denaturation at various temperatures or a cross-linking agent, such as glutaraldehyde. However, this method yields microspheres with a short storage life, low stability and high toxicity.

A sonochemical method has been developed by Suslick and co-workers for the synthesis of nonaqueous liquid-filled microcapsules and air-filled microbubbles [44]. Suslick has shown that micrometre sized gas- or liquid filled proteinaceous microspheres can be produced from various kinds of proteins, such as bovine serum albumin (BSA), human serum albumin (HSA) and hemoglobin (Hb) [44-48]. Suslick reports on microspheres at high concentrations with a long shelf life and high stability. The mechanism of proteinaceous microspheres' preparation obtained by the sonochemical method has been discussed previously and is a direct result of the chemical effects of ultrasound irradiation on an aqueous medium [44]. Indeed, the microspheres formation is a combination of two acoustic phenomena: emulsification and cavitation.

Ultrasonic emulsification creates the microscopic dispersion of the protein solution necessary to form the shape of the proteinaceous microsphere shell. On the other hand, ultrasonic irradiation of liquids produces acoustic cavitation: the formation, growth and implosive collapse of bubbles, which creates transient hot-spots with enormous peak temperatures and production of free radicals [22, 25, 199]. The superoxide radical ($O_2^{-\bullet}$) can create inter-protein disulphide bonds, that cross-link the proteins [44-48]. However, Gedanken and co-workers have been shown that it is possible to form microspheres with proteins that did not

comprise the Cysteine amino acids (a.a.) in their structure, as streptavidin or poly (Glutamic acid) [51]. According to their explanation, hydrophobic interactions or thermal denaturation of the protein after the initial ultrasonic emulsification assists in microspheres formation [51]. Several works [44, 51, 55, 65, 67, 226] have already been performed to clarify the mechanism of proteinaceous microspheres formation by the ultrasound system, however, further complementary studies are needed to establish the mechanism of their formation.

It is our particular interest to engineer microspheres, using BSA and silk fibroin (SF), by ultrasonic method, based on Suslick's procedure [44] and on our previous results, for a better understanding of the mechanism of microspheres formation.

Albumins are globular proteins that are characterized by a low content of hydrophobic a.a. and a high content of Cysteine (seventeen disulphide bonds and one sulfhydryl group) and the charged a.a., Aspartic and Glutamic acids, Lysine and Arginine [150, 155, 227]. Conversely, SF is a fibrous protein and is mainly composed of hydrophobic a.a., without Cysteine residues in its structure. The a.a. composition of SF from *Bombyx mori* is characterized by a high content of Glycine, Alanine and Serine, whose total share in the protein 85 mol %, Tyrosine accounts for 5.3 mol %, and acidic and basic a.a. total is about 3.0 and 1.1 mol %, respectively [184, 228]. This characteristic of a.a. pattern results from the contribution of two polypeptides, i.e., the heavy and light chains. The heavy chain represents about 90% of the total weight of SF and is predominated with its characteristic -(Glycine-Alanine)$_n$- rich sequences over the more heterogeneous primary structure of the light chain [159, 160].

To find the arrangement of different proteins in microspheres structure we analysed and characterized the particles, submitting them to different techniques.

The ability of proteins to form microspheres was studied quantifying the protein concentration, by the Lowry assay [191], on the supernatant, after ultrasound treatment. The influence of the sonochemical method on secondary structure of proteins was determined by Fourier transform infrared (FT-IR) spectroscopy. Particle size as well as the polydispersity index (PDI) of microspheres was evaluated by photon correlation spectroscopy (PCS). It is well

known, that the particle size can significantly affect the properties of the microspheres and is important for their interaction with the biological environment, e.g., as concerns their ability to pass fine capillaries or to leave the vascular compartment via fenestrations after intravenous administration [187]. In addition to the determination of size and its distribution, the zeta-potential was also evaluated by electrophoretic laser Doppler anemometry, to obtain an indication of microspheres surface potential. Since the surface potential of the particles cannot be measured directly, the zeta-potential (electrical potential at the surface of hydrodynamic shear around the colloidal particle) is usually determined as a characteristic parameter for the microparticle charge. This parameter can also allow us to predict physical stability of microspheres dispersion [229]. In fact, the zeta-potential is an important feature for the particle, because a more pronounced zeta-potential value, either positive or negative, favours the particle-suspension stability [230, 231].

The electron microscopic techniques in particular have been employed to characterize the overall structure and shape of the microspheres. In this study, the scanning transmission electron microscopy (STEM) was applied. A lipophilic fluorescent probe was incorporated into the protein microspheres and analysed by confocal microscopy, providing a refined data set and, ultimately, a more precise evaluation of protein arrangement. Additionally, molecular dynamic studies were monitored in order to study the protein performance in aqueous/organic interface. Finally, microspheres were screened for cytotoxicity using a human cancer cell line (RKO) by means of performing a MTT [3-(4,5-dimethylthiazol-2-yl)-2,5-diphenyltetrazolium bromide] assay.

V-2. MATERIALS AND METHODS

V-2.1. Preparation and characterization of protein microspheres

Protein microspheres were prepared according with the method previously described in the Chapter II. The proteinaceous microspheres were produced using different protein concentrations of BSA (0.1; 0.5; 1.0 and 5.0 $g.L^{-1}$) and SF (1.0; 3.0; 5.0 and 10.0 $g.L^{-1}$) and different aqueous/organic ratios [60/40;

80/20 and 95/5 (%)]. The organic solvent used in all these experiments was the *n*-dodecane. The procedure for the further characterization is detailed also in Chapter II, namely: yield of microspheres formation; size and its distribution; zeta-potential, morphology (STEM technique), conformational assessment (FT-IR), confocal analysis, molecular dynamic simulations and stability studies. The cytotoxicity evaluation is described below.

V-2.2. *In vitro* cytotoxicity screening of protein microspheres

In order to evaluate the effect of the produced proteinaceous microspheres on cells, human colon carcinoma (RKO), from American type culture collection (ATCC), was used. The microspheres were previously sterilized via UV radiation during 2 h.

Cells were grown in Dulbecco's modified Eagle's medium (DMEM) with 10% (v/v) fetal bovine serum (FBS) supplemented with 1.0 mM sodium pyruvate, 1.5 $g.L^{-1}$ sodium bicarbonate and 1% (v/v) penicillin/streptomycin (Gibco, Invitrogen Corp., San Diego, California, USA). Cultures were maintained at 37 ºC in a humidified atmosphere containing 5% CO_2. The culture cells were seeded for 48 h prior to all experiments. Once reached ≈ 90% confluency, cells were detached using 0.05% trypsin/ethylenediaminetetraacetic acid (EDTA) and counted by means of hemocytometer. Cells were seeded in 24 well-plates at a density of $1x10^4$ $cells.mL^{-1}$ of medium, for 48 h, after which culture medium was removed and replaced by fresh medium. The cultivated cells were then treated with different concentrations of BSA microspheres (75, 150, 300, 600 and 900 $mg.L^{-1}$), prepared with different ratios of aqueous/organic phase (60/40, 80/20 e 95/5), for another 48 h. Culture medium alone, containing BSA solution and *n*-dodecane, were used as controls. *N*-dodecane at high percentage (40%) was used as positive control.

Several methodologies for cytotoxicity assay are described nowadays as standardized procedures. Cell viability in the presence of microspheres was evaluated by the MTT [3-(4,5-dimethylthiazol-2-yl)-2,5-diphenyltetrazolium bromide] reduction test as previously described [232]. Briefly, culture medium was removed and cells were washed twice with 500 µL of phosphate buffered

saline solution (PBS). A volume of 0.5 mL MTT (final concentration 0.5 $mg.mL^{-1}$, in PBS medium, pH = 7.4), prepared just before usage and maintained in the dark, was added to the RKO cells. Cells were incubated in the dark, for 2 h, at 37 ºC and 5% CO_2. MTT solution was removed and hydrogen chloride 0.04 M in isopropanol was then added, followed by incubation for 2 h, in the dark, to dissolve the formazan crystals. Finally, 100 µL of each well was transferred to 96 well-plates, in triplicates, and absorbance was read at 570 nm in a multiplate reader (Spectramax 340 PC). The survival of RKO cells was expressed as the percentage of absorbance towards control cells (containing only culture medium). Data are expressed as means with standard errors of the means. One way ANOVA followed by the Tukey´s Multiple Comparison test (GraphPad Prism 5.0 for Windows) was employed with statistically significant differences when $P < 0.05$.

All the experiments were performed in triplicate.

V-3. RESULTS AND DISCUSSION

In order to gain further insight into the mechanism and structure of proteinaceous microspheres formation, an extensive physico-chemical characterization was carried out. In this context, as just referred, two well-known proteins, with different contents of a.a. residues, namely BSA, that present higher content of Cysteine a.a., and SF, with no Cysteine residues in its structure, were used. This study was firstly performed using different protein concentrations and different ratios of aqueous/organic phase (water/*n*-dodecane). The ratios of aqueous/organic phase (%) used were: 95/5, 80/20 and 60/40, and for each of these ratios the following concentrations of BSA were employed: 0.1; 0.5; 1.0 and 5.0 $g.L^{-1}$. For SF the following amounts used for each ratio were: 1.0; 3.0; 5.0 and 10.0 $g.L^{-1}$.

SF concentrations used were higher than BSA concentrations, once that with SF concentrations below to 3.0 $g.L^{-1}$ we could not achieve microspheres. This result can be related with the micellization process, in which the polymers tend to self-assemble into geometric (disks, spheres, cylinders) shapes and become suspended in the solution. However, this phenomenon occurs only when the polymer concentration exceeds a threshold known as critical micelle

concentration (CMC). Considering this explanation, one may anticipate that the proteins would be dispersed in a solution below a critical concentration, and will start only to form microspheres at or above that concentration.

V-3.1. Yield of microspheres

Firstly, the efficiency of microspheres formation was monitored by Lowry assay [191]. The effects of protein concentrations and the different aqueous/organic phase ratios used on microspheres formation are shown in Figure V-1. From this figure, it is concluded that as the concentration of protein increases, the microspheres yield increases. It was reached the maximum yield near to 100% at concentration of 5.0 $g.L^{-1}$ and 10.0 $g.L^{-1}$ for BSA and SF, respectively. Conversely, for lower concentrations the yield obtained was significantly different for ratios of 80/20 compared to 95/5. These results, for the lower concentrations (0.1, 0.5, and 1.0 $g.L^{-1}$ for BSA and 3.0, and 5.0 $g.L^{-1}$ for SF), can be explained by the low frequency of the collision of BSA and SF molecules and the density of the microparticle membrane, which in turn decreases the yield of microsphere obtained. The influence of the *n*-dodecane volume fraction on the microspheres formation yield becomes remarkable only when lower protein concentrations are used. For these amounts a higher content of *n*-dodecane promotes higher efficiency of particles formation. This assay further suggests that for the more concentrated protein solutions the yield was approximately 100% for all the ratios tested.

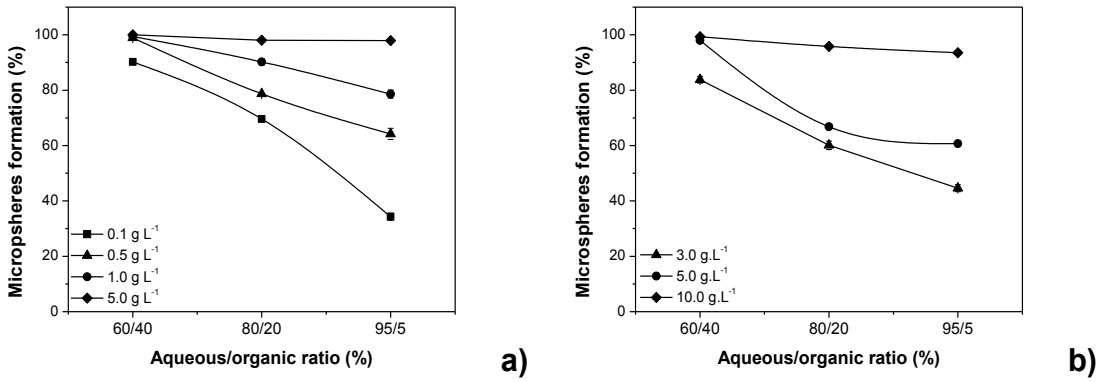

Figure V-1: Yield of BSA (a) and SF (b) microspheres formation using different aqueous/organic ratios (%; 60/40; 80/20 and 95/5) and different protein concentrations (0.1; 0.5; 1.0; 5.0 $g.L^{-1}$ for BSA and 3.0; 5.0; 10.0 $g.L^{-1}$ for SF).

In order to study the different behaviour of microspheres formation for each protein, the initial protein concentration was plotted *versus* levels of protein included in microspheres, suggesting a saturation level relationship as described in Equation V-1. k is a partition constant indicating the tendency of protein to be located at the oil (*n*-dodecane) interface and obviously dependent on the aqueous/oil ratio, and c is the initial protein concentration. Γ_{max} is the maximum amount of protein adsorbed as c increases, and this value was fixed at 100%. In all tested aqueous/*n*-dodecane concentrations potentially 100% of protein tends to stabilize the microspheres.

$$\%\,\mathrm{Protein\ in\ microspheres} = \Gamma_{max}\frac{k \times c}{1 + k \times c}$$

Equation V-1: Saturation level relationship of protein microspheres formation.

The plot concentrations of protein in microspheres as a function of initial protein concentration in solution are shown in Figure V-2.

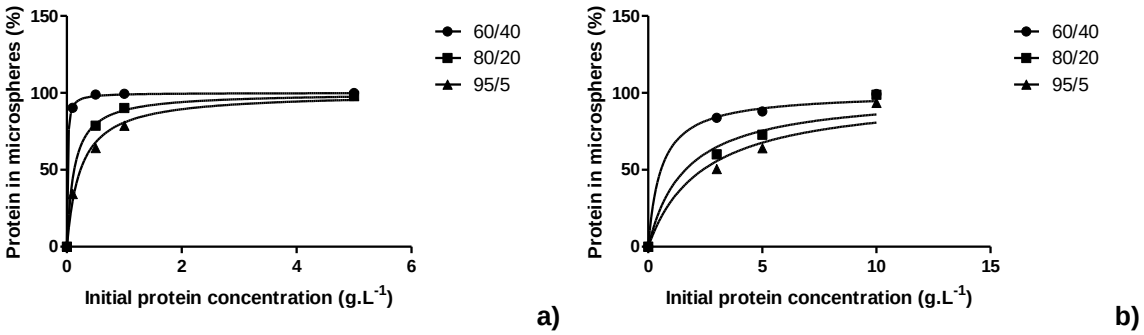

Figure V-2: Saturation curves of BSA (a; 0.1; 0.5; 1.0; 5.0 g.L^{-1}) and SF (b; 3.0; 5.0; 10.0 g.L^{-1}) in the microspheres formation. The curve represents the best fit to Equation V-1.

A nonlinear regression fit of Equation V-1 to the experimental data yielded values of k for BSA and SF (Table V-1). In Figure V-2 all isotherms show a sharp initial rise and then reach maximum adsorption amounts (plateau).

The data in Table V-1 indicate that the k values increase when higher amount of organic phase is added. Thus, the present results demonstrate a higher adsorption of protein when 60/40 of aqueous/organic ratio was used, which corroborate the yield of microspheres formation.

The k values for SF particles present a significant difference when compared with BSA k values. This difference of values can be due to the chemical structure of SF and BSA protein. As just referred, BSA is a globular protein with high content of Cysteine residues and charged a.a.. The use of ultrasound will allow the interactions of charged a.a. with the aqueous phase and the hydrophobic a.a. with the organic phase. Additionally, the presence of Cysteine residues led to the formation of robust bonds (disulphide bonds), which can explain the higher protein adsorption on microspheres formation. On the other hand, in a SF aqueous solution the hydrophobic segments and hydrophilic segments are supposed to disperse randomly [233, 234]. Therefore, the SF molecules have the ability for self-assembly under specific conditions, such as ultrasound conditions. However, the chemical and physical stimulus promoted by ultrasound was not sufficient to obtain higher protein adsorption when compared with BSA microspheres.

Table V-1: Adsorbed protein in microspheres obtained for: BSA (0.1; 0.5; 1.0 and 5.0 g.L^{-1}) and SF (3.0; 5.0 and 10.0 g.L^{-1})

Aqueous/organic ratios (%)	Adsorbed protein in microspheres (L.g^{-1})	
	BSA	SF
95/5	4 ± 0.5	0.4 ± 0.09
80/20	7 ± 0.4	0.6 ± 0.09
60/40	95 ± 6.0	2 ± 0.3

V-3.2. Fourier transform infrared (FT-IR) analysis of proteinaceous microspheres - Conformational assessment

The conformational changes in secondary structure for BSA and SF microspheres were explored. Infrared spectroscopy is a well-established method for the analysis of protein secondary structure. Characteristic bands found in the infrared spectra of proteins and polypeptides include the Amide I, Amide II and

Amide III. These arise from the amide bonds (-CONH-) that link the a.a.. The absorption associated with the Amide I vibrational band is assigned to stretching vibrations of the C=O bond of the Amide and it is detected in the range of 1700-1600 cm^{-1}. Absorption associated with the Amide II band, which falls in 1540-1520 cm^{-1} region, is attributed to the N-H bending and C-H stretching vibrations [235, 236].

In this work it was carried out a deeper study on Amide I band to probe the microspheres' secondary structure. Studies with proteins of known structure have been used to correlate systematically the shape of the Amide I band to secondary structure providing a powerful tool in the analysis of the secondary structure of proteins in aqueous solutions [237, 238]. The Amide I band of proteins typically consists of many overlapping component bands that represent different structural elements such as α-helices, β-sheets, turns and non-ordered or irregular structures. Therefore, the individual component bands cannot be resolved in the experimental spectra. The Fourier deconvolution procedure, sometimes referred as "resolution enhancement" involves narrowing the widths of infrared bands, allowing increased separation of the overlapping components present within the broad band envelope [237-239].

BSA has a globular protein and its secondary structure consists of mainly α-helices [155, 240-242]. For SF untreated samples Silk I (Random coil) conformation is confirmed by intense bands at 1411, 1380, 1334 cm^{-1}, which are considered marker bands for this structure [184]. Table V-2 presents the detailed information of Amide I deconvolution for BSA and SF microspheres obtained. In this approach, the Amide I band was transformed to yield a fitted self-deconvoluted set of bands from which the secondary structure was determined. BSA microspheres presented the same content of α-helix in their structure and the microspheres synthesis by sonochemical method did not disturb the integrity of the protein structure. On the other hand, for SF the deconvolution resulted in an increase of β-sheet content. This data indicates that through microspheres formations, SF acquires mainly a β-sheet conformation, induced by the ultrasound radiation. As a consequence of the sonochemical process, the molecular chains became closer increasing the interactions of side chain groups promoting a higher cristallinity in the microspheres formation.

The FT-IR results show that the secondary structure of fibrous proteins was changed, while globular proteins retain their secondary structure upon the sonication treatment.

Table V-2: Results from the curve fitting of Amide I range of the FT-IR spectrum of proteinaceous microspheres prepared with 5.0 g.L^{-1} of BSA and 10.0 g.L^{-1} of SF, using 60/40 of aqueous/organic ratio

	BSA		SF	
	Untreated[a]	**Micropshere**	**Untreated[b]**	**Micropshere**
β-Sheet	48-32%	39%	29%	59%
α-Helix	52-68%	61%	-	-
Random coil/Silk I	-	-	43%	15%
Turns and bends	-	-	27%	25%

[a] Based on literature values [155, 240, 241].

[b] Based on previous published results of our work group [184].

V-3.3. Particle size and its distribution

The influence of the two different parameters previously considered (aqueous/organic ratios and protein concentrations) was also analysed in terms of size and its distribution for both proteins.

The results are presented in Figure V-3. Data show that particle size is directly related with protein concentration and aqueous/organic ratio.

Figure V-3 highlights the fact that when lower quantity of organic phase and higher protein concentrations are used it is possible to obtain a narrower size distribution of proteinaceous microspheres with a smaller size (nanometre level). An increase of the protein concentrations in the solution, promotes the formation of less polydisperse particles with a smaller size, which can be explained by higher concentration of protein that can wrap the formed microspheres and prevent the growth more easily [243]. However, when the sizes obtained for BSA

and SF microspheres were compared it was found that smaller sizes were achieved for BSA microspheres.

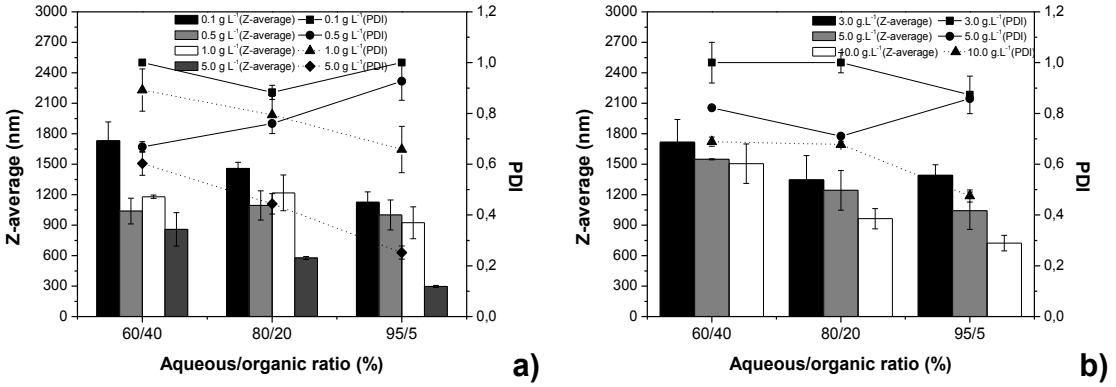

Figure V-3: Particle size (Z-average; nm) and PDI for BSA (a) and SF (b) microspheres, using different aqueous/organic ratios (%; 60/40; 80/20 and 95/5) and different protein concentrations (0.1; 0.5; 1; 5.0 g.L^{-1} for BSA and 3.0; 5.0; 10.0 g.L^{-1} for SF).

According with the results from literature, the formation of the disulphide bonds is the main explanation for BSA microspheres formation, as well as for all proteins containing Cysteine a.a. in their composition [44]. Contrariwise, SF, as just referred, is a fibrous protein and is essentially composed by hydrophobic a.a. with the capacity for self-assembly. Additionally, the secondary structure of SF microspheres shows the formation of crystalline regions that encourage an increase on molecular interactions. However, these hydrophobic interactions were not sufficient to promote the decrease of size. The dimensions and shapes of the supramolecular structure formed from such assemblies depend on a variety of factors, such as geometry of polar head group, and also the shape and the position of each molecule in the protein microsphere [231].

The results obtained can support the idea that the linearity of sizes is directly related to the protein structure, protein concentration and the fraction of *n*-dodecane used. Therefore, it can be concluded that all these parameters considered can affect the microspheres sizes to a certain extent.

V-3.4. Surface charge determinations

The measurement of the surface charge of microspheres showed that

independently of aqueous/organic ratio and concentrations used, they present negative surface charge. Their zeta-potential values varied around -45 mV and -38 mV for the suspension of the BSA and SF, respectively. In most circumstances, the higher the absolute value of the zeta-potential of the microspheres, the larger the amount of charge on their surface, which produces stronger repellent interactions among the microspheres dispersed in the buffer/water and thus resulting in higher stability [230].

V-3.5. Morphology

Figure V-4 shows the STEM photographs obtained for the BSA and SF microspheres. This figure illustrates that these proteinaceous microspheres are clearly spherical homogeneous particles with smooth surfaces. The morphology of spherical shape would offer the highest potential for controlled release and protection of incorporated drugs, as they provide minimum contact with the aqueous environment, as well as the longest diffusion pathways. Comparing particles with any other shape, spherical particles also require the smallest amount of surface-active agent for stabilization, because of their small specific surface area [187]. Moreover, our findings are also consistent with PCS results, since similar sizes were obtained.

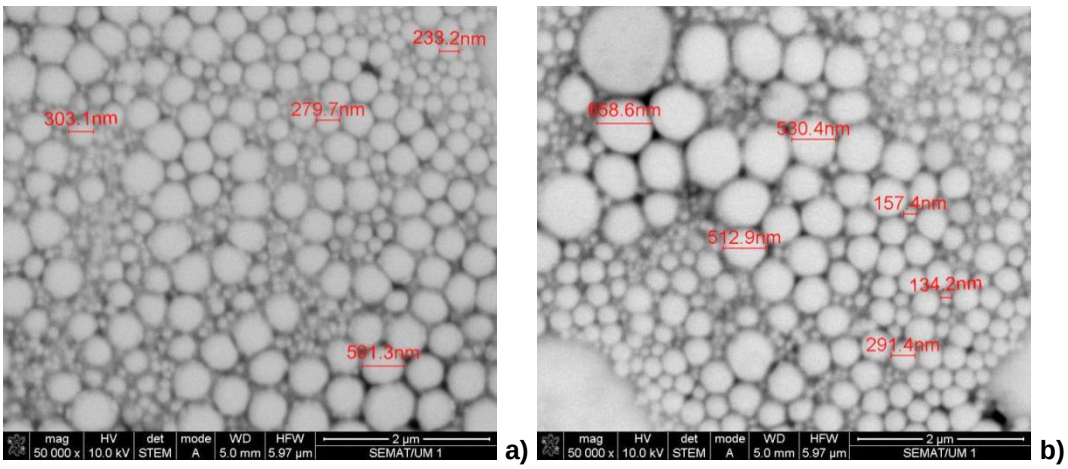

Figure V-4: STEM photographs (x50000 magnification) of proteinaceous microspheres: BSA (a) and SF (b) obtained using an aqueous/organic ratio (%) of 95/5 and with a protein concentration of 5.0 g.L^{-1} and 10.0 g.L^{-1} for BSA and SF, respectively.

V-3.6. Microspheres stability

On microspheres research, suspension stability is other important parameter in materials characterization. Since those colloidal particles can suffer aggregation over time [244], it was made an evaluation of particle size for four months, to assess their physical stability. The zeta-potential was also determined, since this parameter of colloidal particles, due to degradation of some components, can also change over storage time [245]. The data obtained demonstrate a high stability for microspheres using the highest protein concentration. Figure V-5 shows the particle size and the zeta-potential values for BSA and SF microspheres prepared with 5.0 $g.L^{-1}$ and 10.0 $g.L^{-1}$, respectively using different aqueous/organic ratios (60/40; 80/20 and 95/5). Comparing the different fraction of organic phase it can be seen that the microspheres obtained with 5 and 20% of *n*-dodecane, aggregate after three months of storage. It was observed an increase in microspheres sizes distribution and also a tendency of zeta-potential to attain lower negative zeta-potential values.

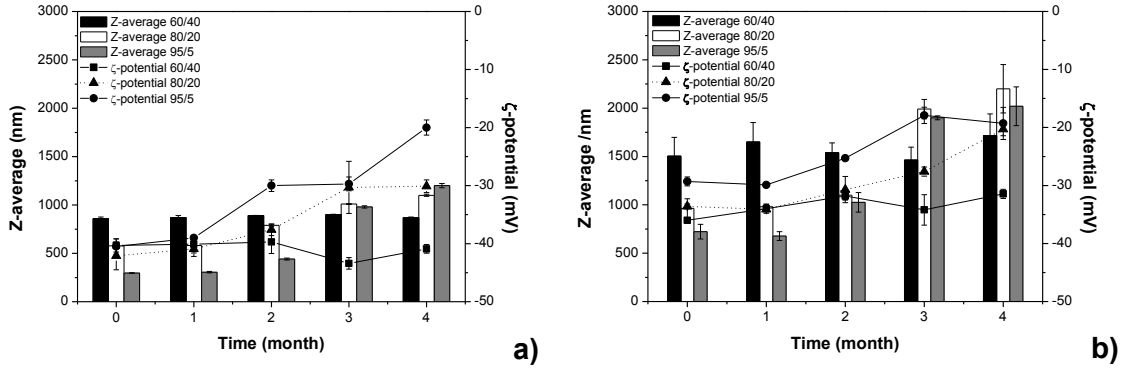

Figure V-5: Particle size (Z-average; nm) and zeta (ζ) -potential (mV), over four months, for BSA (a) and SF (b) microspheres prepared with 5.0 $g.L^{-1}$ and 10.0 $g.L^{-1}$, respectively, for different aqueous/organic ratios (%; 60/40; 80/20 and 95/5).

For BSA concentrations range between 0.1-1.0 $g.L^{-1}$ and SF with 3.0-5.0 $g.L^{-1}$ the particle stability is lower for all ratios used. However, considerable differences between these two proteins were obtained. Figure V-6 shows that after two weeks of storage it was observed an increase on size distribution and the zeta-potential was near to zero, for SF microspheres (5.0 $g.L^{-1}$). Conversely, BSA microspheres (1.0 $g.L^{-1}$) instigated signs of instability only after one month of

storage. This difference can be explained by disulphide bonds present on BSA that forms a robust interaction promoting an increase on microspheres stability. Although, SF can be organized into a well-defined and stable macroscopic structure, due to their hydrophobic interactions that is rather weak when compared with covalent bonds, mainly, when lower protein concentration is used. Considering these results, it is possible to conclude that microspheres prepared with 60/40 of aqueous/organic phase and with highest amount of protein (5.0 $g.L^{-1}$ and 10.0 $g.L^{-1}$ for BSA and SF, respectively) are stable for at least four months.

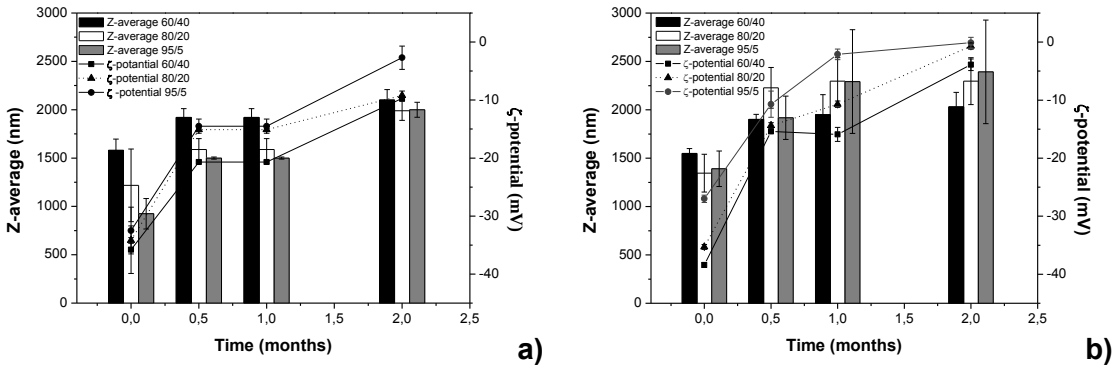

Figure V-6: Particle size (Z-average; nm) and zeta (ζ) -potential (mV) over two months for BSA (a) and SF (b) microspheres prepared with 1.0 $g.L^{-1}$ and 5.0 $g.L^{-1}$, respectively for different aqueous/organic ratios (%; 60/40; 80/20 and 95/5).

V-3.7. Confocal analysis

The confocal analyses allow us to predict the microspheres structure. For that two set experiments were performed. In the first set, proteins were labelled with fluorescein isothiocyanate (FITC; 495 nm/521 nm) and 1,1'-dioctadecyl-3,3,3',3'-tetramethylindodicarbocyanine perchlorate (DID), which is an hydrophobic probe with markedly red-shifted fluorescence excitation and emission spectra. In the second set, the Nile red was chosen because of its capacity of getting a range of fluorescent signals depending of chemical environment. Hydrophobic environments have signals at 489/509 nm (using the green fluorescent protein filter) and less hydrophobic have signals at 550/573 nm (using the rhodamine red dye filter). However, highly hydrophilic signals cannot be seen due to the lower partition coefficient in water [193, 194]. The Imaris

program enabled us to “cut” the microspheres into different planes, allowing us to locate the lipophilic probe in the particles.

Figure V-7 clearly demonstrate that the protein stay at aqueous phase (green colour), while the DID dye remains on the *n*-dodecane phase (red colour).

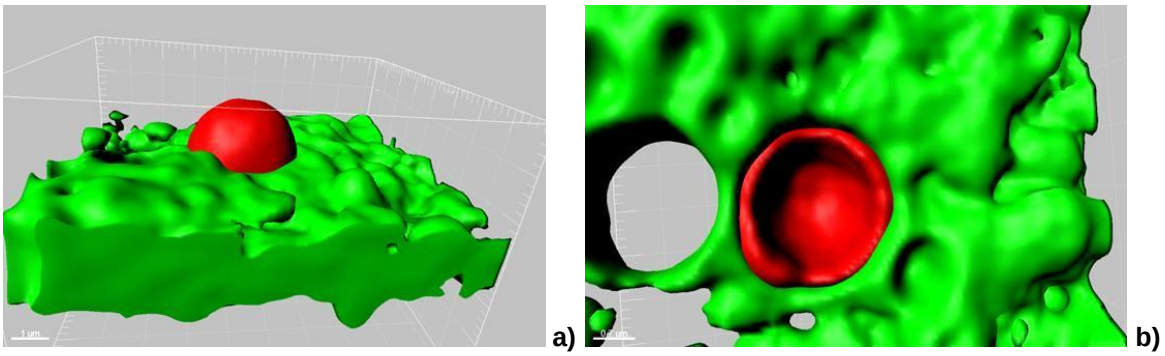

Figure V-7: **Three dimension photographs of microspheres prepared with BSA-FITC and with DID, using 60/40 of aqueous/organic ratio (%): a) side view and b) top view. The green colour represents the BSA-FITC and the red colour corresponds to DID. The BSA protein forms the microspheres walls and the DID is entrapped inside the liquid-filled proteinaceous microspheres.**

Furthermore, the results with Nile red emphasize the protein behaviour at aqueous/organic interface, presenting a green sign in a less hydrophobic medium, while in a polar solvent acquires red sign (Figure V-8 and Figure V-9). These results are also in agreement with the morphology studies.

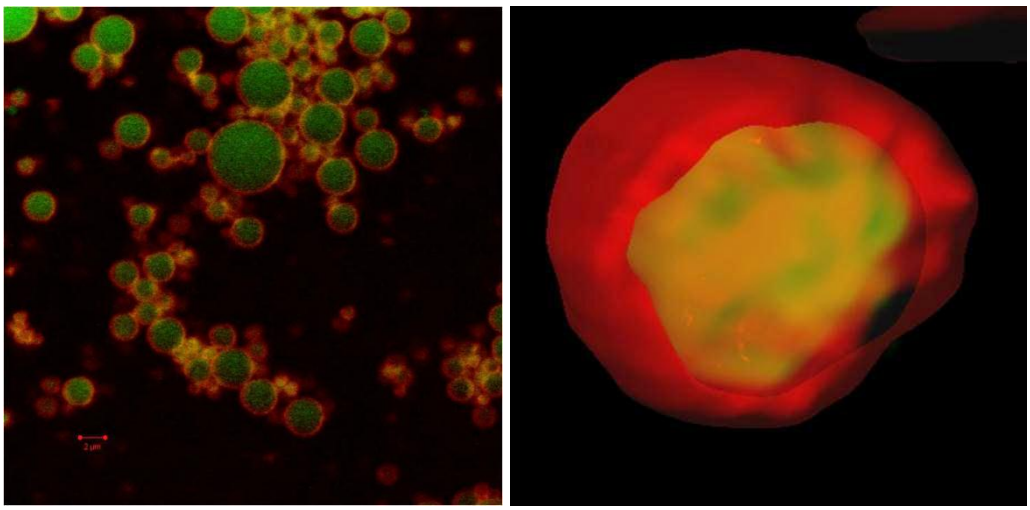

Figure V-8: **Photograph of microspheres prepared with BSA and with Nile red, using 60/40 of aqueous/organic ratio (%): fluorescent signs of Nile red in different medium (in organic solvent Nile red present green colour while in polar solvent acquires red colour).**

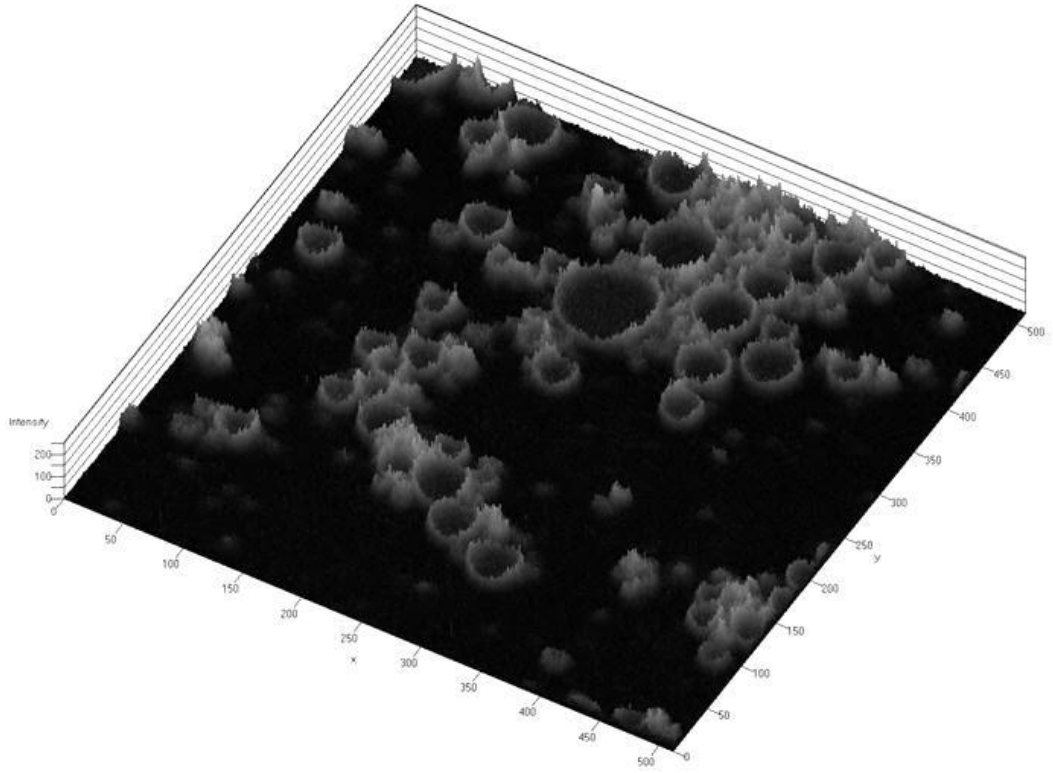

a)

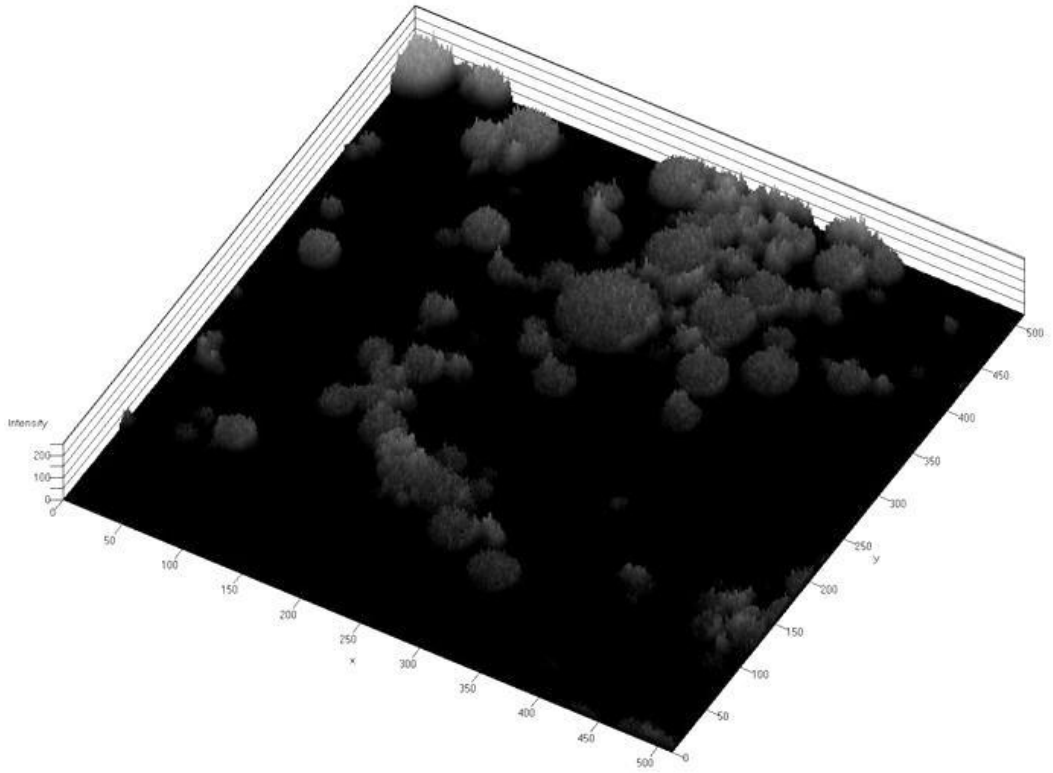

b)

Figure V-9: Photograph of microspheres prepared with BSA and with Nile red, using 60/40 of aqueous/organic ratio (%): a) Red sphere (in the polar solvent) and b) Green sphere (in the organic solvent), cutting in the middle.

V-3.8. Molecular studies of protein behaviour on biphasic system

To assess the behaviour of a globular protein, BSA, through ultrasound system, a molecular modelling study was performed by using GROMACS software [246] with the GROMOS (ffG53A6) force-field [247].

The sonication process was not easily simulated, but to obtain some realistic model, the *n*-dodecane molecules were added randomly and the empty space was filled with water. The procedure, where all the components are randomly distributed through space, seems to be the best way to simulate the sonication process.

The number of *n*-dodecane molecules was chosen so that the final solution is equivalent to a 1:1 mixture of water/*n*-dodecane (v/v). All the simulations were made at 300 K. The results represent 50 ns of simulated time.

Figure V-10 shows BSA in the interface between water and *n*-dodecane. The protein retains some water molecules in the surface interacting with *n*-dodecane, however, demonstrate a preferential orientation in the interface.

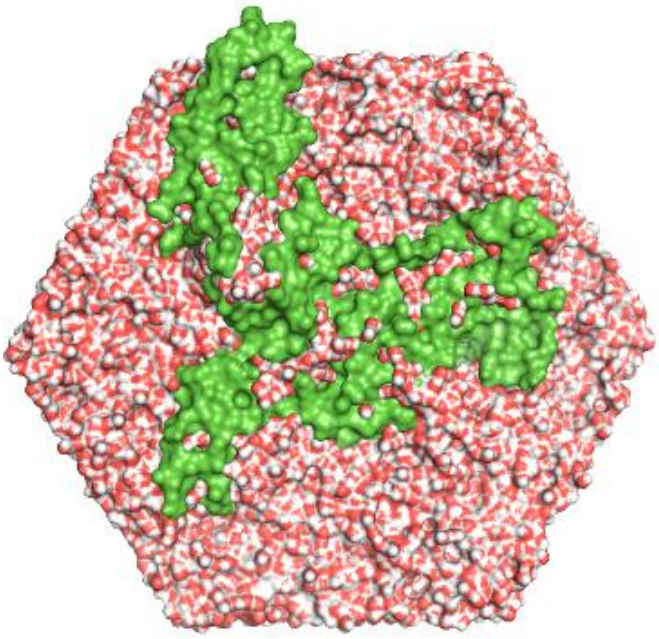

Figure V-10: Molecular dynamic simulation results of BSA in a 1:1 (v:v) mixture of water/*n*-dodecane. BSA (green) in the interface water (red and white)/*n*-dodecane (not shown). The BSA portion that is visible is interacting with *n*-dodecane.

Figure V-11 illustrate the differences between the surfaces of BSA in terms of potential. It is clear that the surface interacting with *n*-dodecane is more hydrophobic (the surface potential is near zero). In contrast, the surface interacting with water clearly has a negative surface potential.

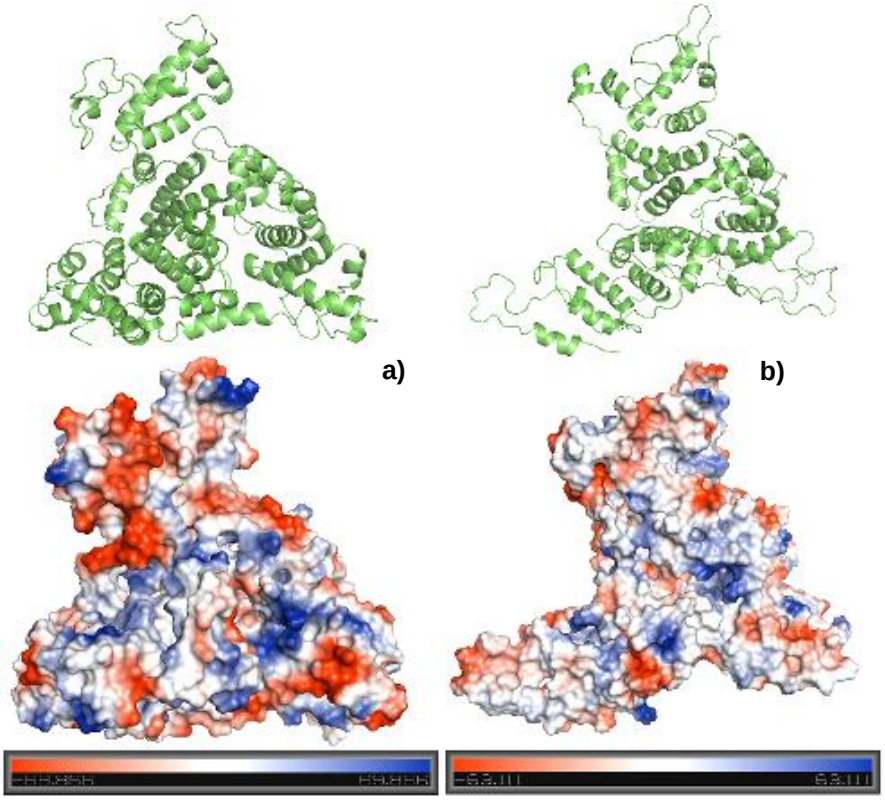

Figure V-11: Representation of the potential surface in vacuum: a) on the surface of BSA facing the water phase; b) on the surface of BSA that lies on the interface water/*n*-dodecane. The potentials were calculated using Pymol.

V-3.9. Proposed mechanism of microspheres formation

Proteins are considered as natural polymers that contain both hydrophobic and hydrophilic segments that could self-assemble in aqueous solution to form distinct structures, such as micelles, vesicles and tubules [248, 249]. SF amorphous regions are composed of a.a. with bulk side groups that have poor orientation, but the repeat a.a. sequence -(Glycine-Alanine)$_n$- tend to form a well oriented β-sheet crystalline regions. The polypeptide chains of BSA can be arranged into a compact globular form, due to the optimization of free energies of many noncovalent and disulphide bonds. Furthermore, a globular protein typically

consists of relatively straight runs of secondary structure joined by stretches of polypeptides that abruptly can change directions [227].

The mechanism of BSA microspheres formation has been described and as a direct result of S-S bonds formation between Cysteine residues of the protein in an oxidative environment promoted by sonochemical method [44]. Moreover, other chemical interactions are involved in this mechanism of proteinaceous microspheres formation, in particular when Cysteine residues are lacking in the protein sequence.

The higher shear forces produced by ultrasound will drive the orientation of polar and nonpolar groups in a biphasic system. The polar and charged side chains, and the polypeptides groups, will be able to form hydrogen bonds with water, but the nonpolar sides chains cannot. This side chains will tend to clump together in the oil droplet surface. This hydrophobic effect - the clustering of hydrophobic side chains from diverse parts of protein sequence - causes protein compactness. The "compactness" produces two favourable results: it minimizes the total hydrophobic surface area in contact with water, and brings the hydrophobic groups close to each other, allowing the van der Waals interactions between them. The hydrophobic interactions in proteins sum up to a substantial energetic contribution, promoting the formation and stabilization of spherical particle. Polar chains do not need to be protected from the solvent, because they can form hydrogen bond with water so they will tend to be distributed on the microspheres surface (Figure V-12).

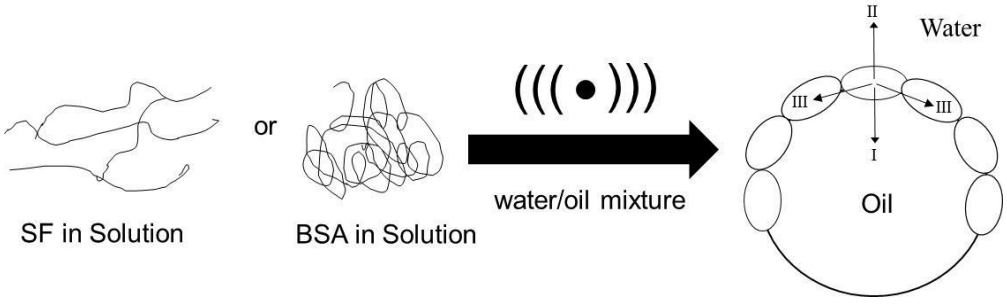

Figure V-12: Schematic representation of the different energy fields involved in formation and stabilization of proteinaceous microspheres, obtained by sonochemical method: I) hydrophobic interaction; II) hydrophilic interaction; III) protein-protein interactions.

V-3.10. Cytotoxicity evaluation

An important parameter that has to be evaluated for biomaterials to be used in medical applications is the cytotoxicity level. This was assessed to our materials through the use of human colon carcinoma (RKO). A RKO cell line was exposed to different concentrations of BSA microspheres, over a period of 48 h (Figure V-13).

Assessment of cell membrane integrity is one of the most common procedures to measure cell viability and cytotoxic effects. In our particular case it was performed by the use of MTT, which can be quantified spectrophotometrically.

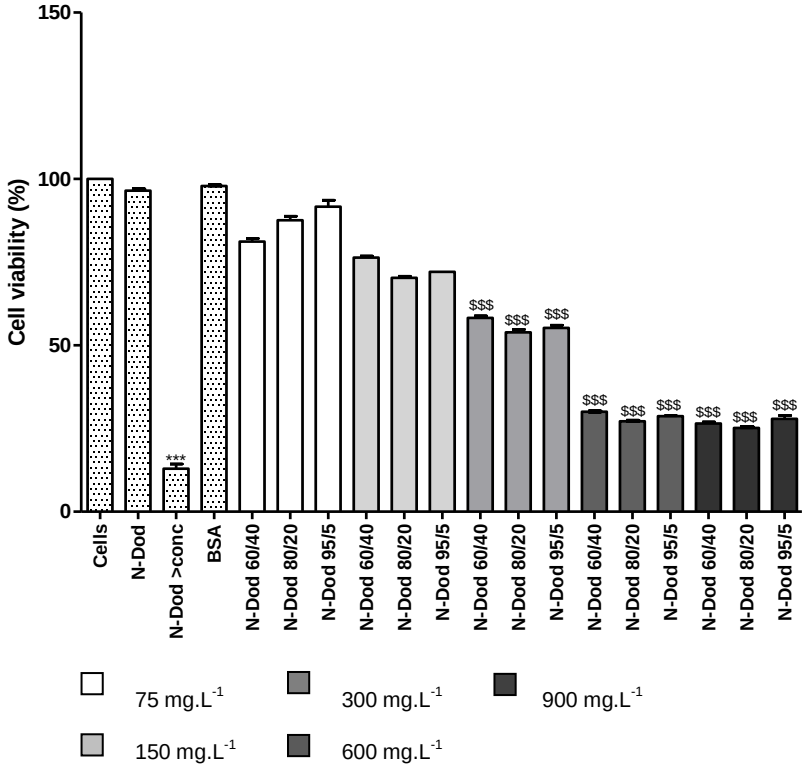

Figure V-13: Effect of BSA microspheres, applying different concentrations, on viability of the human cell line RKO, after 48 h of treatment (*used to compare all the controls: BSA solution, *n*-dodecane at lower and higher concentration, with the control cells and $ used to compare all concentrations with controls = significantly different from all the other tested conditions, $P < 0.05$).

The different microspheres concentrations (75, 150, 300, 600 and 900 $mg.L^{-1}$) were tested and the $ symbols were used to compare all concentrations with controls. Results indicate that BSA particles at concentrations of 75 and

150 mg.L^{-1} do not induce any toxicity for the investigated culturing time. However, at concentrations ranges of 300 and 900 mg.L^{-1}, after 48 h, the viability of the RKO cells decreased in the presence of BSA particles, which suggests moderate cytotoxic effects. In Figure V-13 the * symbol was used to compare all the controls (BSA solution, *n*-dodecane at lower and higher concentration) with the control cells (only cells and medium). As can be seen only *n*-dodecane at the highest concentration is toxic, which is in agreement with previous studies [61].

V-4. CONCLUSIONS

This study pretended to highlight the effects of ultrasound in two different proteins microspheres development. Results show that it is possible to conclude that for the particles formation and stabilization there is not essential the presence of disulphide bonds, but the presence of hydrophobic and hydrophilic interactions. Furthermore, the results obtained show that ultrasound source promote the rearrangement of chains in a regular array to some extent, that can lead to a conformational change, resulting in a more rigid and compact structure.

In this study, it was established that the amount of protein and the *n*-dodecane volume fraction are essential to form and stabilize the proteinaceous microspheres and also to tune their size distribution. Moreover, all these parameters should take into account the protein structure, and the knowledge of this allows a design of different microparticle template.

Further studies are underway in order to use these proteinaceous microspheres as delivery systems (DS) that can be applied in different areas, such as medicine.

CHAPTER VI

MECHANISM OF THE FORMATION OF PROTEINACEOUS MICROSPHERES

HIGHLIGHTS FROM PEPTIDE SIZE AND SEQUENCE

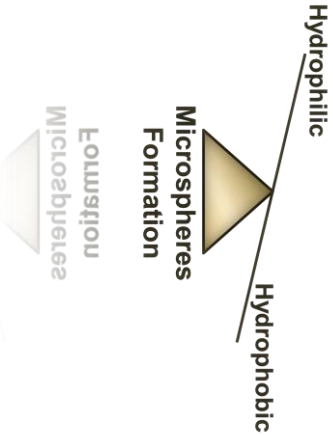

Chapter VI

Mechanism of the formation of proteinaceous microspheres - Highlights from peptide size and sequence[**]

ABSTRACT

The use of ultrasound for the formation of microspheres from protein aqueous solutions and hydrophobic solvents/oil has been widely reported. The previous Chapter (V) demonstrated that there are several factors that should be taken into account, alongside with the amino acid composition of proteins, to obtain structured microspheres. Using a wide range of peptides with variable sizes and sequences with a tailored hydrophilic/hydrophobic ratio, it was elucidated the fundamentals on microspheres formations. The results have shown that the larger peptides with separated and clear hydrophobic and hydrophilic areas lead to more stable and small spheres.

The work presented in this Chapter set the rational to choose certain protein/peptide sequences for designing stable devices for a wide range of application areas.

[**] This chapter is based on the following publication:
Silva R, Ferreira H, Azoia N, Rollet A, Angel U, Güebitz G, Gedanken A, Cavaco-Paulo A, *Mechanism of the formation of proteinaceous microspheres – Highlights from peptide size and sequence*, submitted.

VI-1. INTRODUCTION

The growing interest in nanotechnology has stimulated the discovery and development of new materials that can self-assemble into well-ordered structures at the nanometre scale [250, 251]. Micro and nanoparticles have found diverse and important applications, ranging from the encapsulation of dyes, flavours, and fragrances, to drug delivery systems and to the study of membrane structure, function and reactivity [252-254] . Many molecular components can be used in particle manufacturing, and the ability to combine them into designed architectures containing significant complexity, remains a challenge. Additionally, there are several methods in the literature about the preparation of the different devices [23, 131, 164]. The selection of an appropriate method determines the success or failure of microstructured materials synthesis, because physical properties and applications of micro and nanostructured materials are heavily dependent of preparation method. The importance of choosing a proper procedure in designing these structured materials has been a driving force for the development of new methodologies for several decades. Among a variety of approaches, the utilization of ultrasound has been extensively examined over many years, and is one of the most powerful tools in micro and nanoparticles synthesis. The sonochemical micro and nanosynthesis at the engineered interface of a cavitation microbubble is a combination of physical and chemical effects [15, 23].

The extreme conditions, produced by high intensity ultrasound, at the interface between the gaseous interior of the cavitation microbubble and the surrounding liquid medium can be utilized for carrying out various physical transformations and/or chemical reactions leading to the formation of spherical shells containing either gas or liquid in their inner cavity. Suslick and co-workers have been able to produce stable microspheres from aqueous solutions of proteins and organic solvents using high intensity ultrasound [44-48]. The mechanisms of the formation of these particles have been the subject of much discussion and could stem from the chemical and mass transport effects of ultrasound on an aqueous medium [44, 72]. It was proposed that the particles are

held together by disulphide bonds between protein Cysteine residues, and that a superoxide radical ($O_2^{\bullet-}$), sonochemically produced by acoustic cavitation, is the cross-link agent. Other studies have shown that microspheres can be formed with proteins/peptides that did not contain any Cysteine residues indicating that mass transport effects seem to be the major cause of microsphere formation [51].

In this study, it was used a wide range of peptides with variable sequences, sizes and hydrophilic/hydrophobic ratio in order to investigate the proteinaceous microparticle formation, and achieve a rationale on peptides and proteins for microsphere formation.

The motivation to select peptides is based on the fact that they can be readily designed and synthesized for specific applications unlike large and complex proteins. Instead of studying a protein as a whole for a particular function, one may investigate small sections of peptides chains of the same protein to achieve the same goal and at the same time to go deeper into the chemical structure. This approach has been used to gain a better understanding of microspheres formation mechanism via ultrasound sources allowing the resemblance of some situation found in well-studied protein.

VI-2. MATERIALS AND METHODS

VI-2.1. Peptide development

The sequence of the peptides is described by a one-letter code, which is the symbol commonly used to represent the amino acids (a.a.) residues. The peptide sequences were synthesized by JPT Peptide Technologies GmbH (Berlin, Germany). These peptides were supplied as a lyophilized material. They were analysed by high performance liquid chromatography (HPLC) and mass spectrometry (MS), and their purity was over 70% (HPLC, 220 nm, C18, linear gradient).

VI-2.2. Preparation and characterization of peptide microspheres

Peptide microspheres were prepared according with the method previously described in the Chapter II. The peptide microspheres were produced using a fixed ratio (%) of 60/40 of aqueous/organic phase (*n*-dodecane) and 100 µM was the concentration of peptide aqueous solution used in the assays. The procedure for the further characterization is detailed in Chapter of materials and methods, namely: yield of microspheres formation; size and its distribution; zeta-potential, scanning transmission electron microscopy (STEM), confocal microscopy, molecular dynamic simulations and stability studies.

VI-3. RESULTS AND DISCUSSION

This work was firstly performed using ten different hexapeptides with the general sequence of GXGXGX, where G is Glycine and X can be Alanine, Serine, Leucine or Aspartic Acid. The aim was the evaluation of the effects of the chemical environment on microsphere formation in this small peptide. The results proved that only the peptide with highly hydrophobic residues, like Leucine, form microspheres (approximately 900 nm in diameter and with a polydispersity index, PDI, of 0.8 ± 0.05, presenting a 60% of yield and a negative charge). Alanine restricts the small hexapeptide ability to form microspheres at the solvent-water interface, because it was not hydrophobic enough. Alanine has a smaller side chain when compared with Leucine.

The design of the peptide motifs with a variety of sizes, charges and hydrophobicity was based on the fatty acid model, which has a charged/polar head and an hydrophobic tail. The peptides had the general formula of $[D]_xAA[GAAAA]_y$ with 8-31 residues, with the N-terminus linked to Aspartic Acid (represented as D; 1-4 residues) and a tail of hydrophobic amino acid (Alanine corresponds to A; 6-22 residues), which is interspersed with G for increased flexibility (Glycine corresponds to G).

The data of Table VI-1 show that the amount of Aspartic Acid at the N-terminal leads to an increase in the yield of microsphere formation, to smaller sizes and to high charged microspheres. It is known that highly charged particles

can produce more stable devices, due to their inter-negative repulsive interactions. Furthermore, the increased size of the hydrophobic tail of the GAAAA motif also promotes the enhancement of the yield of microsphere formation, a decrease in size values and high monodispersed fractions. These results indicate that the peptides with concentrated charged areas and clear larger hydrophobic regions lead to smaller sizes and high surface charges, thus improving the microsphere formation yield and microsphere stability.

Table VI-1: Yield (%), Z-average (nm), PDI and zeta-potential (mV) of microspheres obtained for the engineered peptides based on fatty acid model

Peptide (N→C-terminus)	Yield (%)	Z-average (nm)	PDI	Zeta-potential (mV)
[D] AA[GAAAA]	49 ± 9	672 ± 37	0.6 ± 0.03	-14 ± 1
$[D]_2$AA[GAAAA]	60 ± 4	620 ± 36	0.5 ± 0.03	-26 ± 2
$[D]_3$AA[GAAAA]	68 ± 4	633 ± 32	0.6 ± 0.07	-37 ± 1
$[D]_4$AA[GAAAA]	70 ± 3	533 ± 17	0.6 ± 0.06	-39 ± 1
[D]AA$[GAAAA]_5$	89 ± 4	469 ± 15	0.4 ± 0.04	-38 ± 3
$[D]_4$AA$[GAAAA]_5$	98 ± 1	455 ± 14	0.4 ± 0.04	-47 ± 4

In the next set of experiments it was used peptide motifs based on the primary sequence of a secretory leukocyte protease inhibitor (SLIPI) that has in common the potential inhibitory capacity of the human neutrophil elastase (HNE) [255]. To maintain the size of the peptide it was replaced the four Cysteine residues with a range of hydrophilic and hydrophobic residues. Therefore, in each peptide motif, the four Cysteine residues (PCyst) were replaced by Serine (PSer), Tyrosine (PTyr), Histidine (PHis), Phenylalanine (PPhe) or Leucine (PLeu).

The results reported in Table VI-2 indicate higher levels of efficiency in microsphere formation, presenting slightly differences in the yield. With this, it was confirmed that Cysteine is not needed for microspherization and that mass transfer is the major cause for microsphere formation. The peptide with a higher

moiety of hydrophobic a.a. displays an increase in the yield of microsphere formation. The insertion of polar and basic residue in a peptide segment interferes with the balance of hydrophobic/hydrophilic character leading to an increase in the size of the microspheres. The peptide with Histidine presents positive values due to the high quantity of basic Histidine residue in the sequence.

Table VI-2: Yield (%), Z-average (nm), PDI and zeta-potential (mV) of microsphere of the engineered peptides, based on SLPI, with fourteen a.a. residues

Peptide[a] (N→C-terminus)	Yield (%)	Z-average (nm)	PDI	Zeta-potential (mV)
KRCCPDTCGIKCLD	84 ± 2	380 ± 20	0.5 ± 0.01	-26 ± 3
KRSSPDTSGIKSLD	78 ± 1	971 ± 28	0.8 ± 0.01	-16 ± 2
KRYYPDTYGIKYLD	77 ± 0.4	829 ± 25	0.8 ± 0.02	-24 ± 1
KRHHPDTHGIKHLD	76 ± 0.9	840 ± 13	0.7 ± 0.06	+23 ± 3
KRFFPDTFGIKFLD	92 ± 0.6	310 ± 15	0.5 ± 0.03	-20 ± 1
KRLLPDTLGIKLLD	91 ± 1	300 ± 8	0.4 ± 0.04	-26 ± 3

[a] changed a.a. are underline

Figure VI-1 shows the STEM photographs obtained for the peptide microspheres. Figure VI-1 a), b) and c) present spherical particles with smooth surfaces. Although, PSer [Figure VI-1 d)] exhibits a heterogeneous population of microspheres, it did not produce a regular spherical shape when compared with the others peptides. The same behaviour was observed for the microspheres of PHis and PTyr. The inclusion of polar and basic residues may cause different shape assemblies than the other peptides. Furthermore, the photographs obtained for the $[D]_4AA[GAAAA]_5$ and $[D]_2AA[GAAAA]$ peptides [Figure VI-1 a) and b)] also present differences in their sizes. After the self-assembly process induced by the sonochemical method, the peptides may form different structures, because packing of the hydrophobic side chains depends on the size of their corresponded van der Waals surface area. It is clear that the decrease in the

hydrophobic tail favours the increase in size of the microspheres. The morphology of spherical shape obtained for the majority of the peptide microspheres would offer the highest potential for the controlled release and protection of incorporated drugs, as they provide minimum contact with the aqueous environment, as well as the longest diffusion pathways. Compared with other particle shape, spherical ones will require the smallest amount of a surface-active agent for stabilization, because of their small specific surface area [187]. Additionally, our findings are also consistent with photon correlation spectroscopy (PCS) results, since the particle size distribution was very similar.

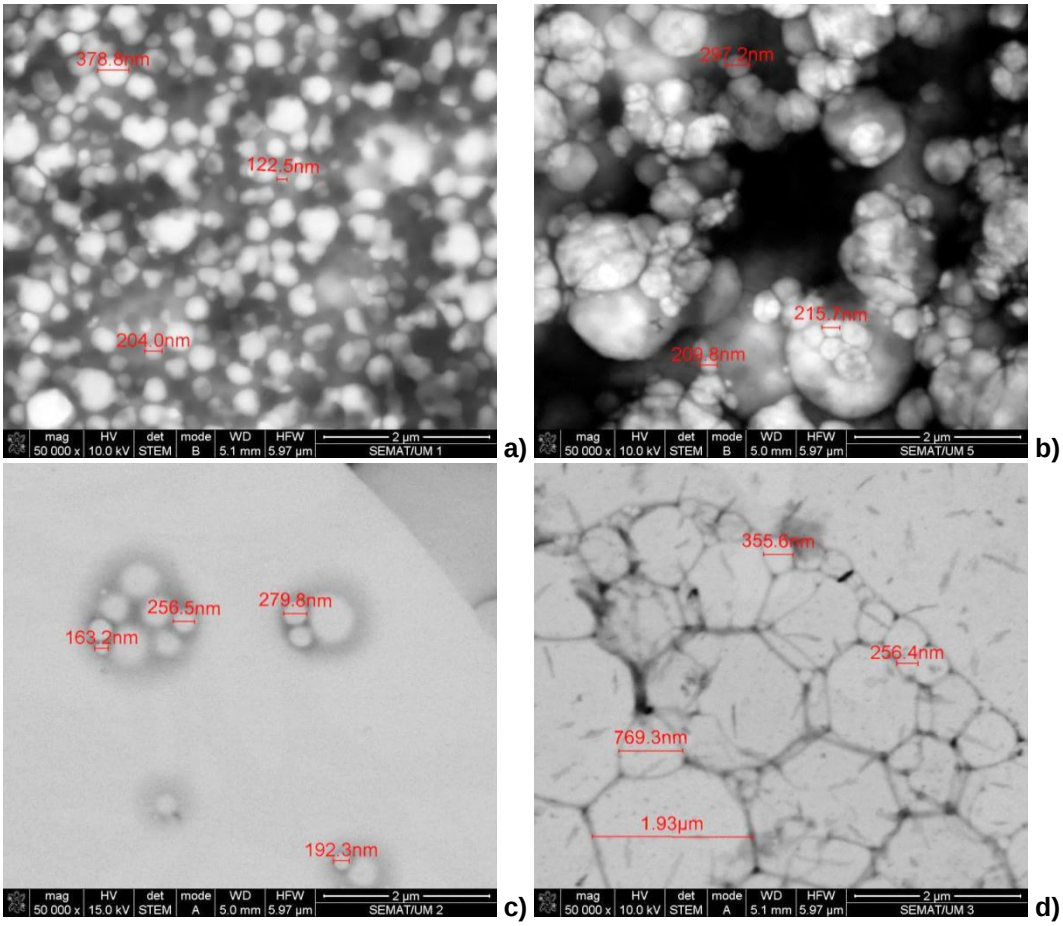

Figure VI-1: STEM images (x50000 magnification) of peptide microspheres: a) $[D]_4AA[GAAAA]_5$; b) $[D]_2AA[GAAAA]$; c) KRFFPDTFGIKFLD; d) KRSSPDTSGIKSLD.

A lipophilic fluorescent probe was incorporated into peptide microspheres and analysed by confocal microscopy, providing a refined data set and, ultimately, a more precise evaluation of peptide arrangement. Nile red is a dye that exhibits solvatochromism and its absorption band varies in spectral position, shape and intensity with the nature of the solvent. The dye is highly fluorescent in organic

solutions, and increasing the polarity of the solvent leads to an enhancement of emission and excitation maxima, when the fluorescent spectra is measured [193, 194].

Figure VI-2 emphasizes the peptide behaviour at an aqueous/organic interface, presenting a green colour in a less hydrophobic medium, while in a nonpolar solvent it acquires a red colour. The results clearly demonstrate the peptide arrangement in microsphere formation, suggesting a more hydrophobic core in its structure. This figure also presents some differences between $[D]_4AA[GAAAA]_5$ and $[D]_2AA[GAAAA]$, attributed to the decrease in the number of hydrophobic residues in peptide motifs that lead to an increase of particles size and to a decrease of peptide microspheres stability. Figure VI-2 b) indicates that this peptide has a tendency to coalesce.

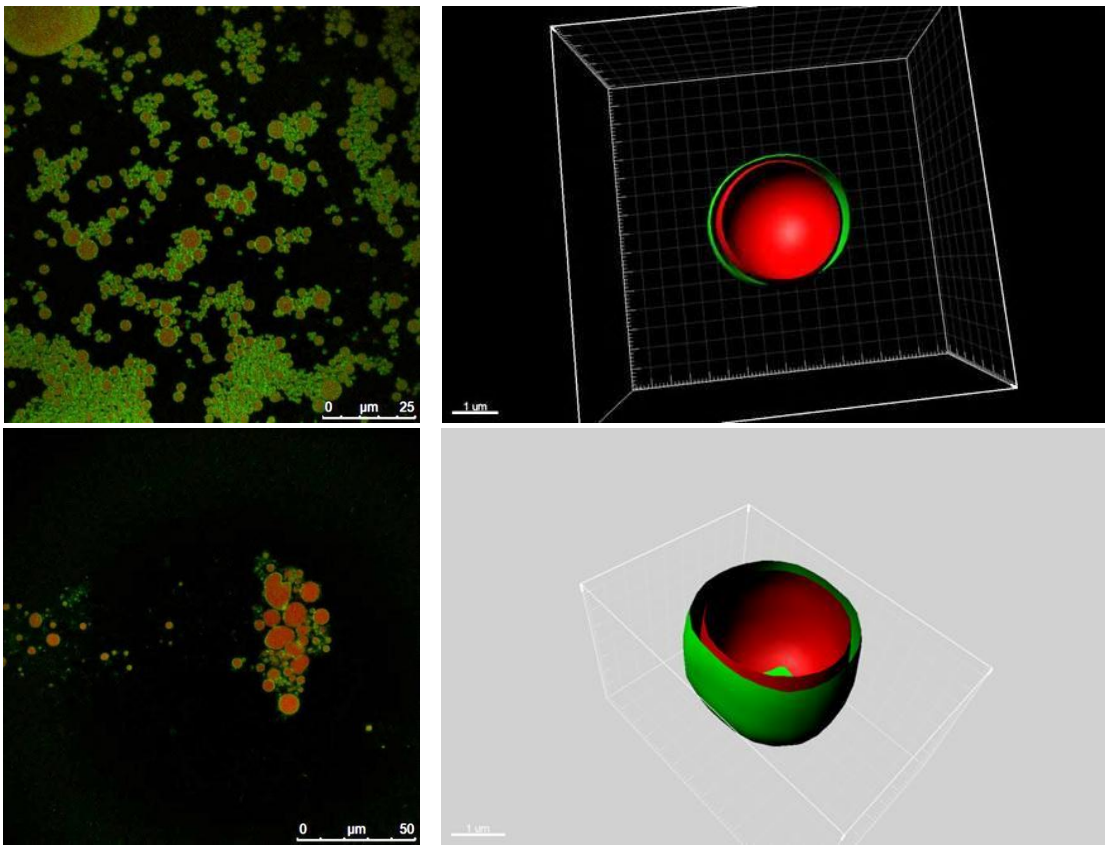

Figure VI-2: **Confocal images of peptide microspheres: a) $[D]_4AA[GAAAA]_5$; b) $[D]_2AA[GAAAA]$, prepared with Nile red (green colour shows the more polar regions excited with laser line of 532 nm and the red colour shows the more nonpolar regions excited with laser line of 488 nm). The three-dimensional (3-D) images evidence the peptide behaviour at an aqueous/organic interface, presenting a green colour in a less hydrophobic medium, while in a nonpolar solvent it acquires a red colour, suggesting a more hydrophobic core in its structure.**

In order to simulate the formation of the microspheres, GROMACS software [246] with a GROMOS (ffG53A6) force-field was used [247]. The sonochemical method is not easily simulated, but to obtain a realistic model it was used fifty peptide molecules randomly distributed in space. Next, the *n*-dodecane molecules were added randomly, and finally, the empty space was filled with water. It was considered that this procedure, where all the components are randomly distributed through space, is the paramount manner in which simulates the sonication process. The number of *n*-dodecane molecules was chosen so that the final solution will be equivalent to a 1:1 mixture of water/*n*-dodecane (v:v). In all of these simulations it was possible to notice that the peptides have some affinity to the interface between the solvents. Figure VI-3 shows that the highly polar groups at the interface interact with the water and that the nonpolar residues interact with the *n*-dodecane.

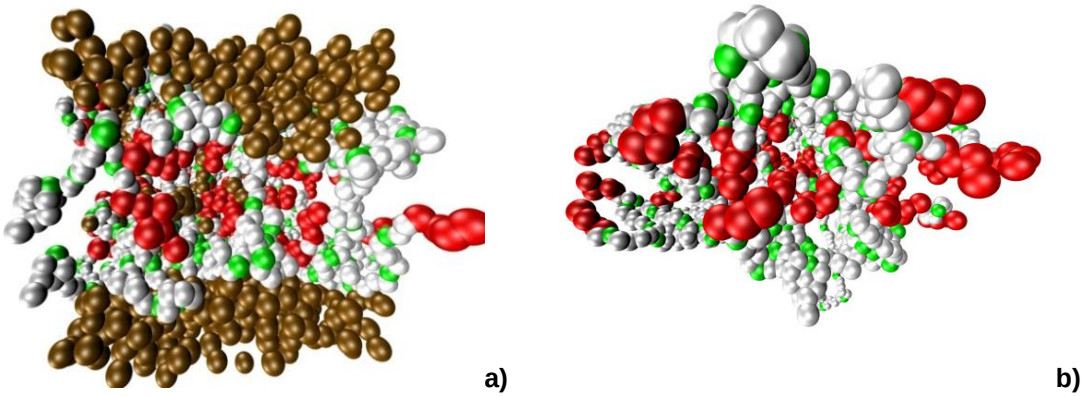

Figure VI-3: Molecular studies of microspheres obtained with peptide $[D]_4AA[GAAAA]_5$: a) peptide stays at the interface, with the polar head (red) towards the water (not shown) and the nonpolar tail (white) facing the *n*-dodecane (brown); b) the peptide in water (not shown) tends to form aggregates, with the polar heads (red) interacting with each other.

The evaluation of the suspension stability of microspheres was performed by measuring the particle size, the surface charge and observing the macroscopic aspect, over four months. Since these colloidal particles can aggregate over time, particularly when stored in an aqueous dispersion, an evaluation of the particle size was done for four months, aimed at evaluating their physical stability [244]. The zeta-potential was also determined, since this parameter of colloidal particles can also change over storage time, due to the degradation of some components [245].

The stability results showed that the peptides based on fatty acid molecules model, can form microspheres with high stability. The degree of hydrophobicity of peptide motifs can significantly affect these data. When hydrophobic residues increase (y=5), the molecules have a tendency to assemble and form peptide matrices with enhanced strength. The [D]AA[GAAAA]$_5$ and [D]$_4$AA[GAAAA]$_5$ peptides revealed the same behaviour over four months. The size distribution and the zeta-potential values were very similar and there was no change in the macroscopic appearance (Figure VI-4). In contrast, the other peptides presented an enhancement in the values of size distribution. Additionally, the zeta-potential values tend to zero, exhibiting instability. The results indicated that the longer is the peptide segment, the greater is the tendency to self-assemble into well-defined and stable microstructures.

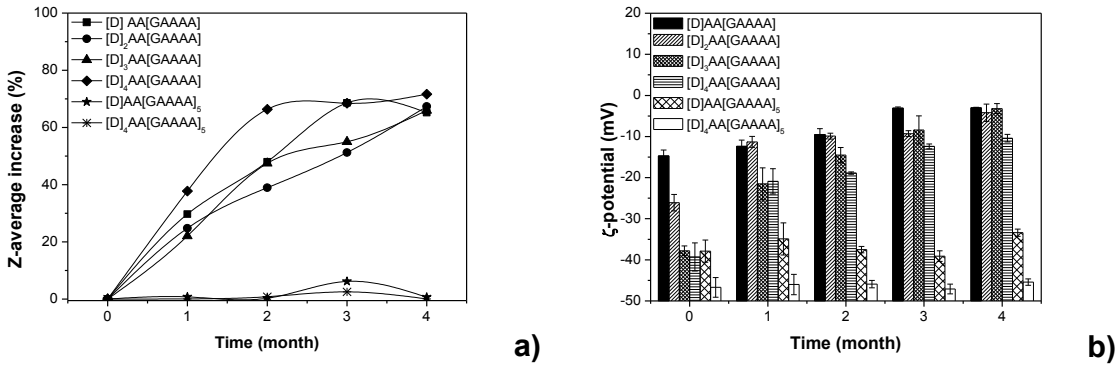

Figure VI-4: Increase of Z-average (nm) (a) and zeta (ζ) -potential (mV) (b) over four months for the peptide microspheres based on fatty acid model.

The stability results for microspheres of PSer, PHis and PTyr, derived from SLIPI, were evaluated and an increase in the particle size was observed after one month of storage (Figure VI-5). Additionally, the zeta-potential value, in the same period of time, was more closer to zero, indicating the tendency of the particles to aggregate. Conversely, for the microspheres of PPhe and PLeu, the values obtained for particle size and zeta-potential, during four months, were very similar.

The results achieved are mainly due to the presence of Cysteine and hydrophobic residues. The Cysteine allows the disulphide bonds between those residues in adjacent peptides to induce robust covalent bonds. Furthermore, the

hydrophobicity of Phenylalanine and Leucine groups prove to be sufficient to promote stable devices.

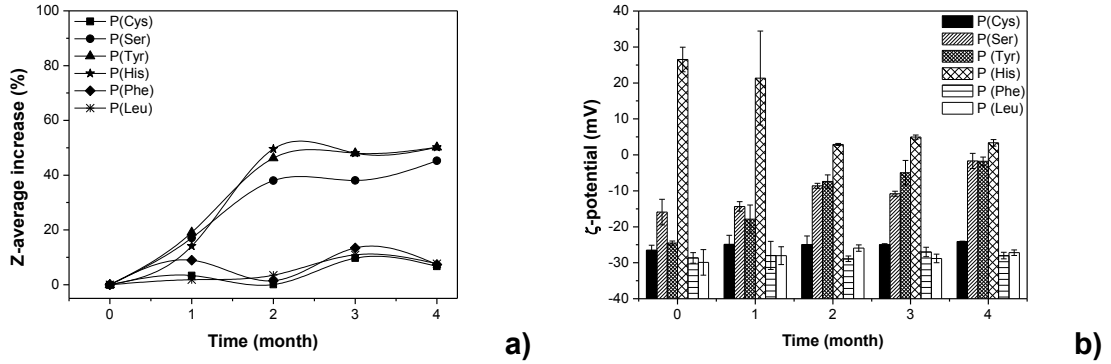

Figure VI-5: Increase of Z-average (nm) (a) and zeta (ζ) -potential (mV) (b) over four months for the peptide microspheres based on SLIPI structure.

To confirm the influence of different poly(amino acids) on microsphere formation poly(Lysine); poly(Serine); poly(Proline); and poly(Alanine) were tested. Table VI-3 shows that only poly(Lysine) did not form microspheres. The polarity and the positive charge of Lysine could compromise microsphere formation. The best result was obtained with poly(Proline) followed by poly(Alanine). They are both hydrophobic, although, the side chain of poly(Proline) is larger than the Alanine side chain. The yield achieved for poly(Serine) microspheres was the lowest. All poly(amino acids) tested present a negative charge.

Table VI-3: Yield (%), Z-average (nm), PDI and zeta-potential (mV) of microspheres obtained for the different poly(amino acids)

Poly (amino acid)	Yield (%)	Z-average (nm)	PDI	Zeta-potential (mV)
Poly(Serine)	29 ± 8	796 ± 27	1 ± 0.02	-11 ± 0.8
Poly(Proline)	60 ± 2	690 ± 16	0.9 ± 0.03	-31 ± 0.5
Poly(Alanine)	50 ± 2	676 ± 36	0.8 ± 0.02	-26 ± 1
Poly(Lysine)	-	-	-	-

VI-4. CONCLUSIONS

In this study, it can be concluded that the microsphere formation is mainly due to the intrinsic properties of a.a. residues and their arrangements in peptides. The higher shear forces produced by ultrasound will drive the orientation of polar and nonpolar groups in a biphasic system (Figure VI-6). This orientation is highly dependent on the positioning of the individual residues in the peptide motif and also on the side chain of each residue. The degree of hydrophobicity is also an important parameter to control, since that higher degree leads to an enhancement of van der Waals interactions between peptide molecules promoting a peptide microsphere compactness and, consequently, higher stabilization.

This work provides the groundwork for the design of sequences for peptides and proteins to reach the stable and controlled size of the microspheres and to improve their physico-chemical properties. Moreover, it is possible to build desired supramolecules with specific properties that can be applied in different research fields.

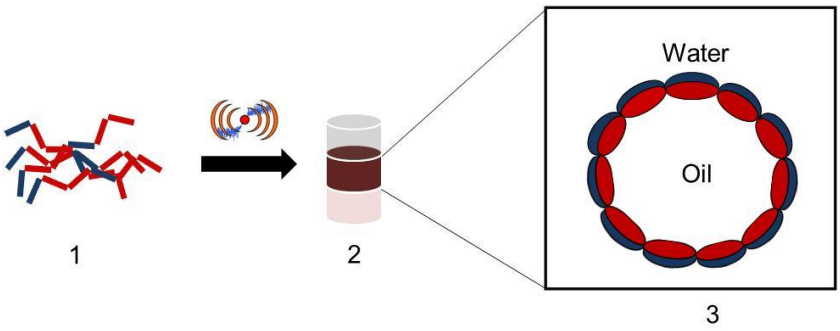

Figure VI-6: **Potential packing pathway of peptide microsphere formation: 1) peptide in solution; 2) microspheres at the interface of aqueous/organic phase; 3) peptide arrangement showing the hydrophilic residues (blue colour) interacting with water and the hydrophobic residues (red colour) interact with the organic phase. The ultrasound sources promote an enhancement of hydrophilic and hydrophobic interactions and form a close ring.**

CHAPTER VII

SONOCHEMICAL PROTEINACEOUS MICROSPHERES FOR WOUND HEALING

Chapter VII

Sonochemical proteinaceous microspheres for wound healing[††]

ABSTRACT

In this Chapter a novel approach is proposed using proteinaceous microspheres of bovine serum albumin (BSA), human serum albumin (HSA) and silk fibroin (SF), based on the previously described sonication conditions, (Chapter V). Different organic solvents, namely *n*-dodecane, mineral oil and vegetable oil, were used as organic phase on microspheres production stage. The ability of these devices to inhibit human neutrophil elastase (HNE) was evaluated using porcine pancreatic elastase (PPE) solution as a model of wound exudates. The results obtained indicated that the level of PPE activity can be tuned by changing the organic solvent present on different protein devices, thus showing an innovative way of controlling the elastase-antielastase imbalance found in chronic wounds. Furthermore, these proteinaceous microspheres were shown to be important carriers of elastase inhibitors causing no cytotoxicity in human skin fibroblasts *in vitro*, making them suitable for biomedical applications, such as chronic wounds.

[††] This chapter is based on the following publication:
Silva R, Ferreira H, Vasconcelos A, Gomes AC, Cavaco-Paulo A, *Sonochemical proteinaceous microspheres for wound healing*, submitted.

VII-1. INTRODUCTION

A wound is the result of disruption of normal anatomic structure and function. Based on the nature of the repair process, wounds can be classified as acute or chronic wounds [180, 256]. Acute wounds are usually tissue injuries that heal completely, with minimal scarring, within the expected time frame, usually 8-12 weeks. Chronic wounds, on the other hand, arise from tissue injuries that heal slowly, that is not healed beyond 12 weeks and often reoccur [180, 256]. Chronic wounds are thus defined as wounds which have failed to proceed through an orderly and timely process to produce anatomic and functional integrity or went through the repair process without establishing a sustained anatomic and functional result. Non-healing chronic wounds, such as decubitis ulcers (bedsores or pressure sores) and leg ulcers (venous, ischaemic or of traumatic origin) and other delayed wounds, are an important and persistent problem in dermatology [257, 258].

Acute wounds have low levels of protein-degrading enzymes, whereas exudates from non-healing chronic wounds contain elevated levels of proteases, like matrix metalloproteinases (MMP) and human neutrophil elastase (HNE) [258-263]. The overproduction of proteolitic enzymes in wound exudates leads to reduced concentrations of growth factors, fibronectin and endogenous levels of protease inhibitors, resulting in imbalance between degradation and remodeling processes [257, 260, 264]. Thus, it has been postulated that lowering protease levels in the chronic wound to levels normally found in acute wounds may accelerate healing in the chronic wound [261, 263, 265]. Due to its involvement in such process, there is extensive literature exploring the different types of inhibitors or inhibitors formulations that may restore the normal levels of these enzymes in the above diseases [266]. The use of fatty acids is known to decrease HNE activity on a chronic wound fluid [267]. The release of oleic acid albumin formulations from derivatized cotton wound dressings had also shown the promotion of wound healing [265, 268]. Nevertheless, several challenges remain that need to be taken into consideration in developing novel wound healing delivery formulations. Even so, there are few studies on the release of oils from protein microspheres to promote the inhibition of high levels of HNE

found on chronic wounds exudate.

The work presented here evaluated the capacity of three different organic solvents (*n*-dodecane, mineral oil and vegetable oil) to inhibit HNE in order to evaluate their ability to be used as a part of a wound management strategy. However, these organic solvents are insoluble in aqueous environments and would require a vehicle to promote the elastase inhibition in the wound environment. For the delivery of such compounds to the target area, proteinaceous devices, based on bovine serum albumin (BSA), human serum albumin (HSA) and silk fibroin (SF) have been used. Serum albumin is one of the most extensively studied and applied proteins in this research field because of its availability, low cost, stability, unusual ligand binding properties and is recognized as the principal transport protein for fatty acids and others lipids that would otherwise be insoluble in the circulating plasma [227, 265, 268, 269]. On the other hand, SF has a long history of use in clinical applications [140]. More recently, this protein has been bioengineered for use in biomaterials as films, three-dimensional (3-D) porous scaffolds, electrospun fibers, hydrogels and microparticles [140, 158, 184, 185, 233, 270-272]. These materials provide mechanical toughness, biocompatibility and biodegradability [141].

In this work, microspheres are produced by means of ultrasonication of a two-phase starting mixture, consisting of protein solution (BSA, HSA or SF) and organic solvent.

The preparation was followed by an extensive physico-chemical characterization. The ability of proteins to form microspheres was performed by quantifying the protein concentration on the supernatant, after ultrasound treatment [191]. Particle size, as well as the polydispersity index (PDI) of microspheres was evaluated by photon correlation spectroscopy (PCS). In addition to the size distribution determination, the zeta-potential was also determined by electrophoretic laser Doppler anemometry, to assess particles surface potential. Both size and zeta-potential, as well as macroscopic aspect observation, were determined every week in order to evaluate their physical-stability over time. The scanning transmission electron microscopy (STEM) was employed to characterize the overall structure and shape of particles. Furthermore, the inhibitory activity of these protein microemulsions containing different organic

solvents was tested using porcine pancreatic elastase (PPE) solution as a model of wound exudates. Finally, these devices were screened for cytotoxicity using a human cell line monitored with a metabolic test.

VII-2. MATERIALS AND METHODS

VII-2.1. Preparation and characterization of protein microspheres

Protein microspheres were prepared according with the method previously described in the Chapter II. The protein devices were produced using a fixed ratio (%) of 60/40 of aqueous/organic phase and 5.0 $g.L^{-1}$ of BSA and HSA and 10.0 $g.L^{-1}$ of SF were the concentrations of proteins aqueous solution used in the assays. Three different organic phases were tested: *n*-dodecane, mineral and vegetable oil. The procedure for the further characterization is detailed in Chapter II, namely: yield of microspheres formation; size and PDI; zeta-potential, morphology (STEM technique). The assay to determine the activity loss of PPE as well as the cytotoxicity screening is described below.

VII-2.2. *In vitro* determination of porcine pancreatic elastase (PPE) activity loss over time in presence of proteinaceous microspheres

The activity of PPE was measured according to a method previously reported with some modifications [273]. In brief, 30 µL of enzyme was mixed with 900 µL of reaction buffer 100 mM tris(hydroxymethyl)aminomethane hydrochloride (Tris-HCl), pH 8.0. The reaction was started with the addition of 70 µL of 4.4 mM of succinyl-alanine-alanine-*p*-nitroanilide (Suc-Ala-Ala-Ala-*p*-nitroanilide), a synthetic substrate for PPE. The reaction was carried out for 5 min, at 25 °C, and the cleavage of the substrate was monitored spectrophotometrically at 410 nm using a Heλios γ ThermoSpectronic spectrophotometer (Unicam). One unit is defined as the amount of enzyme that will hydrolyse 1.0 µmol of Succinyl-alanine-alanine-*p*-nitroanilide ($Suc(Ala)_3$-*p*NA) per minute at 25 °C, pH 8.0. To examine the inhibitory activity of the organic solvents, different concentrations of proteinaceous microspheres were added to a fixed amount of

PPE solution. The protein microspheres used for these studies are the following: BSA; HSA and SF. The incubation was carried out at 25 °C and, at determined time points, aliquots were collected to monitor the decrease in elastase activity. Measurements were recorded in triplicate and the results were expressed as mean value ± standard deviation.

VII-2.3. Cytotoxicity screening

The cytotoxicity of microspheres prepared from different proteins was evaluated using murine embryonic fibroblasts cells (MEFs), isolated from E13.5 embryos and normal human skin fibroblasts (BJ5ta), from American type culture collection (ATCC).

The BJ5ta cell line (normal human skin fibroblasts) was maintained according to ATCC recommendations (4 parts Dulbecco's modified Eagle's medium (DMEM) containing 4 mM L-glutamine, 4.5 $g.L^{-1}$ glucose, 1.5 $g.L^{-1}$ sodium bicarbonate and 1 part of Medium 199, supplemented with 10% (v/v) of fetal bovine serum (FBS), 1% (v/v) of Penicillin/Streptomycin solution and 10 $\mu g.mL^{-1}$ hygromycin B). The cells were maintained at 37 ºC in a humidified atmosphere of 5% CO_2. Culture medium was refreshed every 2 to 3 days.

Cells were seeded at a density of 10 x 10^3 cells/100 µL/well on 96-well tissue culture polystyrene (TCPS) plates (TPP, Switzerland) in the day before experiments and then exposed to different microspheres concentrations, as well as to different controls solutions (BSA; HSA and SF solutions; vegetable oil) added to fresh culture medium. At 24, 48 and 72 h of exposure, cell viability was determined using the alamarBlue® assay (Invitrogen, EUA). AlamarBlue cell viability reagent functions as a cell health indicator by using the reducing power of living cells to quantitatively measure the proliferation of various human and animal cell lines, allowing to establish relative cytotoxicity of agents within various chemical classes. When cells are alive, they maintain a reducing environment within the cytosol of the cell. In this assay, viable cells continuously convert resazurin (blue and non-fluorescent) to resorufin (red and highly fluorescent), increasing the overall fluorescence and colour of the media surrounding cells. 10 µL of alamarBlue compound were added to each well containing 100 µL of culture medium. After 4 h of incubation at 37 ºC the absorbance at 570 nm, using

600 nm as a reference wavelength, was measured in a microplate reader (Spectramax 340PC).

The quantity of resorufin formed is directly proportional to the number of viable cells. Data are expressed as means with standard errors of the means. Two-way ANOVA followed by post hoc Bonferroni test (GraphPad Prism 5.0 for Windows) was employed with statistically significant differences when $P < 0.05$.

The samples were tested at least in triplicates per two independent experiments.

VII-3. RESULTS AND DISCUSSION

In this work, devices based on proteins, such as BSA, HSA and SF, to delivery oils were developed and characterized. Therefore, this study presents an original system to control high levels of elastase found on chronic wounds.

VII-3.1. Characterization of proteinaceous microspheres

The characterization of the microspheres obtained with these different proteins was focused in the study of microspheres formation yield, particle size, PDI, zeta-potential and morphology. All the experiments were done with three different organic solvents and, while *n*-dodecane present twelve carbons linked by saturated bonds, mineral oil and vegetable oil present different degrees of saturated and unsaturated fats.

Firstly, to determine the successful yield of protein that forms microspheres with different organic solvent, the Lowry procedure was used.

Table VII-1, Table VII-2 and Table VII-3 show the results obtained for BSA, HSA and SF microspheres, respectively. The proteinaceous microspheres evidence a high yield on particles formation independently of the organic solvent used. However, these devices exhibit a slight difference of the mean size (Z-average) when vegetable oil and mineral oil were applied, relatively to the microspheres obtained with *n*-dodecane. It is known that certain properties of fatty acid residues in the molecule of triacylglycerol have significant effects on the

fluidity of the oil. The "zig-zag" organization of single bonds enables the chains to be lined up close to each other and intermolecular interactions, such as van der Waals interactions, can take place promoting the size reduction, which explain the results obtained for *n*-dodecane. This system inhibits fluid flow, resulting in the relatively high viscosity of the oils. On the other hand, the presence of double bonds, can produce "kinks" in the geometry of the molecules. This prevents the chains becoming close to form intermolecular contacts, which results in an increased capability of the fluid to flow and, consequently, a highest size was achieved.

This assay further suggests that the SF present the highest Z-average values when compared with BSA and HSA. According with our previous studies (Chapter V) [72] this is mainly due to the differences that exist in the macromolecular structures of proteins.

The PDI values were similar, without significant changes, in the presence of different organic solvents and proteins. Moreover, there was no difference on the yield of particles formation, particle sizes and PDI, when the proteinaceous microspheres were prepared in phosphate buffered saline solution (PBS) medium or in deionized water (H_2O).

Another characteristic of polymeric microspheres that is of extreme interest is zeta-potential, which is a function of the surface charge of the particles [274]. The proteinaceous particles, prepared with the three different organic solvents, present a negative charge on their surfaces (Table VII-1, Table VII-2 and Table VII-3). Negligible changes in zeta-potential values were observed between different organic solvents used. However, the results show that the zeta-potential value dropped significantly when protein microspheres are prepared with PBS solution (pH 7.4). Studies of current literature suggest that the zeta-potential is related to both surface charge and the local environment of the particle (composition of the surrounding solvent, the environmental pH value and ions in the suspension) [275-277]. Nevertheless, the zeta-potential is not an actual measurement of the individual molecular surface charge; rather, it is a measurement of the electric double layer produced by the surrounding ions in solution (i.e. counter ions). The effect of pH on the zeta-potential of the protein particles is explainable by considering that the surfaces of these materials contain pH-dependent ionisable functional groups, both acidic and basic, that can undergo

dissociation and protonation [278]. The results advise that the use of deionized water (H_2O, pH 5.5) augmented the negative charge on the particles surfaces.

Table VII-1: Effect of organic phase (40%) on the yield value (%), Z-average (nm), PDI and zeta-potential (mV) on the formulation of BSA prepared in different dispersing medium (H_2O and PBS)

Organic phase	Yield (%)	Z-average (nm)	PDI	Zeta-potential (mV)	
				H_2O	PBS
n-dodecane	100 ± 0	960 ± 186	0.5 ± 0.07	-43 ± 2	-15 ± 1
Mineral oil	100 ± 0	1203 ± 141	0.6 ± 0.02	-40 ± 0	-16 ± 1
Vegetable oil	100 ± 0	1382 ± 551	0.5 ± 0.04	-42 ± 1	-18 ± 1

Table VII-2: Effect of organic phase (40%) on the yield value (%), Z-average (nm), PDI and zeta-potential (mV) on the formulation of HSA prepared in different dispersing medium (H_2O and PBS)

Organic phase	Yield (%)	Z-average (nm)	PDI	Zeta-potential (mV)	
				H_2O	PBS
n-dodecane	99 ± 1	1117 ± 111	0.4 ± 0.01	-41 ± 2	-16 ± 1
Mineral oil	97 ± 0	1608 ± 114	0.6 ± 0.06	-39 ± 2	-13 ± 1
Vegetable oil	94 ± 0	1676 ± 275	0.5 ± 0.08	-42 ± 4	-13 ± 1

Table VII-3: Effect of organic phase (40%) on the yield value (%), Z-average (nm), PDI and zeta-potential (mV) on the formulation of SF prepared in different dispersing medium (H_2O and PBS)

Organic phase	Yield (%)	Z-average (nm)	PDI	Zeta-potential (mV)	
				H_2O	PBS
n-dodecane	98 ± 1	1505 ± 193	0.6 ± 0.07	-37 ± 3	-12 ± 0
Mineral oil	88 ± 2	1930 ± 159	0.7 ± 0.04	-39 ± 2	-12 ± 0
Vegetable oil	90 ± 1	2006 ± 125	0.6 ± 0.08	-39 ± 2	-14 ± 3

Suspension stability is another important parameter for materials characterization in microemulsion research. Nevertheless, stability studies were performed over four months analyzing the macroscopic aspect and measuring the size distribution and zeta-potential, in order to evaluate their physical stability (Figure VII-1). An increase in size is observed over time when aggregation of particles occurs. Size of proteinaceous devices did not otherwise change over four months.

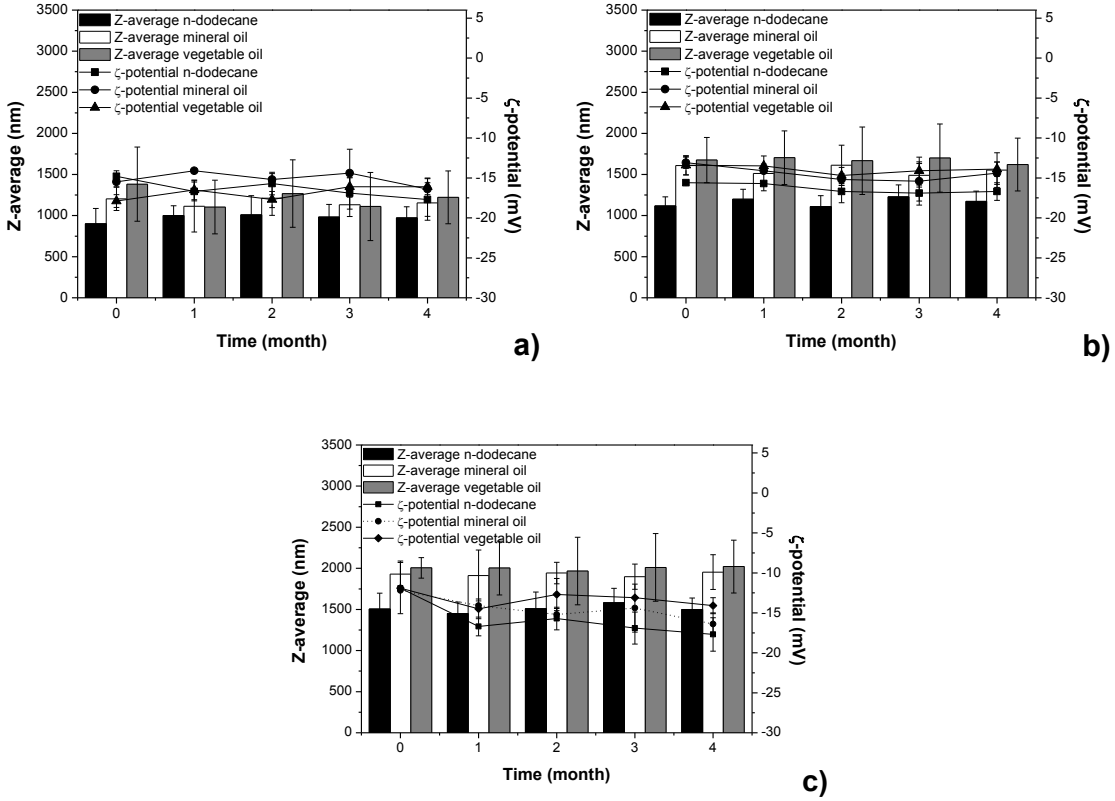

Figure VII-1: Z-average (nm) and zeta (ζ) -potential (mV) over time frame of four months for different protein formulations prepared in PBS medium: a) BSA (5.0 g.L^{-1}) b) HSA (5.0 g.L^{-1}) and c) SF (10.0 g.L^{-1}).

For a suspension system, zeta-potential is also an important index, which reflects the intensity of repulsive force among particles and the stability of dispersion. The reduced net charge on the surface and the accompanying reduction in repulsive forces between particles led to aggregation. However, after the time storage of proteinaceous devices, no noticeable aggregates or obvious changes in zeta-potential were observed when microspheres were prepared in H_2O or PBS medium. The electrostatic repulsive forces present in these emulsions were sufficient to promote the stability over the time frame of storage.

The use of electron microscopy can provide valuable information on particle size, shape and structure. STEM is an important technique to depict particle morphology and surface features. Figure VII-2 evidences the spherical shape of proteinaceous particles. The spherical shape would offer the highest potential for controlled release and protection of incorporated drugs, as they provide minimum contact with the aqueous environment, as well as the longest diffusion pathways. Comparing particles with any other shape, spherical particles also require the smallest amount of surface-active agent for stabilization, because of their small specific surface area [187]. The STEM photographs are also consistent with PCS results, once that the particle size distribution was very similar.

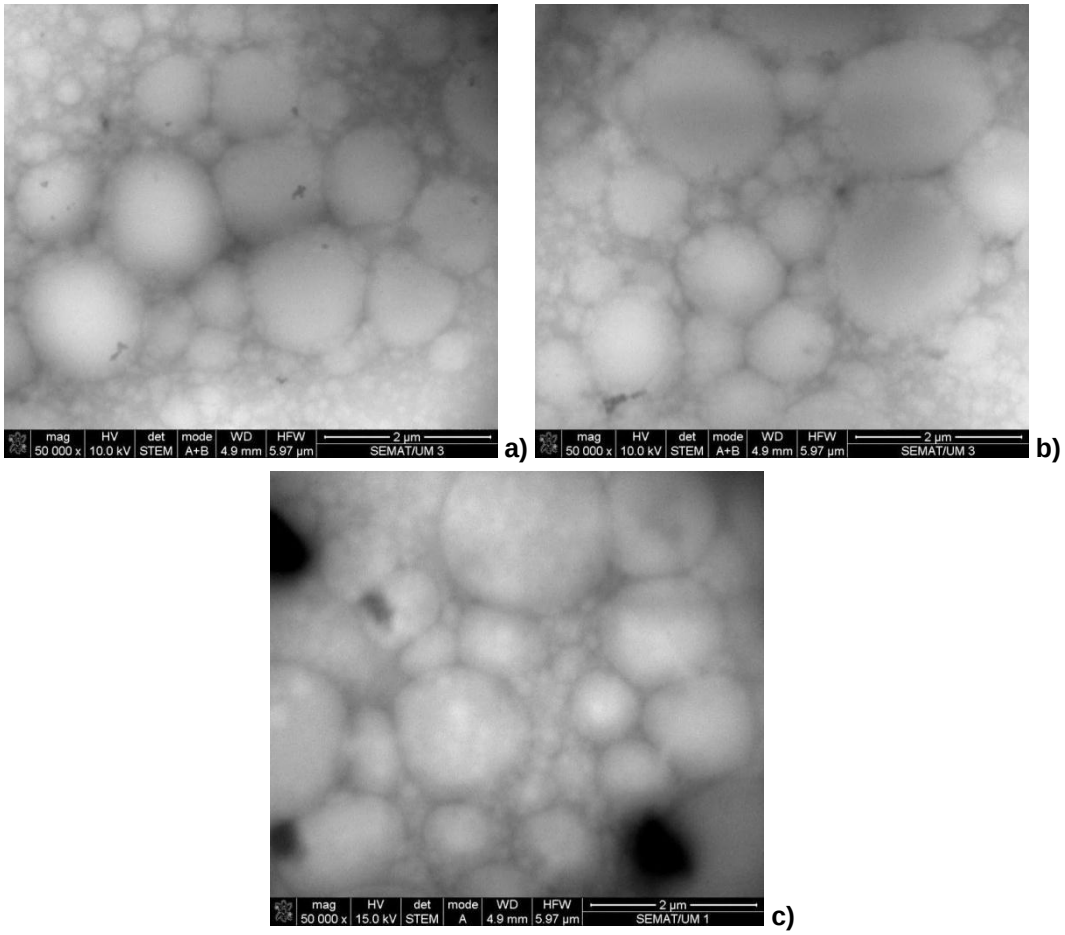

Figure VII-2: STEM images (x50000 magnification) of proteinaceous microspheres prepared with vegetable oil: a) BSA (5.0 g.L^{-1}) b) HSA (5.0 g.L^{-1}) and c) SF (10.0 g.L^{-1}).

VII-3.2. Inhibitory activity

The major goal of this work is the development of proteinaceous devices with a specific biological functionality: the inhibition of elastase in chronic wounds. For this purpose, it was important to determine the inhibitory activity of the different organic solvents incorporated into protein devices.

Figure VII-3 depicts the activity loss obtained with the highest concentration of proteinaceous microspheres used (5.0 $g.L^{-1}$ for BSA and HSA and 10.0 $g.L^{-1}$ for SF), after 5 min of incubation with PPE. It can be observed that after 5 min it was achieved more than 40% of activity loss for all the proteinaceous microspheres prepared with different solvents. Nevertheless, both mineral and vegetable oil present higher activity loss than *n*-dodecane, specially when SF was used as carrier. This result can be due to the presence of monounsaturated and polyunsaturated fatty acids in different ratios on mineral and vegetable oil, when compared with *n*-dodecane, which is composed by saturated chains. Oleic acid, for example, has been shown to be effective in the wound healing process [265, 268] . Additionally, a survey of the literature reveals the importance of chain length in the inhibitory capacity, indicating that a minimal chain length of fatty acids is a prerequisite [267, 279].

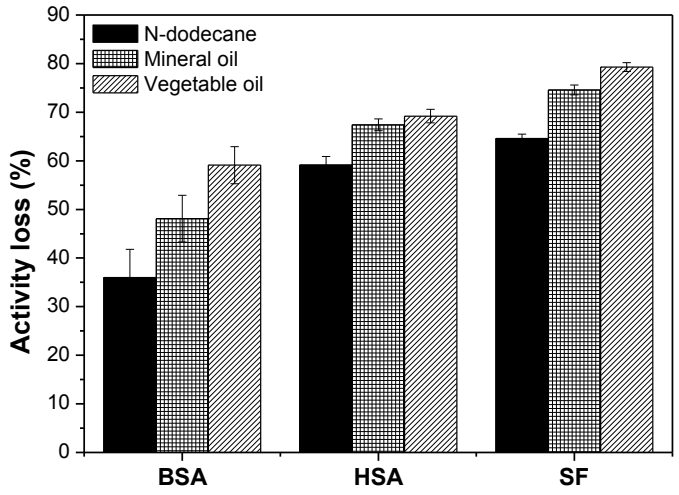

Figure VII-3: Activity loss of PPE obtained after 5 min of incubation at 25 ºC with BSA (5.0 $g.L^{-1}$), HSA (5.0 $g.L^{-1}$) and SF (10.0 $g.L^{-1}$) microspheres prepared with different organic phases: *n*-dodecane, mineral and vegetable oil.

Considering all the mentioned aspects, the vegetable oil was used as standard conditions for all subsequent preparations.

The controlled release of vegetable oil present in proteinaceous microspheres was also assessed. To determine the inhibitory activity of vegetable oil, decreasing protein microspheres amounts were incubated with PPE solution, at 25 ºC. At determined time points, aliquots were taken to determine the residual activity. From the results obtained (Figure VII-4) it is evident that for high protein microspheres concentrations, PPE activity rapidly decreases, suggesting a promising system to modulate elastase activity. For lower protein microspheres concentrations, the decrease in activity of PPE was not so pronounced. This leads to the conclusion that the decrease in PPE activity is dependent on protein devices concentration, once that higher concentrations of proteinaceous microspheres lead to a higher content of the entrapped vegetable oil.

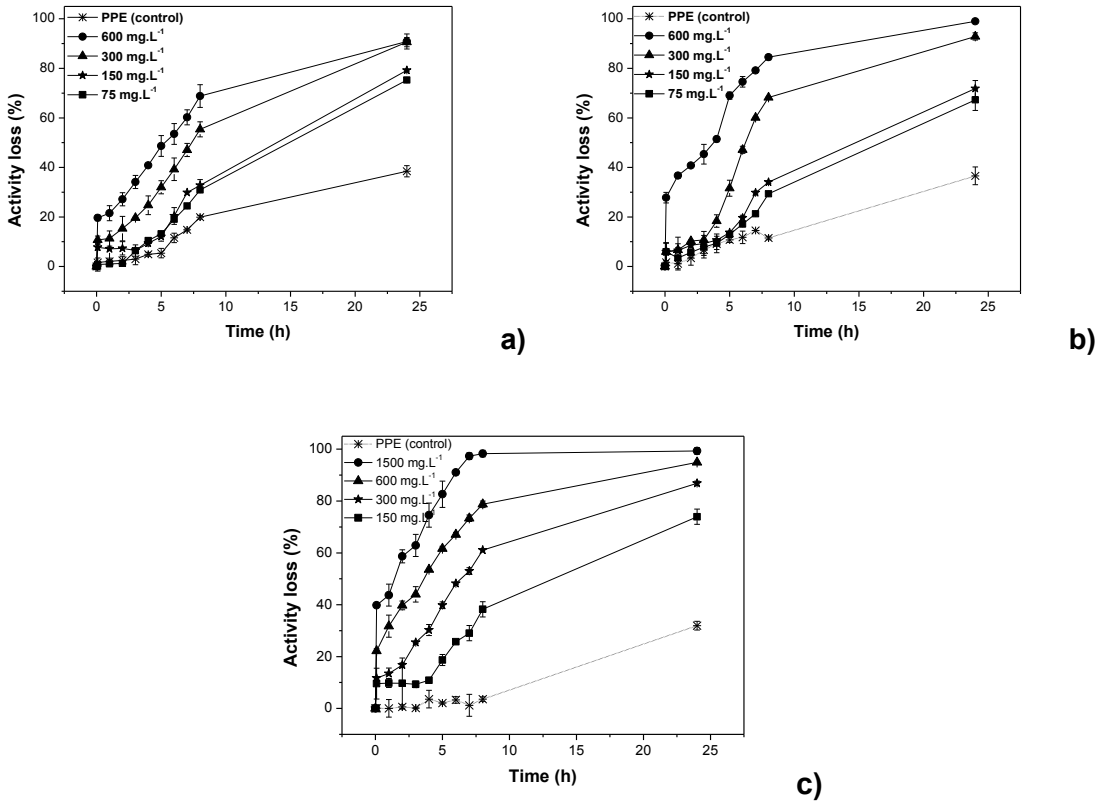

Figure VII-4: Activity loss of PPE, obtained after 24 h of incubation, at 25 ºC, in the presence of different concentrations of BSA (a: 75, 150, 300 and 600 mg.L^{-1}), HSA (b: 75, 150, 300 and 600 mg.L^{-1}) and SF (c: 150, 300, 600 and 1500 mg.L^{-1}) microspheres incorporating vegetable oil.

It is noteworthy that when SF is used as a carrier, a faster decrease of PPE activity is observed, revealing that the PPE solution is rapidly in contact with vegetable oil encapsulated into the SF microspheres. The data obtained can be related with the cristallinity degree of SF induced by ultrasound which was not sufficient to promote a more rigid structure, leading to an easier degradation or even the formation of cracks, allowing a rapidly diffusion out of vegetable oil.

The results obtained for albumin microspheres can be related with their concentration in the devices. Previous reports indicated that albumin can increase enzyme activity [265, 280]. Recently, the use of oleic acid/BSA formulations showed acceleration of the elastase activity, while requiring increased oleic acid concentrations to override the elastase activation properties of the albumin [265, 280]. A possible explanation is that higher concentrations of BSA may stabilize the enzyme, by promoting aggregation or association of the albumin protein, which in turn may hinder the enzymatic turnover of available substrate. An alternative explanation is that the higher albumin concentration serves as an additional substrate for elastase hydrolysis and thereby decreases the level of enzyme available for chromophoric peptide substrate analysis [265, 268].

These results further suggest differences between the two albumin proteins, bovine albumin and human albumin, in their capacity to inhibit PPE enzyme. The primary structures of HSA and BSA are homologous by 80% [155]. The difference between these two proteins is mainly due to the replacement of some hydrophobic amino acids (a.a.) in their sequence and this replacement can promote different affinities to fatty acids [155, 227]. Spector and co-workers [281] reported the affinity of BSA and HSA to several fatty acids, showing that the unsaturated fatty acids were bound more tightly to HSA than to BSA. This fact can explain the highest activity loss when HSA is used as a device.

VII-3.3. Cytotoxicity evaluation

The biocompatibility of proteinaceous devices incorporating the vegetable oil was assessed through the use of fibroblast *in vitro* cultures. A preliminary screening was made using murine embryonic fibroblasts cells (MEFs) as a

measure of global cytotoxicity. In this study, a wide range of protein concentrations (from 75 to 5000 mg.L^{-1} for BSA, HSA and from 150 to 10000 mg.L^{-1} for SF) used for inhibition assays was evaluated and no toxicity was observed for the range concentrations of 75-300 mg.L^{-1} and 150 to 600 mg.L^{-1} for BSA and SF, respectively. The results obtained with MEFs were then confirmed with human skin fibroblasts (BJ5ta), testing the range protein microspheres concentrations that did not promote any damage to the MEFs.

The effect of all tested conditions over BJ5ta was evaluated after 24, 48 and 72 h (Figure VII-5). Results indicate that neither protein solutions (BSA, HSA and SF), nor vegetable oil induced any toxicity in this time frame ($P > 0.05$).

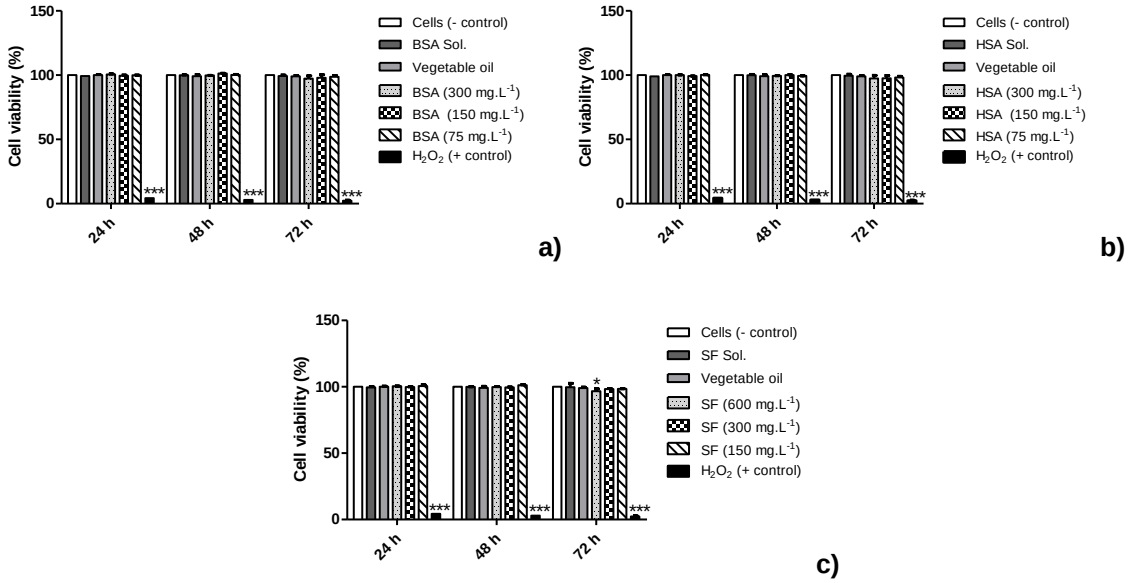

Figure VII-5: BJ5ta cell viability at 24, 48 and 72 h of culture with different materials solutions and different concentration of BSA (a), HSA (b) and SF (c) microspheres incorporating vegetable oil. Values for tested samples are presented as a function of the control (cells cultured with culture medium, scored 100%). Statistically significant differences are observed. The results obtained were compared among each other and with the control: * *P* <0.05, * *P* <0.001.**

It is possible to observe in Figure VII-5 that the range concentrations of 75-300 mg.L^{-1} of BSA microspheres containing the vegetable oil did not affect the viability of human skin fibroblasts cells for a period of 72 h, suggesting that microspheres can be safely applied to the skin at these concentrations. Similar data is displayed for the viability of BJ5ta cells, in the presence of HSA particles, which further provides the evidence of no cytotoxic effects after 72 h. However,

the use of 600 mg.L^{-1} of SF microspheres on human fibroblasts cells is statistically different when compared with control cells (* $P < 0.05$), which suggests a mild cytotoxicity.

VII-4. CONCLUSIONS

In this study, a promising microemulsion system was characterized and selected microemulsions were explored for their ability as potential elastase inhibitors.

This work outlines the feasibility of using different organic solvents to produce proteinaceous devices. The choice of organic phase interferes with the characteristics of the microspheres and such knowledge allows the design of materials with specific properties. After their production and subsequent characterization, the inhibitory activity was evaluated against PPE solution and it was found that vegetable oil presents higher inhibitory efficiency. Furthermore, the effective nature of protein should be considered, once that SF demonstrated to be more capable of transferring vegetable oil in an aqueous solution under conditions of pH properties mimicking wound fluid.

The cytotoxicity screening indicated that the developed protein particles are not cytotoxic in a wide range of concentrations (75 to 300 mg.L^{-1} for BSA and HSA and 150 to 300 mg.L^{-1} for SF) over 72 h of exposure. However, for those proteinaceous microspheres concentrations, the highest value attained for the inhibitory activity of PPE was achieved for HSA and BSA. Therefore, it is necessary to find a compromise between the ability to inhibit the elastase and their cytotoxicity, when formulations are developed.

The results presented here strongly demonstrate the value of *in vitro* experiments with respect to the influence of proteinaceous devices to study single factors in the wound healing process. Nevertheless, it must be kept in mind that wound healing is rather complex, although the understanding of these properties may help to support the further refinement of protein devices for improved wound healing.

CHAPTER VIII

PROTEIN MICROSPHERES AS SUITABLE DEVICES FOR PIROXICAM RELEASE

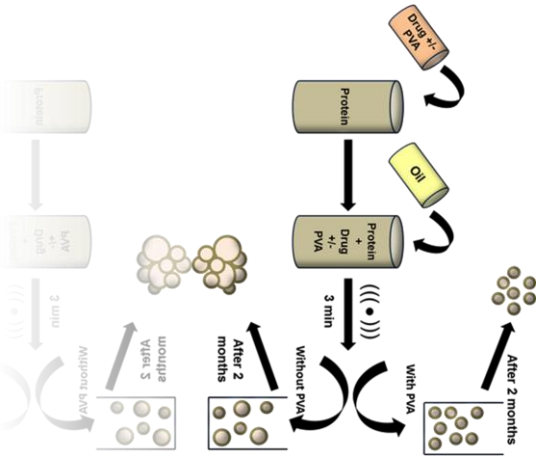

Chapter VIII

Protein microspheres as suitable devices for piroxicam release[‡‡]

ABSTRACT

Bovine serum albumin-piroxicam (BSA-piroxicam) and human serum albumin-piroxicam (HSA-piroxicam) -piroxicam microspheres were sonochemically prepared and characterized based on the previous results achieved in the Chapter V [95/5 (%) of aqueous/organic phase]. The use of polyvinyl alcohol (PVA) lead to an improvement of formulation characteristics, including smaller size, lower polydispersity index (PDI), higher entrapment efficiency and higher stability. The release kinetics of these proteinaceous microspheres was determined in presence of protease, indicating an anomalous drug transport mechanism (diffusion and polymer degradation). In presence of higher protease concentration, BSA microspheres exhibit Case II transport, leading to zero order release (polymer degradation). These proteinaceous devices did not show cytotoxicity against human skin fibroblasts *in vitro*, for range concentrations below to 300 $mg.L^{-1}$, greatly supporting their potential application in the treatment of inflammatory diseases.

[‡‡] This chapter is based on the following publication:
Silva R, Ferreira H, Carvalho A, Gomes AC, Cavaco-Paulo A, *Protein microspheres as suitable devices for piroxicam release*, submitted.

VIII-1. INTRODUCTION

Non-steroidal anti-inflammatory drugs (NSAIDs) are the most widely used drugs in the treatment of inflammatory diseases, such as rheumatic disease, but are also being increasingly used for non-rheumatic conditions, including acute and chronic pain, biliary and ureteric colic, dysmenorrheal inflammation and fever [282]. The mechanism of action of NSAIDs is mediated by its capacity to inhibit cyclo-oxygenase (COX) activity. The COX enzyme can be divided into two isoforms - a constitutive isoform (COX-1), which is responsible for maintaining normal function in the gastrointestinal and renal tracts, for example, and an inducible isoform (COX-2), which is found in areas of inflammation and in the brain [283]. It has been suggested that the anti-inflammatory actions of NSAIDs are due to the inhibition of COX-2, whereas the unwanted side-effects are due to the inhibition of COX-1 [284-286]. The vast majority of NSAIDs currently available are not selective for COX-2 and can thus cause the adverse reactions so commonly seen during NSAIDs treatment [284-286]. Therefore, the entrapment in microspheres of the NSAIDs, such as piroxicam, which are not selectively targeting COX-2, could be useful to minimize their adverse reactions.

Various types of macromolecular substances, such as synthetic and natural polymers have been used in drug delivery research, as they can effectively deliver the drug to target the action site and thus increasing the therapeutic benefit, while minimizing the side effects [9, 148, 287-289]. Recently, protein microspheres have been shown efficacy as biodegradable and biocompatible carrier, which can incorporate a variety of drugs in relatively non-specific fashion [61, 66, 69, 70, 75].

Albumin is a promising material and has been extensively investigated as drug delivery system (DDS), because of its biodegradability and low toxicity [134, 137]. In addition, albumin proteins has a functionality for transporting different macromolecules in the bloodstream to target organs making it a potential macromolecular carrier for the site-directed delivery of drugs [227]. Previous studies demonstrate that 3 min of sonication promote high entrapment efficiency of anti-cancer drugs in bovine serum albumin (BSA) microspheres [61, 66].

In this work, a sonochemical method was used to produce microspheres of BSA and human serum albumin (HSA) and to incorporate piroxicam into them. The production was followed by an extensive physico-chemical characterization of microspheres. Moreover, further miniaturization of the microspheres, to improve their colloidal stability, was performed via different stabilizers: polyvinyl alcohol (PVA), pluronic acid F68 (pluronic F68) and tween 80. The ability of proteins to form microspheres was evaluated by quantifying protein concentration with the Lowry assay on the supernatant after ultrasound treatment [191]. Particle size, as well as the polydispersity index (PDI), of microspheres, was evaluated by photon correlation spectroscopy (PCS). It is well known that the particle size can significantly affect the microspheres properties and is important for their interaction with the biological environment [187]. Particle size values are thus crucial in the development and optimization of preparation process. In addition the zeta-potential of microspheres was also evaluated by electrophoretic laser Doppler anemometry, to obtain an indication of surface potential. The scanning transmission electron microscopy (STEM) has been employed to characterize the overall structure and shape of the microspheres. The entrapment efficiency of piroxicam in microspheres was assessed and the release profile was evaluated in the presence of a protease.

Finally, microspheres were screened for cytotoxicity using a metabolic assay on a human cell line.

VIII-2. MATERIALS AND METHODS

VIII-2.1. Preparation and characterization of protein microspheres

Protein microspheres were prepared according with the method previously described in the Chapter II. The protein devices were produced using a fixed ratio (%) of 95/5 of aqueous/organic phase (vegetable oil), 3000 µM of drug (piroxicam) and 5.0 $g.L^{-1}$ was the concentration of protein aqueous solution used in the assays.

The procedure for the characterization of microspheres obtained is detailed in

the Chapter of materials and methods, namely: yield of microspheres formation, entrapment efficiency of piroxicam into protein microspheres, size and its distribution, zeta-potential, morphology (STEM technique) and stability studies.

The procedure used to study enzymatic degradation and the drug release kinetics, as well as the cytotoxicity evaluation is described below.

VIII-2.2. *In vitro* enzymatic degradation studies

The enzymatic degradation of the developed carrier systems was investigated by incubating the microspheres in phosphate buffered saline solution (PBS, 0.01 M, pH = 7.4) with different concentrations of protease, subtilisin from *Bacillus* sp. (E.C.3.4.21.62), (0.075, 0.50 and 3.0 $U.mL^{-1}$). The selected enzyme was used to mimicking the enzymatic environment of the human body and as a trigger for drug release.

The microspheres were incubated at room temperature under constant shacking (50-60 rpm). At determined time points, aliquots were taken and the piroxicam release was monitored by absorbance measurements at wavelength of 353 nm using a Heλios γ ThermoSpectronic spectrophotometer (Unicam). The quantification of the release was established by a standard absorbance curve. All the release experiments were carried out in triplicate and for a period of 6 days. Results are reported as average ± standard deviation.

VIII-2.3. Drug release kinetics

The release behaviour of compounds from polymeric systems can be determined by fitting the release data to the empirical relationship given by the Ritger-Peppas equation (Equation VIII-1). M_t/M_∞ is the fractional drug release at time t, t is the release time; k is the kinetic constant, and *n* is the diffusion exponent characteristic of the release mechanism.

$$\frac{M_t}{M_\infty} = k \times t^n$$

Equation VIII-1: Ritger-Peppas equation.

To determine *n* values for proteinaceous microspheres, Equation VIII-1 is transformed in Equation VIII-2, and *n* is determined from the slope of the plot of log (% release) *versus* log t.

$$\log(\%\,\text{released}) = \log\left(\frac{M_t}{M_\infty}\right) = \log k + n \times \log t$$

Equation VIII-2: Modified Ritger-Peppas equation.

VIII-2.4. Cytotoxicity screening

The cytotoxicity of BSA and HSA microspheres, containing piroxicam, was evaluated using murine embryonic fibroblasts cells (MEFs), isolated from E13.5 embryos and normal human skin fibroblasts (BJ5ta), from American type culture collection (ATCC).

The BJ5ta cell line (normal human skin fibroblasts) was maintained according to ATCC recommendations (4 parts Dulbecco's modified Eagle's medium (DMEM) containing 4 mM L-glutamine, 4.5 $g.L^{-1}$ glucose, 1.5 $g.L^{-1}$ sodium bicarbonate and 1 part of Medium 199, supplemented with 10% (v/v) of fetal bovine serum (FBS), 1% (v/v) of Penicillin/Streptomycin solution and 10 $\mu g.mL^{-1}$ hygromycin B). The cells were maintained at 37 ºC in a humidified atmosphere of 5% CO_2. Culture medium was refreshed every 2 to 3 days.

Cells were seeded at a density of 10 x 10^3 cells/100 µL/well on 96-well tissue culture polystyrene (TCPS) plates (TPP, Switzerland), in the day before of experiments, and then exposed to different microspheres concentrations, as well as to different controls solutions (BSA and HSA solutions, vegetable oil; PVA solution; piroxicam solution) added to fresh culture medium. At 24, 48 and 72 h of exposure, cell viability was determined using the alamarBlue® assay (Invitrogen, EUA). AlamarBlue cell viability reagent functions as a cell health indicator by using the reducing power of living cells to quantitatively measure the proliferation of various human and animal cell lines, allowing to establish relative cytotoxicity of agents within various chemical classes. When cells are alive, they maintain a reducing environment within the cytosol of the cell. In this assay, viable cells continuously convert resazurin (blue and non-fluorescent) to resorufin (red, highly

fluorescent), increasing the overall fluorescence and colour of the media surrounding cells. 10 µL of alamarBlue compound were added to each well containing 100 µL of culture medium. After 4 h of incubation at 37 ºC the absorbance at 570 nm, using 600 nm as a reference wavelength, was measured in a microplate reader (Spectramax 340PC).

The quantity of resorufin formed is directly proportional to the number of viable cells. Data are expressed as means with standard errors of the means. Two-way ANOVA followed by post hoc Bonferroni test (GraphPad Prism 5.0 for Windows) was employed with statistically significant differences when $P < 0.05$.

The samples were tested at least in triplicates per two independent experiments.

VIII-3. RESULTS AND DISCUSSION

VIII-3.1. Influence of stabilizer addition in protein microspheres characterization parameters

In this work, matrices based on BSA and HSA proteins, were produced and characterized. To ensure microspheres suitability for the intended type of application and to enable a focused development of dispersions with specific properties, the characteristics of the dispersions have to be known in detail.

In a previous study [72] (Chapter V) it was demonstrated that smaller sizes are obtained with 95/5 (%) of aqueous/organic phase. Based on these results, the addition of different stabilizers, namely PVA, tween 80 and pluronic F68, on formulations was evaluated.

Firstly, the efficiency of microspheres formation was monitored with the Lowry assay [191]. The addition of stabilizer for the production of protein devices did not affect the yield of microspheres formation (≈ 100%).

The effect of stabilizers on microspheres size was then evaluated. In this experiment, PVA was the first adopted stabilizer and BSA microspheres of different sizes were successfully prepared controlling PVA amount (Table VIII-1). Results show that when PVA quantity is increased, the size of proteinaceous

microspheres becomes much smaller. From Table VIII-1, it is possible to verify that not only the size of BSA microspheres gets effectively smaller, within a certain range, with the increasing of PVA amount, but also the particle size distribution, determined as PDI, becomes narrower. There are two main explanations for these observations. Firstly, the tiny particles make wavy movement and collide each other in an emulsion leading to particles aggregation. The polymerization degree of PVA used in the experiment can change the viscosity of an aqueous solution decreasing the wavy movement speed and the collision of the tiny particles. Secondly, the adsorption of PVA on the surface of proteinaceous microspheres can lower the surface energy and further agglomeration of proteinaceous microspheres [165, 290].

Table VIII-1: Effect of PVA on Z-average (nm), PDI and zeta-potential (mV) values of BSA microspheres

PVA amount (%)	Z-average (nm)	PDI	Zeta-potential (mV)
0	402.9 ± 65.1	0.44 ± 0.03	-15.6 ± 1.5
2	392.7 ± 20.1	0.35 ± 0.01	-4.7 ± 0.3
4	378.1 ± 40.6	0.18 ± 0.08	-3.9 ± 0.6
6	340.4 ± 15.6	0.15 ± 0.06	-3.8 ± 0.2
8	257.9 ± 5.90	0.06 ± 0.04	-3.9 ± 0.1
10	259.1 ± 4.20	0.06 ± 0.06	-3.7 ± 0.3

Besides PVA, others macromolecular stabilizers have been tested, namely, pluronic F68 and tween 80 (Table VIII-2). However, PVA, when compared with pluronic F68 and tween 80, presented a high ability to reduce the particle sizes and, at the same time, decrease the PDI, promoting a monomodal distribution of BSA microspheres. The optimization of stabilizer amount was achieved at 8%, as higher percentages of PVA did not represent significant change in microspheres size. This ratio was used as standard conditions for all subsequent preparations.

Apart from size determination, zeta-potential was also evaluated to obtain an indication of microspheres surface potential. The surface potential of the particles cannot be measured directly, the zeta-potential (electrical potential at the surface of hydrodynamic shear around the colloidal particle) is usually determined as a characteristic parameter for the particle charge [229, 291]. The BSA microspheres possess a zeta-potential around -15 mV, suggesting the presence of negative charge on the microspheres surfaces (Table VIII-1). Nevertheless, the zeta-potential of the particles decreased significantly in the presence of stabilizers (Table VIII-1 and Table VIII-2).

Table VIII-2: Effect of different stabilizers, PVA (8%), pluronic F68 (8%) and tween 80 (8%), on Z-average (nm), PDI and zeta-potential (mV) values of BSA microspheres

Stabilizers (8%)	Z-average (nm)	PDI	Zeta-potential (mV)
PVA	247.9 ± 5.9	0.060 ± 0.04	-3.9 ± 0.1
Pluronic F68	392.1 ± 60.1	0.29 ± 0.05	-2.9 ± 0.4
Tween 80	386.3 ± 17.1	0.28 ± 0.06	-3.5 ± 0.1

A survey of the literature reveals that the measurement of zeta-potential allows predict about the stability for colloidal dispersion [275, 276, 278]. In general, particle aggregation of charged particles (high zeta-potential) is less likely to occur, due to electric repulsion. However, this rule cannot be strictly applied to the systems containing steric stabilizers, because the adsorption of the steric stabilizers will decrease the zeta-potential, due to the shift in the shear plane of the particle [109].

HSA was also tested in this work and the data presented on Table VIII-3 substantiate that HSA contributed to a small increase on the Z-average value, when compared with BSA. In spite of the 80% of homology, present on the primary structures of the two proteins, the replacement of some hydrophobic amino acids (a.a.) by others (e.g. HSA has a single Tryptophan amino acid while BSA holds two Tryptophan's in its sequence [155, 227], can explain this

difference on the size obtained, once that, the properties of each amino acid demonstrated to be essential in the physico-chemical parameters of microspheres [72, 73]. Conversely, the zeta-potential of HSA microspheres is very similar to BSA microspheres.

Table VIII-3: Effect of PVA on Z-average (nm), PDI and zeta-potential (mV) values of HSA microspheres

PVA amount (%)	Z-average (nm)	PDI	Zeta-potential (mV)
0	451.8 ± 14.6	0.47 ± 0.02	-17.1 ± 1.6
8	296.9 ± 1.3	0.070 ± 0.01	-3.9 ± 1.1

VIII-3.2. Piroxicam entrapment

The entrapment efficiency of piroxicam into BSA and HSA microspheres was assessed spectrophotometrically. Entrapment efficiency refers to the ratio of quantity entrapped/adsorbed drug in relation to the total (theoretical) amount of drug used for microspheres production.

Figure VIII-1 shows that PVA proved to be successful in enhancing drug incorporation efficiency in both types of proteinaceous devices prepared.

Piroxicam entrapment efficiency is an important factor, once that the release rate is usually dependent on drug concentration gradient [132]. Furthermore, higher levels of drug incorporation lead to a wider concentration gap between the polymeric/protein microspheres and the release medium and can cause a higher diffusion rate.

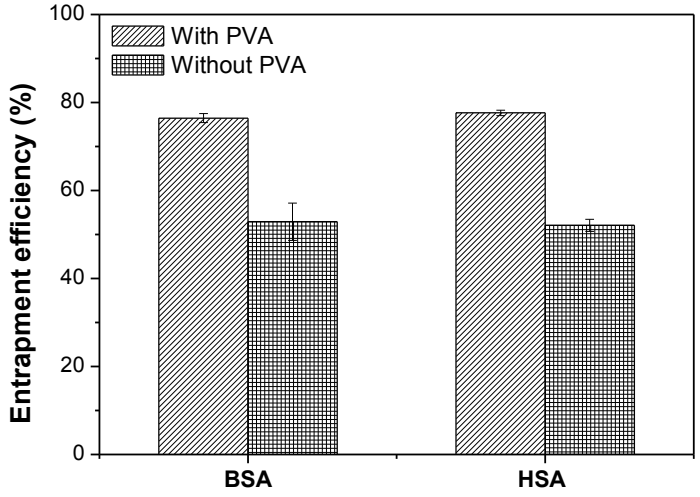

Figure VIII-1: Effect of PVA (8%) on the entrapment efficiency of piroxicam (initial concentration of 3000 µM) into BSA (5.0 g.L^{-1}) and HSA (5.0 g.L^{-1}) microspheres.

As previously demonstrated, the PVA addition led to a submicron size and a relatively narrow particle size distribution. The drug incorporation in microspheres resulted in a slightly bigger particles with similar PDI values (Figure VIII-2).

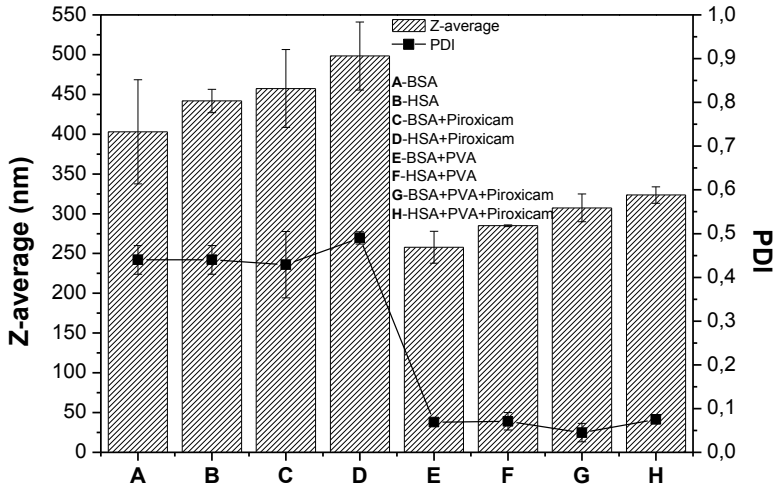

Figure VIII-2: Z-average (nm) and PDI of different formulations, prepared with BSA (5.0 g.L^{-1}) and HSA (5.0 g.L^{-1}), piroxicam (3000 µM), with or without PVA (8%).

The zeta-potential results (Figure VIII-3) evidence that the presence of piroxicam did not affect significantly the surface charge of proteinaceous microspheres.

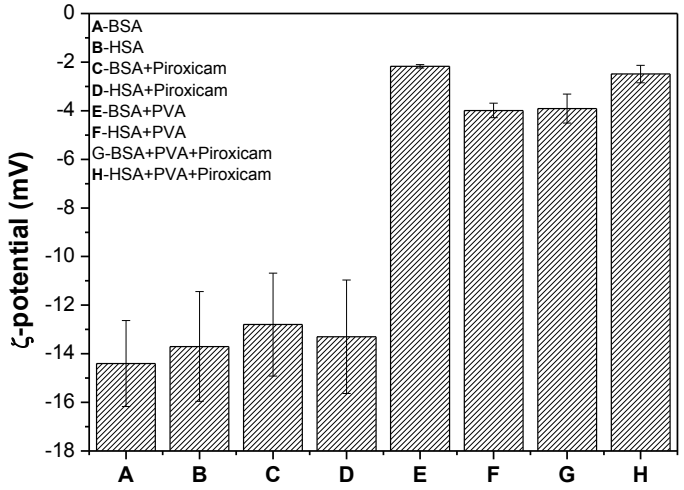

Figure VIII-3: Zeta (ζ) -potential (mV) of different formulations prepared with BSA (5.0 g.L^{-1}) and HSA (5.0 g.L^{-1}), piroxicam (3000 µM), with or without PVA (8%).

VIII-3.3. Stability studies

Since those colloidal particles can suffer destabilization over time [244], particularly when stored in an aqueous dispersion, particle size was monitored for two months after preparation in order to evaluate their physical stability. The zeta-potential was also determined, since this parameter can change over time, due to degradation of components of the colloidal particles [245]. In an electrostatically stabilized dispersion, charges generated on the surface of particles prevent or control agglomeration. Steric stabilization takes place when large molecules adsorb onto the surface of particles, thus introducing physical barriers between them [276]. A combination of electrostatic and steric mechanisms produces electrosteric stabilization preventing microspheres agglomeration.

Figure VIII-4 demonstrates that the presence of PVA increases microspheres' stability, as the size and zeta-potential measurements were roughly stable over time. Conversely, the entrapment of piroxicam without PVA leads to an increase

on Z-average values and decrease zeta-potential values (≈ 0 mV), after one week of storage. Furthermore, the stabilization of microemulsion with PVA is attributed to the adsorbed chain molecules of PVA on the surface, which have ceaseless thermal motion, resulting in dynamically rough surface preventing coalescence by repulsive entropic force.

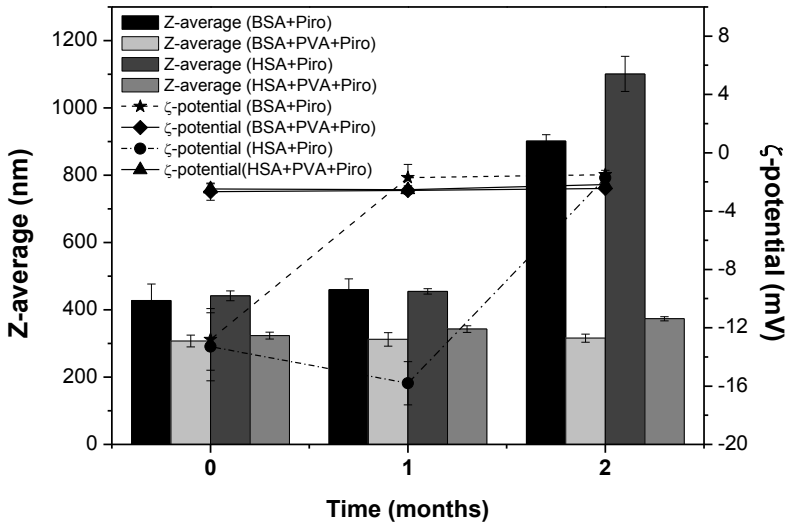

Figure VIII-4: Z-average (nm) and zeta (ζ) -potential (mV) over a timeline of two months for different formulations prepared with BSA (5.0 g.L^{-1}) and HSA (5.0 g.L^{-1}), piroxicam (3000 µM), with or without PVA (8%).

VIII-3.4. Morphology

STEM photographs, in Figure VIII-5, illustrate that the obtained BSA microspheres are clearly spherical homogeneous particles with smooth surfaces. It was possible to verify that the use of stabilizers (PVA) promoted some restrictions on visualization of microspheres, due to their surface tension. The morphology of HSA microspheres was also evaluated and presents a similarly spherical shape. This morphology would offer the highest potential for controlled release and protection of incorporated drugs, as they provide minimum contact with the aqueous environment, as well as the longest diffusion pathways. Comparing particles with any other shape, spherical particles also require the smallest amount of surface-active agent for stabilization, because of their small

specific surface area [187]. These results are also in agreement with PCS results, once that the particle size distribution was very similar.

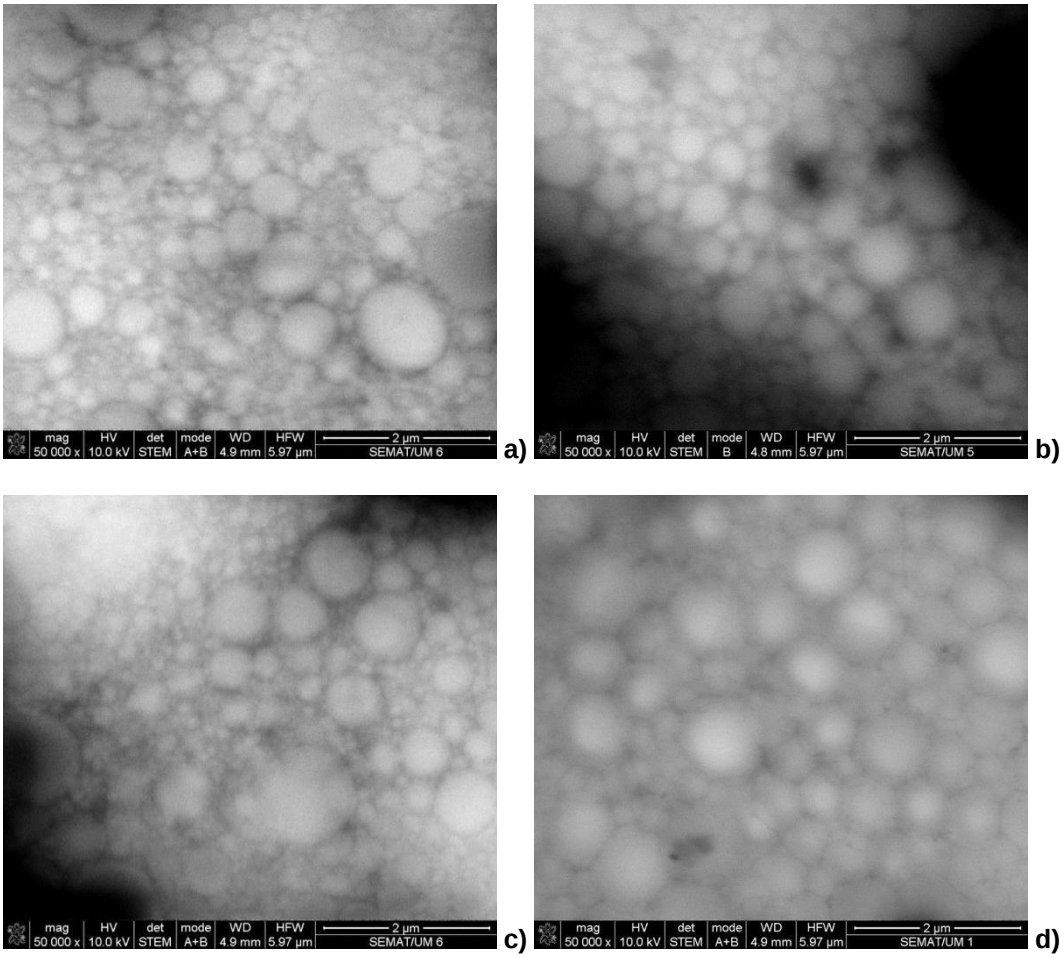

Figure VIII-5: STEM images (x50000 magnification) of protein microspheres: a) BSA (5.0 g.L^{-1}) + Piroxicam (3000 µM); b) BSA (5.0 g.L^{-1}) + PVA (8%) + Piroxicam (3000 µM); c) HSA (5.0 g.L^{-1}) + Piroxicam (3000 µM); d) HSA (5.0 g.L^{-1}) + PVA (8%) + Piroxicam (3000 µM).

VIII-3.5. *In vitro* release profile

The two developed systems in this study aimed to be used as carriers of an anti-inflammatory molecule are: BSA-piroxicam microspheres and HSA-piroxicam microspheres. One important and desired property is biodegradation when designing DDS. Biodegradable polymers are able to release the entrapped drug as their degradation take places. Thus, by controlling the degradation rate of polymeric materials the drug release can be identically monitored.

The release profile of BSA and HSA-based particles, prepared with 5.0 $g.L^{-1}$ of protein, 8% of PVA and with 3000 µM of piroxicam, in the presence of protease enzyme are presented in Figure VIII-6. The release can be divided into two phases: an initial burst in the first hours and a continuous release over the remaining time.

The burst release of piroxicam is associated with those piroxicam molecules dispersing close to microspheres surface, which diffuse out in the initial incubation time.

There are several factors that affect the release of the entrapped drug. It was possible to verify that BSA particles display a faster release of piroxicam, compared with the release obtained with HSA microspheres. This result can be attributed to the fact that smaller particles have a larger surface area, therefore, most of the associated drug would be at or near the particle surface leading to a fast drug release. On the other hand, the observed higher sizes of HSA particles, can explain the longer sustained release compared to smaller particles.

Different concentrations of protease (0.073, 0.50 and 3.0 $U.mL^{-1}$) were used for piroxicam release trigger on protein devices and the results of Figure VIII-6 evidence that the higher concentration lead to the most rapid diffuse out of drug.

A number of mathematical models have been proposed to describe the mechanisms of drug release from polymeric devices. The Higuchi [292], Korsmeyer [293] and Peppas [294, 295] equations are the most widely used to date and are mainly based on the Fickian diffusion equation.

In order to analyse the release mechanism of piroxicam from the proteinaceous microspheres and the effect of the protease concentrations over the release behaviour, the obtained data was processed using the empirical expression proposed by Ritger-Peppas [294] presented in the previously point of materials and methods.

For a sphere, a Fickian diffusion of first-order is observed when n has the limiting value of 0.43; if $n = 0.85$ occurs Case II transport (polymer relaxation/degradation), leading to zero-order release. Finally, when n lies between 0.43 and 0.85, Anomalous transport is observed coupling Fickian diffusion and polymer degradation [294, 295].

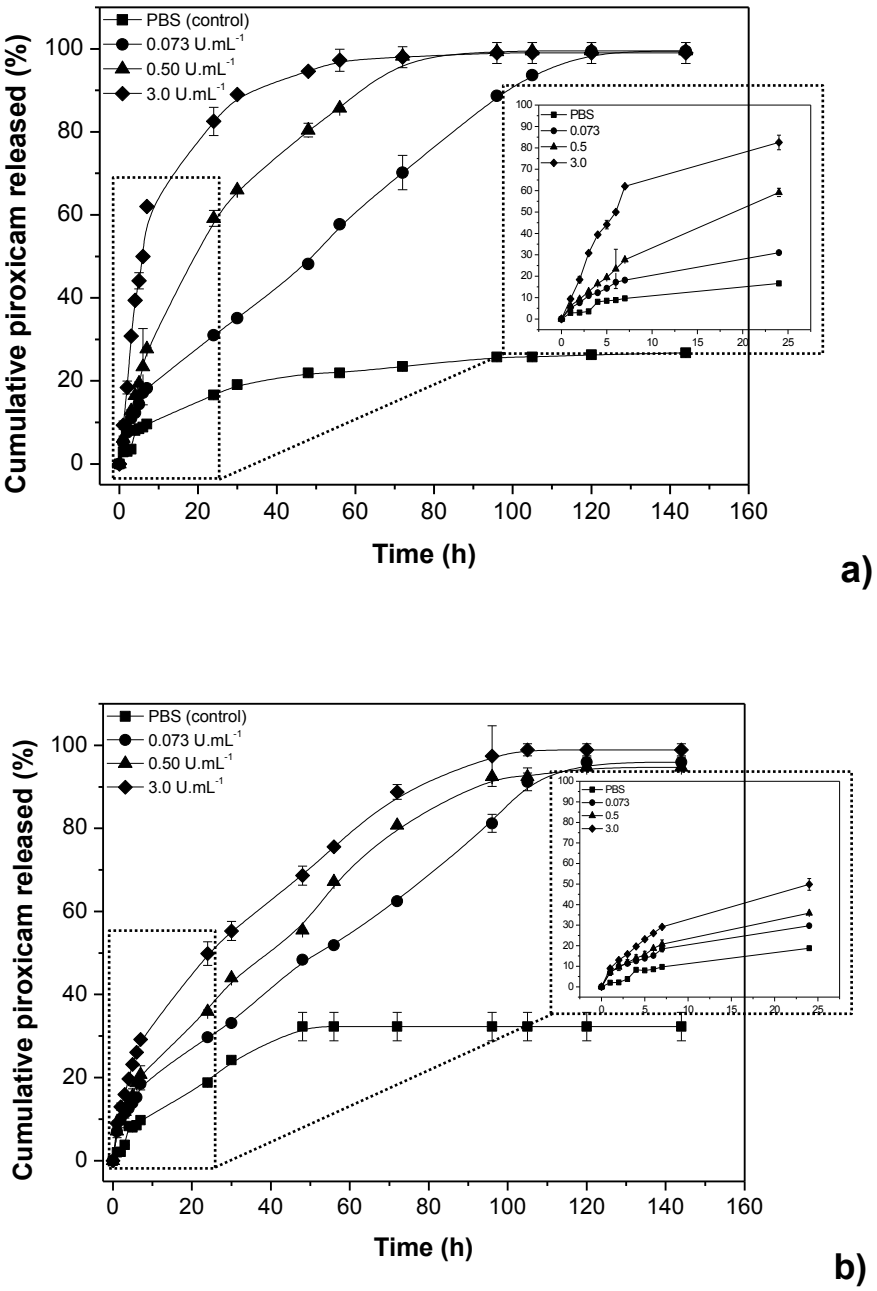

Figure VIII-6: ***In vitro*** **release profile of piroxicam from BSA (a) and HSA (b) microspheres incubated with different concentrations of protease (0.073, 0.50 and 3.0 U.mL^{-1}) and with PBS buffer solution (control). The first 24 h of release is enlarged for all the conditions.**

In HSA microspheres (Table VIII-4), the drug transport mechanism obtained for all experimental conditions was Non-Fickian diffusion or Anomalous (indication of the superposition of both extreme phenomena: drug diffusion and macromolecular chain relaxation/degradation). This result indicates that neither absolute Fickian diffusion (as result of pure drug diffusion) nor Case II-zero order

(because of polymer chain relaxation/degradation) was the predominant mechanism in this case. Therefore, it can be concluded that the protease concentration does not significantly influences the drug transport mechanism, affecting solely the diffusion coefficient value.

In Table VIII-4 is possible to observe that BSA microspheres in the presence of higher protease concentrations present a higher *n* value indicating the Case II-zero order nature, which means that the piroxicam release is mainly due to the macromolecular chain relaxation indicating the degradation of BSA microspheres.

The proteins chemical nature reveal a significant influence in the drug transport mechanism (Anomalous and Case II-zero order nature), when higher enzyme concentrations are used, affecting the diffusion coefficient value. Moreover, correlation coefficient "R^2" is above the permissible range, that is, 0.95, further supporting the validity of the results.

Table VIII-4: Piroxicam release kinetic data obtained from fitting experimental release data to Ritger-Peppas Equation VIII-2, where "*n*" is the diffusion exponent and R^2 is the correlation coefficient

Protease ($U.mL^{-1}$)	BSA		HSA	
	n	***R^2***	***n***	***R^2***
0.073	0.568	0.987	0.529	0.988
0.50	0.699	0.994	0.526	0.996
3.0	0.859	0.987	0.544	0.993

VIII-3.6. Cytotoxicity evaluation

The biocompatibility of the piroxicam entrapped on proteinaceous devices was assessed in fibroblast cultures. A preliminary screening was made using murine embryonic fibroblasts cells (MEFs), as a measure of global cytotoxicity. In this study, a wide range of protein concentrations (from 75 to 5000 $mg.L^{-1}$) used

for inhibition assays was evaluated and no toxicity was observed for the range concentrations of 75-300 mg.L^{-1}.

The results obtained with MEFs were then confirmed with human skin fibroblasts, testing the range protein concentrations (75-300 mg.L^{-1}) that did not induced any damage to MEFs cells.

The effect of all tested conditions on BJ5ta was evaluated after 24, 48 and 72 h of culture, in order to establish the effect of drug entrapped in proteinaceous microspheres (BSA and HSA) on exposed BJ5ta (Figure VIII-7 and Figure VIII-8). Results indicate that neither protein solutions (BSA and HSA), PVA solution (PVA Sol.) nor vegetable oil induce any toxicity for the investigated culture times ($P > 0.05$). However, it is clear that the effect of piroxicam, in a concentration of 0.5 mM, on human fibroblasts cells is statistically different when compared to control cells (*** $P < 0.001$) and with the other tested samples (••• $P < 0.001$).

In Figure VIII-7 it is possible to verify that after 72 h of exposure to 300 mg.L^{-1} of BSA microspheres containing piroxicam, the viability of BJ5ta decreased, suggesting moderate cytotoxicity effects when compared with cells control (** $P < 0.01$). Comparisons of different concentrations of BSA microspheres, containing piroxicam, with the other tested samples were also performed and statistically significant differences were obtained for the 300 mg.L^{-1} concentration, after 72 h (+ symbol: BSA Sol. *Vs* 300 mg.L^{-1} BSA; # symbol: Vegetable oil *Vs* 300 mg.L^{-1} BSA; δ symbol: 150 and 75 mg.L^{-1} BSA *Vs* 300 mg.L^{-1} BSA, $P < 0.05$).

In Figure VIII-8, similar data is displayed for the viability of BJ5ta cells in contact with HSA microspheres, containing piroxicam, which further provides the evidence of cytotoxic effects after 72 h, when 300 mg.L^{-1} of HSA microspheres concentration is used (+ symbol: BSA Sol. *Vs* 300 mg.L^{-1} BSA; # symbol: Vegetable oil *Vs* 300 mg.L^{-1} BSA; δ symbol: 150 and 75 mg.L^{-1} BSA *Vs* 300 mg.L^{-1} BSA, $P < 0.05$ and ** symbol: Cells *Vs* 300 mg.L^{-1} BSA $P < 0.01$). Statistically, it is possible to observe that the range concentrations of 75-150 mg.L^{-1} of proteinaceous microspheres containing piroxicam, did not significantly affect the viability of human skin fibroblasts cells for a period of 72 h, indicating that microspheres can be safely applied at these concentrations.

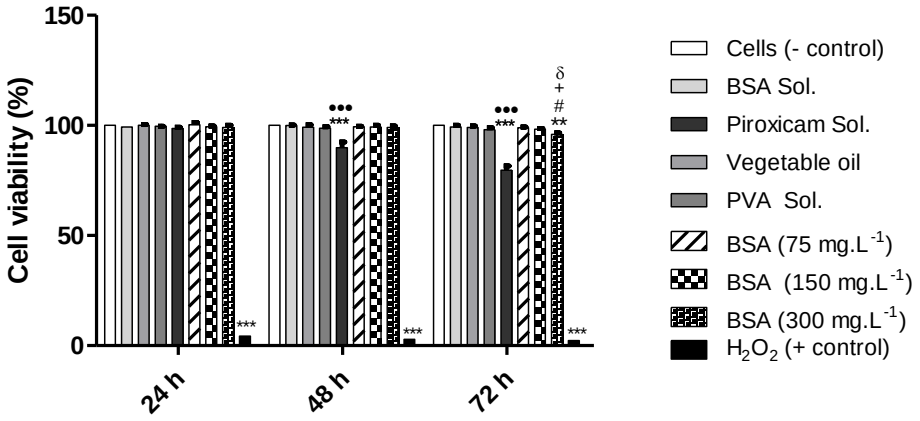

Figure VIII-7: BJ5ta cell viability at 24, 48 and 72 h of culture with different solutions and different concentrations of BSA microspheres containing piroxicam (75, 150 and 300 mg.L^{-1}). Values for tested samples are presented in relation to the control (cells cultured with culture medium scored 100% of viability). Statistically significant differences are indicated. * = significantly different from cells control; • = significantly different from other tested conditions; + = significantly different from BSA Sol.; # = significantly different from Vegetable oil; δ = significantly different from 75, 150 and 300 mg.L^{-1} of BSA microspheres.

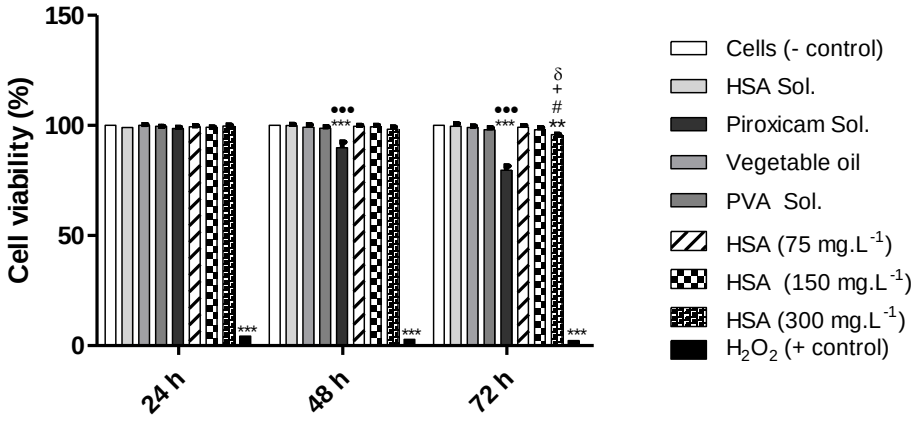

Figure VIII-8: BJ5ta cell viability at 24, 48 and 72 h of culture with different solutions and different concentrations of HSA microspheres containing piroxicam (75, 150 and 300 mg.L^{-1}). Values for tested samples are presented in relation to the control (cells cultured with culture medium scored 100% of viability). Statistically significant differences are indicated. * = significantly different from cells control; • = significantly different from other tested conditions; + = significantly different from HSA Sol.; # = significantly different from Vegetable oil; δ = significantly different from 75, 150 and 300 mg L^{-1} of HSA microspheres.

VIII-4. CONCLUSIONS

The present study demonstrates the ability of proteinaceous microspheres to entrap the anti-inflammatory drug piroxicam. BSA and HSA microspheres were produced with predictable and reproducible size by a sonochemical method. Furthermore, the incorporation of PVA into the prepared formulations resulted in improved characteristics, including smaller size, lower size distribution, higher stability and higher entrapment efficiency of piroxicam.

The kinetics of piroxicam entrapped in BSA or HSA microspheres release mechanism was shown to be dependent on the protein and on protease concentration. The fast release is achieved when the drug is entrapped into BSA microspheres and in the presence of high protease concentration (3.0 $U.mL^{-1}$). However, if it is necessary a slower release the piroxicam should be incorporated in HSA microspheres.

This fact, along with the cytocompatibility observed with human skin fibroblasts, indicates that these proteins may potentially be used as potential bioactive carriers for treatment of inflammatory diseases. In this sense, such drug carriers with a specific size range can be invaluable therapeutic tools for other pathologies where the NSAIDs can be useful, such as cancer, Alzheimer and artherosclerosis [282, 296-298].

CHAPTER IX

COTTON AND NONWOVEN GAUZES BANDAGES: A SUPPORT FOR PROTEINACEOUS MICROSPHERES

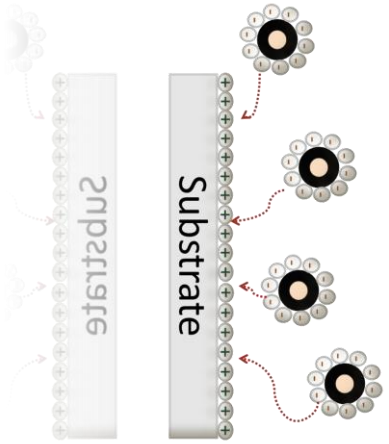

Chapter IX

Cotton and nonwoven gauzes bandages: A support for proteinaceous microspheres[§§]

ABSTRACT

The use of active ingredients in wound management have evolved alongside the pharmaceutical agents and dressings used to deliver them. However, the development of gauzes dressings with specific properties still remains a challenge for several medical applications, thus the search for the new gauzes bandages.

Being protein microspheres production process optimized, it was considered pertinent their application onto a textile support. Thus, bovine serum albumin-piroxicam (BSA-piroxicam) microspheres were attached onto cotton and nonwoven gauzes using two different methodologies (incubation and sonochemical methodology). The attachment of proteinaceous microspheres using sonochemical radiation, promotes the binding onto cotton and nonwoven gauzes by a one-step process. In fact, the short time ultrasound treatment (3 min) proved to be the more efficient methodology, due to the increase of mass transport effects.

The results also demonstrated that the previous activation of surface gauzes, with the cationic product, led to an enhancement of proteinaceous microspheres attached onto cotton and nonwoven gauzes and, consequently, to a higher piroxicam release. Furthermore, these protein devices show extraordinary ability to delivery piroxicam, greatly supporting their potential application in the biomedical fields.

[§§] This chapter is based on the following publication:
Silva R, Ferreira H, Cavaco-Paulo A, *Cotton and nonwoven gauzes bandages: A support for proteinaceous microspheres*, submitted.

IX-1. INTRODUCTION

The use of textiles in medicine has a long tradition. An important field of application is in wound care and prevention of chronic wounds [180]. Among the long list of textile materials, bandages and wound dressings gained great popularity [178]. The exploit of textile materials was supported by availability, prices and re-usability [299]. Along with the technology development of functional textiles, their use in wound healing and prevention of chronic wounds has reached a new quality of interactivity between biological tissues and textiles [178]. These fibres were shown to favour wound occlusion, exudate transport, and drug dispensation with much reduced distress to the patient [180, 300]. Despite the fact that traditional textiles fulfilled primary quality approaches like biocompatibility, flexibility, strength, etc., there is an increasing need for specified functions [301]. In particular, the controlled release of bioactive molecules to counteract the progression of infection and inflammation such as in chronic wounds management was considered a step forward in this research area [302]. The local delivery of drugs by topical administration or by delivery device may enable the maintenance of high local drug concentration for an extended duration release without exceeding systematic toxicity. This is an important feature, because the use of anti-inflammatory drugs, such as piroxicam that is very useful to counteract local inflammation, can be absorbed through blood vessels and could originate severe side effects on both the gastrointestinal and kidney [303, 304].

Controlled delivery dressings can provide an excellent means of delivering drugs to wound sites in a consistent and sustained fashion over long periods of time without the need for frequent dressing change [305].

There is a need to develop new dressings that can be useful in the treatment of local infections, where it may be beneficial to the increase of the local concentrations of anti-inflammatory drugs, while avoiding high systemic doses, thus reducing patient exposure to an excess of drug beyond that required at the wound site [306, 307]. Furthermore, a dressing that will deliver an active substance to a wound site in a controlled fashion for a sustained period of about a week could help solve or minimize the non-compliance patients.

Several biodegradable devices from both natural and synthetic polymers have been produced by different processes in recent years, for use as drug carriers. Biodegradable polymers can release larger quantities of pharmaceutical agents and their degradation properties can be tailored for a specific application [8, 148, 308]. Natural polymers such as proteins are attractive, since they exhibit superior biocompatibility and biodegradability [69, 140, 309].

In the present work, piroxicam, sonochemical entrapped on bovine serum albumin (BSA) microspheres was attached onto cotton and nonwoven gauzes in order to produce a functionalized biomaterial with the ability to deliver the pharmaceutical agent in a control manner.

IX-2. MATERIALS AND METHODS

IX-2.1. Preparation and characterization of protein microspheres containing piroxicam

Protein microspheres were prepared according with the method described previously in Chapter II. The protein devices were produced using a fixed ratio (%) of 95/5 of aqueous/organic phase (vegetable oil), 8% of polyvinyl alcohol (PVA), 3000 µM of piroxicam and 5.0 $g.L^{-1}$ was the concentration of protein aqueous solution used in the assays. The procedure for the further characterization is detailed in Chapter II. The methodologies used to attach the proteinaceous devices onto cotton and nonwoven gauzes as well as the evaluation of piroxicam release are described below.

IX-2.2. Chemical activation of gauzes

IX-2.2.1. Cationization of cotton and nonwoven gauzes

The gauzes were cationized using the exhaust method already described [310]. The cationization was performed in sealed, stainless steel pots of 120 cm^3 capacity in a laboratory scale dyeing machine (AHIBA Spectradye, from Datacolor International) with infrared temperature control.

The treatment was carried out using a material: liquor ratio of 1:20, 10% (on weight of the fabric) of poly(diallyldimethylammonium chloride) (PDDA) (Figure IX-1) and 5.0 g.L^{-1} of sodium hydroxide (NaOH) over 60 min at 50 ºC. Then the gauzes were washed thoroughly with deionized water.

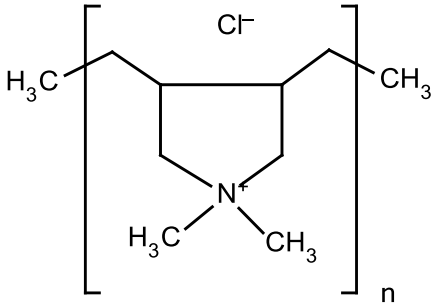

Figure IX-1: Chemical structure of poly (diallyldimethylammonium chloride).

IX-2.2.2. Determination of the cationization efficiency on the gauze surface

The cationization at the surface of gauzes (cotton and nonwoven) were analysed by staining of treated samples and controls (cotton and nonwoven gauzes without cationization treatment) with a Comassie brilliant blue G250 (Acid Blue 90; C.I. 42655). The staining was executed in AHIBA machine, previously referred, using 1 g.L^{-1} of Comassie dye, at 60 ºC for 60 min. After staining, the samples were washed with deionized water until no more dye could be detected in the washing solution. The colour measurements were determined using a spectrophotometer (illuminant D_{65} at 600 nm) (Spectraflash, from Datacolor International) coupled to a computer. The colour strength was evaluated as K/S (Equation IX-1) at maximum absorption wavelength (600 nm). The ratio between absorption coefficient (K) and scattering coefficient (S) is related to reflectance data by applying Kubelka-Munk's law at each wavelength, and it is proportional to dye concentration [311, 312]. R is the light reflection, K is the absorption coefficient and S is the scattering coefficient. All the samples were measured using at least triplicate samples.

$$\frac{K}{S} = \frac{1-R^2}{2\times R}$$

Equation IX-1: Determination of K/S using the simplified Kubelka-Munk's law.

IX-2.3. Attachment of proteinaceous microspheres, containing piroxicam, onto gauzes bandages

In order to obtain the attachment of proteinaceous microspheres, containing piroxicam, onto gauzes (0.1 g) two sets of experiments were applied, namely incubation and sonochemical method. The attachment of microspheres by incubation procedure was carried out in two different steps. First, the microspheres were produced and submitted to an extensive physico-chemical characterization. After, they were incubated with the gauzes in a water shaking bath at room temperature (25 ºC) over 24 h under constant shacking (50 rpm). Several controls were run simultaneously: a control test with non-cationized gauzes (cotton and nonwoven) and a control test with cationized gauzes (cotton and nonwoven) without microspheres, incubated with phosphate buffered saline solution (PBS, 0.01 M, pH=7.4). After incubation, the samples were removed and washed with deionized water.

The attachment of proteinaceous microspheres via sonochemical method was performed in one-step reaction. In this case, the gauzes were added to the biphasic system, consisting of protein solution and vegetable oil, applying the same conditions described in Chapter II (II-4.2.). The control samples were the gauzes (cotton and nonwoven, cationized and non-cationized) in PBS submitted to ultrasound treatment in the same conditions. The remaining solution was centrifuged, using the centricon tubes, and the protein concentration in the supernatant and the amount of piroxicam entrapped was determined (Chapter II). Finally, the samples gauzes were collected and washed with deionized water.

All measurements were performed using at least duplicate samples.

IX-2.4. Evaluation of proteinaceous microspheres attached onto gauzes based on ninhydrin reaction

The presence of protein microspheres in the gauzes samples, was evaluated using the ninhydrin (2,2-dihydroxyindane-1,3-dione) reagent. Ninhydrin is most commonly used to detect, the terminal amines or Lysine residues in peptides and proteins [313, 314]. This is a chemical reagent used to detect ammonia or

primary and secondary amines. When reacting with these free amines, a deep blue or purple colour, known as Ruhemann's purple, is produced (Figure IX-2).

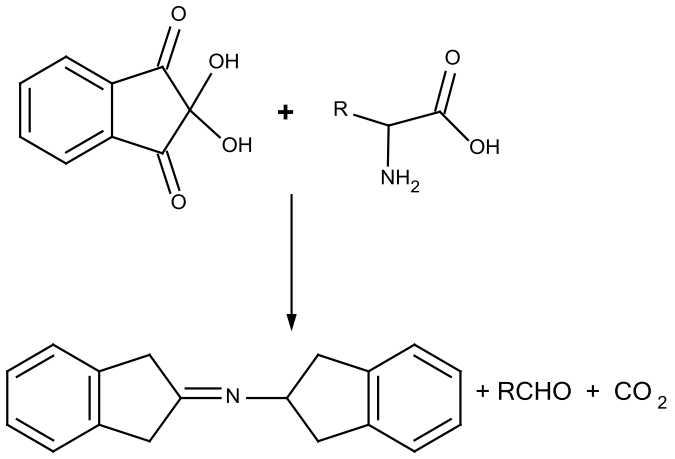

Figure IX-2: Mechanism of reaction of amino acids with ninhydrin to form Ruhemann's purple product (Adapted from Friedman [314]).

For this assay, the gauzes samples were dried at 60 ºC and then incubated with ninhydrin solution (0.5%), at 60 ºC, over 30 min. This test was performed in the gauzes samples after proteinaceous microspheres attachment by incubation and ultrasound treatment, and in controls gauzes samples (cotton and nonwoven cotton samples gauzes, cationized and non-cationized, without microspheres).

IX-2.5. Quantification of piroxicam released from proteinaceous microspheres attached onto gauzes bandages

The release of piroxicam by the microspheres attached onto gauzes was assessed by incubation of the textile samples, and control samples (gauzes without microspheres) in deionized water (pH 5.5). The deionized water was used to mimic the skin pH (5.5 - 5.6) [315]. At determined time points, aliquots were taken, and the piroxicam release was monitored by absorbance measurements at wavelength of 353 nm using a Helios γ ThermoSpectronic spectrophotometer (Unicam). The quantification of the piroxicam released was established by a standard absorbance curve. The release studies were carried out in in triplicate and for a period of 6 days. Results are reported as mean value ± standard deviation.

IX-3. RESULTS AND DISCUSSION

In this work, matrices based on BSA protein, were produced and characterized.

In a previous study [76] (Chapter VIII), it was shown that smaller sizes are obtained with 95/5 (%) of aqueous/organic phase and with 8% of stabilizer. After testing some different stabilizers it was demonstrated that the most competent is the PVA. The results evidence high entrapment efficiency (≈ 80%) of piroxicam into BSA microspheres. Piroxicam entrapment efficiency is an important factor, once that the release rate is usually dependent on drug concentration gradient [132]. Furthermore, higher levels of drug incorporation lead to a wider concentration gap between the protein microspheres and the release medium and can cause a higher diffusion rate.

These conditions were used as standard conditions for all subsequent tests.

IX-3.1. Attachment of proteinaceous microspheres, containing piroxicam, onto cotton and nonwoven gauzes

Considering special advantages and high potentialities of the application of microstructures materials in textile industry, especially for producing high performance textile, this study report the application of microstructured proteinaceous material containing an anti-inflammatory drug for biomedical application.

In this work, two different methodologies were used to attach the BSA microspheres, containing the anti-inflammatory drug, onto cotton and nonwoven gauzes bandages. First, the microspheres were previously prepared, characterized and subsequently incubated with gauzes (cationized and non-cationized) in shaking water bath, at 25 ºC and 50 rpm.

In the other set of experiments, the attachment of microspheres was carried out in one-step reaction using the ultrasound system. This attachment procedure did not present significant differences on physico-chemical characteristics of BSA microspheres containing piroxicam. The efficiency of microspheres formation

was ≈ 100% and the entrapment efficiency of piroxicam was ≈ 76%. The values of zeta-potential were also very similar (-5 ± 0.5 mV), as well as the Z-average and polydispersity index (PDI) values (280 ± 10 nm and 0.095 ± 0.001, respectively).

Taking into account that microspheres present negative surfaces charge, our aim is the activation of the gauzes surfaces in order to obtain a positive charge. Consequently, a higher electrostatic interaction has been expected between the negative surface charge of BSA microspheres and the positive surface charge of gauzes. The covalent addition of cationizer products to cotton is used extensively to improve anionic dye fastness [316]. This study reports not only the cationization of cotton gauzes but also the nonwoven gauzes using PDDA. The reason to submit the nonwoven gauze to cationization process is due to the presence of viscose (67%), containing hydroxyl groups as the cotton fibre. These hydroxyl groups acquire a negative charge when they are ionisable, decreasing the electrostatic interactions with the BSA microspheres and thus the need for cationization process of gauzes.

The cationized samples and the control samples (cotton and nonwoven gauzes no cationized) were dyed with Comassie blue, known as an acid dye, to evaluate cationization efficiency. When dyed, ionic bonding with fibre cationic sites accounts for fixation of coloured anions in the dyed material. The efficiency of cationization process was determined based on colour strength (K/S) and the values are given in the Figure IX-3. Comparing the K/S values of the cationized and the non-cationized gauzes (cotton and nonwoven) it is possible to conclude that Comassie dye has a more affinity for the cationized fibre when compared with non-cationized fibre, demonstrating the strong electrostatic interactions between the negative charge of dye molecules and the positive charge present at the gauzes surfaces.

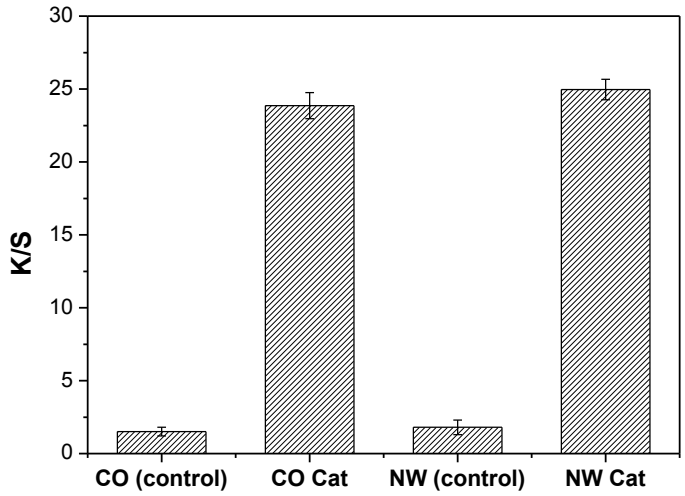

Figure IX-3: K/S values (λ=600 nm) for the cationized samples (cotton and nonwoven gauzes represented as CO Cat and NW Cat, respectively) and the control samples (non-cationized cotton and nonwoven gauzes, represented as CO control and NW control, respectively) dyed with Comassie brilliant blue G250. The K/S was calculated according with the Equation IX-1.

The proposed methods to attach the BSA microspheres, containing piroxicam, onto cotton and nonwoven gauzes bandages (cationized and non- cationized) were evaluated using the ninhydrin reagent, which is applied to detect amino acids (a.a.) on proteins. When ninhydrin react with amines present on proteins a visible purple colour will be developed [313, 314].

Figure IX-4 shows the images, after the addition of ninhydrin, being possible to verify that all the samples (cationized and non-cationized) present a blue colour, correspondent to the presence of protein at gauzes surface. However, the results suggest a more pronounced blue colour for the cationized samples, evidencing the higher protein attachment onto positively charged surfaces. Furthermore, the ultrasound treatment seems to be more efficient once that a greater uniformity of the colour was achieved. In this case, the protein transfer from solution to gauze surface is improved by ultrasound induction in a more uniform manner.

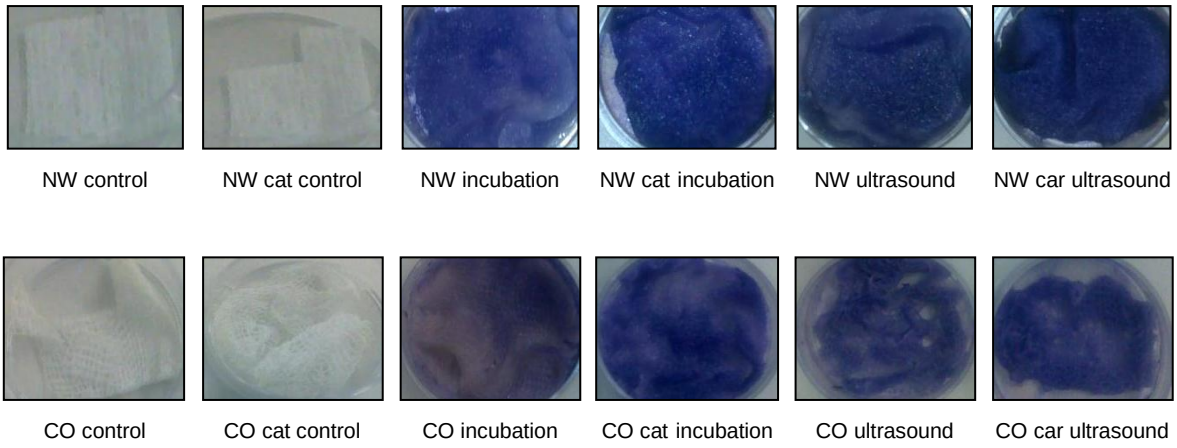

Figure IX-4: **Images of developed colour after 30 min of ninhydrin application on the microspheres attached onto cotton (a) and nonwoven (b) gauzes bandages by sonication or incubation method (cotton and nonwoven gauzes represented as CO and NW, and cotton and nonwoven gauzes cationized represented as CO cat and NW cat, respectively). The control samples were incubated or sonicated with PBS (non-cationized gauzes: cotton and nonwoven without microspheres, symbolized as CO control and NW control, respectively; cationized gauzes: cotton and nonwoven without microspheres, represented as CO cat control and NW cat control, respectively).**

IX-3.2. Morphology of gauzes bandages with microspheres

The morphological analysis of the fibres was carried out using scanning electron microscopy (SEM), which is the most widely used of the surface analytical techniques. SEM represents an invaluable tool for studying surface topography and failure analysis. The technique, which enables qualitative three-dimensional (3-D) imaging of surface features, clearly illustrated that with both methodologies, incubation and ultrasound treatment, it was possible to attach the BSA microspheres, containing piroxicam, onto the cotton and nonwoven gauzes (Figure IX-5 and Figure IX-6).The microphotographs also suggest that the presence of positive charges on the gauzes surfaces increment the microspheres attachment, being possible to visualise a layer of microspheres covering almost completely the surface of the gauze fibres. These data corroborate the ninhydrin results.

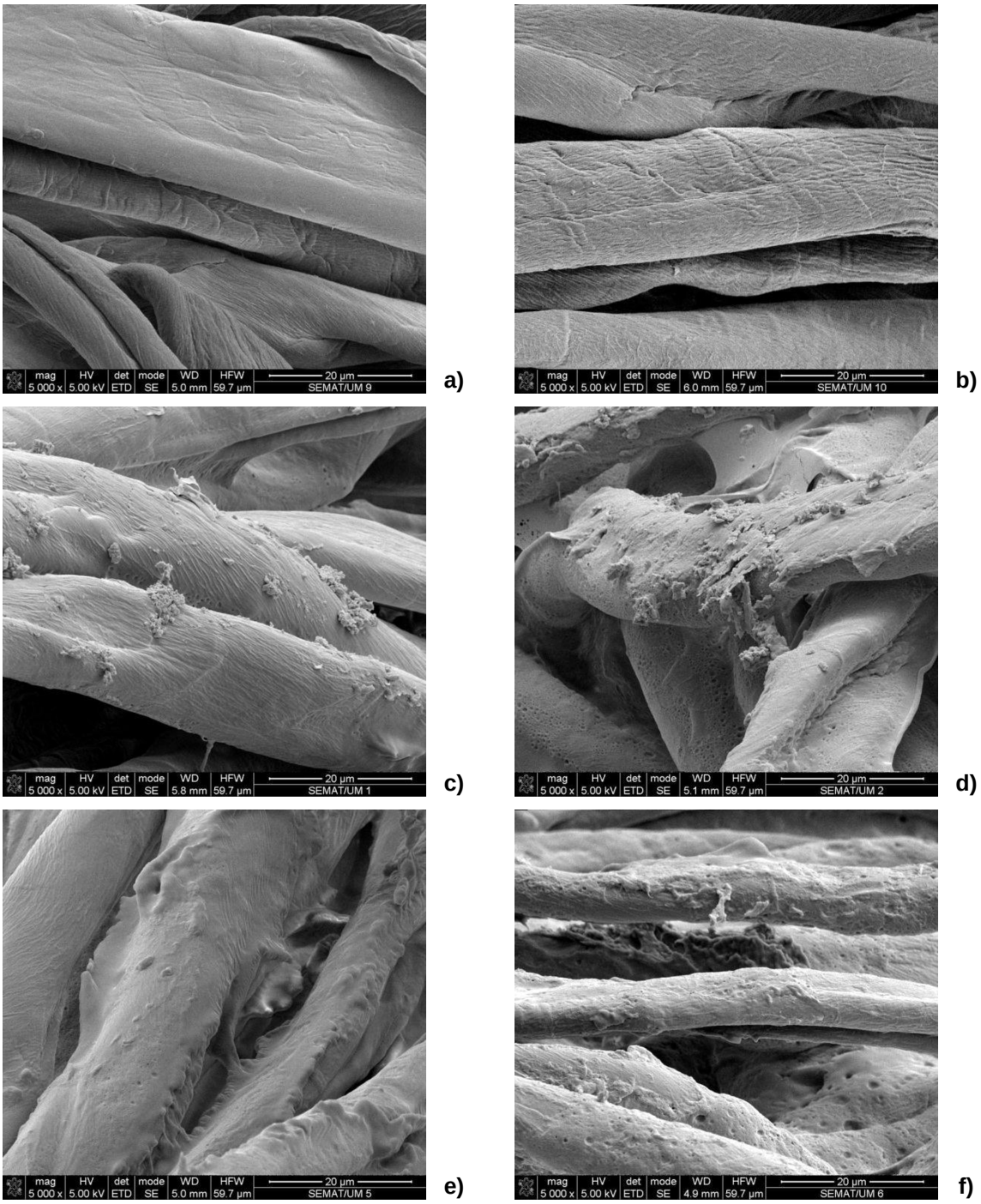

Figure IX-5: SEM microphotography's (x5000 magnification) of cotton gauzes bandages: a) and b) control (cationized and non-cationized without microspheres, respectively); c) non-cationized - incubation treatment; d) cationized - incubation treatment; e) non-cationized - ultrasound treatment; f) cationized - ultrasound treatment.

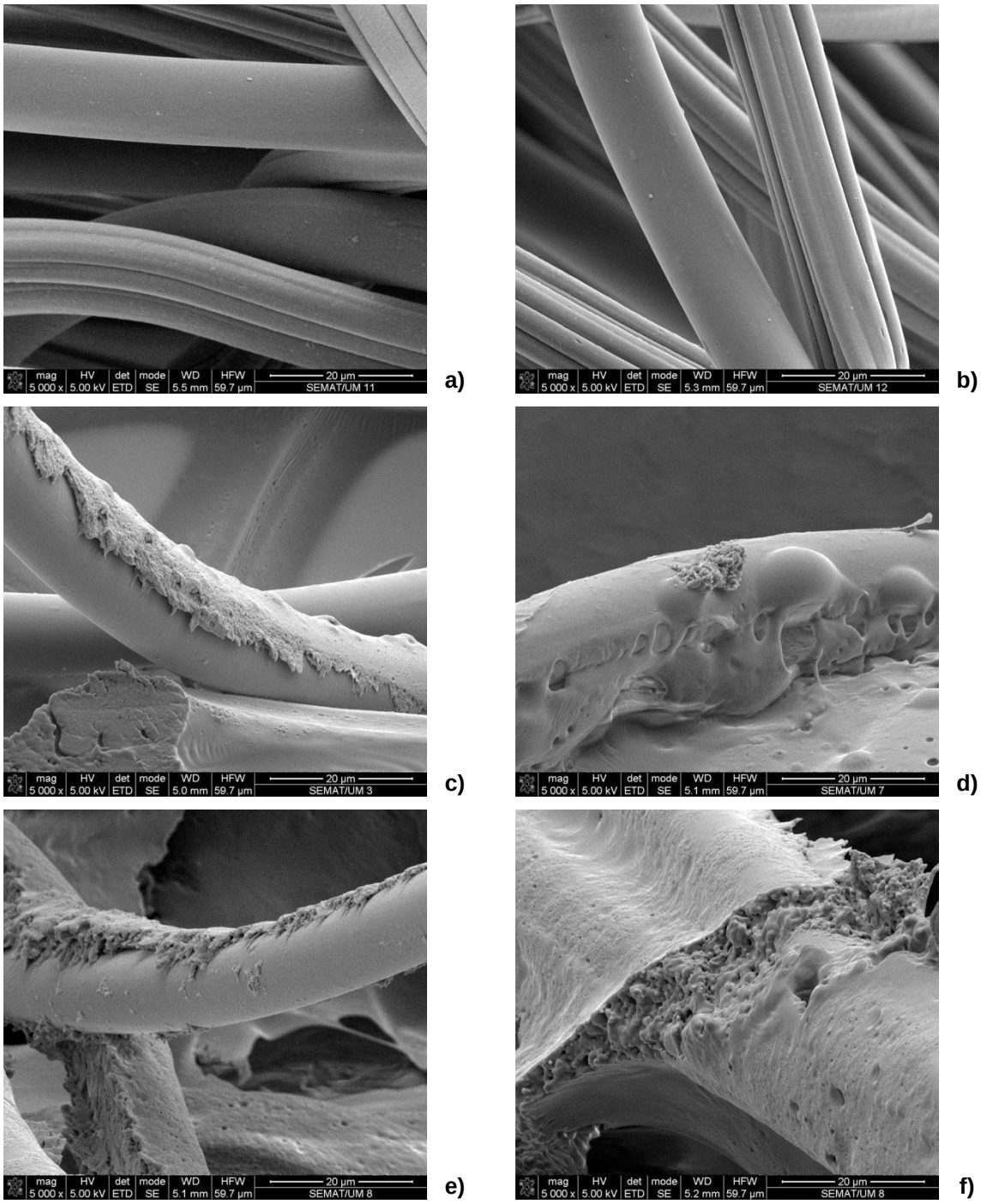

Figure IX-6: **SEM microphotography's (x5000 magnification) of nonwoven gauzes bandages: a) and b) control (cationized and non-cationized, without microspheres, respectively); c) non-cationized-incubation treatment; d) cationized - incubation treatment; e) non-cationized - ultrasound treatment; f) cationized - ultrasound treatment.**

IX-3.3. *In vitro* release profile of piroxicam from cotton and nonwoven gauzes bandages

The release behaviour of polymeric microspheres is one of the most important features of the drug/polymer formulations, because of the proposed application in sustained drug delivery.

The release profile of BSA-based particles was performed in wet gauzes bandages (immediately after ultrasound or incubation treatment) and in dried gauzes bandages (samples dried at room temperature).

The release of piroxicam it was observed mainly in the first hours. The burst release of piroxicam is associated with those piroxicam molecules dispersing close to microspheres surface, which diffuse out in the initial incubation time (Figure IX-7 and Figure IX-8).There are several factors that affect the release of the entrapped drug in protein microspheres. It was possible to verify that BSA particles display a higher release of piroxicam, when they are attached by sonochemical methodology [Figure IX-7 b) and Figure IX-8 b)]. This result can be attributed to the fact that ultrasound phenomena in liquid media enhance mass transports of their constituents in a non-homogeneous fashion allowing the fast attachment on the fibres gauzes.

The beneficial use of the ultrasound is realized through its chemical, mechanical or physics effects on the process or product [317]. Conversely, the attachment by incubation treatment with a constant stirring is not plentiful to promote an efficient treatment, which can explain the longer sustained release of piroxicam. The amount of piroxicam release can be related with its microsphere entrapped quantity and attached onto fibres surface.

Incubation and ultrasound treatment with the above characteristics appear to have the same behaviour effects on the release of piroxicam in cationized gauzes bandages (Figure IX-7 and Figure IX-8). As it was mentioned, the cationization process promotes the presence of positive charges on the gauzes surfaces that would favour the attachment of the BSA microspheres, which presents a negative surface charge, onto the structure of the gauzes material (cotton and nonwoven). Therefore, the improvement of electrostatics interactions, between the microspheres and the cationized gauzes, can promotes a higher

released of piroxicam. These data also suggested that lowest concentration of piroxicam released is achieved with gauzes bandages dried. This result can be attributed to the fact that the drying process can lead to a premature disruption of BSA microspheres and, consequently, a lost in the content of piroxicam. It is also necessary to note that in dried samples the hydration of the textile material may be more difficult or occurs more slowly and, consequently, can decrease the diffusion of piroxicam to the medium.

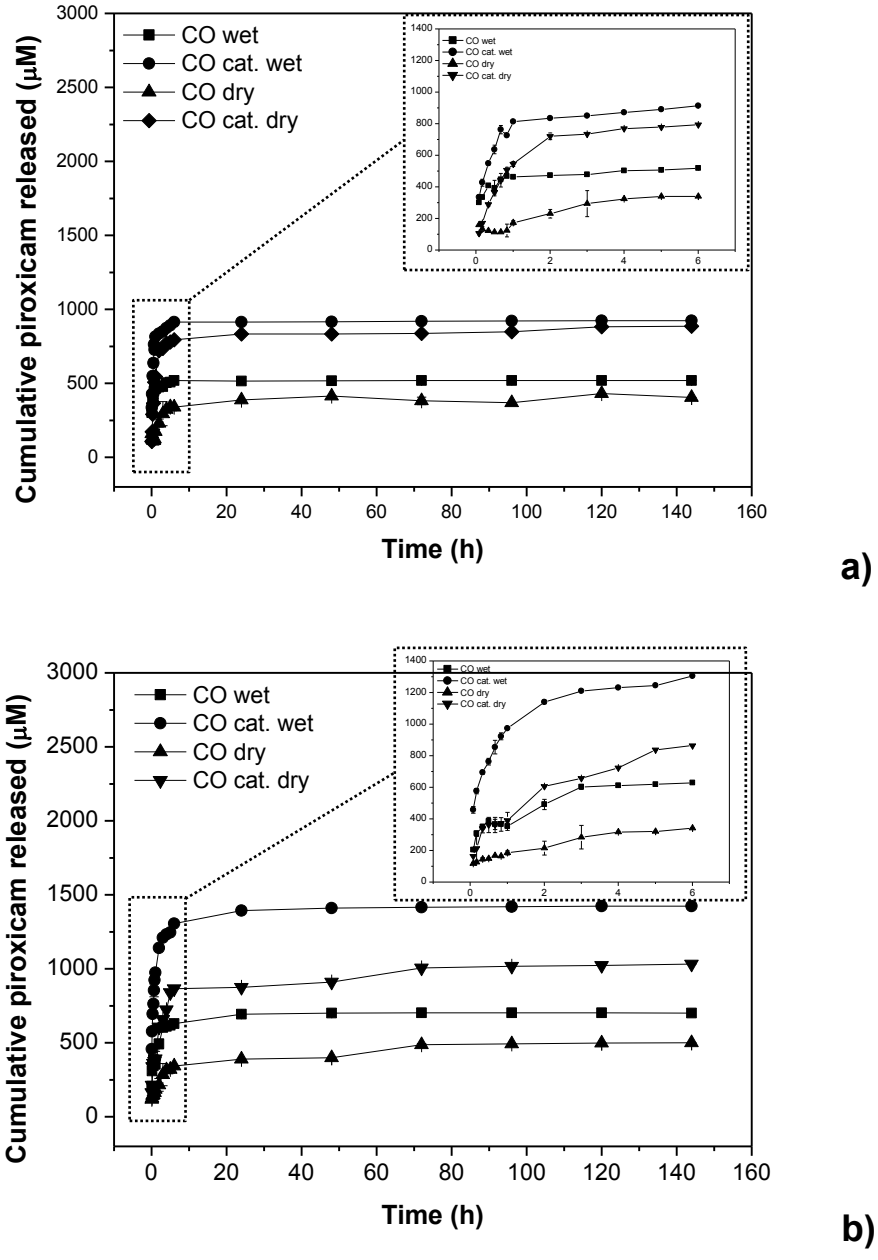

Figure IX-7: ***In vitro*** **release profile of piroxicam entrapped on BSA microsphere from cotton gauzes bandages: (a) incubation treatment (b) sonochemical treatment. The first 6 hours of release is enlarged for all the conditions.**

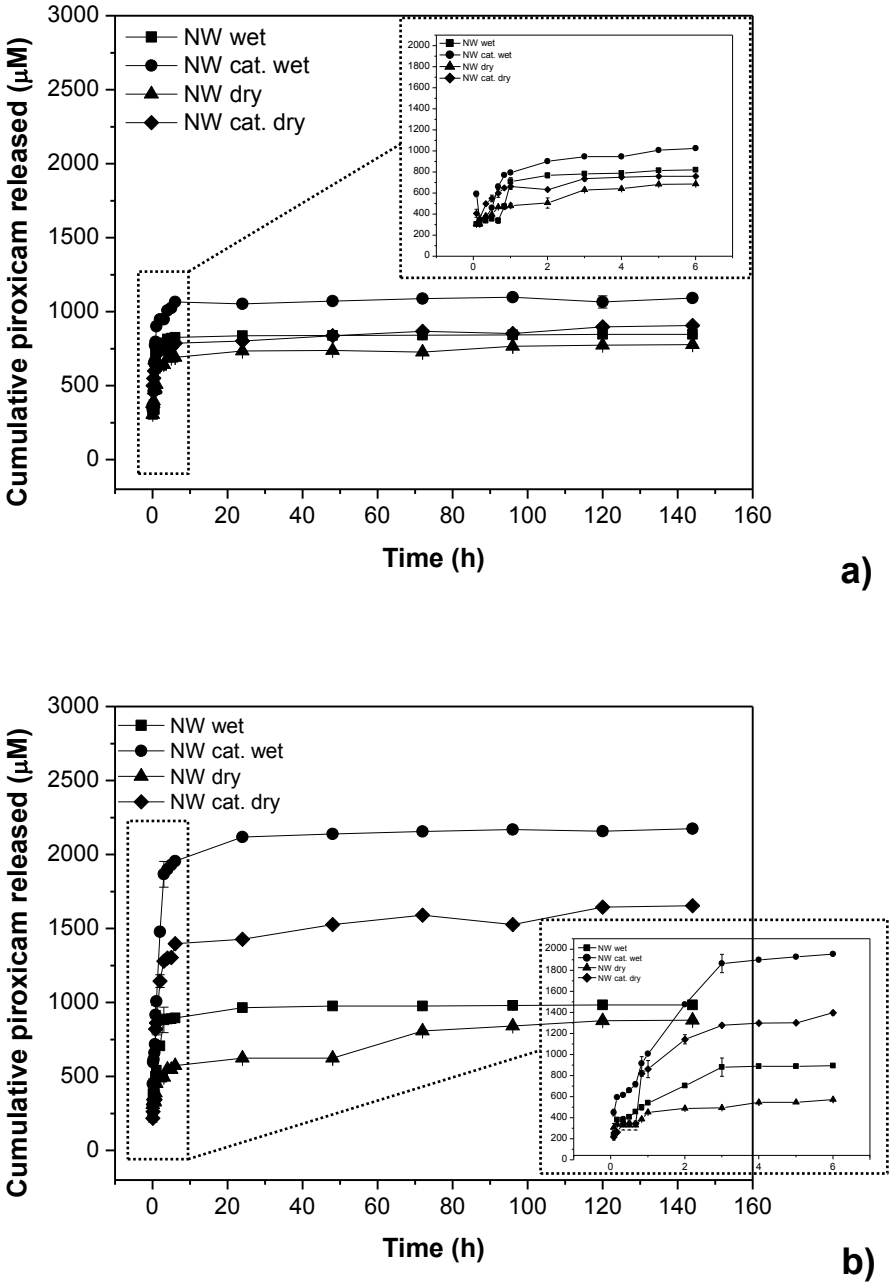

Figure IX-8: ***In vitro*** **release profile of piroxicam entrapped on BSA microsphere from nonwoven gauzes bandages: (a) incubation treatment (b) sonochemical treatment. The first 6 hours of release is enlarged for all the conditions.**

The gauzes porosity nature reveals a significant influence in the attachment of BSA microspheres, affecting the drug delivery concentrations. The results show that independently of the methodology used to immobilize the BSA microspheres, the nonwoven gauze shows a higher concentration of piroxicam released over the time. Being more closed and compact than cotton gauzes, this type of fibre structure can offer a better support for microspheres' attachment.

Considering that the assumed application of the product is for one-way used only, no fastness tests were included in the investigation plan at this stage.

IX-4. CONCLUSIONS

The present study demonstrates the attachment ability of proteinaceous microspheres, containing an anti-inflammatory drug, onto different gauzes, cotton and nonwoven. The continuous application of shear stress provided by stirring or ultrasound waves was able to promote the attachment of BSA-particles onto gauze bandages. Furthermore, the chemical activation of gauzes, using the PDDA as cationizer reagent, improved the content of BSA microspheres at the fibres surfaces and, consequently, a higher concentration of piroxicam was released. However, the highest release was achieved when the attachment process was performed by sonochemical method. The short time treatment (3 min) improves the mass transport effects enhancing the microspheres attachment. The capacity of ultrasound to attach the microspheres to gauzes was made by one-step reaction, providing a reduction in the products consumption, shorter process time and a greater uniformity of the treatment.

The release of piroxicam entrapped in BSA microspheres was shown to be dependent on the gauzes structure. The fastest and highest concentration of piroxicam released can be reached when the proteinaceous microspheres were attached on nonwoven gauzes.

The results achieved, indicate that these functionalized gauze bandages may potentially be used as powerful bioactive carriers for wound healing. Furthermore, such drug carriers can be helpful for several pathologies where the piroxicam can be useful.

CHAPTER X

GENERAL DISCUSSION, FINAL REMARKS AND FUTURE PERSPECTIVES

Chapter X

General discussion, final remarks and future perspectives

GENERAL DISCUSSION

The objective of this dissertation was the development and characterization of delivery systems (DS) sonochemically prepared. These systems can be useful for entrapment and release of bioactive agents. To accomplish this aim, two based materials were selected: phospholipids and proteins. Herein a summary of major achievements will be given.

The general discussion of the research work produced in this thesis, which intends from Chapter III to IX, was divided in the following items:

- Liposomes;
- Protein microspheres.

LIPOSOMES

The feasibility to prepare liposomes with predictable sizes via ultrasound sources was demonstrated in the Chapter III. Sonication is a powerful technique that can be used to reduce the liposomes size in a relative short time treatment, due to their high energy released over treatment. In order to achieve dependable and reproducible results, with this technique, several parameters were controlled, namely time of treatment, power input and distance of ultrasound tip from the base of the vessel. The results obtained demonstrated that the cavitation events promoted by sonochemical methodology are directly dependent on the parameters previously described and, also, on the wave behaviour.

The choice of tip placement was based on estimated wavelength of 77.1 mm, which allows the calculation of the anti-node ($\lambda/4$; 19 mm) and node point ($\lambda/2$; 38 mm). The anti-node point is where the maximum of vibration and

amplitude of wavelength occurs and, consequently, more pronounced cavitation events and the associated phenomena. It was also shown that the behaviour of a longitudinal wave should give a constructive interference at anti-nodal point and destructive at the nodal point. Thus, the calorimetric and dosimetric procedure was employed to characterize the events that occur at the node and anti-node points. The results prove that the energy and the hydroxyl radicals (•OH) production are higher at 19 mm of depth and using the maximum of amplitude (40%). The results for the energy deposition increase with the power input for both depths (19 and 38 mm). However, the results for •OH formation showed that at 19 mm ($\lambda/4$) position displayed a significant increase in •OH radical production at 40% of amplitude. The reason for this fact is that whilst cavitation bubble implosion is regarded as necessary for •OH radical formation, and is also a contributor of heat, other factors are present which contribute for heat energy to the solution when conditions do not favour •OH radical production.

These parameters were taken into account to verify how they interfere with the reduction of liposomes size. The results demonstrated that at 19 mm and with 40% of amplitude it was possible to obtain smaller sizes and a more homogeneous population after few minutes of treatment when compared with the results achieved for 38 mm of depth. However, after a total time treatment of 21 min there was no significant differences on the reduction of liposomes size for these two depths.

The further Chapter (Chapter IV) described the ultrasonic effects on peptides incorporated on phospholipids aggregates. In this Chapter it were explored the potentialities of liposomes to incorporate two synthetic peptides, linked to fluorescent dye, which can be used in the cosmetic field. The treatments with ultrasound were carried out at anti-nodal and nodal points, using the lowest (20%) and the highest amplitude (40%). According to the previous results, the total treatment time necessary to decrease the liposomes sizes was 12 min and this time frame was used for the subsequent preparations. The results were in agreement with the previously data where the smaller sizes were obtained with the 19 mm of tip placement and using 40% of amplitude. The peptide motifs differ in the position of the charged group (Lysine; K) in the peptide structure. These

changes in the peptide motif lead to changes in the physico-chemical characteristics of liposomes.

The zeta-potential results demonstrate differences on the surface of vesicles when these two peptides were incorporated. The peptide with the Lysine residue distributed along the sequence (LLLL**K**LLLL**K**LLLL**K**LLLL**K)** can be located on the polar surface of liposomes and consequently promote an enhancement on the values of zeta-potential (≈ 7 mV). The incorporation of this peptide on phospholipids aggregates leads to an amorphous shape of liposomes. Conversely, the peptide with the Lysine residue in the extremity of the peptide fragment (LLLLLLCLCLLL**K**A**K**A**K**) allows the location of the others residues inside of the core vesicle, due to their hydrophobicity. Consequently, the surface of liposomes did not suffer a significant change on the zeta-potential values and the morphology studies demonstrate a more homogeneous shape, presenting a “rode” shape.

PROTEINS

In this dissertation, the other main aim was to fully investigate the mechanism of protein microspheres formation by ultrasound sources. The microspheres were produced by means of ultrasonication of two-phase starting mixture, consisting of protein solution and organic solvent, using the same power input energy, 40% of amplitude, which is the maximum of power input to prepare microspheres. The use of this condition favours the cavitation events at the aqueous/organic interface and, consequently, the mass transport effects.

Chapter V reported the use of two proteins, specifically bovine serum albumin (BSA) and silk fibroin (SF), to produce microspheres. BSA is a soluble globular protein, presenting a high content of Cysteine residues, while SF is an insoluble fibrous protein without Cysteine residues in its chemical constitution. In this Chapter, it was found that the amount of protein and the organic volume fraction are essential to form and stabilize the proteinaceous devices and also tune their size distribution. The knowledge of this proves to be an important tool to predict sizes particles ranging from 300 to 1500 nm. Additionally, the conformation assessment, obtained with Fourier transform infrared (FT-IR) analysis after

microspheres formation, confirmed a change on the secondary structure leading to more ordered structure (enhancement on the β-sheet content), while the globular protein (BSA) maintains its secondary structure upon ultrasound treatment. This result accomplished with the molecular studies and with the confocal analysis, which demonstrates the protein arrangement in a biphasic system, allows us to predict that the mass transport effects is the main mechanism of protein microspheres formation. This phenomena brings the hydrophobic groups close to each other allowing the van der Waals interactions between them, summing up to a substantial energetic contribution, favouring the formation and stabilization of spherical particle. The polar chains can form hydrogen bond with the aqueous phase and will be distributed around microspheres surface. Another important characteristic on the microspheres characterization is the cytotoxicity. Polymeric materials to be used in medical applications should be biocompatible. Cytotoxicity, as initial phase in testing biocompatibility, detects cell death or other negative effect of materials on cellular functions. The cytotoxicity screening was assessed to our materials through the use of human cell line, establishing that the use of high concentrations of microspheres (above 300 $mg.L^{-1}$), accomplished with the high ratio of organic phase (40% of *n*-dodecane), lead to a moderate cytotoxicity effects.

The followed Chapter (Chapter VI) reported deeper studies on the mechanism of the protein microspheres using wide ranges of peptides with a variable size and sequence and a tailored hydrophobic/hydrophilic ratio. The results proved that larger peptides with a separated clear hydrophobic and hydrophilic areas lead to a more stable and small spheres. The formation of peptide microspheres show to be dependent of the intrinsic properties of amino acids (a.a.) residues and their arrangements in the peptide sequences. The use of sonochemical methodology promotes high shear forces driving the orientation of polar and nonpolar groups in biphasic system. The proof of the concept was attained with molecular dynamic studies and confocal analysis, demonstrating the polar residues interacting with aqueous phase and the affinity of hydrophobic residues with the *n*-dodecane.

Based on the concept of delivery devices, the Chapter VII described a novel approach using proteinaceous microspheres of BSA, human serum albumin

(HSA) and SF containing different organic solvents, namely, *n*-dodecane, mineral and vegetable oil, to reduce the activity of HNE found in high levels on chronic wounds. The inhibitory activity was evaluated against porcine pancreatic elastase (PPE), used as a model of wound exudates, and it was found that the vegetable oil presents higher inhibitory efficiency. This was explained by the incidence of monounsaturated and polyunsaturated fatty acids present in different ratios on mineral and vegetable oil when compared with *n*-dodecane. Moreover, the chemical nature of proteins also interferes with the elastase inhibition, once that SF demonstrated to be the more capable device for this purpose. Subsequently, the *in vitro* experiments were performed to investigate the effects on cell viability. The cytotoxicity screening reveals that the developed microspheres are not cytotoxic against human fibroblast in a range concentrations of 75-300 $mg.L^{-1}$ for BSA and HSA, and 150-300 $mg.L^{-1}$ for SF after 72 h of exposure. However, in those concentrations SF is no longer the best device to inhibit the elastase. Therefore, there is a need to find a compromise between the ability to inhibit the elastase and their cytotoxicity when formulations are developed.

The Chapter VIII reported the entrapment of piroxicam, which is an anti-inflammatory drug commonly used in the treatment of inflammatory diseases, into BSA and HSA microspheres. The results have shown that the use of lowest ratio of organic phase (5%) led to smallest sizes (≈ 300 nm). However, their sizes distribution (measured in term of polydispersity index, PDI) is high. To circumvent this drawback it were tested different stabilizers in the BSA and HSA microspheres preparation to achieve a monodispersed population (Chapter VIII). The results demonstrated that the polyvinyl alcohol (PVA) is the most efficient and that 8% is the amount required to achieve a monodispersed population for both protein-based devices. The use of PVA led to an increase on the entrapment efficiency of piroxicam, as well as the BSA-piroxicam and HSA-piroxicam stability over the time. The release kinetics of the protein-based devices was determined in the presence of protease, used to mimic the enzymatic environment of the human body and as a trigger for the drug release. This assay indicates an Anomalous drug transport mechanism (diffusion and polymer degradation). Although, the presence of an higher protease concentration led to a complete degradation of BSA matrix, exhibiting

Case II transport. Concomitantly, the cytotoxicity evaluation in human fibroblasts demonstrated that these protein-based devices can be safely applied in the range concentrations below 300 $mg.L^{-1}$.

Chapter IX, exploited the potential of the combinatorial strategy in textile-based wound dressing employing the previous characterized devices. In the aforementioned Chapter VIII it was performed the physico-chemical characterization of the BSA-piroxicam devices, prepared with PVA, demonstrating a negative charge on the microspheres surfaces. Thus, prior to the attachment of microspheres, the cotton and nonwoven gauzes were submitted to a cationization process in order to acquire the positive charge on their surfaces. The cationization of gauzes led to an increase of the electrostatic interactions between the protein microspheres and the surfaces gauzes. The attachment of proteinaceous devices using sonochemical radiation promotes the binding onto cotton and nonwoven gauzes by one-step-process, and an enhancement of this device on their surface was observed. The attachment of protein microspheres showed to be dependent on the gauzes structure. The fastest and the highest concentration of piroxicam released were reached with nonwoven gauzes. This type of fibre structure offers a better support for microspheres attachment, once that is more closed and compact than cotton gauzes.

FINAL REMARKS

The following points summarize the work carried under the scope of this thesis.

SONOPRODUCTION OF PARTICLES…

- It was possible to develop nano and micron size particles, by sonochemical method, using two different materials: phospholipids and protein-based materials.
- The sonochemical methodology employed has shown to be adequate to produce these systems, which allowed, to some extent, tailor the properties of the nano and microparticles, namely their size and its distribution, surface charge and morphology.

…FOR DELIVERY PURPOSES

- Liposome-based particles have shown its capacity to entrap different synthetic peptides.
- Protein-based particles were able to entrap and release bioactive agents in a sustained fashion. Piroxicam presented high entrapment efficiency, and was released with an initial burst, followed by a state of lower release up to six days.
- The devices, based on protein material, containing piroxicam, were attached onto cotton and nonwoven gauzes and the release piroxicam was achieved, greatly supporting their application for textile-based wound dressings.

As conclusion, these systems present an outstanding potential for delivery applications.

In the proposed strategy, ultrasound systems aim to fill different roles to obtain these DS. Further understanding of intrinsic properties of these developed systems allows their optimization in order to enhance their potentialities. When gathering all the information from each of the studies, it can be drawn that the developed liposomes and protein-based particles present potential to be used as carriers for bioactive molecules.

In summary, the results demonstrate the potential of sonochemical method to develop liposomes and protein-based nano and micron size systems for the above proposed strategy. This confirms that the milestones for this work were achieved.

FUTURE PERSPECTIVES

A number of valuable results were obtained in this research project which will hopefully be of utility in future investigations. The usefulness of sonochemical methodology for the development of an efficient lipidic and proteinaceous delivery platforms for the delivery of bioactive agents are the most significant contributions of this thesis. The next steps may include the following studies:

- To undertake *in vivo* studies to assess the potential of protein microspheres to induce wound healing in animal models, as well as the potential of anti-inflammatory ability of protein-piroxicam microspheres.

- To enhanced the site-specific of drug delivery by using receptor-targeting ligands.

- To explore new applications of the developed systems as carriers for cosmetics uses.

- Upgrading the sonoproduction of particles from laboratory scale to a large scale-process.

REFERENCES

REFERENCES

1. Barat, A., M. Crane, and H.J. Ruskin, *Quantitative Multi-Agent Models for Simulating Protein Release From PLGA Bioerodible Nano- and Microspheres.* Journal of Pharmaceutical and Biomedical Analysis, 2008. **48**(2): p. 361-368.
2. Basinska, T., *Hydrophilic Core-Shell Microspheres: A Suitable Support for Controlled Attachment of Proteins and Biomedical Diagnostics.* Macromolecular Bioscience, 2005. **5**: p. 1145-1168.
3. Müller, R.H., K. Mäder, and S. Gohla, *Solid Lipid Nanoparticles (SLN) for Controlled Drug Delivery - A Review of the State of the Art.* European Journal of Pharmaceutics and Biopharmaceutics, 2000. **50**(1): p. 161-177.
4. Torchilin, V.P., *Targeted Polymeric Micelles for Delivery of Poorly Soluble Drugs.* Cellular and Molecular Life Sciences, 2004. **61**(19): p. 2549-2559.
5. Lasic, D.D., *The Mechanism of Vesicle Formation.* Biochem J., 1988. **256**(1): p. 1-11.
6. Svenson, S. and D. Tomalia, *Dendrimers in Biomedical Applications - Reflections on the Field.* Advanced Drug Delivery Reviews, 2005. **57**(15): p. 2106-2129.
7. Lensen, D., D.M. Vriezema, and J.C.M. van Hest, *Polymeric Microcapsules for Synthetic Applications.* 2008. **8**: p. 991-1005.
8. Couvreur, P. and C. Vauthier, *Nanotechnology: Intelligent Design to Treat Complex Disease.* Pharmaceutical Research, 2006. **23**(7): p. 1417-1450.
9. Couvreur, P., et al., *Nanotechnologies for Drug Delivery: Application to Cancer and Autoimmune Diseases.* Progress in Solid State Chemistry, 2006. **34**(2-4): p. 231-235.
10. Jong, W.H.D. and P.J. Borm, *Drug Delivery and Nanoparticles: Applications and Hazards.* International Journal of Nanomedicine, 2008. **3**(2): p. 133-149.

11. Liechty, W.B., et al., *Polymers for Drug Delivery Systems.* Annual Review of Chemical and Biomolecular Engineering, 2010. **1**(1): p. 149-173.

12. Suslick, K.S. and G.J. Price, *Applications of Ultrasound to Materials Chemistry.* Annual Review of Materials Research, 1999(29): p. 295–326.

13. Suslick, K.S. and W.L. Nyborg, *Ultrasound: Its Chemical, Physical and Biological Effects.* The Journal of the Acoustical Society of America, 1990. **87**(2): p. 919-920.

14. Mason, T.J. and D. Peters, *Practical Sonochemistry: Uses and Applications of Ultrasound*. second ed. 2002: Horwood publishing, Chischester, West Sussex, UK.

15. Shchukin, D.G. and H. Mohwald, *Sonochemical Nanosynthesis at the Engineered Interface of a Cavitation Microbubble.* Physical Chemistry Chemical Physics, 2006. **8**(30): p. 3496-3506.

16. Mason, T.J., *Advances in Sonochesmistry*. Vol. 5. 1999, Stamford, Connecticut: Jai Press Inc. 325.

17. Suslick, K.S., et al., *Acoustic Cavitation and its Chemical Consequences.* Philosophical Transactions A Royal Society Lond., 1999. **357**: p. 335-353.

18. Gandhi, K. and R. Kumar, *Sonochemical reaction engineering.* Sadhana, 1994. **19**(6): p. 1055-1076.

19. Suslick, K.S. and L.A. Crum, *Sonochemistry and Sonoluminescence*. Encyclopedia of Acoustics. 1997, New York: Wiley-Interscience. 271-281.

20. Ashokkumar, M., et al., *Bubbles in an Acoustic Field: An Overview.* Ultrasonics Sonochemistry, 2007. **14**(4): p. 470-475.

21. Gong, C. and D.P. Hart, *Ultrasound Induced Cavitation and Sonochemical Yields.* Journal of the Acoustical Society of America, 1998. **104**: p. 1-16.

22. Rae, J., et al., *Estimation of Ultrasound Induced Cavitation Bubble Temperatures in Aqueous Solutions.* Ultrasonics Sonochemistry, 2005. **12**(5): p. 325-329.

23. Bang, J.H. and K.S. Suslick, *Applications of Ultrasound to the Synthesis of Nanostructured Materials.* Advanced Materials, 2010. **22**: p. 1039-1059.

24. Makino, K., M.M. Mossoba, and P. Riesz, *Chemical effects of ultrasound on aqueous solution. Formation of hydroxyl radicals and hydrogen atoms.* Journal of Physical Chemistry, 1982. **87**: p. 1369-1377.

25. Mason, T.J., et al., *Dosimetry in Sonochemistry: The Use of Aqueous Terephthalate Ion as a Fluorescence Monitor.* Ultrasonics Sonochemistry, 1994. **1**(2): p. 91-95.

26. Hart;, E.J. and A. Henglein, *Free radical and free Atom Reactions in the Sonolysis of Aqueous Iodide and Formate Solutions.* Journal of Physical Chemistry, 1985.

27. Price, G. and E.J. Lenz, *The Use of Dosimeters to Measure Radical Production in Aqueous Sonochemical Systems.* Ultrasonics 1993. **31**(6): p. 451-455.

28. Fang, X., G. Mark, and C. von Sonntag, *OH Radical Formation by Ultrasound in Aqueous Solutions. Part I: The Chemistry Underlying the Terephtalate Dosimeter.* Ultrasonics Sonochemistry, 1996. **3**: p. 57-63.

29. Huang, C., *Studies on Phosphatidylcholine Vesicles. Formation and Physical Characteristics.* Biochemistry, 1969. **8**(1): p. 344-52.

30. Finer, E.G., A.G. Flook, and H. Hauser, *Mechanism of Sonication of Aqueous Egg Yolk Lecithin Dispersions and Nature of the Resultant Particles.* Biochimica et Biophysica Acta (BBA) - Lipids and Lipid Metabolism, 1972. **260**(1): p. 49-58.

31. Zasadzinski, J.A., *Transmission Electron Microscopy Observations of Sonication-Induced Changes in Liposome Structure.* Biophysical journal, 1986. **49**(6): p. 1119-1130.

32. New, R.R.C., *Liposomes - A Practical Approach*. The Partical Aproaches Series, ed. Rickwood D. and H. B.D. 1990, New York: Oxford University Press. 301.

33. Almog, R., R. Forward, and C. Samsonoff, *Stability of Sonicated Aqueous Suspensions of Phospholipids Under Air.* Chemistry and Physics of Lipids 1991. **60**: p. 93-99.

34. Lasic, D.D., *Liposomes - from Physics to Applications*. 1993, New York: Elsevier.

35. Maulucci, G., et al., *Particle Size Distribution in DMPC Vesicles Solutions Undergoing Different Sonication Times.* Biophysical journal, 2005. **88**(5): p. 3545-3550.

36. Woodbury, D.J., et al., *Reducing Liposome Size with Ultrasound: Bimodal Size Distributions.* Journal of Liposome Research, 2006. **16**(1): p. 57-80.

37. Pereira-Lachataignerais, J., et al., *Study and Formation of Vesicle Systems with Low Polydispersity Index by Ultrasound Method.* Chemistry and Physics of Lipids, 2006. **140**(1-2): p. 88-97.

38. Kim, S.H., et al., *Effect of Sonication and Freezing-Thawing on the Aggregate Size and Dynamic Surface Tension of Aqueous DPPC Dispersions.* Journal of Colloid and Interface Science, 2007. **311**(1): p. 217-227.

39. Richardson, E.S., W.G. Pitt, and D.J. Woodbury, *The Role of Cavitation in Liposome Formation.* Biophysical journal, 2007. **93**(12): p. 4100-4107.

40. Yamaguchi, T., et al., *Effects of Frequency and Power of Ultrasound on the Size Reduction of Liposome.* Chemistry and Physics of Lipids, 2009. **160**(1): p. 58-62.

41. Silva, R., et al., *Effect of Ultrasound Parameters for Unilamellar Liposome Preparation.* Ultrasonics Sonochemistry, 2010. **17**(3): p. 628-632.

42. Silva, R., et al., *Incorporation of Peptides in Phospholipid Aggregates Using Ultrasound.* Ultrasonics Sonochemistry, 2008. **15**: p. 1026-1032.

43. Ramírez, R., et al., *Liposome Formation with Wool Lipid Extracts Rich in Ceramides.* Journal of Liposome Research, 2009. **19**(1): p. 77-83.

44. Suslick, K.S. and M.W. Grinstaff, *Protein Microencapsulation of Nonaqueous Liquids.* Journal of the American Chemical Society, 1990(112): p. 7807-7809.

45. Grinstaff, M.W. and K.S. Suslick, *Air-filled Proteinaceous Microbubbles: Synthesis of an Echo-Contrast Agent.* Chemistry, 1991. **88**(17): p. 7708-7710.

46. Grinstaff, M.W. and K.S. Suslick, *Nonaqueous Liquid Filled Microcapsules.* Polymer Preparation, 1991. **32**: p. 255.

47. Suslick, K.S., et al., *Characterization of Sonochemically Prepared Proteinaceous Microspheres.* Ultrasonics Sonochemistry, 1994. **1**(1): p. S65-S68.

48. Wong, M. and K.S. Suslick, *Sonochemically Produced Hemoglobin Microbubbles.* Materials Research Society Symposium Proceedings, 1995. **372**: p. 89.

49. Avivi, S., et al., *The Preparation of Magnetic Proteinaceous Microspheres Using The Sonochemical Method.* Biochimica et Biophysica Acta, 2001. **1527**(3): p. 123-129.

50. Makino, K., et al., *Sonochemically Prepared Bovine Serum Albumin Microcapsules: Factors affecting The size Distribution and the Microencapsulation Yield.* Colloids and Surfaces B: Biointerfaces, 2001. **22**(3): p. 251-255.

51. Avivi, S. and A. Gedanken, *S-S bonds Are Not Required For The Sonochemical Formation of Proteinaceous Microspheres: The Case of Streptavidin.* Biochemical Journal, 2002. **366**(3): p. 705-707.

52. Makino, K., et al., *Sustained Release of Hydrophobic Materials From Sonochemically Prepared Bovine Serum albumin Microcapsules.* Colloids and Surfaces B: Biointerfaces, 2002. **23**(1): p. 59-64.

53. Avivi, et al., *An Easy Sonochemical Route for the Encapsulation of Tetracycline In Bovine Serum Albumin Microspheres.* Journal of the American Chemical Society, 2003. **125**(51): p. 15712-15713.

54. Shchukin, D.G., et al., *Modified Polyelectrolyte Microcapsules as Smart Defense Systems.* Chemistry of Materials, 2004. **16**(18): p. 3446-3451.

55. Avivi, S. and A. Gedanken, *The Preparation of Avidin Microspheres Using the Sonochemical Method and the Interaction of the Microspheres with Biotin.* Ultrasonics Sonochemistry, 2005. **12**(5): p. 405-409.

56. Petrov, A.I., D.V. Volodkin, and G.B. Sukhorukov, *Protein-Calcium Carbonate Coprecipitation: A Tool for Protein Encapsulation.* Biotechnology Progress, 2005. **21**: p. 918-925.

57. Shchukin, D.G., et al., *Gas-Filled Polyelectrolyte Capsules.* Angewandte Chemie International Edition, 2005. **44**(21): p. 3310-3314.

58. Toublan, F.J.J., S. Boppart, and K.S. Suslick, *Tumor Targeting by Surface-Modified Protein Microspheres.* Journal of American Chemical Society, 2006. **128**: p. 3472-3473.

59. Cavalieri, F., et al., *Tethering Functional Ligands onto Shell of Ultrasound Active Polymeric Microbubbles.* Biomacromolecules, 2006. **7**(2): p. 604-611.

60. Avivi, S. and A. Gedanken, *Are Sonochemically Prepared Alpha-Amylase Protein Microspheres Biologically Active?* Ultrasonics Sonochemistry, 2007. **14**(1): p. 1-5.

61. Grinberg, O., et al., *Characterization and Activity of Sonochemically-Prepared BSA Microspheres Containing Taxol - An Anticancer Drug.* Ultrasonics Sonochemistry, 2007. **14**(5): p. 661-666.

62. Grigoriev, D., et al., *Interfacial Assembly of Partially Hydrophobic Silica Nanoparticles Induced by Ultrasonic Treatment.* Small, 2007. **3**(4): p. 665-671.

63. Teng, X.R., D.G. Shchukin, and H. Mohwald, *A Novel Drug Carrier: Lipophilic Drug-Loaded Polyglutamate/Polyelectrolyte Nanocontainers.* Langmuir, 2007. **24**(2): p. 383-389.

64. Cavalieri, F., et al., *Ultrasonic Synthesis of Stable, Functional Lysozyme Microbubbles.* Langmuir, 2008. **24**(18): p. 10078-10083.

65. Han, Y., et al., *Stability and Size Dependence of Protein Microspheres Prepared by Ultrasonication.* Journal of Materials Chemistry, 2008. **18**(42): p. 5162-5166.

66. Grinberg, O., et al., *Sonochemically Prepared BSA Microspheres Containing Gemcitabine, And Their Potential Application in Renal Cancer Therapeutics.* Acta Biomaterialia, 2009. **5**(8): p. 3031-3037.

67. Angel , U., et al., *Microspheres of Mixed Proteins.* Chemistry- European Journal, 2010. **16**: p. 2108-2114.

68. Borodina, T., et al., *Vitamin E Microspheres Embedded Within a Biocompatible Film for Planar Delivery.* Advanced Engineering Materials, 2010: p. n/a-n/a.

69. Grinberg, O. and A. Gedanken, *The Development and Characterization of Starch Microspheres Prepared by a Sonochemical Method for the Potential Drug Delivery of Insulin.* Macromolecular Chemistry and Physics, 2010. **211**: p. 924-931.

70. Skirtenko, N., et al., *One-Step Preparation of Multifunctional Chitosan Microspheres by a Simple Sonochemical Method.* Chemistry European Journal, 2010. **16**: p. 562-567.

71. Zhou, M., et al., *Sonochemical Synthesis of Liquid-Encapsulated Lysozyme Microspheres.* Ultrasonics Sonochemistry, 2010. **17**(2): p. 333-337.

72. Silva, R., et al., *Insights on the Mechanism of Protein Microspheres Formation.* Submitted, 2011.

73. Silva, R., et al., *Mechanisms of the Formation of Proteinaceous Microspheres – Highlights from Peptide Size and Sequences* Submitted, 2011.

74. Silva, R., et al., *Protein Disulfide Isomerase-Induced Refolding of Ribonuclease A Micropsheres.* Submitted, 2011.

75. Silva, R., et al., *Sonochemical Proteinaceous Microspheres for Wound Healing.* Submitted, 2011.

76. Silva, R., et al., *Protein Microspheres as Suitable Devices for Piroxicam Release.* Submitted, 2011.

77. Suslick, K.S., et al., *Sonochemical Synthesis of Armorphous Iron.* Nature, 1991. **353**: p. 414-416.

78. Grinstaff, M.W., et al., *Effect of Cavitation Conditions on Amorphous Metal Synthesis.* Ultrasonics, 1992. **30**(3): p. 168-172.

79. Suslick, K.S., M. Fang, and T. Hyeon, *Sonochemical Synthesis of Iron Colloids.* Journal of the American Chemical Society, 1996. **118**(47): p. 11960-11961.

80. Zhang, J., et al., *Sonochemical Formation of Single-Crystalline Gold Nanobelts.* Angewandte Chemie International Edition, 2006. **45**(7): p. 1116-1119.

81. Wu, C., B.P. Mosher, and T. Zeng, *Rapid Synthesis of Gold and Platinum Nanoparticles Using Metal Displacement Reduction with Sonomechanical Assistance.* Chemistry of Materials, 2006. **18**(13): p. 2925-2928.

82. Suslick, K.S., T. Hyeon, and M. Fang, *Nanostructured Materials Generated by High-Intensity Ultrasound: Sonochemical Synthesis and Catalytic Studies.* Chemistry of Materials, 1996. **8**(8): p. 2172-2179.

83. Zhu, Y., et al., *Sonochemical Synthesis of Titania Whiskers and Nanotubes.* Chemical Communications, 2001(24): p. 2616-2617.

84. Jeevanandam, P., Y. Koltypin, and A. Gedanken, *Synthesis of Nanosized α-Nickel Hydroxide by a Sonochemical Method.* Nano Letters, 2001. **1**(5): p. 263-266.

85. Zhou, S.-M., et al., *Sonochemical Synthesis of Mass Single-Crystal PbS Nanobelts.* Journal of Solid State Chemistry, 2005. **178**(1): p. 399-403.

86. Zhu, J.-J., et al., *Sonochemical Method for the Preparation of Monodisperse Spherical and Rectangular Lead Selenide Nanoparticles.* Langmuir, 2002. **18**(8): p. 3306-3310.

87. Li, C.P., et al., *Hydrocarbon and Carbon Nanostructures Produced by Sonochemical Reactions of Organic Solvents on Hydrogen-Passivated Silicon Nanowires under Ambient Conditions.* Chemistry of Materials, 2005. **17**(23): p. 5780-5788.

88. Sun, X.-H., et al., *Templating Effect of Hydrogen-Passivated Silicon Nanowires in the Production of Hydrocarbon Nanotubes and Nanoonions via Sonochemical Reactions with Common Organic Solvents under Ambient Conditions.* Journal of the American Chemical Society, 2002. **124**(50): p. 14856-14857.

89. Gedanken, A., *Using Sonochemistry for the Fabrication of Nanomaterials.* Ultrasonics Sonochemistry, 2004. **11**(2): p. 47-55.

90. Edwards, K.A. and A.J. Baeumner, *Liposomes in analyses.* Talanta, 2006. **68**: p. 1421-1431.

91. Bangham, A.D. and R.W. Horne, *Negative Staining of Phospholipids and their Structural Modification by Surface-Active Agents as Observed in the Electron Microscope.* Journal of Molecular Biology, 1964. **8**(5): p. 660-668, IN2-IN10.

92. Gregoriadisbrenda, G. and E. Ryman, *Liposomes as Carriers of Enzymes or Drugs: A New Approach to the Treatment of Storage Diseases.* Biochemical Journal, 1971. **124**: p. 58.

93. Sharma, A. and U.S. Sharma, *Liposomes in Drug Delivery: Progress and Limitation.* International Journal of Pharmaceutics, 1997. **154**: p. 123-140.

94. Jones, M.N. and D. Chapman, *Micelles, Monolayers and Biomembranes*. Cell Biochemistry and Function, ed. W.L. Inc. Vol. 14. 1996, New York: John Wiley & Sons, Ltd. 252.

95. Florkin, M. and E.H. Stotz, *Lipid Metabolism of Compreensive Biochemistry*. Vol. 18. 1967, New York: Elsivier.

96. Keller, A., *The Structure and Function of Macromolecules*, in *Phospholipids*. 2008, Avon High School.

97. Edwards, K.A. and A.J. Baeumner, *Liposomes in Analyses.* Talanta, 2006. **68**(5): p. 1421-1431.

98. Vemuri, S. and C.T. Rhodes, *Preparation and Characterization of Liposomes as Therapeutic Delivery Systems: A Review.* Pharmaceutica Acta Helvetiae, 1995. **70**(2): p. 95-111.

99. Fendler, J.H., *Membrane Mimetic Chemistry*. 1982, New York: John Wiley & Sons, Inc.

100. Hope, M.J., et al., *Production of Large Unilamellar Vesicles by a Rapid Extrusion Procedure. Characterization of Size Distribution, Trapped Volume and Ability to Maintain a Membrane Potential.* Biochimica et Biophysics Acta, 1985. **812**: p. 55-65.

101. Perkins, W.R., et al., *The Determination of Liposome Captured Volume.* Chemistry and Physics of Lipids, 1993. **64**(1-3): p. 197-217.

102. Bangham, A.D., M.M. Standish, and J.C. Watkins, *Diffusion of Univalent Ions Across the Lamellae of Swollen Phospholipids.* Journal of Molecular Biology, 1965. **13**: p. 238.

103. Gómez-Hens, A. and J. Manuel Fernández-Romero, *The Role of Liposomes in Analytical Processes.* TrAC Trends in Analytical Chemistry, 2005. **24**(1): p. 9-19.

104. Brotchie, A., F. Grieser, and M. Ashokkumar, *Effect of Power and Frequency on Bubble-Size Distributions in Acoustic Cavitation.* Physical Review Letters, 2009. **102**(8): p. 084302.

105. Lee, C., J. Barnett, and P.D. Reaven, *Liposomes Enriched in Oleic Acid are Less Susceptible to Oxidation and have Less Proinflammatory Activity when Exposed to Oxidizing Conditions.* Journal of Lipid Research, 1998. **39**(6): p. 1239-1247.

106. Laguerre, M., J. Lecomte, and P. Villeneuve, *Evaluation of the Ability of Antioxidants to Counteract Lipid Oxidation: Existing Methods, New Trends and Challenges.* Progress in Lipid Research, 2007. **46**(5): p. 244-282.

107. Zuidam, N.J., et al., *Physical (in) Stability of Liposomes upon Chemical Hydrolysis: The role of Lysophospholipids and Fatty Acids.* Biochimica et Biophysica Acta (BBA) - Biomembranes, 1995. **1240**(1): p. 101-110.

108. Zuidam, N.J. and D.J.A. Crommelin, *Differential Scanning Calorimetric Analysis of Dipalmitoylphosphatidylcholine-Liposomes Upon Hydrolysis.* International Journal of Pharmaceutics, 1995. **126**(1-2): p. 209-217.

109. Heurtault, B., et al., *Physico-Chemical Stability of Colloidal Lipid Particles.* Biomaterials, 2003. **24**(23): p. 4283-4300.

110. Suntres, Z.E. and A. Omri, *The Role of Liposomal Antioxidants in Oxidative Stress*, in *Nanocarrier Technologies: Frontiers of Nanotherapy*, M.R. Mozafari, Editor. 2006, Springer: Dordrecht, The Netherlands. p. 221.

111. Kates, M., *Biology of halophilic bacteria, Part II.* Cellular and Molecular Life Sciences, 1993. **49**(12): p. 1027-1036.

112. Kruus, P., et al., *Formation and Mechanical Stability of Phospholipids Vesicles.* Membrane 1997. **17**: p. 257-262.

113. Rabinovich-Guilatt, L., et al., *Phospholipid Hydrolysis in a Pharmaceutical Emulsion Assessed by Physicochemical Parameters and New Analytical Method.* European Journal of Pharmaceutics and Biopharmaceutics, 2005. **61**: p. 69-76.

114. Jones, M., *The Surface Properties of Phospholipids Liposomes Systems and their Characterization.* Advanced Colloid Interface Science, 1995. **54**: p. 93-128.

115. Maurer, N., D.B. Fenske, and P.R. Cullis, *Developments in liposomal drug delivery systems.* Expert Opinion on Biological Therapy, 2001. **1**(6): p. 923-947.

116. Gregoriadis, G., *Engineering liposomes for drug delivery: progress and problems.* Trends in Biotechnology, 1995. **13**(12): p. 527-537.

117. Woodle, M.C., *Sterically Stabilized Liposome Therapeutics.* Advanced Drug Delivery Reviews, 1995. **16**: p. 249-265.

118. Senior, J. and G. Gregoriadis, *Is Half-Life of Circulating Liposomes Determined by Changes in their Permeability?* Febs Letters, 1982. **145**(1): p. 109-114.

119. Woodle, M.C. and D.D. Lasic, *Sterically Stabilized Liposomes.* Biochimica et Biophysica Acta, 1992. **1113**: p. 171-199.

120. Lasic, D.D., *Sterically Stabilized Vesicles.* Angewandte Chemie International Edition in English, 1994. **33**(17): p. 1685-1698.

121. Bocca, C., et al., *Phagocytic Uptake of Fluorescent Stealth and Non-Stealth Solid Lipid Nanoparticles.* International Journal of Pharmaceutics, 1998. **175**(2): p. 185-193.

122. Gabizon, A., et al., *Tumor Cell Targeting of Liposome-Entrapped Drugs with Phospholipid-Anchored Folic Acid-PEG Conjugates.* Advanced Drug Delivery Reviews, 2004. **56**(8): p. 1177-1192.

123. Stella, B., et al., *Design of Folic Acid-Conjugated Nanoparticles for Drug Targeting.* Journal of Pharmaceutical Sciences, 2000. **89**(11): p. 1452-1464.

124. Joshi, R., et al., *Free Radical Scavenging Behavior of Folic Acid: Evidence for Possible Antioxidant Activity.* Free Radical Biology and Medicine, 2001. **30**(12): p. 1390-1399.

125. Ansell, S.M., et al., *Antibody Conjugation Methods for Active Targeting of Liposomes*. 2000. p. 51-67.

126. Matzku, S., et al., *Tumour Targeting with Antibody-Coupled Liposomes: Failure to Achieve Accumulation in Xenografts and Spontaneous Liver Metastases.* Cancer Immunology, Immunotherapy, 1990. **31**(5): p. 285-291.

127. Immordino, M.L., F. Dosio, and L. Cattel, *Stealth Liposomes: Review of the Basic Science, Rationale, and Clinical Applications, Existing and Potential.* International Journal of Nanomedicine, 2006. **1**(3): p. 297–315.

128. Ranade, V.V. and M.A. Hollinger, *Role of Polymers in Drug Delivery*, in *Drug delivery systems second edition*. 2003, CRC Press LLC: Boca Raton, Florida.

129. Antonietti, M. and K. Landfester, *Polyreactions in Miniemulsions.* Progress in Polymer Science, 2002. **27**(4): p. 689-757.

130. Asua, J.M., *Miniemulsion polymerization.* Progress in Polymer Science, 2002. **27**(7): p. 1283-1346.

131. Anton, N., J.-P. Benoit, and P. Saulnier, *Design and Production of Nanoparticles Formulated from Nano-Emulsion Templates-A Review.* Journal of Controlled Release, 2008. **128**(3): p. 185-199.

132. Xu, Y. and Y. Du, *Effect of Molecular Structure of Chitosan on Protein Delivery Properties of Chitosan Nanoparticles.* International Journal of Pharmaceutics, 2003. **250**(1): p. 215-226.

133. Petsko, G.A. and D. Ringe, *Protein Structure and Function* 2005, New Science Press London.

134. Weber, C., et al., *Desolvation Process and Surface Characterisation of Protein Nanoparticles.* International Journal of Pharmaceutics, 2000. **194**(1): p. 91-102.

135. Suslick, K., (Champaign, IL, US), Toublan, Farah Jean-jacques, (Urbana, IL, US), Boppart, Stephen A., (Champaign, IL, US), Marks, Daniel L., (Urbana, IL, US), *Surface Modified Protein Microparticles*. 2007: United States.

136. Maham, A., et al., *Protein-Based Nanomedicine Platforms for Drug Delivery.* Small, 2009. **5**(15): p. 1706-1721.

137. Müller, B.G., H. Leuenberger, and T. Kissel, *Albumin Nanospheres as Carriers for Passive Drug Targeting: An Optimized Manufacturing Technique.* Pharmaceutical Research, 1996. **13**(1): p. 32-37.

138. Langer, K., et al., *Optimization of the Preparation Process for Human Serum Albumin (HSA) Nanoparticles.* International Journal of Pharmaceutics, 2003. **257**(1-2): p. 169-180.

139. Langer, K., et al., *Human Serum Albumin (HSA) Nanoparticles: Reproducibility of Preparation Process and Kinetics of Enzymatic Degradation.* International Journal of Pharmaceutics, 2008. **347**(1-2): p. 109-117.

140. Wang, X., et al., *Silk Microspheres for Encapsulation and Controlled Release.* Journal of Controlled Release, 2007. **117**(3): p. 360-370.

141. Altman, G.H., et al., *Silk-Based Biomaterials.* Biomaterials, 2003. **24**(3): p. 401-416.

142. Latha, M.S., et al., *Progesterone Release from Glutaraldehyde Cross-Linked Casein Microspheres: In vitro Studies and in vivo Response in Rabbits.* Contraception, 2000. **61**(5): p. 329-334.

143. Latha, M.S. and A. Jayakrishnan, *A New Method for the Synthesis of Smooth, Round, Hydrophilic Protein Microspheres using Low Concentrations of Polymeric Dispersing Agents.* Journal of Microencapsulation, 1995. **12**(1): p. 7-12.

144. Berthold, A., K. Cremer, and J. Kreuter, *Collagen Microparticles: Carriers for Glucocorticosteroids.* European Journal of Pharmaceutics and Biopharmaceutics, 1998. **45**(1): p. 23-29.

145. Swatschek, D., et al., *Microparticles Derived from Marine Sponge Collagen (SCMPs): Preparation, Characterization and Suitability for Dermal Delivery of All-trans Retinol.* European Journal of Pharmaceutics and Biopharmaceutics, 2002. **54**(2): p. 125-133.

146. Muvaffak, A., I. Gurhan, and N. Hasirci, *Prolonged Cytotoxic Effect of Colchicine Released From Biodegradable Microspheres.* Journal of Biomedical Materials Research Part B: Applied Biomaterials, 2004. **71B**(2): p. 295-304.

147. Young, S., et al., *Gelatin as a Delivery Vehicle for the Controlled Release of Bioactive Molecules.* Journal of Controlled Release, 2005. **109**(1-3): p. 256-274.

148. Won, Y.-W. and Y.-H. Kim, *Recombinant Human Gelatin Nanoparticles as a Protein Drug Carrier.* Journal of Controlled Release, 2008. **127**(2): p. 154-161.

149. Kratz, F., *Albumin as a Drug Carrier: Design of Prodrugs, Drug Conjugates and Nanoparticles.* Journal of Controlled Release, 2008. **132**(3): p. 171-183.

150. Peters, T.J., *Serum Albumin.* Adv. Protein Chem., 1985. **37**: p. 161-245.

151. Carter, D.C., et al., *Three-Dimensional Structure of Human Serum Albumin.* Science, 1989. **244**(4909): p. 1195-1198.

152. Carter, D.C. and J.X. Ho, *Structure of Serum Albumin.* Adv. Protein Chem., 1994. **45**: p. 153–203.

153. Fasano, M., et al., *The Extraordinary Ligand Binding Properties of Human Serum Albumin.* IUBMB Life, 2005. **57**(12): p. 787-796.

154. Bertucci, C. and E. Domenici, *Reversible and Covalent Binding of Drugs to Human Serum Albumin: Methodological Approaches and Physiological Relevance.* Current Medicinal Chemistry, 2002. **9**: p. 1463-1481.

155. Yampolskaya, G.P., B.N. Tarasevich, and A.A. Elenskii, *Secondary Structure of Globular Proteins in Adsorption Layers at the Solution-Air Interface by the Data of Fourier Transform IR Spectroscopy.* Colloid Journal, 2005. **67**(3): p. 385-391.

156. Scheffel, U., et al., *Albumin Microspheres for Study of the Reticuloendothelial System.* Journal of Nuclear Medicine, 1972. **13**(7): p. 498-503.

157. Zolle, I., et al., *Human Serum Albumin Milimicrospheres for Studies Reticuloentothelial System.* The Journal of Nuclear Medicine, 1970. **11**: p. 379-380.

158. Nazarov, R., H.-J. Jin, and D.L. Kaplan, *Porous 3-D Scaffolds from Regenerated Silk Fibroin.* Biomacromolecules, 2004. **5**(3): p. 718-726.

159. Lotz, B. and F. Colonna Cesari, *The Chemical Structure and the Crystalline Structures of Bombyx mori Silk Fibroin.* Biochimie, 1979. **61**(2): p. 205-214.

160. Yamaguchi, K., et al., *Primary Structure of the Silk Fibroin Light Chain Determined by cDNA Sequencing and Peptide Analysis.* Journal of Molecular Biology, 1989. **210**(1): p. 127-139.

161. Zhou, P., et al., *Structure of Bombyx mori Silk Fibroin Based on the DFT Chemical Shift Calculation.* The Journal of Physical Chemistry B, 2001. **105**(50): p. 12469-12476.

162. Fontenot, K. and F.J. Schork, *Sensitivities of Droplet Size and Stability in Monomeric Emulsions.* Industrial & Engineering Chemistry Research, 1993. **32**(2): p. 373-385.

163. Taylor, P., *Ostwald Ripening in Emulsions.* Colloids and Surfaces A: Physicochemical and Engineering Aspects, 1995. **99**(2-3): p. 175-185.

164. Li, M., O. Rouaud, and D. Poncelet, *Microencapsulation By Solvent Evaporation: State of the Art for Process Engineering Approaches.* International Journal of Pharmaceutics, 2008. **363**(1-2): p. 26-39.

165. Feczkó, T., J. Tóth, and J. Gyenis, *Comparison of the Preparation of PLGA-BSA Nano- and Microparticles by PVA, Poloxamer and PVP.* Colloids and Surfaces A: Physicochemical and Engineering Aspects, 2008. **319**(1-3): p. 188-195.

166. Zhou, F., et al., *Influences of Surfactant (PVA) Concentration and pH on the Preparation of Copper Nanoparticles by Electron Beam Irradiation.* Radiation Physics and Chemistry, 2008. **77**(2): p. 169-173.

167. Mu, L. and P.H. Seow, *Application of TPGS in Polymeric Nanoparticulate Drug Delivery System.* Colloids and Surfaces B: Biointerfaces, 2006. **47**(1): p. 90-97.

168. Cohen-Sela, E., et al., *A New Double Emulsion Solvent Diffusion Technique for Encapsulating Hydrophilic Molecules in PLGA Nanoparticles.* Journal of Controlled Release, 2009. **133**(2): p. 90-95.

169. Lee, J., et al., *Amphiphilic Amino Acid Copolymers as Stabilizers for the Preparation of Nanocrystal Dispersion.* European Journal of Pharmaceutical Sciences, 2005. **24**(5): p. 441-449.

170. Hans, M.L. and A.M. Lowman, *Biodegradable Nanoparticles for Drug Delivery and Targeting* Current Opinion in Solid State and Materials Science, 2002. **6**(4): p. 319-327.

171. Lee, T.M., et al., *Engineered Microsphere Contrast Agents for Optical Coherence Tomography.* Opt. Lett., 2003. **28**(17): p. 1546-1548.

172. Thassu, D., Y. Pathak, and M. Deleers, *Nanoparticulate Drug-Delivery Systems: An Overview*. Vol. 166. 2007, New York: Informa Healthcare USA, Inc. 382.

173. Langer, R. and N.A. Peppas, *Advances in Biomaterials, Drug Delivery, and Bionanotechnology.* AIChE Journal, 2003. **49**(12): p. 2990-3006.

174. Chellat, F., et al., *Study of Biodegradation Behavior of Chitosan-Xanthan Microspheres in Simulated Physiological Media.* Journal of Biomedical Materials Research, 2000. **53**(5): p. 592-599.

175. Grassi, M. and G. Grassi, *Mathematical Modelling and Controlled Drug Delivery: Matrix Systems.* Current Drug Delivery, 2005. **2**: p. 97-116.

176. Ratner, B.D., *Biomaterials Science: An Introduction to Materials in Medicine*. 2004, San Diego, California: Elsivier Academic Press. 867.

177. Zahedi, P., et al., *A Review on Wound Dressings With an Emphasis on Electrospun Nanofibrous Polymeric Bandages.* Polymers for Advanced Technologies, 2009. **21**: p. 77-95.

178. Wollina, U., et al., *Functional Textiles in Prevention of Chronic Wounds, Wound Healing and Tissue Engineering.* eBooks Collection 1997-2009, 2003. **31**: p. 82-97.

179. Ovington, L.G., *Advances in Wound Dressings.* Clinics in Dermatology, 2007. **25**(1): p. 33-38.

180. Boateng, J.S., et al., *Wound Healing Dressings and Drug Delivery Systems: A Review.* Journal of Pharmaceutical Sciences, 2008. **97**: p. 2892-2923.

181. Angel, U., et al., *Attaching Different Kinds of Proteinaceous Nanospheres to a Variety of Fabrics Using Ultrasound Radiation.* Israel Journal of Chemistry, 2010. **50**: p. 524-529.

182. Gouveia, I.C., *Synthesis and Characterization of a Microsphere-Based Coating for Textiles with Potential as an In Situ Bioactive Delivery Dystem.* Polymers for Advanced Technologies, 2010: p. n/a-n/a.

183. Silva, R., H. Ferreira, and A. Cavaco-Paulo, *Cotton and Nonwoven Gauzes Bandages: A Support for Proteinaceous Microspheres* Submitted, 2011.

184. Vasconcelos, A., G. Freddi, and A. Cavaco-Paulo, *Biodegradable Materials Based on Silk Fibroin and Keratin.* Biomacromolecules, 2008. **9**(4): p. 1299-1305.

185. Vasconcelos, A., et al., *Protein Matrices for Improved Wound Healing: Elastase Inhibition by a Synthetic Peptide Model.* Biomacromolecules, 2010. **11**(9): p. 2213-2220.

186. Malvern, I., *Size Theory*, in *Zetasizer Nano Series*. 2005, Malvern Instruments Ltd.: Worcestershire.

187. Bunjes, H., *Characterization of Solid Lipid Nanoparticles and Microparticle*, in *Lipospheres in Drug Targets and Delivery Approaches, Methods and Applications*, C. Nastruzzi, Editor. 2005, CRC Press LLC: Boca Raton, Florida. p. 41-66.

188. Malvern, I., *Zeta-potential Theory*, in *Zetasizer Nano Series*. 2005, Malvern Instruments Ltd.: Worcestershire.

189. Schmid, G., *Nanoparticles From Theory to Application*. 2004, Weinheim: WILEY-VCH Verlag GmbH & Co. KGaA,. 445.

190. Bogner, A., et al., *Wet STEM: A New Development in Environmental SEM for Imaging Nano-Objects Included in a Liquid Phase.* Ultramicroscopy, 2005. **104**(3-4): p. 290-301.

191. Lowry, O.H., et al., *Protein Measurement with Folin-Phenol Reagent.* Journal of Biological Chemistry, 1951. **193**(1): p. 265-275.

192. Semwogerere, D. and E. Weeks, *Confocal Microscopy.* Encyclopedia of Biomaterials and Biomedical Engineering, 2005: p. 1-10.

193. Anandan, S. and M. Yoon, *Photoinduced Electron Transfer Studies of Nile Red in the Presence of TiO2 Colloidal Nanoparticles.* Spectrochimica Acta Part A: Molecular and Biomolecular Spectroscopy, 2004. **60**(4): p. 885-888.

194. Greenspan, P. and S.D. Fowler, *Spectrofluorometric Studies of the Lipid Probe, Nile Red.* Journal of Lipid Research, 1985. **26**: p. 781-789.

195. Edwards, K.A. and A.J. Baeumner, *Analysis of Liposomes.* Talanta, 2006. **68**(5): p. 1432-1441.

196. Kiyoshi, M., S. Yuklo, and H. Masao, *Formation and Mechanical Stability of Phospholipid Vesicles.* Membrane, 1992. **17**(4): p. 257-262.

197. Basto, C., T. Tzanov, and A. Cavaco-Paulo, *Combined Ultrasound-Laccase Assisted Bleaching of Cotton.* Ultrasonics Sonochemistry, 2007. **14**(3): p. 350-354.

198. Kumar, A., et al., *Gas-Liquid Mass Tranfer Studies in Sonochemical Reactors.* Industrial & Engineering Chemistry Research, 2004. **43**: p. 1812-1819.

199. Little, C., M. El-Sharif, and M.J. Hepher, *The Effect of Solution Level on Calorific and Dosimetric Results in a 70 kHz Tower Type Sonochemical Reactor.* Ultrasonics Sonochemistry, 2007. **14**(3): p. 375-379.

200. Marczak, W., *Water as a Standard in the Measurements of Speed of Sound in Liquids.* The Journal of the Acoustical Society of America, 1997. **102**(5): p. 2776-2779.

201. Genot, C., et al., *Characterization and Stability During Storage of Liposomes Made of Muscle Phospholipids.* Lebensm.-Wiss. U.-Technol., 1999. **32**: p. 167-174.

202. Korgel, B.A., J.H. van Zanten, and H.G. Monbouquette, *Vesicle Size Distributions Measured by Flow Field-Flow Fractionation Coupled with Multiangle Ligth Scatering.* Biophsysical Journal, 1998. **74**: p. 3264-3272.

203. Fromherz, P. and D. Ruppel, *Lipid Vesicle Formation-The Transition From Open Disks to Closed Shells.* Febs Letters, 1985. **179**: p. 155-159.

204. Lasch, J., V. Weissig, and M. Brandl, *Preparation of Liposomes In: Liposomes: A Practical Approach.* Oxford University Press., 2003: p. 3-27.

205. Brandl, M., et al., *Liposome Preparation using High-Pressure Homogenizers. In: Liposome Tecnology: Liposome Preparation and Related Techniques.* CRC Press, 1993: p. 49-65.

206. Dai, C., et al., *Preparation and Characterization of Liposomes-in-Alginate (LIA) for Protein Delivery System.* Colloids and Surfaces, 2005. **47**: p. 205-210.

207. Mugabe, C., A.O. Azghani, and A. Omri, *Preparation and Characterization of Dehydration-Rehydration Vesicles Loaded with Aminoglycoside and*

Macrolide Antibiotics. International journal of pharmaceutics 2006. **307**: p. 244-250.

208. Hollmann, A., et al., *Characterization of Liposomes Coated with S-Layer Proteins from Lactobacilli.* Biochimica et Biophysica Acta (BBA), 2007. **1768**: p. 393-400.

209. Kheirolomoom, A., et al., *Acoustically-Active Microbubbles Conjugated to Liposomes: Characterization of a Proposed Drug Delivery Vehicle.* Journal of controlled release, 2007. **118**: p. 275-284.

210. Patil, M.N. and A.B. Pandit, *Cavitation-A Novel Technique for Making Stable Nano-Suspensions.* Ultrasonics Sonochemistry, 2007. **14**(5): p. 519-530.

211. Stathopulos, P.B., et al., *Sonication of Proteins Causes Formation of Aggregates that Resemble Amyloid.* Protein Science, 2006. **13**: p. 3017-3027.

212. Hawkins, C.I. and M.J. Davies, *Generation and Propagation of Radical Reactions on Proteins.* Biochimica et Biophysica Acta, 2001. **1504**: p. 196-219.

213. Wood, R.W. and A.L. Loomis, *The Physiological and Biological Effects of High Frequency Sound Waves of Great Intensity.* Philosophical Magazine, 1927. **4**: p. 414-436.

214. Li, T., et al., *Gene Transfer with Echo-enhanced Contrast Agents: Comparison Between Albunex, Optison, and Levovist in Miceâ€ Initial Results1.* Radiology, 2003. **229**(2): p. 423-428.

215. Bittner, B., et al., *Recombinant Human Erythropoietin (rhEPO) Loaded Poly(lactide-co-glycolide) Microspheres: Influence of the Encapsulation Technique and Polymer Purity on Microsphere characteristics.* European Journal of Pharmaceutics and Biopharmaceutics, 1998. **45**(3): p. 295-305.

216. Jiang, W., et al., *Biodegradable Poly(lactic-co-glycolic acid) Microparticles for Injectable Delivery of Vaccine Antigens.* Advanced Drug Delivery Reviews, 2005. **57**(3): p. 391-410.

217. Wolf, M., et al., *Stabilisation and Determination of the Biological Activity of - Asparaginase in Poly(,-lactide-co-glycolide) Nanospheres.* International Journal of Pharmaceutics, 2003. **256**(1-2): p. 141-152.

218. DeLano, W.L. *The PyMOL Molecular Graphics System*. 2002 [cited; Available from: http://www.pymol.org.

219. Wimmer, R., et al., *Versatile Interactions of the Antimicrobial Peptide Novispirin with Detergents and Lipids.* Biochemistry, 2005. **45**(2): p. 481-497.

220. Bessalle, R., et al., *Structure-Function Studies of Amphiphilic Antibacterial Peptides.* Journal of Medicinal Chemistry, 1993. **36**(9): p. 1203-1209.

221. Ahlin, P., et al., *Investigation of Polymeric Nanoparticles as Carriers of Enalaprilat for Oral Administration.* International Journal of Pharmaceutics, 2002. **239**(1-2): p. 113-120.

222. Arias, J.L., et al., *Synthesis and Characterization of Poly(ethyl-2-cyanoacrylate) Nanoparticles with a Magnetic Core.* Journal of Controlled Release, 2001. **77**(3): p. 309-321.

223. Malmsten, M., *Soft Drug Delivery Systems.* Soft Matter, 2006. **2**: p. 760-769.

224. Missirlis, D., R. Kawamura, and N. Tirelli, *Thermally-Induced Glass Gormation from Hydrogel Nanoparticles.* Soft Matter, 2006. **2**(12): p. 1067-1075.

225. Gedanken, A., *Preparation and Properties of Proteinaceous Microspheres Made Sonochemically.* Chemistry-European Journal, 2008. **14**: p. 3840-3853.

226. Han, Y., et al., *Sonochemical Synthesis of Magnetic Protein Container for Targeted Delivery.* Macromolecular Rapid Communications, 2008. **29**: p. 1203-1207.

227. Peters Jr, T., J.T.E. C.B. Anfinsen, and M.R. Frederic, *Serum Albumin*, in *Advances in Protein Chemistry*. 1985, Academic Press. p. 161-245.

228. Zhou, C.Z., et al., *Fine Organization of Bombyx mori fibroin Heavy Chain Gene.* Nucleic Acids Res., 2000. **28**(12): p. 2413-2419.

229. Chansiri, G., et al., *Effect of Surface Charge on the Stability of Oil/Water Emulsions during Steam Sterilization.* Journal of Pharmaceutical Sciences, 1999. **88**(4): p. 454-458.

230. Feng, S.-S. and G. Huang, *Effects of Emulsifiers on the Controlled Release of Paclitaxel (Taxol®) from Nanospheres of Biodegradable Polymers* Journal of Controlled Release, 2001. **71**(1): p. 53-69.

231. Cao, Z., et al., *The Preparation of Regenerated Silk Fibroin Microspheres.* Soft Matter, 2007(3): p. 910 - 915.

232. Silva J. P., et al., *Oxidative Stress Protection by Newly Synthesized Nitrogen Compounds with Pharmacological Potential.* Life Sciences, 2006. **78**(11): p. 1256-1267.

233. Kim, U.-J., et al., *Three-Dimensional Aqueous-Derived Biomaterial Scaffolds from Silk Fibroin.* Biomaterials, 2005. **26**(15): p. 2775-2785.

234. Tanaka, K., S. Inoue, and S. Mizuno, *Hydrophobic Interaction of P25, Containing Asn-linked Oligosaccharide Chains, With the H-L complex of Silk Fibroin Produced by Bombyx mori* Insect Biochemistry and Molecular Biology, 1999. **29**(3): p. 269-276.

235. Haris, P.I. and F. Severcan, *FTIR Spectroscopic Characterization of Protein Structure in Aqueous and Non-Aqueous Media.* Journal of Molecular Catalysis B: Enzymatic 1999. **7**(1-4): p. 207-221.

236. Chittur, K.K., *FTIR/ATR for Protein Adsorption to Biomaterial Surfaces.* Biomaterials, 1998. **19**(4-5): p. 357-369.

237. Byler, D.M. and H. Susi, *Examination of the Secondary Structure of Proteins by Deconvolved FTIR Spectra.* Biopolymers, 1986. **25**: p. 469-487.

238. Dong, A., P. Huang, and W.S. Caughey, *Protein Secondary Structures in Water from Second-Derivative Amide I Infrared Spectra.* Biochemistry, 1990. **29**(13): p. 3303-3308.

239. Kong H., et al., *Deconvolution of Overlapped Peaks Based on the Exponentially Modified Gaussian Model in Comprehensive Two-Dimensional Gas Chromatography* Journal of Chromatography A, 2005. **1086**(1-2): p. 160-164.

240. Gülseren, I., et al., *Structural and Functional Changes in Ultrasonicated Bovine Serum Albumin Solutions.* Ultrasonics Sonochemistry, 2007. **14**(2): p. 173-183.

241. Fu, K., et al., *FTIR Characterization of the Secondary Structure of Proteins Encapsulated within PLGA Microspheres.* Journal of Controlled Release, 1999. **58**(3): p. 357-366.

242. Takeda, K., M. Shigeta, and K. Aoki, *Secondary Structures of Bovine Serum Albumin in Anionic and Cationic Surfactant Solutions.* Journal of Colloid and Interface Science, 1987. **117**(1): p. 120-126.

243. Zhang, G.Q., et al., *Ultrasonic-Assisted Preparation of Monodisperse Iron Oxide Nanoparticles.* Materials Letters, 2007. **61**(11-12): p. 2204-2207.

244. Bala, I., S. Hariharan, and M.N. Kumar, *PLGA Nanoparticles in Drug Delivery: The State of the Art.* Critical Reviews in Therapeutic Drug Carrier Systems, 2004. **21**(5): p. 387-422.

245. Bala, I., et al., *Design of Biodegradable Nanoparticles: A Novel Approach to Encapsulating Poorly Soluble Phytochemical Ellagic Acid.* Nanotechnology, 2005. **16**: p. 2819-2822.

246. Hess, B., et al., *GROMACS 4: Algorithms for Highly Efficient, Load-Balanced, and Scalable Molecular Simulation.* Journal of Chemical Theory and Computation, 2008. **4**(3): p. 435-447.

247. Oostenbrink, C., et al., *A Biomolecular Force Field Based on the Free Enthalpy of Hydration and Solvation: The GROMOS Force-Field Parameter Sets 53A5 and 53A6.* Journal of Computational Chemistry, 2004. **25**: p. 1656-1676.

248. Rathore, O. and D.Y. Sogah, *Self-Assembly of β-Sheets into Nanostructures by Poly(alanine) Segments Incorporated in Multiblock*

Copolymers Inspired by Spider Silk. Journal of the American Chemical Society, 2001. **123**(22): p. 5231-5239.

249. Gente, G., A. Iovino, and C. La Mesa, *Supramolecular Association of a Triblock Copolymer in Water.* Journal of Colloid and Interface Science, 2004. **274**(2): p. 458-464.

250. Santoso, S.S., S. Vauthey, and S. Zhang, *Structures, Function and Applications of Amphiphilic Peptides.* Current Opinion in Colloid & Interface Science, 2002. **7**(5-6): p. 262-266.

251. Zhang, S., et al., *Design of Nanostructured Biological Materials Through Self-Assembly of Peptides and Proteins.* Current Opinion in Chemical Biology, 2002. **6**(6): p. 865-871.

252. Branco, M.C. and J.P. Schneider, *Self-Assembling Materials for Therapeutic Delivery.* Acta Biomaterialia, 2009. **5**(3): p. 817-831.

253. Vauthey, S., et al., *Molecular Self-Assembly of Surfactant-Like Peptides to form Nanotubes and Nanovesicles.* Proceedings of the National Academy of Sciences of the United States of America, 2002. **99**(8): p. 5355-5360.

254. Childers, W.S., et al., *Peptide Membranes in Chemical Evolution.* Current Opinion in Chemical Biology, 2009. **13**(5-6): p. 652-659.

255. Ashcroft, G.S., et al., *Secretory Leukocyte Protease Inhibitor Mediates Non-Redundant Functions Necessary for Normal Wound Healing.* Nat Med, 2000. **6**(10): p. 1147-1153.

256. Lazarus, G.S., et al., *Definitions and Guidelines for Assessment of Wounds and Evaluation of Healing.* Archives of Dermatology 1994. **130**(4): p. 489-493.

257. Grinnell, F. and M. Zhu, *Identification of Neutrophil Elastase as the Proteinase in Burn Wound Fluid Responsible for Degradation of Fibronectin.* The Journal of Investigative Dermatology, 1994. **103**(2): p. 155-161.

258. Yager, D.R., et al., *Ability of Chronic Wound Fluids to Degrade Peptide Growth Factors is Associated with Increased Levels of Elastase Activity*

and Dimished Levels of Proteinase Inhibitors. Wound Repair and Regeneration, 1997. **5**(1): p. 23-32.

259. Chen, C., et al., *Molecular and Mechanistic Validation of Delayed Healing Rat Wounds as a Model for Human Chronic Wounds.* Wound Repair and Regeneration, 1999. **7**(6): p. 486-494.

260. Shapiro, S.D., *Proteinases in Chronic Obstructive Pulmonary Disease.* Biochemical Society Transactions, 2002. **30**(2): p. 98-102.

261. Lobmann, R., G. Schultz, and H. Lehnert, *Proteases and the Diabetic Foot Syndrome: Mechanisms and Therapeutic Implications.* Diabetes Care, 2005. **28**(2): p. 461-471.

262. Trengove, N.J., S.R. Langton, and M.C. Stacey, *Biochemical Analysis of Wound Fluid from Nonhealing and Healing Chronic Leg Ulcers.* Wound Repair and Regeneration, 1996. **4**(2): p. 234-239.

263. Yager, D.R. and B.C. Nwomeh, *The Proteolytic Environment of Chronic Wounds.* Wound Repair and Regeneration, 1999. **7**(6): p. 433-441.

264. Schönfelder, U., et al., *Influence of Selected Wound Dressings on PMN Elastase in Chronic Wound Fluid and Their Antioxidative Potential In Vitro.* Biomaterials, 2005. **26**(33): p. 6664-6673.

265. Edwards, J.V., P. Howley, and I.K. Cohen, *In vitro Inhibition of Human Neutrophil Elastase by Oleic Acid Albumin Formulations from Derivatized Cotton Wound Dressings.* International Journal of Pharmaceutics, 2004. **284**(1-2): p. 1-12.

266. Edwards, P.D. and P.R. Bernstein, *Synthetic Inhibitors of Elastase.* Medicinal Research Reviews, 1994. **14**(2): p. 127-194.

267. Ashe, B.M. and M. Zimmerman, *Specific Inhibition of Human Granulocyte Elastase by cis-unsaturated Fatty Acids and Activation by the Corresponding Alcohols.* Biochemical and Biophysical Research Communications, 1977. **75**(1): p. 194-199.

268. Edwards, J.V., et al., *Protease Inhibition by Oleic Acid Transfer From Chronic Wound Dressings to Albumin.* International Journal of Pharmaceutics, 2007. **340**(1-2): p. 42-51.

269. Edwards, J.V., et al., *Modified Cotton Gauze Dressings that Selectively Absorb Neutrophil Elastase Activity in Solution.* Wound Repair and Regeneration, 2001. **9**(1): p. 50-58.

270. Kim, U.-J., et al., *Structure and Properties of Silk Hydrogels.* Biomacromolecules, 2004. **5**(3): p. 786-792.

271. Jin, H.-J., et al., *Biomaterial Films of Bombyx Mori Silk Fibroin with Poly(ethylene oxide).* Biomacromolecules, 2004. **5**(3): p. 711-717.

272. Jin, H.-J., et al., *Electrospinning Bombyx mori Silk with Poly(ethylene oxide).* Biomacromolecules, 2002. **3**(6): p. 1233-1239.

273. Tanaka, H., et al., *A Sensitive and Specific Assay for Granulocyte Elastase in Inflammatory Tissue Fluid Using L-pyroglutamyl-L-prolyl-L-valine-p-nitroanilide.* Clinica Chimica Acta, 1990. **187**(2): p. 173-180.

274. Attard, P., D. Antelmi, and I. Larson, *Comparison of the Zeta Potential with the Diffuse Layer Potential from Charge Titration.* Langmuir, 2000. **16**(4): p. 1542-1552.

275. Zhang, Y., et al., *Zeta-Potential: A Surface Electrical Characteristic to Probe the Interaction of Nanoparticles with Normal and Cancer Human Breast Epithelial Cells.* Biomedical Microdevices, 2008. **10**(2): p. 321-328.

276. Mandzy, N., E. Grulke, and T. Druffel, *Breakage of TiO2 Agglomerates in Electrostatically Stabilized Aqueous Dispersions.* Powder Technology, 2005. **160**(2): p. 121-126.

277. Liao, D.L., G.S. Wu, and B.Q. Liao, *Zeta-Potential of Shape-Controlled TiO2 Nanoparticles with Surfactants.* Colloids and Surfaces A: Physicochemical and Engineering Aspects, 2009. **348**(1-3): p. 270-275.

278. Berg, J.M., et al., *The Relationship Between pH and Zeta-Potential of ~ 30 nm Metal Oxide Nanoparticle Suspensions Relevant to in vitro Toxicological Evaluations.* Nanotoxicology, 2009. **3**(4): p. 276-283.

279. Siedle, B., A. Hrenn, and I. Merfort, *Natural Compounds as Inhibitors of Human Neutrophil Elastase.* Planta Med, 2007. **73**(05): p. 401,420.

280. Machovich, R. and W.G. Owen, *Denatured Proteins as Cofactors for Plasminogen Activation.* Archives of Biochemistry and Biophysics, 1997. **344**(2): p. 343-349.

281. Spector Arthur A. , John Kathryn , and J.E. Fletcher, *Binding of Long-Chain Fatty Acids to Bovine Serum Albumin.* Journal of Lipid Research, 1969. **10**: p. 56-67.

282. Lúcio, M., et al., *Use of Liposomes to Evaluate the Role of Membrane Interactions on Antioxidant Activity.* Analytica Chimica Acta, 2007. **597**(1): p. 163-170.

283. Fröhlich, J.C., *Prostaglandin Endoperoxide Synthetase Isoenzymes: The Clinical Relevance of Selective Inhibition.* Annals of the Rheumatic Diseases, 1995. **54**(12): p. 942-943.

284. Brooks, P., *Use and Benefits of Nonsteroidal Anti-inflammatory Drugs.* The American Journal of Medicine, 1998. **104**(3, Supplement 1): p. 9S-13S.

285. Tomisato, W., et al., *Membrane Permeabilization by Non-steroidal Anti-inflammatory Drugs.* Biochemical and Biophysical Research Communications, 2004. **323**(3): p. 1032-1039.

286. Goosen, C., et al., *Correlation Between Physicochemical Characteristics, Pharmacokinetic Properties and Transdermal Absorption of NSAID's.* International Journal of Pharmaceutics, 1998. **163**(1-2): p. 203-209.

287. Couvreur, P., et al., *Nanoparticles as Microcarriers for Anticancer Drugs.* Advanced Drug Delivery Reviews, 1990. **5**(3): p. 209-230.

288. Allémann, E., R. Gurny, and E. Doelker, *Drug Loaded Nanoparticles: Preparation Methods and Drug Targeting Issues* European Journal of Pharmaceutics and Biopharmaceutics, 1993. **39**: p. 173-191.

289. Truong-Le, V.L., et al., *Gene Transfer by DNA-Gelatin Nanospheres.* Archives of Biochemistry and Biophysics, 1999. **361**(1): p. 47-56.

290. Chen, J. and E. Dickinson, *Protein/Surfactant Interfacial Interactions Part 1. Flocculation of Emulsions Containing Mixed Protein + Surfactant.* Colloids and Surfaces A: Physicochemical and Engineering Aspects, 1995. **100**: p. 255-265.

291. Azarmi, S., et al., *Optimization of a Two-Step Desolvation Method for Preparing Gelatin Nanoparticles and Cell Uptake Studies in 143B Osteosarcoma Cancer Cells.* Journal of Pharmacy & Pharmaceutical Sciences, 2006. **9**: p. 124-132.

292. Higuchi, T., *Rate of Release of Medicaments from Ointment Bases Containing Drugs in Suspension.* Journal of Pharmaceutical Sciences, 1961. **50**: p. 874-875.

293. Korsmeyer, R.W., et al., *Mechanisms of Solute Release from Porous Hydrophilic Polymers.* International Journal of Pharmaceutics, 1983. **15**(1): p. 25-35.

294. Ritger, P.L. and N.A. Peppas, *A Simple Equation for Description of Solute Release I. Fickian and Non-Fickian Release from Non-Swellable Devices in the form of Slabs, Spheres, Cylinders or Discs.* Journal of Controlled Release, 1987. **5**(1): p. 23-36.

295. Siepmann, J. and N.A. Peppas, *Modeling of Drug Release from Delivery Systems Based on Hydroxypropyl Methylcellulose (HPMC).* Advanced Drug Delivery Reviews, 2001. **48**(2-3): p. 139-157.

296. Cao, G. and R.L. Prior, *Comparison of Different Analytical Methods for Assessing Total Antioxidant Capacity of Human Serum.* Clinical Chemistry, 1998. **44**(6): p. 1309-1315.

297. Behl, C., *Alzheimer's Disease and Oxidative Stress: Implications for Novel Therapeutic Approaches.* Progress in Neurobiology, 1999. **57**(3): p. 301-323.

298. De Zwart, L.L., et al., *Biomarkers of Free Radical Damage : Applications in Experimental Animals and in Humans.* Free Radical Biology and Medicine, 1999. **26**(1-2): p. 202-226.

299. Harding, K., K. Cutting, and P. Price, *The Cost-Effectiveness of Wound Management Protocols of Care.* British Journal of Nursing, 2000. **10**: p. 216-7.

300. Miraftab, M., et al., *Fibres for wound dressings based on mixed carbohydrate polymer fibres.* Carbohydrate Polymers, 2003. **53**(3): p. 225-231.

301. Jones, V.J., *The Use of Gauze: Will it Ever Change?* International Wound Journal, 2006. **3**: p. 79-88.

302. Degim, Z., *Use of Microparticulate Systems to Accelerate Skin Wound Healing.* Journal of Drug Targeting, 2008. **16**(6): p. 437-448.

303. Dahl, J.B. and H. Kehlet, *Non-Steroidal Anti-Inflammatory Drugs: Rationale for Use in Several PostOperative Pain.* British Journal of Anaesthesia, 1991. **66**: p. 703-712.

304. Álvarez-Soria, M.A., et al., *Long term NSAID treatment inhibits COX-2 synthesis in the knee synovial membrane of patients with osteoarthritis: differential proinflammatory cytokine profile between celecoxib and aceclofenac.* Annals of the Rheumatic Diseases, 2006. **65**(8): p. 998-1005.

305. Wang, B., T. Siahaan, and R. Soltero, eds. *Drug Delivery - Principles and Applications*. 2005, John Wiley & Sons.

306. Lee, J.W., J.H. Park, and J.R. Robinson, *Bioadhesive-Based Dosage Forms: The Next Generation.* Journal of Pharmaceutical Sciences, 2000. **89**: p. 850-866.

307. Uhrich, K.E., et al., *Polymeric Systems for Controlled Drug Release.* Chemical Reviews, 1999. **99**(11): p. 3181-3198.

308. Kocbek, P., et al., *Targeting Cancer Cells using PLGA Nanoparticles Surface Modified with Monoclonal Antibody.* Journal of Controlled Release, 2007. **120**(1-2): p. 18-26.

309. Xu, W., G. Ke, and X. Peng, *Studies on the Effects of the Enzymatic Treatment on Silk Fine Powder.* Journal of Applied Polymer Science, 2006. **101**: p. 2967-2971.

310. Subramanian Senthil Kannan M. , et al., *Influence of Cationization of Cotton on Reactive dyeing.* Journal of Textile and Apparel, Technology and Management, 2006. **5**(2): p. 1-22.

311. Harold, R.W., *Textiles: Apperance Analysis and Shade Sorting.* Textile Chemical Coloration, 1987. **19**: p. 23-31.

312. Macdonald, R., *Colour Physics for Industry* 1987, England: Society of Dyers and Colourists.

313. Meyer, H., *The Ninhydrin Reaction and its Analytical Applications.* Biochemistry, 1957. **67**: p. 333-340.

314. Friedman, M., *Applications of the Ninhydrin Reaction for Analysis of Amino Acids, Peptides, and Proteins to Agricultural and Biomedical Sciences.* Journal of Agricultural and Food Chemistry, 2004. **52**(3): p. 385-406.

315. Braun-Falco, O. and H. Korting, *Normal pH value of human skin.* Hautarzt, 1986. **37**(3): p. 126-129.

316. Seong, H.S. and S.W. Ko, *Synthesis, Application and Evaluation of Cationising Agents for Cellulosic Fibres.* Journal of the Society of Dyers and Colourists, 1998. **114**(4): p. 124-129.

317. Jambrak, A.R., et al., *Effect of Ultrasound Treatment on Solubility and Foaming Properties of Whey Protein Suspensions.* Journal of Food Engineering, 2008. **86**: p. 281-287.